online issn: 1307-6892

irc 2021
XV. international research conference
proceedings

open science index 15 2021

july 22-23, 2021 berlin germany
international scholarly and scientific research & innovation

Open Science

Open Science Philosophy

Open science encompasses unrestricted access to scientific research articles, access to data from public research, and collaborative research enabled by information and communication technology tools, models, and incentives. Broadening access to scientific research publications and data is at the heart of open science. The objective of open science is to make research outputs and its potential benefits available to the entire world and in the hands of as many as possible:

- Open science promotes a more accurate verification of scientific research results. Scientific inquiry and discovery can be sped up by combining the tools of science and information technologies. Open science will benefit society and researchers by providing faster, easier, and more efficient availability of research outputs.
- Open science reduces duplication in collecting, creating, transferring, and re-using scientific material.
- Open science increases productivity in an era of tight budgets.
- Open science results in great innovation potential and increased consumer choice from public research.
- Open science promotes public trust in science. Greater citizen engagement leads to active participation in scientific experiments and data collection.

Open Science Index

The Open Science Index (OSI) currently provides access to over thirty thousand full-text journal articles and is working with member and non-member organizations to review policies to promote and assess open science. As part of the open science philosophy, and by making open science a reality; OSI is conducting an assessment of the impact of open science principles and restructuring the guidelines for access to scientific research. As digitalization continues to accelerate science, Open science and big data hold enormous promise and present new challenges for policymakers, scientific institutions, and individual researchers.

OSI is helping the global scientific research community discover, evaluate, and access high-quality research output. Renowned for its editorially curated and refereed collection of the highest-quality publications, OSI has always been and will remain free-of-charge.

OSI provides an efficient and thorough discovery process to the open science research database and provides links and free access to full-text articles. There are 50 open access journal categories that are curated and refereed by international scientific committees, the in-house editorial team, and trusted partners. Since its inception in 2007, OSI has made more than thirty thousand peer-reviewed open access full-text journal articles (PDF versions) freely available online without cost, barriers, or restrictions.

Open Science Access

With the Open Science Index, researchers can discover and access trusted peer-reviewed open access full-text scientific research articles with confidence. OSI helps researchers find appropriate non-profit open access journals to publish their work.

OSI gives one-click access to online full-text PDFs and expands the reach to global society by giving users free access from anywhere around the globe. Through cutting-edge open science collaboration, in an innovative public partnership, the non-profit OSI is devoted to making science open and reusable.

To learn more, visit online at waset.org

Open Science

Open Society

An open society allows individuals to change their roles and to benefit from corresponding changes in status. Open science depends to a greater or lesser extent on digital technologies and innovations in structural processes by an open society. When realized, open science research and innovation can create investment opportunities for new and better products and services and therefore increase competitiveness and employment. Open science research and innovation is a key component of thematic open science priorities. Central to the open science digital infrastructure is enabling industry to benefit from digital technology and to underpin scientific advances through the development of an open society. Open science research and innovation can also contribute to society as a global actor because scientific relations can flourish even where global relations are strained. Open science has a critical role across many areas of decision making in providing evidence that helps understand the risks and benefits of different open science choices. Digital technology is making the conduct of open science and innovation more collaborative, more global, and more open to global citizens. Open society must embrace these changes and reinforce its position as the leading power for science, for new ideas, and for investing sustainably in the future.

It is apparent in open society that the way science works is fundamentally changing, and an equally significant transformation is taking place in how organizations and societies innovate. The advent of digital technology is making research and innovation more open, collaborative, and global. These exchanges are leading open society to develop open science and to set goals for research and innovation priority. Open science goals are materializing in the development of scientific research and innovation platforms and greater acceptance of scientific data generated by open science research. Open science research and innovation do not need help from open society to come up with great ideas, but the level of success ideas ultimately reach is undoubtedly influenced by regulation, financing, public support, and market access. Open society is playing a crucial role in improving all these success factors.

Open Science

Open science represents a new approach to the scientific process based on cooperative work and new ways of diffusing knowledge by using digital technologies and collaborative tools. These innovations capture a systemic change to the way science and research have been carried out for the last fifty years. Science is shifting from the standard practice of publishing research results in scientific publications after the research and reviews are completed. The shift is towards sharing and using all available knowledge at an earlier stage in the research process. Open science is to science what digital technology is to social and economic transactions: allowing end users to be producers of ideas, relations, and services and in doing so, enabling new working models, new social relationships and leading to a new modus operandi for science. Open science is as important and disruptive as e-commerce has been for the retail industry. Just like e-commerce, the open science research paradigm shift affects the whole business cycle of doing science and research. From the selection of research subjects to the carrying out of research, to its use and re-use, to the role of universities, and that of publishers are all dramatically changed. Just as the internet and globalization have profoundly changed the way we do business, interact socially, consume culture, and buy goods, these changes are now profoundly impacting how one does research and science.

The discussion on broadening the footprint of science and on novel ways to produce and spread knowledge gradually evolved from two global trends: Open Access and Open Source. The former refers to online, peer-reviewed scholarly outputs, which are free to read, with limited or no copyright and licensing restrictions, while open source refers to software created without any proprietary restriction and which can be accessed and freely used. Although open access became primarily associated with a particular publishing

or scientific dissemination practice, open access already sought to induce a broader practice that includes the general re-use of all kinds of research products, not just publications or data. It is only more recently that open science has coalesced into the concept of a transformed scientific practice, shifting the focus of researchers' activity from publishing as fast as possible to sharing knowledge as early as possible. Open science is defined as the idea that scientific knowledge of all kinds should be openly shared as early as is practical in the discovery process. As a result, the way science is done in the future will look significantly different from the way it is done now. Open science is the ongoing evolution in the modus operandi of doing research and organizing science. This evolution is enabled by digital technology and is driven by both the globalization of the scientific community and increasing public demand to address the societal challenges of our times. Open science entails the ongoing transitions in the way research is performed, researchers collaborate, knowledge is shared, and science is organized.

Open science impacts the entire research cycle, from the inception of research to its publication, and on how this cycle is organized. The outer circle reflects the new interconnected nature of open science, while the inner circle shows the entire scientific process, from the conceptualization of research ideas to publishing. Each step in the scientific process is linked to ongoing changes brought about by open science, including the emergence of alternative systems to establish a scientific reputation; changes in the way quality and impact of research are evaluated; the growing use of scientific blogs; open annotation; and open access to data and publications. All institutions involved in science are affected, including research organizations, research councils, and funding bodies. The trends are irreversible, and they have already grown well beyond individual projects. Theses changes predominantly result from a bottom-up process driven by a growing number of researchers who increasingly employ social media in their research and initiate globally coordinated research projects while sharing results at an early stage in the research process.

Open science is encompassed in five schools of thought:

- the infrastructure school, concerned with technological architecture
- the public school, concerned with the accessibility of knowledge creation
- the measurement school, concerned with alternative impact assessment
- the democratic school, concerned with access to knowledge
- the pragmatic school, concerned with collaborative research

According to the measurement school, the reputation and evaluation of individual researchers are still mainly based on citation-based metrics. The h-index is an author-level metric that attempts to measure both the productivity and citation impact of the publications of a scientist or scholar. The impact factor is a measure reflecting the average number of citations to articles published in an academic journal and is used as a proxy for the relative importance of a journal.

Numerous criticisms have been made of citation-based metrics, primarily when used, and often misused, to assess the performance of individual researchers. These metrics:

- are often not applicable at the individual level
- do not take into account the broader social and economic function of scientific research
- are not adapted to the increased scale of research
- cannot recognize new types of work that researchers are performing

Web-based metrics for measuring research output, popularized as altmetrics, have recently received much attention: some measure the impact at the article level, others make it possible to assess the many outcomes of research in addition to the number of scientific articles and references. The current reputation and evaluation system has to adapt to the new dynamics of open science and acknowledge and incentivize

engagement in open science. Researchers engaging in open science have growing expectations that their work, including intermediate products such as research data, will be better rewarded or taken into account in their career development. Vice-versa, the use, and reuse of open data will require appropriate codes of conduct requiring, for example, the proper acknowledgment of the original creator of the data.

These ongoing changes are progressively transforming scientific practices with innovative tools to facilitate communication, collaboration, and data analysis. Researchers that increasingly work together to create knowledge can employ online tools and create a shared space where creative conversation and collaboration can occur. As a result, the problem-solving process can be faster, and the range of problems that can be solved can be expanded. The ecosystem underpinning open science is evolving very rapidly. Social network platforms for researchers already attract millions of users and are being used to begin and validate more research projects.

Furthermore, the trends towards open access are redefining the framework conditions for science and thus have an impact on how open innovation is produced by encouraging a more dynamic circulation of knowledge. It can enable more science-based startups to emerge thanks to the exploitation of openly accessible research results. Open science, however, does not mean free science. It is essential to ensure that intellectual property is protected before making knowledge publicly available in order to subsequently attract investments that can help translate research results into innovation. If this is taken into account, fuller and broader access to scientific publications and research data can help to accelerate innovation. Investments that boost research and innovation in open science would benefit society with fewer barriers to knowledge transfer, open access to scientific research, and greater mobility of researchers. In this context, open access can help overcome the barriers that innovative organizations face in accessing the results of research funded by the public.

Open innovation

An open society is the largest producer of knowledge, but the phenomenon of open science is changing every aspect of the scientific method by becoming more open, inclusive, and interdisciplinary. Ensuring open society is at the forefront of open science means promoting open access to scientific data and publications alongside the highest standards of research integrity. There are few forces in this globe as engaging and unifying as science. The universal language of science maintains open channels of communication globally. Open society can maximize its gains through maintaining its presence at the highest level of scientific endeavor, and by promoting a competitive edge in the knowledge society of the information age. The ideas and initiatives described in this publication can stimulate anyone interested in open science research and innovation. It is designed to encourage debate and lead to new ideas on what and open society should do, should not do, or do differently.

An open society can lead to a research powerhouse; however, open society rarely succeeds in turning research into innovation and in getting research results to the global market. Open society must improve at making the most of its innovation talent, and that is where open innovation comes into play. The basic premise of open innovation is to open up the innovation process to all active players so that knowledge can circulate more freely and be transformed into products and services that create new markets while fostering a stronger culture of entrepreneurship. Open innovation is defined as the use of purposive inflows and outflows of knowledge to accelerate internal innovation. This original notion of open innovation was primarily based on transferring knowledge, expertise, and even resources from one company or research institution to another. This notion assumes that firms can and should use external ideas as well as internal ideas, and internal and external paths to market, as they seek to improve their performance. The concept of open innovation is continually evolving and is moving from linear, bilateral transactions and collaborations

towards dynamic, networked, multi-collaborative innovation ecosystems. This means that a specific innovation can no longer be seen as the result of predefined and isolated innovation activities but rather as the outcome of a complex co-creation process involving knowledge flows across the entire economic and social environment. This co-creation takes place in different parts of the innovation ecosystem and requires knowledge exchange and absorptive capacities from all the actors involved, whether businesses, academia, financial institutions, public authorities, or citizens.

Open innovation is a broad term, which encompasses several different nuances and approaches. Two main elements underpin the most recent conceptions of open innovation: the users are in the spotlight and invention becomes an innovation only if users become a part of the value creation process. Notions such as user innovation emphasize the role of citizens and users in the innovation processes as distributed' sources of knowledge. This kind of public engagement is one of the aims of open science research and innovation. The term 'open' in these contexts has also been used as a synonym for 'user-centric'; creating a well-functioning ecosystem that allows co-creation and becomes essential for open innovation. In this ecosystem, relevant stakeholders are collaborating along and across industry and sector-specific value chains to co-create solutions for socio-economic and business challenges. One important element to keep in mind when discussing open innovation is that it cannot be defined in absolutely precise terms. It may be better to think of it as a point on a continuum where there is a range of context-dependent innovation activities at different stages, from research to development through to commercialization, and where some activities are more open than others. Open innovation is gaining momentum thanks to new large-scale trends such as digitalization and the mass participation and collaboration in innovation that it enables. The speed and scale of digitalization are accelerating and transforming the way one designs, develops, and manufactures products, the way one delivers services, and the products and services themselves. It is enabling innovative processes and new ways of doing business, introducing new cross-sector value chains and infrastructures.

Open society must ensure that it capitalizes on the benefits that these developments promise for citizens in terms of tackling societal challenges and boosting business and industry. Drawing on these trends, and with the aim of helping build an open innovation ecosystem in open society, the open society's concept of open innovation is characterized by:

- combining the power of ideas and knowledge from different actors to co-create new products and find solutions to societal needs
- creating shared economic and social value, including a citizen and user-centric approach
- capitalizing on the implications of trends such as digitalization, mass participation, and collaboration

In order to encourage the transition from linear knowledge transfer towards more dynamic knowledge circulation, experts agree that it is essential to create and support an open innovation ecosystem that facilitates the translation of knowledge into socio-economic value. In addition to the formal supply-side elements such as research skills, excellent science, funding and intellectual property management, there is also a need to concentrate on the demand side aspects of knowledge circulation, making sure that scientific work corresponds to the needs of the users and that knowledge is findable, accessible, interpretable and reusable. Open access to research results aims to make science more reliable, efficient, and responsive and is the springboard for increased innovation opportunities, e.g. by enabling more science-based startups to emerge. Prioritizing open science does not, however, automatically ensure that research results and scientific knowledge are commercialized or transformed into socio-economic value. In order for this to happen, open innovation must help to connect and exploit the results of open science and facilitate the faster translation of discoveries into societal use and economic value.

Open Science

Collaborations with global partners represent important sources of knowledge circulation. The globalization of research and innovation is not a new phenomenon, but it has intensified in the last decade, particularly in terms of collaborative research, international technology production, and worldwide mobility of researchers and innovative entrepreneurs. Global collaboration plays a significant role both in improving the competitiveness of open innovation ecosystems and in fostering new knowledge production worldwide. It ensures access to a broader set of competencies, resources, and skills wherever they are located, and it yields positive impacts in terms of scientific quality and research results. Collaboration enables global standard-setting, allows global challenges to be tackled more effectively, and facilitates participation in global value chains and new and emerging markets.

To learn more, visit online at waset.org

Open Science

Scholarly Research Review

The scholarly research review is a multidimensional evaluation procedure in which standard peer review models can be adapted in line with the ethos of scientific research, including accessible identities between reviewer and author, publishing review reports and enabling greater participation in the peer review process. Scholarly research review methods are employed to maintain standards of quality, improve performance, provide credibility, and determine suitability for publication. *Responsible Peer Review Procedure:* Responsible peer review ensures that scholarly research meets accepted disciplinary standards and ensures the dissemination of only relevant findings, free from bias, unwarranted claims, and unacceptable interpretations. Principles of responsible peer review:

• Honesty in all aspects of research
• Accountability in the conduct of research
• Professional courtesy and fairness in working with others
• Good stewardship of research on behalf of others

The responsibilities of peer review apply to scholarly researchers at all stages of peer review: Fairness, Transparency, Independence, Appropriateness and Balance, Participation, Confidentiality, Impartiality, Timeliness, Quality and Excellence, Professionalism, and Duty to Report.

Scholarly Research Review Traits:
• Scholarly Research Review Identities: Authors and reviewers are aware of each other's identity

• Scholarly Research Review Reports: Review reports are published alongside the relevant article

• Scholarly Research Review Participation: The wider academic community is able to contribute to the review process

• Scholarly Research Review Interaction: Direct reciprocal discussion between author(s) and reviewers, and/or between reviewers, is allowed and encouraged

• Scholarly Research Pre-review Manuscripts: Manuscripts are made immediately available in advance of any formal peer review procedures

• Scholarly Research Review Final-version Reviewing: Editorial revision of the language and format is conducted on the final version of the manuscript for publication

• Scholarly Research Review Platforms: The scholarly research review process is independent of the final publication of the manuscript and it is facilitated by a different organizational entity than the venue of publication

All submitted manuscripts are subject to the scholarly research review process, in which there are three stages of evaluation for consideration: pre-review manuscripts, chair-review presentation, and final-review manuscripts. All submitted full text papers, that may still be withstand the editorial review process, are presented in the conference proceedings. Manuscripts are tracked and all actions are logged by internal and external reviewers according to publication policy. External reviewers' editorial analysis consists of the evaluation reports of the conference session chairs and participants in addition to online internal and external reviewers' reports. Based on completion of the scholarly research review process, those manuscripts meeting the publication standards are published 10 days after the event date.

To learn more, visit online at waset.org

TABLE OF CONTENTS

Aeroelastic Robust Optimisation of a Composite Plate Wing Using Surrogate Modelling

M. Sharifi, J-C. Chassaing, A. Vincenti

***Abstract*—**Aeroelastic optimisation of wing structure using composite materials has become a matter of interest in aeronautics due to their high strength-to-weight and stiffness-to-weight ratio. In the present work the properties of these materials have been investigated in order to achieve an optimal aeroelastic behaviour. First, the aeroelastic model needs to be created. The Doublet Lattice Method (DLM) has been employed in order to compute aerodynamic loads of a subsonic incompressible flow. The structure is modelled using the Finite Element Method (FEM) and is then coupled with DLM in order to study the aeroelastic behaviour of the plate wing. Different aeroelastic solvers have been developed such as the V-g method and the p-k method. Using these solvers, the aeroelastic response of a straight or a swept wing has been validated. After next step is the formulation of the optimisation problem. More precisely, the main objective of the optimisation procedure is to alleviate the velocity at which an aeroelastic instability may occur. However multiple difficulties are faced during this step such as the presence of a discontinuity of the response surface of the critical velocity and the problem associated with the computational time of the forward uncertainty propagation methods such as Monte Carlo. The discontinuity of the response surface is caused by a mode switch and can result in a drastic change in the value of the flutter velocity when the parametric uncertainties due to the manufacturing process are taken into account such as randomness in ply angles and thicknesses of a composite laminate. First, a robust optimisation framework is deployed by combining a genetic algorithm and a Gaussian Process Regression approach. However, the treatment of discontinuous response surfaces using this meta model, may result in a loss of accuracy in determining the optimal solution. In order to alleviate this drawback, a second approach is proposed by using a Gaussian Process Emulator (GPE) in order to fit directly the modal eigenvalues at a given speed that are continuous functions of the material properties and can be predicted accurately using a surrogate model. The latter then emulates a stability margin which depends on the values of the damping calculated using the eigenvalues. The optimisation problem is thus formulated to reduce the probability that the stability margin becomes negative. In the end, optimal aeroelastic layups are determined for various rectangular, tapered and forward or backward composite plates.

***Keywords*—** Aeroelastic flutter, composite structures, uncertainty quantification, robust optimisation

M. Sharifi is with Sorbonne Université, CNRS, Institut Jean Le Rond d'Alembert, UMR 7190, F-75005 Paris, France (e-mail: mahshid.sharifi@sorbonne-universite.fr).

J-C. Chassaing is with Sorbonne Université, CNRS, Institut Jean Le Rond d'Alembert, UMR 7190, F-75005 Paris, France (e-mail: jean-camille.chassaing@sorbonne-universite.fr).

A. Vincenti is with Sorbonne Université, CNRS, Institut Jean Le Rond d'Alembert, UMR 7190, F-75005 Paris, France (e-mail: angela.vincenti@sorbonne-universite.fr).

2-Way Fluid-Structure Interaction of a Wing

Morteza Raki

***Abstract*—**As for Aircraft wing, its design and construction have special importance in the aerospace industry so that working on these fields plays an important role in the expenses and operation of the whole system. Designing an airplane wing is considered a Multiphysics major due to solid and fluid calculations which are classified in different subjects. In this regard, one of the significant topics which are investigated by researchers and scientists is the aeroelastic investigation on aircraft wing and to design optimization in this field, it is needed to concentrate on fluid-structure interaction. The present paper aims to study the 2-way fluid-structure interaction of a wing. First and foremost, there are some theoretical calculations based on 2-way fluid-structure interaction to be done to be able to simulate the problem in ANSYS software. Then the results are detected to be analyzed.

***Keywords*—**Aircraft Wing, Fluid-Structure Interaction, Stress, Strain, Deformation.

Morteza Raki is with the Concordia University, Canada (e-mail: raki.morteza@hotmail.com).

Numerical Investigation of a Biomagnetic Fluid in a Stenosed Bifurcated Artery with and without Elastic Behavior

M. Adnan Anwar, Kaleem Iqbal, Mudassar Razzaq

***Abstract*—** In recent years, fluid-structure interaction (FSI) analysis has generated tremendous interest in interdisciplinary sciences problems. With the advancement of computational capabilities, solving a large problem becoming more and more feasible and efficient. In this numerical study, the idea is to model the incompressible Newtonian blood flow passing through an asymmetric stenosed bifurcated artery in the presence of a non-uniform magnetic field. The Biomagnetic Fluid Dynamics (BFD) model describes both magnetization and electrical conductivity of blood. A monolithic Arbitrary Lagrangian-Eulerian (ALE) formulation is used by two-way fluid-structure interaction coupling. A stable P2-P1 finite element pair is employed to approximate the velocity and pressure spaces independently for discretization. The resulting nonlinear algebraic system is linearized by implementing Newton's procedure. A comparative analysis is made for the elastic walls and rigid walls in comparison with the velocity magnitude, pressure fields, wall shear stress in a stenosed bifurcated artery. A comparable difference is plotted in velocity and wall shear stresses. The results show that the elastic behavior of the wall should not be ignored, since it possesses significant importance in hemodynamic studies.

***Keywords*—** arbitrary Lagrangian Eulerian, finite element method, stenosed bifurcated artery, bio magnetic fluid.

M. Adnan Anwar is with the Department of Mathematics, School of Science and Engineering, Lahore University of Management Sciences, Opposite Sector U, DHA, Lahore Cantt., 54792, Pakistan, adnan.anwar@lums.edu.pk

Kaleem Iqbal is with the Department of mathematics, Quaid-i-Azam University, Islamabad, 15320, Islamabad, Pakistan, kaleemiqbal3@gmail.com

Mudassar Razzaq is with the Department of Mathematics, School of Science and Engineering, Lahore University of Management Sciences, Opposite Sector U, DHA, Lahore Cantt., 54792, Pakistan, mudassar.razzaq@lums.edu.pk

Vulnerability Analysis for Risk Zones Boundary Definition to Support a Decision Making Process at CBRNE Operations

Aliaksei Patsekha, Michael Hohenberger, Harald Raupenstrauch

***Abstract*—**An effective emergency response to accidents with chemical, biological, radiological, nuclear, or explosive materials (CBRNE) that represent highly dynamic situations needs immediate actions within limited time, information and resources. The aim of the study is to provide the foundation for division of unsafe area into risk zones according to the impact of hazardous parameters (heat radiation, thermal dose, overpressure, chemical concentrations). A decision on the boundary values for three risk zones is based on the vulnerability analysis that covered a variety of accident scenarios containing the release of a toxic or flammable substance which either evaporates, ignites and/or explodes. Critical values are selected for the boundary definition of the Red, Orange and Yellow risk zones upon the examination of harmful effects that are likely to cause injuries of varying severity to people and different levels of damage to structures. The obtained results provide the basis for creating a comprehensive real-time risk map for a decision support at CBRNE operations.

***Keywords*—**boundary values, CBRNE threats, decision making process, hazardous effects, vulnerability analysis, risk zones

I. Introduction

EMERGENCY response is the stage of the disaster management process that needs immediate actions and attracts the most attention and resources. The way it has been planned and the way the hazardous situation is managed will have a significant influence on post-disaster recovery and future development possibilities [1]. An effective emergency response and evacuation management plans are meant to save people's lives, protect public and private property, keep the environment safe and meet basic human needs after an emergency has occurred.

The CBRNE, natural or human caused threats and accidents are still urgent at present, though they usually do not occur often; however, the civil defense system always has to be ready for a rapid response [2]. The focus of the research is mainly on CBRNE threats and incidents that are caused by the deliberate operation with as well as by the misuse of chemical (C), biological (B), radioactive (R), nuclear (N) materials and explosives (E) (e.g. structural failures, releases of toxic substances, leaks of flammable materials, terrorist attacks, etc.).

CBRNE agents can often cause mass destruction, but this is not necessarily the case despite many of them have the potential to do so. The CBRNE classification based on the time of the incident, the impact magnitude and the availability of the materials [3] proves that CBRNE incidents represent highly dynamic situations where every minute counts and where there is a need for rapid and effective measures to save lives, protect health and stabilize the situation. These actions are in the field of duty of first responders (usually firefighters, police officers, paramedics or emergency medical technicians) for whom operations with CBRNE substances represent an enormous challenge with regard to the decision-making processes. For example, CBRNE accidents oblige emergency personnel to evacuate masses that necessitate the sudden movement of many people. But the work on informing the area residents and providing them with a safety evacuation plan is a far complicated matter and needs both broader and more specific skills than emergency plans normally needed even in the largest buildings. A place for people's relocation from an exposed area should be determined within an adequate vision of the threat evolution, especially in a case of fast-approaching hazards [4]. Or we can mention another difficulty for rescue operations and its phases (e.g. victims' treatment, control or containment of fire and other hazards) when responders should consider the possibility of the site contamination with CBRNE agents that pose an immediate threat to the health and safety of the emergency personnel [5].

The time is another obvious factor which provides additional pressure on decision makers. Though, even in an acute emergency, an assessment, however brief, is needed to ensure that any action undertaken is effective [1]. Usually, in Europe the average response time is between ten and twenty minutes [6]. The opening time span (up to 15-20 min) after the initial hazardous occurrence are considered of paramount importance that results in a situation where emergency personnel have only a few minutes to find the most effective way to limit casualties generated by CBRNE hazards [7], [8]. Accidents such as an ammonium nitrate explosion occurred at the West Fertilizer Company facility in West (Texas, US) on April 17, 2013 where 15 people were killed (12 of them were emergency responders unprepared for an accident of such magnitude), 260 were injured, make clear that a suitable risk assessment is of central importance, especially in the first response phase.

The authors would like to thank the Austrian Federal Ministry of Agricultre, Regions and Tourism and the Austrian Research Promotion Agency (FFG) with their Security Research Program (KIRAS) for the funding support of the ERIMAPS project.

Aliaksei Patsekha, Michael Hohenberger, and Harald Raupenstrauch are with the Montanuniversitaet Leoben, Franz-Josef-Strasse 18, 8700 Leoben (e-mail: aliaksei.patsekha@unileoben.ac.at, michael.hohenberger@unileoben.ac.at, harald.raupenstrauch@unileoben.ac.at).

Summing things up, we can conclude that first responders and their advisors should possess the right qualifications and comprehensive knowledge that is key to managing CBRNE events. The information on propagation of hazardous effects is of a great importance as it is used to define the borders of "risk zones" which determine the behavior and decisions of the emergency personnel.

Within the "ERIMAPS – Real-time risk maps for decision support at CBRNe operations" project, an attempt is made to develop the foundation for creating a comprehensive real-time risk map that will be based on simple impact calculations, available with a minimum of input parameters and reckon with spatial demographic data to provide assistance in a decision making process.

II. Main Part

There are different methods to divide an incident adjacent area to zone types according to their threat rate. For this reason qualitative and quantitative approaches are mainly used [9]-[11]. For the purpose of this work it was decided to make a combined classification for zoning of hazardous areas, according to the values of defined during planned impact modeling characteristics.

A distinctive feature of the carried-out vulnerability analysis is a joint risk-based assessment of hazardous impacts on people on the one hand, and buildings and facilities – on the other. This approach provides an opportunity to consider a wide range of threats which occur in a case of a CBRNE accident in an urban environment.

Hazardous consequences and impact analysis are addressed from the point of the final result of the ERIMAPS project that is to develop the background for creating a software solution for the representation of a real-time risk map and to investigate the applicability of a risk-based assessment of the hazardous area. This includes implementation of a completely new approach to simplify the calculation process of hazardous impacts and linking it with the data from geographic information systems (GIS) as well as atmospheric information. Cross light of this research scope is described in [12], [13] with the main specific feature in using various modeling software to estimate the consequences of a hazardous incident. But generally applied models (CFD, ALOHA, HAMS-GPS, MET, etc.) are not fully suited for the purpose of the project because of their complicity, computational power and time demands, limited access, need in validation or reconfiguration from industrial to the urban environment and so on [14], [15].

Risk zones: Expected output parameters for the vulnerability analysis are decided on the chosen calculation models where hazardous impacts are estimated by heat radiation, thermal dose, overpressure and toxic concentration values. Those to be defined values are used to divide the hazardous area and specify it in certain risk zones which should be presented in a graphic form for more convenient use by emergency personnel during the operation.

It was suggested to implement commonly recommended color scheme for zones marking-out when a hazard is going to reach the defined dangerous level. So the Red – Orange – Yellow colors are used to give some natural feeling of being in an unsafe or risky area.

The 'Red zone' marks the most dangerous area and is the closest to the initial hazardous occurrence (fire, explosion, toxic release). It is in the circumference where fatal injuries and collapsed structures can be expected. The 'Orange zone' is still dangerous, the people there are likely to be hospitalized, but it is rather unlikely that a healthy person gets fatally injured there. However, more vulnerable people are still at risk of dying in this zone. The 'Yellow zone' is primarily dangerous for vulnerable population and risk groups, such as children or people who are unable to flee. But if the evacuation is conducted within a certain time frame, fatalities are unlikely. If necessary, green color could be used to mark clearly safe areas, where no hazardous impacts are expected. General approach to divide a hazardous area into the risk zones considering the resulted impact on people and structures is summarized in Table I.

TABLE I
Approach to the Risk Zone Categorization

Risk zone color	Grade of hazardous impact	
	on people	on structures and buildings
Red	Possibility of fatality	Heavy damage
Orange	Irreversible consequences	Moderate damage
Yellow	Reversible consequences	Minor damage

Hazardous effects: There are three main group effects due to fires, explosions and toxic releases: heat radiation, pressure waves and exposure to toxic substances. Besides the process conditions and source terms, they are dependent on the type and amount of the substance involved and are distance and duration sensitive.

Thermal radiation harmful effects on the human body and structures are the most frequent threats during CBRNE accidents. The impact analysis to identify peoples' vulnerabilities has been primarily conducted to determine the boundary values for the risk zones. Effects of heat radiation and thermal dose were examined to decide these zones specification. During the process, injuries caused by heat radiation and thermal dose (from redness or blister formation on the skin to charring, heat inhalation trauma) and pain limits from the thermal radiation intensity were discussed as well as indirect effects of thermal radiation (effect of clothing, smoke inhalation, structural effects). In Table II the heat radiation and thermal dose critical values to define the risk zones that were adopted considering recommendations [11], [16], [17] are presented.

Thermal radiation intensity of 1.5 kW/m² for the 'Yellow zone' is chosen as a pain threshold value whereas thermal dose here is based on the high probability of getting first degree burns. The limits of 3 kW/m^2 and 200 kJ/m^2 for the 'Orange zone' are set up on the possibility that people there are likely to be hospitalized (onset of serious injury and second degree burns are expected), but lethal outcome for a healthy person is rather unlikely (escape time to avoid serious consequences is about 60 seconds). The heat radiation and thermal dose for the 'Red zone' are for a 1% chance of fatality

(type of injury – third-degree burns) for continuous (up to 90 seconds) exposure. Also specific values of the heat radiation are added in Table II to manage the safety and health of on the scene disaster responders that is critical for obvious reasons [18].

Analysis of thermal radiation harmful effects on structures allowed defining values to corresponding risk zones (Table II). The expected damages were addressed from the point of their possible threat to people in the surroundings and a time span for which they are relevant (e.g. pool and jet fires can last for hours and fireballs and vapor cloud explosions are usually finished within seconds) [16]. So for the 'Red zone' critical heat flux value is compliant with heavy damage to housing (e.g. auto-ignition of textiles and wood) or process equipment. The 'Orange zone' boundaries were decided on the damage type that is related to ignition of surfaces and rupture or other type of failure of structural elements (for exposure durations more than 30 min). Less severe damage level (serious discoloration of the material surfaces, peeling-off of paint and/or substantial deformation of constructional elements) is accepted for the 'Yellow zone'. In addition, it was decided to use a supplementary scale of heat radiation values to anticipate indirect injuries which can occur through structural damage (from distortion of substructure components and glass breakage to plastic melting and fuel ignition) to people who stay indoors or in close proximity to buildings (see "humans (indirect effect)" option in Table II).

TABLE II
CRITICAL VALUES SELECTED FOR THE DEFINITION OF THE RISK ZONES (FOR FIRES AND EXPLOSIONS)

Hazardous parameter	Hazard targets	Zone color		
		Yellow	Orange	Red
Heat radiation [kW/m^2]	- humans	1.5	3	6.3
	- responders (EN469 clothing)	3	4.6 [a]	6.3 [b]
	- responders (EN1486 clothing)	4.6	6.3 [a]	10 [b]
	- structures	2	12	35
	- humans (indirect effect) [c]	2	4	12
Thermal dose [kJ/m^2]	- humans	125	200	375 / 250 [d]
Overpressure [kPa]	- humans	2	5	14
	- structures	3.5	17	35
	- humans (indirect effect) [c]	0.5	5	8

[a]It is possible to perform incident related activities depending on the firefighter's clothing with a maximum time set at 3 min (EN469) and 5 min (EN1486).
[b]It is possible to escape from a heat radiation contour (not allowed to perform incident related activities).
[c]Probability of indirect injuries to people indoors or in direct proximity to buildings or structures.
[d]Thermal dose for exposure to fireballs.

Another assessed scenario of hazardous events is related to explosions. The main direct harmful effect to humans (and surrounding facilities) is the sudden increase in pressure that occurs as a blast wave passes. The most vulnerable human organs are ears and lungs because of their high sensitivity to jump-in pressure (blast lung is the most common fatal injury). Despite there are various consequences of an explosion (pressure waves, missile flight, heat radiation, crater formation, earth shocks) for the differentiation of the risk zones the peak overpressure is used as the key parameter.

According to assumed method of the risk zone categorization, severe damage to structures and housing is present in a case of overpressure more than 35 kPa that provides a threshold value for the 'Red zone' (Table II). Moderate and light damage predefine criteria for the 'Orange' and 'Yellow' zones: 17 and 3.5 kPa, respectively. Similar to heat radiation effects, to consider a possibility of indirect trauma to people indoors due to overpressure, additional values are chosen to cover injuries occurring through damage to window frames, house ceilings, roofs and walls, etc.

Harmful effects of toxic action represent the third group of hazardous consequences during the CBRNE events that are assessed here. The damage degree a toxic chemical can inflict on its surroundings is determined by the toxicity of the material, the duration of exposure and the dose received due to its dispersion. Within the project scope it was decided to focus on the inhalation intoxication and its corresponding effects as the main threat to the majority of people present in the emergency area. The concentration of the substance for which it is still toxic as well the impact duration affects exposure limits. Within the established goals of the project, as we were looking at short-term affecting in emergency cases, AEGLs (Acute Exposure Guideline Levels) and ERPG (Emergency Response Planning Guideline) were under consideration as emergency exposure limits. After conducting the comparative analysis, it was decided to use AEGLs as the focal and more flexible system in terms of exposure duration to define the risk zones.

Three threshold limit values in the AEGLs represent a different degree of toxic effects severity for five relatively short exposure periods – 10 min, 30 min, 1 hour, 4 hours, and 8 hours. These exposure levels are applicable to all members of the general population, including susceptible individuals. The following risk zone categorization based on AEGLs and corresponding severity of the toxic effects is accepted. Level 1 of AEGL is used for the 'Yellow' risk zone when notable discomfort, irritation, certain asymptomatic non-sensory effects are the main characteristic features. Irreversible or other serious, long lasting adverse health effects or an impaired ability to escape can be used for the description of the 'Orange zone' according to AEGL 2. Level 3 – for the 'Red zone' – is a case of life threatening health effects or death.

TABLE III
AEGLS VALUES FOR A SELECTION OF INDUSTRIAL TOXIC GASES

Gas	Risk zone color	AEGLs	Concentration [ppm] for the exposure period of				
			10 min	30 min	1 hour	4 hours	8 hours
Ammonia	Yellow	AEGL 1	30	30	30	30	30
	Orange	AEGL 2	220	220	160	110	110
	Red	AEGL 3	2700	1600	1100	550	390
Chlorine	Yellow	AEGL 1	0.50	0.50	0.50	0.50	0.50
	Orange	AEGL 2	2.8	2.8	2.0	1.0	0.71
	Red	AEGL 3	50	28	20	10	7.1

Individual AEGLs values for two of many major industrial gases that represent a toxic hazard through their manufacture, storage and transporting are given in Table III [19].

In terms of the research goals, AEGLs values for the exposure duration from 10 min to 1 hour are of great interest as they present useful information for first responders who should decide on immediate actions to deal with such dangerous situations like a release of toxic chemicals.

III. Conclusion

Following a disaster, initial assessments should be rapid and provide the information required to start an appropriate response aimed to save lives, protect health and stabilize the situation. Hazards definition plays the main part in this process. Several scenarios of CBRNE events which are related to the fire and/or explosion incidents or toxic releases are applied as a basis for main threats and hazard identification. Possible consequences due to the occurring heat radiation, blast wave and toxicity for people and facilities are used for the risk zones categorization. More specifically, the boundary values for these zones are based on the people's injury severity and the level of damage to structures or buildings.

The obtained results in the short-term in combination with data from geographic information systems provide necessary conditions for creating the injury pattern catalog and developing a building classification to support hazards impact assessment over the course of a CBRNE accident.

On a wider scale, the conducted research provides the foundation to develop a real-time risk map for decision support system during the CBRNE operations especially if an emergency occurs in an urban environment. A distinctive feature of the proposed approach is a multilayered map that covers different kinds of risks to humans and building structures which would definitely help to answer the central question from the ERIMAPS project: "What happens in an event in the next few minutes, who and how many will be affected, where is the focus and what resources are required?".

Acknowledgment

The ERIMAPS project is a cooperation between Montanuniversitaet Leoben, Die Johanniter Austria, the Austrian Federal Ministry of Defence, the Professional Fire Brigade Graz, the Professional Fire Brigade Vienna and Flammpunkt GmbH.

References

[1] Emergency response - World Health Organization. Available from https://www.who.int/water_sanitation_health/hygiene/emergencies/em2002chap4.pdf, accessed 01 March 2020.

[2] A. Baums, Response to CBRNE and human-caused accidents by using land and air robots. Automatic Control and Computer Sciences, 51(6) (2017) 410–416.

[3] CBRNE Health Information Resources - Section 1: Introduction to CBRNE Concepts. Available from https://www.nlm.nih.gov/dis_courses/cbrne/01-000.html, accessed 01 March 2020.

[4] S. Marsella, N. Sciarretta, CBRN Events and Mass Evacuation Planning. Enhancing CBRNE Safety & Security: Proceedings of the SICC 2017 Conference, (2018) 353–363.

[5] Introduction to CBRNE Terrorism: An Awareness Primer and Preparedness Guide for Emergency Responders. Available from http://jumpjet.info/Emergency-Preparedness/Disaster-Mitigation/NBC/Introduction_to_CBRNE_Terrorism.pdf, accessed 02 March 2020.

[6] Oesterreichisches Rotes Kreuz, Rahmenvorschrift Rettungsdienst, 226. Praesidentenkonferenz, 2014

[7] J.-L. Vincent, E. Abraham, P. Kochanek, F.A. Moore, M.P. Fink, Textbook of Critical Care, seventh ed., Elsevier - Health Sciences Division, Philadelphia, United States, 2017.

[8] Initial operational response to a CBRN incident. Available from https://www.jesip.org.uk/uploads/media/pdf/CBRN%20JOPs/IOR_Guidance_V2_July_2015.pdf, accessed 03 March 2020.

[9] G.G. Noll, M.S. Hildebrand, G.D. Rudner, R. Schnepp, Hazardous materials: Managing the incident, fourth ed., Jones & Bartlett Learning, Burlington, MA, 2019.

[10] C.J.H. van den Bosch, R.A.P.M. Weterings (Eds.), Methods for the calculation of physical effects: due to releases of hazardous materials (liquids and gases) ('Yellow Book'), third ed., Committee for the Prevention of Disasters, The Hague, 2005.

[11] U. Hauptmanns, Process and Plant Safety, Springer Berlin Heidelberg, 2014.

[12] B. Yoo, S.D. Choi, Emergency Evacuation Plan for Hazardous Chemicals Leakage Accidents Using GIS-based Risk Analysis Techniques in South Korea. International Journal of Environmental Research and Public Health, 16(11) (2019) 1948.

[13] Y. Ghajari, A. Alesheikh, M. Modiri, R. Hosnavi, M. Abbasi, Spatial Modelling of Urban Physical Vulnerability to Explosion Hazards Using GIS and Fuzzy MCDA. Sustainability, 9(7) (2017) 1274.

[14] J. Burman, L. Jonsson, Issues when linking computational fluid dynamics for urban modeling to toxic load models: The need for further research. Atmospheric Environment, 104 (2015) 112–124.

[15] M. Ciccotti, F. Spagnolo, M. Palmery, Safety in the Transport of Hazardous Substances in Residential Areas: Cases of the Release of TIC (Chlorine, Propane, and Butane) at Low Temperatures. Enhancing CBRNE Safety & Security: Proceedings of the SICC 2017 Conference, (2018) 71–79.

[16] C.J.H. van den Bosch, L. Twilt, R.A.P.M. Weterings, et al., Methods for the determination of possible damage to people and objects resulting from releases of hazardous materials (Green Book), thirst ed., Committee for the Prevention of Disasters, Den Haag, 1992.

[17] S. Mannan (Ed.), Lees' Loss Prevention in the Process Industries, Hazard Identification, Assessment and Control, fourth ed., Elsevier, Amsterdam, 2012.

[18] Maximum allowable exposure to different heat radiation levels. Available from http://content.publicatiereeksgevaarlijkestoffen.nl/documents/PGS29/Raport%20IFV_20160509_Heat_radiation_contours_final.pdf, accessed 05 February 2020.

[19] Access Acute Exposure Guideline Levels (AEGLs) Values. Available from https://www.epa.gov/aegl/access-acute-exposure-guideline-levels-aegls-values, accessed 12 February 2020.

Miniaturized Wideband Single-Feed Patch Antenna for C-Band Applications

Abdelheq Boukarkar, Omar Guermoua

***Abstract*—**In this paper, we propose a miniaturized and wideband patch antenna for C-band applications. The antenna miniaturization is obtained by loading shorting vias along one patch edge. At the same time, the wideband performance is achieved by combining two resonances using one feed line. The measured results reveal that the antenna covers the frequency band 4.32 GHz to 6.52 GHz (41%) with a peak gain and a peak efficiency of 5.5 dBi and 87%, respectively. The antenna occupies a relatively small size of only 26 x 22 x 5.6 mm^3, making it suitable for compact wireless devices requiring a stable unidirectional gain over a wide frequency range.

***Keywords*—** Miniaturized antennas, patch antennas, stable gain, wideband antennas.

I. Introduction

IN recent years, the need for designing small size radio frequency (RF) devices is increasing significantly. Indeed, modern wireless systems require antennas with lightweight, low profile, and low cost that can be integrated into the RF front end easily. Patch antennas are attractive candidates as they meet the requirements mentioned above. However, in some wireless applications, a conventional patch antenna may not be suitable due to its narrow impedance bandwidth of less than 5% in most cases. Hence, bandwidth enhancement is needed under the constraints of maintaining a compact size and a stable gain with unidirectional radiation patterns.

Several works targeting bandwidth enhancement of patch antennas have been proposed [1]–[15]. The common method of improving the working bandwidth consists of introducing slots adequately into the antenna structure [1]–[7]. By controlling the shape and the position of the slots, different resonant modes can be excited and combined accordingly to widen the working bandwidth. An illustrative example is demonstrated in [2], where a V-shaped slot is etched on the radiating triangular patch to enhance the impedance bandwidth. In this design, an additional resonant mode TM_{11} is generated by the insertion of the V-shaped slot. Another approach of bandwidth enhancement exploits the coupling between the main radiating element and some parasitic strips or patches [8] –[12]. For instance, in [8], two additional resonances are obtained by introducing multiple parasitic patches which are placed carefully near a radiating triangular element. By adopting this technique, a considerable improvement of the working bandwidth is realized (about 13.8% evaluated at 10 dB of return loss). Metamaterials can also be used to broaden the working bandwidth, as illustrated in [13]–[15]. For instance, in [13], a metamaterial-based rectangular patch antenna with wideband performance is obtained by manipulating the structure and the position of an additional metasurface. The antenna's impedance bandwidth is enhanced clearly as it reaches 36%.

In this paper, the proposed approach consists of combining two resonances from two shorted radiating patches. Shorting vias are loaded carefully along one radiating edge for antenna miniaturization. The radiating elements are fed concurrently for more antenna compactness. The operating frequencies are controlled easily by adjusting the length of the patches. The proposed antenna realizes a comparatively wide operating bandwidth of 41% on a relatively small platform of 26 x 22 x 5.6 mm^3. The antenna can be employed in c-band applications, for instance, in Worldwide Interoperability for Microwave Access (WiMAX), working around 5.8 GHz.

The paper is organized as follows. In Section II, the antenna design guidelines, including the working mechanism, are provided. In Section III, the simulated and measured results, as well as a comparison study with some recent works, are given. The conclusion of this work is drawn in Section IV.

II. Antenna Geometry and Design Guidelines

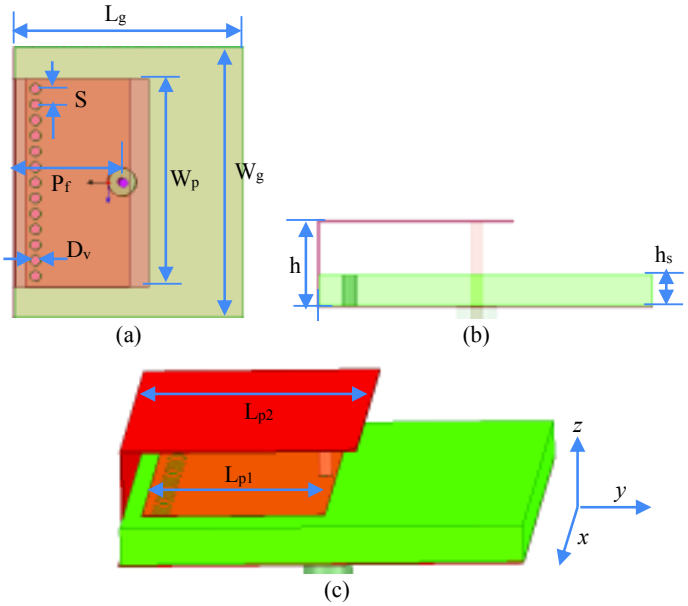

Fig. 1 Structure of the proposed antenna; (a) top view (b) side view, (c) perspective view

A. Boukarkar and O. Guermoua are with École Supérieure Ali CHABATI, Algiers, 16000, Algeria (corresponding author, phone: +213666570816; email: abdelheq.boukarkar@gmail.com).

TABLE I
ANTENNA DIMENSIONS

Parameter	W_g	L_g	L_{p1}	L_{p2}	h	h_s	W_p	P_f	D_v	S
Value (mm)	26	22	10	12.8	5.6	2	20	10.5	1	1.5

The structure of the proposed antenna is shown in Fig. 1, and its dimensions are depicted in Table I. The antenna consists of two radiating patches. The first radiating patch is printed on the F4B substrate with a thickness of h_s=2 mm, a relative permittivity of ε_r=2.65, and a loss tangent of 0.002. Metalized vias are loaded onto one radiating edge to reduce the patch's length by approximately a half. At the same time, a sheet of copper is bent and soldered adequately to the antenna's ground plane to form the second radiating patch. The two patches are fed simultaneously using a probe feed coaxial cable. The position of the probe feed P_f controls the bandwidth impedance. The lengths of the patches L_{p1} and L_{p2} are evaluated using the following equations:

$$L_{p1} = \frac{\lambda_{g_1}}{4} + h_s \quad (1)$$

$$\lambda_{g_1} \approx \frac{c}{f_1\sqrt{\varepsilon_r}} \quad (2)$$

$$L_{p2} = \frac{\lambda_{g_2}}{4} + h \quad (3)$$

$$\lambda_{g_2} \approx \frac{c}{f_2\sqrt{\varepsilon_r}} \quad (4)$$

where λ_{g1} and λ_{g2} are the guided wavelengths corresponding to the operating frequencies f_1 and f_2, respectively. The antenna resonances are combined adequately to broaden the impedance bandwidth. The antenna working frequencies are chosen arbitrarily to cover some C-band applications. Indeed, one can easily select the working bandwidth by adjusting the length of the two patches L_{p1} and L_{p2}.

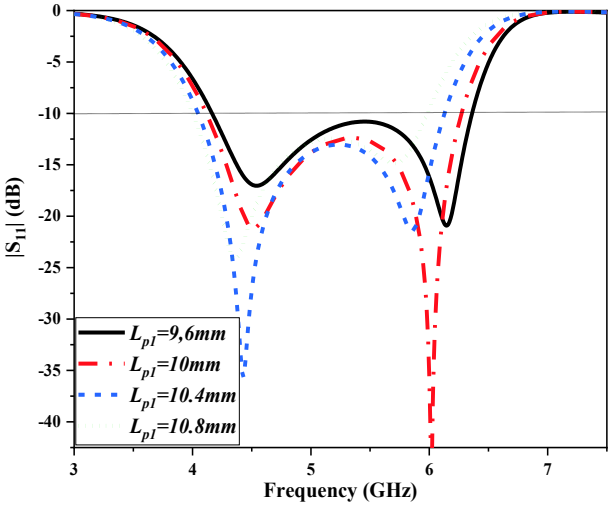

Fig. 2 The simulated reflection coefficient |S11| when the length of the patch L_{p1} is tuned

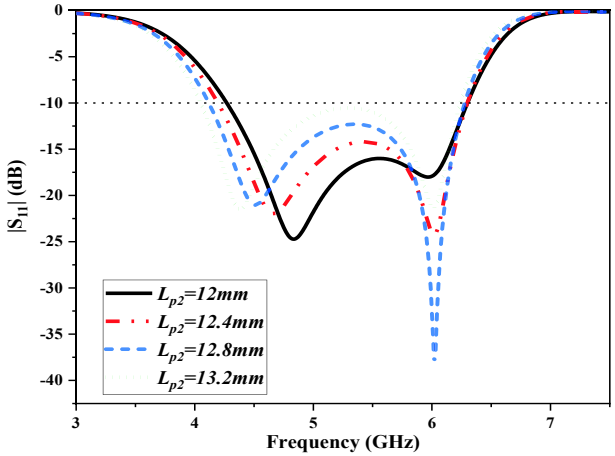

Fig. 3 The simulated reflection coefficient |S11| when the length of the patch L_{p2} is tuned

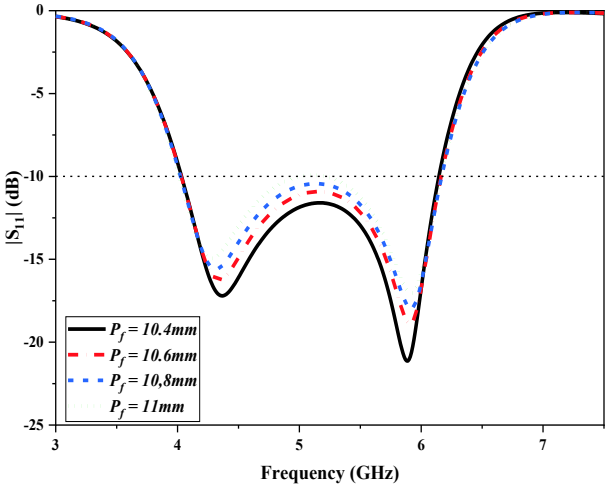

Fig. 4 The simulated reflection coefficient |S11|when the position of the feed point P_f is tuned

To understand more the working mechanism and the design guidelines, three parametric studies are performed using High-Frequency Structure Simulator (HFSS) software. The first parametric study investigates the effects of tuning the patch's length L_{p1} on the resonant frequencies. We note that the lower operating frequency remains stable during the tuning of L_{p1}, as shown in Fig. 2. Similarly, we have concluded from the second parametric study that the lower operating frequency can be controlled by adjusting the length L_{p2} without affecting much the upper resonance. The corresponding reflection coefficient |S11| is shown in Fig. 3. The last parametric study deals with the position of the feed line P_f. Indeed, the antenna impedance matching is ensured easily by selecting an adequate feed position P_f as demonstrated in Fig. 4. The current distribution, at the lower and the upper resonant frequencies, is given in Fig. 5. We note that each patch can be excited separately. To validate the proposed approach, an antenna prototype is fabricated and tested. The next section is devoted to the simulation and measurement results.

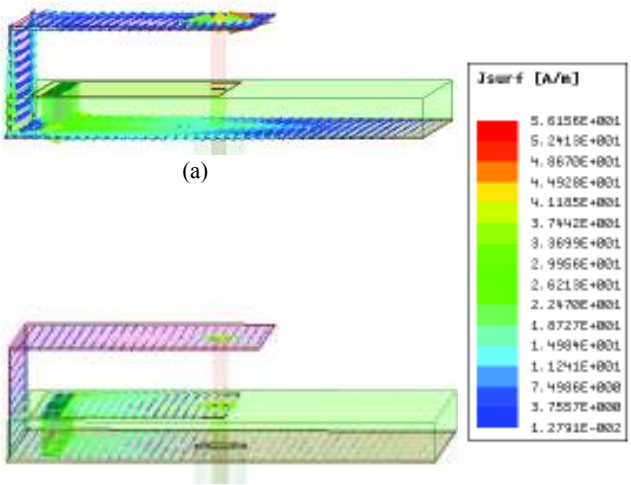

(a)

(b)

Fig. 5 The current distribution at the resonant frequencies; (a) f_1 = 4.2 GHz, (b) f_2 = 6.2 GHz

III. Simulated and Measured Results

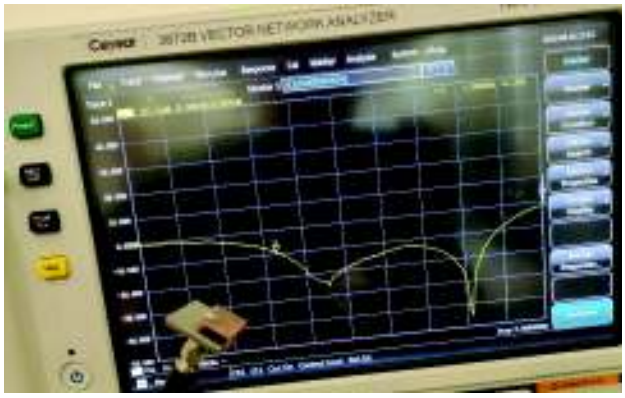

Fig. 6 Photograph of the antenna with the $|S_{11}|$ measurement setup

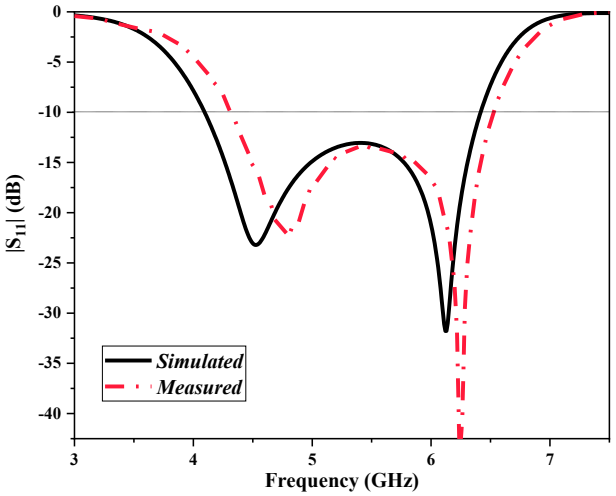

Fig. 7 The simulated and measured reflection coefficient $|S_{11}|$

The photograph of the fabricated antenna with the $|S_{11}|$ measurement setup is shown in Fig. 6. The second radiating patched formed by the copper sheet is soldered carefully to the antenna's ground plane. The antenna reflection coefficient is measured using a 3672B vector network analyzer. The simulated and measured $|S_{11}|$ is shown in Fig. 7.

The measured results reveal that the antenna covers the operating band 4.32 GHz to 6.65 GHz with a good impedance matching. The small discrepancies between the simulated and measured results are attributed mainly to the measurement setup and fabrication tolerances. The antenna radiation patterns are obtained in SATIMO anechoic chamber. The radiation patterns measurement setup is shown in Fig. 8.

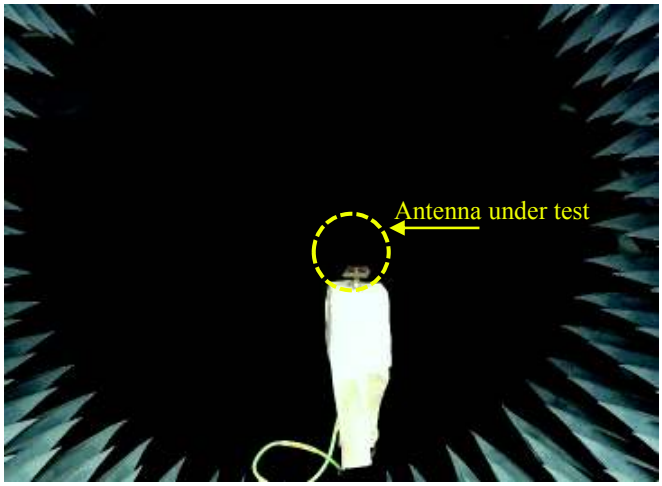

Fig. 8 The radiation pattern measurement setup

To demonstrate the stability of the patterns, three frequency samples are selected. The frequency points correspond to the lower, the middle, and the upper limit of the operating bandwidth. The simulated and measured patterns at f_L=4.32 GHz, f_m=5.42 GHz, and f_u=6.52 GHz are compared in Fig. 9. We note that, in all the cases, the simulated and measured results agree well. The measured gains and efficiencies vary from 4.3 dBi to 5.5 dBi and 82% to 87%, respectively. To highlight the contributions made in this paper, a comparison study with some recently published papers is displayed in Table II. The antennas' sizes, operating frequencies, bandwidths, average gains, efficiencies, and the used approaches are provided. The design in [7] realizes a comparatively wide bandwidth of 52.7% with an average gain of 6 dBi. In comparison, the proposed design has a slightly smaller size. The antenna presented in [9] occupies a larger area with comparatively higher gain and 20.1% of impedance bandwidth. In [15], the antenna has a compact size; however, its impedance bandwidth is relatively low. One can note the trade-off between antenna profile and the working bandwidth. The larger the profile is, the wider the impedance bandwidth.

The proposed antenna exhibits acceptable performance in terms of overall size, operating bandwidth, and average gain. In current wireless systems, compact RF components are highly recommended. As the proposed design is small, it can be used to form an antenna array.

TABLE II
COMPARISON STUDY

Reference	[7]	[9]	[15]	**Proposed**
Size (λ_0)	0.52 x 0.35 x 0.06	1.09 x 1.09 x 0.03	0.36 x 0.36 x 0.04	0.37 x 0.31 x 0.08
Frequencies (GHz)	1.62–2.78	2.19–2.68	5.31–5.92	4.67–5.84
Bandwidth (%)	52.7	20.1	10.86	41%
Average gain (dBi)	6	9.5	4.17	5
Average efficiency (%)	N.M*	88	72	85
Approach	Etching slots	Parasitic patches	Metamaterials loading	Stacked shorted patches

- We note that λ_0 is the free-space wavelength evaluated at the lower limit of the working bandwidth.
- * N.M: Not Mentioned.

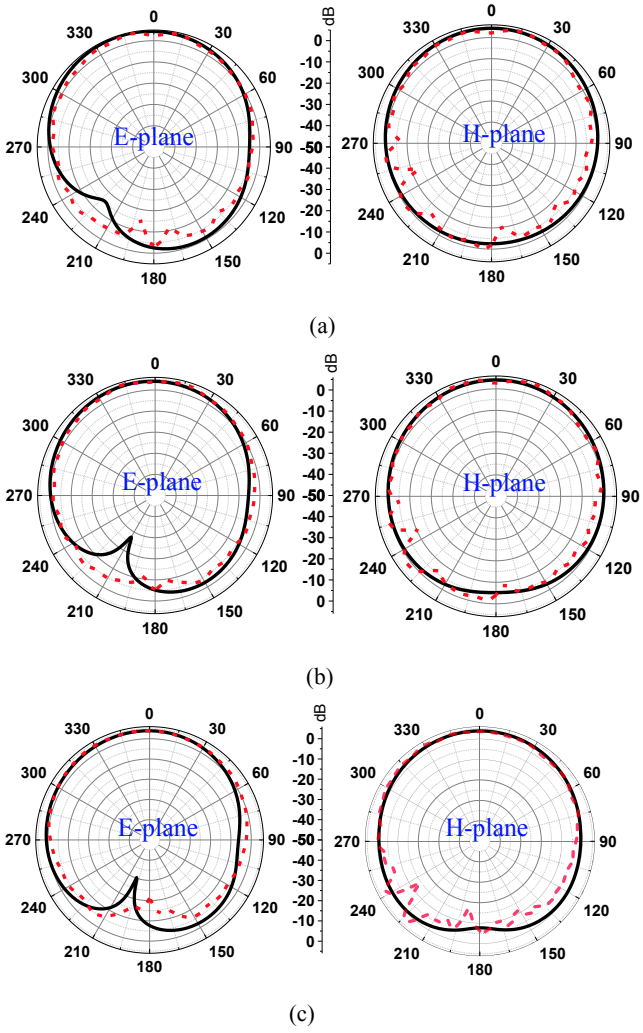

(a)

(b)

(c)

Fig. 9 The simulated and measured radiation pattern (sold line: simulated, dashed line: measured); (a) f_L=4.32 GHz, (b) f_m=5.42 GHz, (c) f_u=6.52 GHz

IV. CONCLUSION

In this paper, a simple design of a miniaturized patch antenna with wideband performance is achieved. The two operating frequencies are combined and controlled easily by adjusting the corresponding patch lengths L_{p1} and L_{p2}. The antenna exhibits comparatively acceptable performances in terms of operating bandwidth, gain, and efficiency with a miniaturized size of only 25 x 25 x 6.2 mm^3. As a suggestion for future work, the proposed design may be used as an antenna element of a miniaturized phased array antenna covering some C-band applications.

REFERENCES

[1] M. Min and L. Guo, "Design of a Wideband Single-Layer Reflectarray Antenna Using Slotted Rectangular Patch With Concave Arms," IEEE Access, vol. 7, pp. 176197-176203, 2019.

[2] H. Wong, K. K. So and X. Gao, "Bandwidth Enhancement of a Monopolar Patch Antenna With V-Shaped Slot for Car-to-Car and WLAN Communications," IEEE Transactions on Vehicular Technology, vol. 65, no. 3, pp. 1130-1136, March 2016.

[3] N. Liu, L. Zhu and W. Choi, "A Low-Profile Wide-Bandwidth Planar Inverted-F Antenna Under Dual Resonances: Principle and Design Approach," IEEE Transactions on Antennas and Propagation, vol. 65, no. 10, pp. 5019-5025, Oct. 2017.

[4] A. Bekasiewicz and S. Koziel, "Cost-Efficient Design Optimization of Compact Patch Antennas With Improved Bandwidth," IEEE Antennas and Wireless Propagation Letters, vol. 15, pp. 270-273, 2016.

[5] T. F. A. Nayna, F. Ahmed and E. Haque, "Bandwidth enhancement of a rectangular patch antenna in X band by introducing diamond shaped slot and ring in patch and defected ground structure," 2017 International Conference on Wireless Communications, Signal Processing and Networking (WiSPNET), Chennai, 2017, pp. 2512-2516.

[6] N. Liu, L. Zhu and W. Choi, "A Differential-Fed Microstrip Patch Antenna With Bandwidth Enhancement Under Operation of TM10 and TM30 Modes," IEEE Transactions on Antennas and Propagation, vol. 65, no. 4, pp. 1607-1614, April 2017.

[7] W. An, X. Wang, H. Fu, J. Ma, X. Huang and B. Feng, "Low-Profile Wideband Slot-Loaded Patch Antenna With Multiresonant Modes," in IEEE Antennas and Wireless Propagation Letters, vol. 17, no. 7, pp. 1309-1313, July 2018.

[8] K. D. Xu, H. Xu, Y. Liu, J. Li and Q. H. Liu, "Microstrip Patch Antennas With Multiple Parasitic Patches and Shorting Vias for Bandwidth Enhancement," IEEE Access, vol. 6, pp. 11624-11633, 2018.

[9] D. Yang, H. Zhai, C. Guo and H. Li, "A Compact Single-Layer Wideband Microstrip Antenna With Filtering Performance," IEEE Antennas and Wireless Propagation Letters, vol. 19, no. 5, pp. 801-805, May 2020.

[10] Z. Liang, J. Liu, Y. Zhang and Y. Long, "A Novel Microstrip Quasi Yagi Array Antenna With Annular Sector Directors," IEEE Transactions on Antennas and Propagation, vol. 63, no. 10, pp. 4524-4529, Oct. 2015.

[11] J. Wu, Y. Yin, Z. Wang and R. Lian, "Broadband Circularly Polarized Patch Antenna With Parasitic Strips," IEEE Antennas and Wireless Propagation Letters, vol. 14, pp. 559-562, 2015.

[12] J. Zhang, L. Zhu, Q. Wu, N. Liu and W. Wu, "A Compact Microstrip-Fed Patch Antenna With Enhanced Bandwidth and Harmonic Suppression," IEEE Transactions on Antennas and Propagation, vol. 64, no. 12, pp. 5030-5037, Dec. 2016.

[13] N. Nasimuddin, Z. N. Chen and X. Qing, "Bandwidth Enhancement of a Single-Feed Circularly Polarized Antenna Using a Metasurface: Metamaterial-based wideband CP rectangular microstrip antenna.," in IEEE Antennas and Propagation Magazine, vol. 58, no. 2, pp. 39-46, April 2016.

[14] S. Ahdi Rezaeieh, M. A. Antoniades and A. M. Abbosh, "Gain Enhancement of Wideband Metamaterial-Loaded Loop Antenna With Tightly Coupled Arc-Shaped Directors," IEEE Transactions on Antennas and Propagation, vol. 65, no. 4, pp. 2090-2095, April 2017.

[15] M. Ameen and R. K. Chaudhary, "Metamaterial-based circularly polarised antenna employing ENG-TL with enhanced bandwidth for WLAN applications," Electronics Letters, vol. 54, no. 20, pp. 1152-1154, 2018.

A Study on Kinetic of Nitrous Oxide Catalytic Decomposition over CuO/HZSM-5

Y. J. Song, Q. S. Xu, X. C. Wang, H. Wang, C. Q. Li

***Abstract*—**The catalyst of copper oxide loaded on HZSM-5 was developed for nitrous oxide (N_2O) direct decomposition. The kinetic of nitrous oxide decomposition was studied for CuO/HZSM-5 catalyst prepared by incipient wetness impregnation method. The external and internal diffusion of catalytic reaction were considered in the investigation. Experiment results indicated that the external diffusion was basically eliminated when the reaction gas mixture GHSV was higher than $9000h^{-1}$ and the influence of the internal diffusion was negligible when the particle size of the catalyst CuO/HZSM-5 was small than 40-60 mesh. The experiment results showed that the kinetic of catalytic decomposition of N_2O was a first-order reaction and the activation energy and the pre-factor of the kinetic equation were 115.15kJ/mol and of 1.6×10^9, respectively.

***Keywords*—**Catalytic decomposition, CuO/HZSM-5, kinetic, nitrous oxide.

Y. J. Song is with the Beijing Institute of Petrochemical Technology, Beijing 102617, CHINA (phone: 86-10-81292038; e-mail: songyongji@bipt.edu.cn).

Q. S. Xu is with the Beijing Institute of Petrochemical Technology, Beijing 102617, CHINA (e-mail: xuqingsheng@bipt.edu.cn).

X. C. Wang is with the Beijing Institute of Petrochemical Technology, Beijing 102617, CHINA (e-mail: wangxincheng@bipt.edu.cn).

H. Wang is with the Beijing Institute of Petrochemical Technology, Beijing 102617, CHINA (e-mail: wanghong@bipt.edu.cn).

C. Q. Li is with the Beijing Institute of Petrochemical Technology, Beijing 102617, CHINA (e-mail: Licuiqing@bipt.edu.cn).

Structuring of Multilayer Aluminum Nickel by Lift-Off Process using Cheap Negative Resist

[1,*] Asghar. Muhammad Talal

***Abstract*—** Lift-Off technique of the photoresist for metal patterning in integrated circuit (IC) packaging has been widely utilized in the field of microelectromechanical systems and semiconductor component manufacturing. The main advantage lies in cost-saving, reduction in complexity, and maturity of the process. The selection of photoresist depends upon many factors such as cost, thickness of the resist, comfortable and valuable parameters extraction. In the present study, an extremely cheap dry film photoresist E8015 of thickness 38-micrometer is processed for the first time for edge profiling, according to author´s best knowledge. Successful extraction of the helpful parameter range for resist processing is performed. An undercut angle of 66 to 73 degrees is realized by parameter variation like exposure energy and development time. Finally, 10-micrometer thick metallic multilayer aluminum nickel is lifted off on the plain silicon wafer. Possible applications lie in controlled self-propagating reactions within structured metallic multilayer that may be utilized for IC packaging in the future.

***Keywords*—** Lift-Off, IC packaging, Photoresist, Multilayer

I. Introduction

The metal lift-off process is a convenient and straightforward method of patterning structures of alternating thicknesses. The structures can be of varying thicknesses depending upon the edge profile obtained [1]. In the lift-off process, it is generally said that the feature size is dependent upon the initial photoresist thickness. With a thick layer of the photoresist, higher is the multilayer feature size that can be realized at the end of the process. One can expect higher aspect ratio copper pillars, solder balls, and metal-glass nanotubes [2].

Additionally, step coverage during the structuring process is another crucial factor determining the success of the lift-off process, and that is associated with the deposition technique. Inadequate step coverage due to directional deposition during the electron beam deposition is beneficial for the lift-off, whereas a complete step coverage due to sputtering leads to poor metal lift-off [3]. The double-layer photoresist technique has been utilized to overcome problems associated with the lift-off. However, this method has drawbacks like individual resist chemical compatibility to resist remover, interlayer sliding, and poor adhesion [4]. So, by the general rule that for a thicker photoresist, one can expect final metallization structures to be thicker. But for this, a good photoresist undercut is required to form a discontinuous metal layer. And if it can be achieved, then thicker multilayer structures can be structured. This stands as a hypothesis of this research work.

Muhammad Talal Asghar is with the Technical University of Ilmenau, Germany (e-mail: talal.asghar@tu-ilmenau.de).

II. Method and Materials

The photoresist under consideration is dry resist E8015 from the laminar series registered under the trademark of eternal technology corporation. It is formulated as a negative tone photoresist based on the acid-catalyzed thermal cross-linking when exposed to the i-line exposure. Physically, it consists of 3 layers with a photoactive layer in the center and a mylar protective sheet on the top and bottom. Former applications of this photoresist lie in print and etch, tent and etch, and plating process during printed circuit board manufacturing.

Fig. 1 Structure of photoresist E8015

Due to the first-ever investigation for the lithography process on this photoresist, it was evident to investigate multiple parameters for the conclusive determination of optimum parameter range. Important parameters include lamination temperature, exposure energy, development time, HMDS (Hexa-methyl disilicate) application, pre-exposure heating, post-exposure heating.

A. Lamination

A dry photoresist coating process is complicated compared to a liquid photoresist that requires a mature spin coating technique [5]. Nitrogen bubble production during the lamination and the adhesivity in between silicon wafer and dry film photoresist are important factors determining the success of lamination.

Wafers cleaned using the piranha solution (H_2O_2: H_2SO_4) in ratio 1:5 and hexamethyldisilazane (HMDS) applied were passed through GBC 3500 laminator at various speeds. The lamination speed levels were preset by the laminator. Before the lamination process, the top protective layer is removed from the resist and the bottom one is removed after the exposure, leaving behind the photoactive layer ready for development.

Fig. 2 GBC 3500 dry film laminator

B. Exposure and Development

The experimental matrix was designed based upon the information processed from the photoresist datasheet and maximum interplay of exposure energy and development time as presented in TABLE I. The exposure energy was changed through the entire spectrum from high dosage to low dosage against the development time for the accurate determination of optimum parameters and their following effects.

TABLE I: EXPERIMENTAL MATRIX

Exposure Energy (mJ/cm²)	Development Time (minutes)			
35	04:00	04:30	05:00	05:30
45	04:00	04:30	05:00	05:30
55	04:00	04:30	05:00	05:30
70	04:00	04:30	05:00	05:30
120	04:00	04:30	05:00	05:30
160	04:00	04:30	05:00	05:30
380	04:00	04:30	05:00	05:30
450	04:00	04:30	05:00	05:30
520	04:00	04:30	05:00	05:30

Glass mask containing various structures was selected for exposure using an i-liner MA8 (Mask aligner). The selection of the mask aligner was made based on the availability of the equipment. Projection mode method was employed. It was convenient because of the reason that in contact mode, the mask may get attached to the photoresist that is disadvantageous to the lift-off process. Development was performed using the Na_2CO_3 solution of 5 % concentration, followed by water rinsing and N_2 gas drying. Visual inspection of the resist after the development is performed to check for the possible sign of delamination of the photoresist.

Fig. 3 Dark field mask

C. Wafer Sectioning

For evaluating the edge profile, the wafers were sectioned with the diamond tool along crystal planes. The sectioned samples, almost 100 mm x 4 mm were then placed inside a holder and inspected with the optical microscope (Zeiss – AXIOTECH HAL 100) and scanning electron microscope (Hitachi S-4800) in cross-sectional view. Necessary undercut and straight photoresist profile studies were performed.

Fig. 4 Wafer sectioning

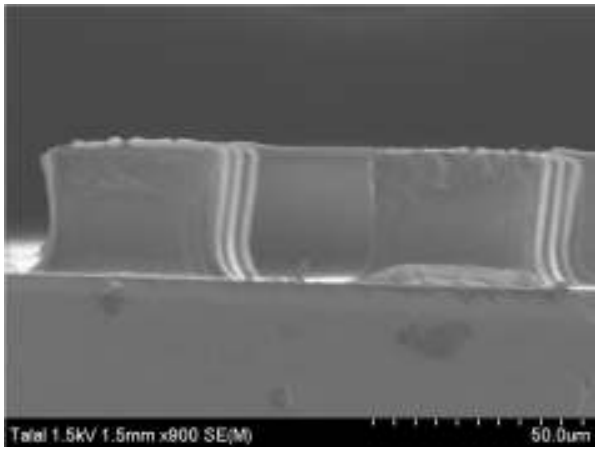

Fig. 5 Resist after exposure

D. Sputtering

10-micrometer thick magnetron sputtered Al/Ni reactive multilayer with an individual bilayer thickness of 20 nanometers was deposited on the sectioned wafer samples. Microscopic characterization using the optical microscope was performed for the top view image processing.

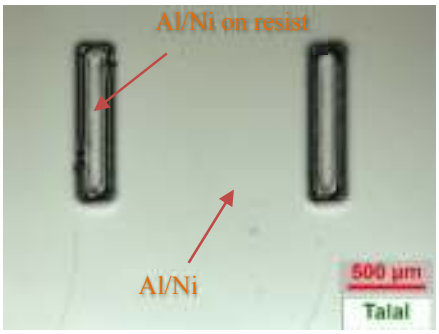

Fig. 6 Top view image of reactive multilayer deposited on wafer

For the resist removal, samples were placed inside intelligent fluid "SH5" at 65 °C for 3 hours, followed by the isopropyl alcohol rinse for 30 seconds and quick damp rinse in water for 3 minutes. Then the residuals were removed with technistrip P1316 at 60 °C for 30 minutes, followed by the water rinsing for 3 minutes in the quick damp rinse.

III. Results and Discussion

A. Optimum Conditions

Silicon wafer with hexamethyldisilazane (HMDS) application and lamination temperature of 120 °C and speed 2 exhibited good lamination. Bubbling due to nitrogen outgassing that is usually observed in thick resist was limited to a minimum. At a lower speed level due to excessive heating, resist was destroyed, leading to delamination as illustrated in Fig. 7. Whereas at higher speed, it was difficult to handle the lamination process leading to poor adhesion.

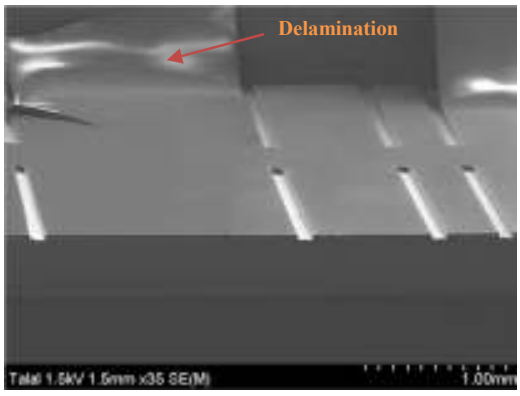

Fig. 7 Delamination of resist

B. Undercut

At exposure energy of 35 mJ/cm^2 with a development time of 5:30 minutes and exposure energy of 45 mJ/cm^2 with a development time of 5:00 minutes, an undercut angle of 66 to 77 degrees is realized as illustrated in Fig. 8 and Fig. 9.

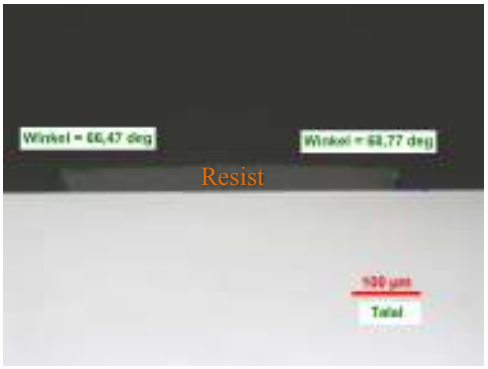

Fig. 8 Exposure energy: 35 mJ/cm^2, Development time: 5:30 minutes

Fig. 9 Exposure energy: 45 mJ/cm^2, Development time: 5:00 minutes

C. Straight Profile

Experimental matrix designed concluded in results depicting the overall performance of resist. In addition to the undercut profile that was necessary for lift-off of multilayer, resist exhibited straight profile at multiple parameter combinations. Initial experiments moved from high exposure energy of 520 mJ/cm^2 to 55 mJ/cm^2. A straight photoresist profile with an almost 90-degree angle was realized at all these parameter ranges, as illustrated in Fig. 10.

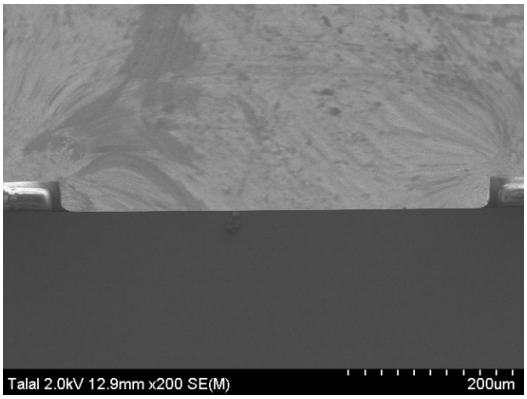

Fig. 10 Straight edge profile

D.Lift-Off

Magnetron sputtered Al/Ni reactive layers on top of resist were removed due to lift-off during the stripping of resist. Lift-off was successful in the case of both parameters set as mentioned before. However, in the case of 35 mJ/cm^2 and development time of 5:30 minutes, rough edges were obtained after the lift-off.

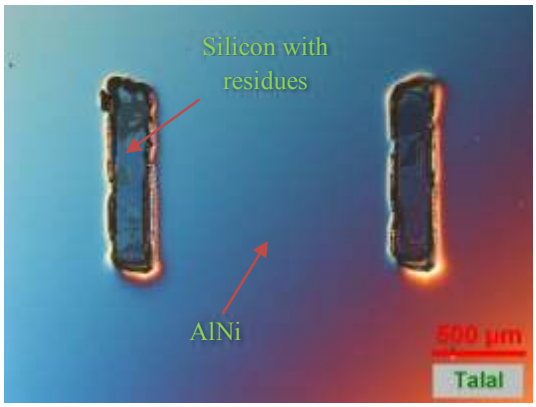

Fig. 11 Lift-off - Exposure energy: 35 mJ/cm^2, Development time: 5:30 minutes

For 45 mJ/cm^2 and a development time of 5:00 minutes, a relatively smooth edge contour has confirmed that there is no continuity existing between the stripped resist and the metal present on the top of the remaining resist.

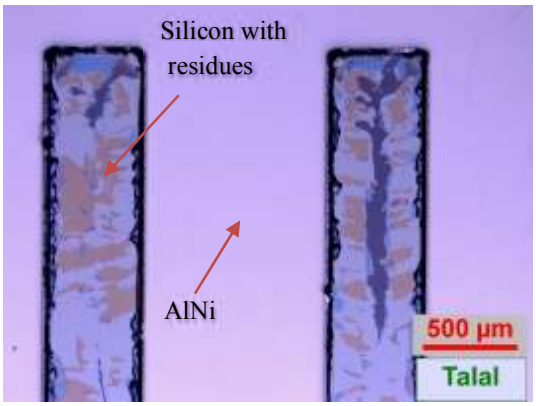

Fig. 12 Lift-off - Exposure energy: 45 mJ/cm^2, Development time: 5:00 minutes

E. Consistent Delamination

Photoresist delamination usually appears in an inconsistent pattern. However, during one of the experiments at the parameter mentioned above, an additional step of 2 minutes of water rinsing was added to check the photoresist behavior. A unexpected behavior was observed resembling to delamination where the resist was lifted from the bottom silicon wafer. This behavior was continuous in a sense that every third structure was showing the repeated behavior.

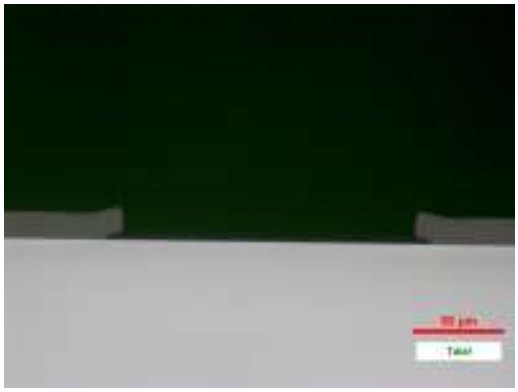

Fig. 13 Consistent resist lifting from silicon wafer

F. Overview

Throughout the experimentation, apparently there was not a considerable undercut achieved that is necessary for the lift-off process. From high exposure energy of 520 mJ/cm^2 to low exposure energy of 55 mJ/cm^2, a straight edge profile with a 90-degree angle was achieved. However, at low exposure energy of 35 mJ/cm^2, 45 mJ/cm^2 and high development time of 5 minutes, 5:30 minutes a considerable undercut angle was achieved. This concludes that the undercut angle is the combined function of low exposure energy and high development time.

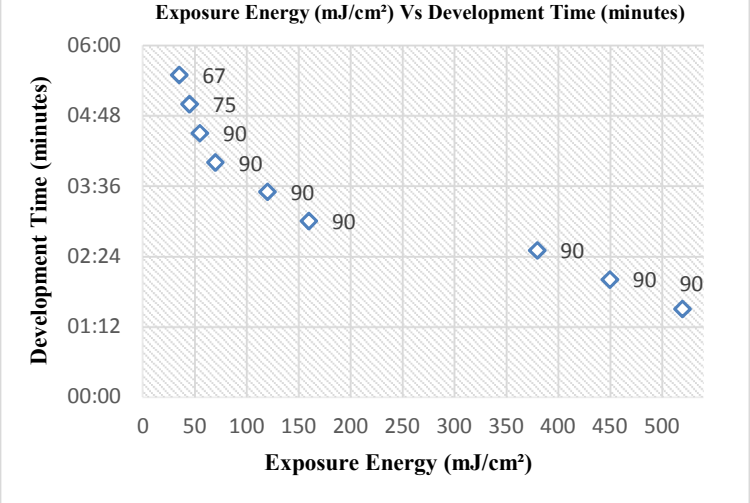

Fig. 14 Overview of the process

IV. CONCLUSION

Dry film photoresist E8015 is successfully optimized for straight and undercut profiles. 10-micrometer multilayer Al/Ni was lifted off due to resist stripping, which demonstrates a discontinuous step coverage due to sputtering. It is evident that with a considerable edge profile, it is possible to lift-off the multilayers to higher thickness. The structured multilayers can be tested for the electrical spark test for controlling the heat propagation reaction that results in high heat release. Possible applications could be the joining of chips in micromechanical systems and integrated circuit (IC) packaging.

REFERENCES

[1] C.Michelle,H. Soon Wee,S.Nandar, L.Ebin, R. Vempati Srinivas, D.Pinjala, "Development of negative profile of dry film resist for metal lift off process," Proc. Electron. Packag. Technol. Conf. EPTC, pp. 884–888, 2009, doi: 10.1109/EPTC.2009.5416418.

[2] C.Chunwei , P.Robert, N.Edward , L.Sam, M.Stephen, P.Georg, B.Rozalia , "Development of thick negative photoresists for electroplating applications," Proc. SPIE 6923, Advances in Resist Materials and Processing Technology XXV, 69233E, 2008, https://doi.org/10.1117/12.773986

[3] D. W. Widmann, "Metallization for Integrated Circuits Using a Lift Off Technique," IEEE J. Solid-State Circuits, vol. 11, no. 4, pp. 466–471, 1976, doi: 10.1109/JSSC.1976.1050760.

[4] R. C. Dorf, "Electronics,Power Electronics,Optoelectronics,Microwaves,Electromagnetics and Radar, " vol. 1, pp. 1-888, 2015.

[5] S. Niranjan, B. Parija & S. Panigrahi, "Fundamental understanding and modeling of spin coating process: A review," Indian J Phys 83, pp. 493–502, 2009, https://doi.org/10.1007/s12648-009-0009-z

A.Muhammad Talal Muhammad Talal Asghar received the BSC. Mechanical Engineering (2016) from UET Taxila, Pakistan and the MSC. Micro and Nanotechnologies (2021) from Technical University of Ilmenau, Germany. His entire engineering and college education was fully funded through prestigious scholarships awarded to high achievers. On the side, he found and led multiple top organizational positions in an engineering institute. In 2016, he joined Qazi enterprisers limited Islamabad, research & development center and worked as the process development engineer of engineering projects. He also had the chance to work as an internee in top multinational firms like TESLA industries Islamabad and DESCON engineering Pvt Ltd. In 2019, he worked as a graduate research assistant in the department of micro and nanotechnologies (ZMN) at TU Ilmenau. Since then he has been working in CIS forschung instiut fur mikrosensorik Erfurt, Germany writing his master thesis. He is involved in MEMS and engineering process development, device design, analysis, electronics, and material characterizations in the research and development domain.

An Approach to Capture, Evaluate and Handle Complexity of Engineering Change Occurrences in New Product Development

Mohammad Rostami Mehr, Seyed Arya Mir Rashed, Arndt Lueder, Magdalena Mißler-Behr

***Abstract*—**This paper represents the conception that complex problems do not necessary need similar complex solutions in order to cope with the complexity. Furthermore, a simple solution based on established methods can provide a sufficient way dealing with the complexity. To verify this conception, the presented paper focuses on the field of change management as a part of new product development process in automotive sector. In the field of complexity management, dealing with increasing complexity is essential, while, only non-flexible rigid processes that are not designed to handle complexity are available. The basic methodology of this paper can be divided in four main sections: 1) analyzing the complexity of the change management, 2) literature review in order to identify potential solutions and methods, 3) capturing and implementing expertise of experts from change management filed of an automobile manufacturing company and 4) systematical comparison of the identified methods from literature and connecting these with defined requirements of the complexity of the change management in order to develop a solution. As a practical outcome, this paper provides a method to capture the complexity of engineering changes (EC) and includes it within the EC evaluation process, following case-related process guidance to cope with the complexity. Furthermore, this approach supports the conception that dealing with complexity is possible while utilizing rather simple and established methods by combining them in to a powerful tool.

***Keywords*—**Complexity management, new product development, engineering change management, flexibility.

I. Introduction

THE increase of complexity in business environment implies more complex internal transactions in every section of a company. High complexity affects the decision behavior in a negative way and leads to inefficiency. This is mainly reasoned by the mangle of traditional management approaches focusing on problems in an isolated and a linear way. Considering the research focus of this paper, two main issues appear while dealing with complexity in EC:

(1) There are many established methods and recourses in companies that represent useful tools but are not suitable in the conventional and isolated way of use in order to cope with the increasing complexity or including it to the decision-making specially in the EC process.
(2) The EC process is rigid and therefore is not matching complexity and its features.

This paper offers a rational linkage of established methods and recourses considering their usefulness within the scope of complexity management, following the fundamental philosophy by solving complex problems with relatively simple solutions and efficient use of available recourses. In order to solve these two issues, following requirements can be deduced for the solution approach. First, the necessity regarding EC from a system point of view will be evaluated. The systemic perspective provides the main framework for complexity management. Secondly, the EC process has to be framed more flexible to be able to cope with the complexity. Later in this paper, the requirements for the approach of this paper will be defined.

Complexity is often described as a systems attribute, thus a host of different system components (variety), which are related to each other (connectivity) and can alter over time. The main issue of complex systems is the enormous non-transparency and the consequential unknown causes and effects [1]. Dealing with complexity successfully means ensuring sufficient transparency and flexibility in order to handle the existing complexity.

Proceeding this paper, the authors analyzed the usage of system thinking in the automotive industry focused on the New Product Development (NPD) Process [2]. In this context the system consists of new products, processes and resources needed to produce a new product. In common NPD processes, a product is developed concurrently by emerging processes and resources based on engineering processes, Fig. 1. Although engineering processes may differ in different organizations, engineering change management (ECM) is indispensable as one of the most important elements of these processes. Also, from a system point of view, ECM can be considered as a sub-system of NPD. ECM is a highly complex process [3] and covers adjustments and modifications during NPD and afterwards, meaning a new replacement technical condition called EC [4]. Hamraz, Caldwell and Clarkson [5] give a literature overview of 427 publications addressing EC as well as ECM and categorize these within the following three main topics:

- Pre-Change Stage - Publications in this topic focus on people, process or product-oriented research to reduce the impact of EC.
- In-Change Stage – Publications in this topic focus on organizational issues, strategic guidelines or tools & methods to ease the handling of EC.
- Post-Change Stage – Publications in this topic focus on

M. Rostami Mehr is with Volkswagen AG, Germany (e-mail: m.rostamimehr@yahoo.com):

temporal, qualitative or cost-oriented impacts of EC for future learning.

Thus, it appears that ECM and EC are a highly explored topic, but this has rarely been in the context of complexity. Li has investigated ECM in NPD in the context of complexity management to provide an answer to the question of how the resources of NPD can be allocated to ECM in an optimal way [6]. Störm has studied EC in order to improve the lead time of information transfer and analyze the impact of lean product development for the improvement of EC [7]. Also, Eger et al. explore the interaction of design engineering and other involved parts in order to reduce the cost of changes in product [8]. Reddi et al. have analyzed the interaction between NPD and ECM to understand which parameters and actors are involved when this occurs. It is shown that there are no methods or tools provided in order to deal with complexity in NPD and form an efficient ECM process [9]. Although researchers such as Leng et al. or Subrahmanian et al. have studied ECM in complex NPD situations [10], [11], the ECM processes − such as basic reference processes e.g., the German Association of the Automotive Industry [12] – do not imply complexity either and are relatively rigid in design. Therefore, it is not clear how to form flexible ECM processes for complex NPD where engineers are able to select an EC process based on the current condition of an NPD project, in order to adapt the evolved processes and resources for changes in product. Aside from flexible EC processes, a tool for assigning priority in implementing EC is also missing. Kocar and Akgunduz introduced a priority index for comparing changes with each other, but there remains no method or tool for assigning priority in evaluating the processes of change [13].

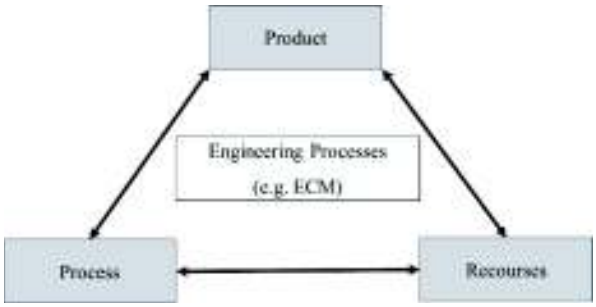

Fig. 1 ECM in the context of the PPR-Process

Ignoring complexity leads to a missed opportunity in terms of the potential competitive factor. Additionally, the negligence may result in extra costs, diminished quality or loss of time. In other words, negative impacts on basic business criteria such as time-to-market or profitability are anticipated. This conception assumes complexity as a comprehensive effect which occurs at and affects different levels of a system, see Fig. 2. This paper ties in with this perspective regarding the necessity of including complexity as an essential factor for the estimation of EC. Therefore, in the following chapters, some fundamental information about NPD and ECM is provided. These two complex systems will form a basis to approach a solution, which will be established incrementally, step by step. First of all, the relevant requirements of the approach will be deduced and further explained. Based on this, the main solution approach will be realized in 3 correlated components:

(1) Evaluation of complexity – Systematic gathering of the system components and potential interactions (system thinking) as well as successive dedication of these in the main cluster (complexity catalogue).
(2) Evaluation process – Selection of a suitable method for evaluation of the complexity catalogue in order to estimate every EC by means of its potential complexity.
(3) Case related process guidance – Defining different strategies to effectively and flexibly handle the estimated complexity of each EC.

The presented approach can be classified as a tool to ease the handling of EC in the change stage [5]. The added value lies in the explicit aspect of complexity within EC and its inclusion in the solution.

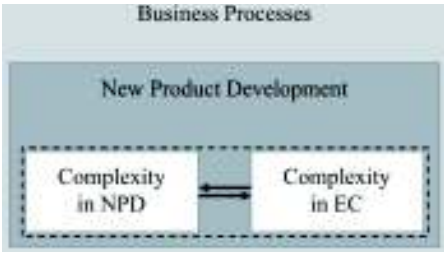

Fig. 2 Hierarchically structured perspective of the system and complexity of EC

II. Complexity in NPD

NPD processes are sequences of activities and steps that an enterprise applies to conceptualize, construct, and commercialize a product. These steps and activities are mostly mental and organizational rather than physical [14]. If NPD processes are considered as a system which has a product as an output by response to demand from a market, the nature of dependencies within this system is a significant driver of complexity [15]. This is a significant part of the car-manufacturing process and includes the organizational units of product development, production, purchasing, sales and marketing, and finance, Fig. 3. Overall processes include high-level hierarchical processes, such as strategy etc. IT systems consist of all IT hardware and software such as PLC (Product Life Cycle) management systems, data banks, servers, etc. Under every organizational unit, the corresponding processes and their interrelations in the context of system engineering can be applied; in fact, the number of processes in some cases, such as in automobile industries, can exceed 1,000 [1]. This interrelation, especially in large projects in the automobile industry, results in enormous information flow. In addition to the high number of processes and interdependencies, product complexity can be categorized under NPD processes. In the industrialization era, most products comprise a high number of connected parts or elements that undergo rapid changes [16]. Products are characterized by a large number of variants due to the mass-customization paradigm. Another feature of NPD

processes in recent decades is uncertainty regarding the time-to-market, market demand, fluctuation of demand, available technology, speed of development of new technologies, and the required resources such as human resources and capital [17]. With the presence of features such as uncertainty and a high number of involved, interrelated processes and dynamics, NPD processes can be categorized as a complex part of an enterprise.

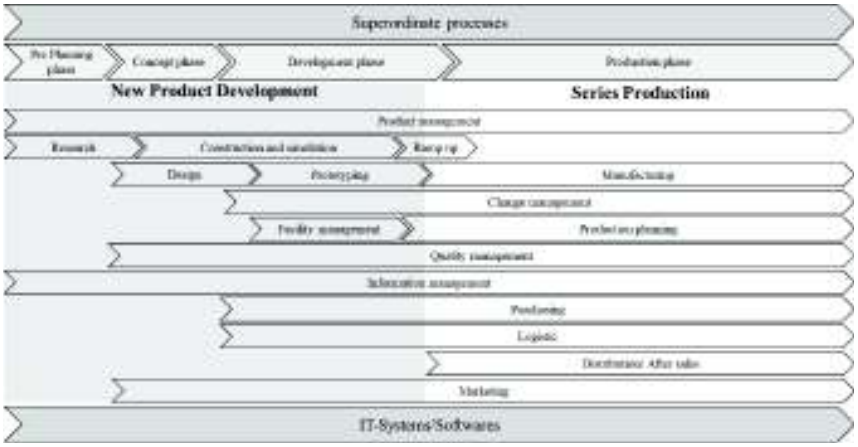

Fig. 3 Business processes of a car manufacturing company (derived from [18])

From another perspective, business processes of car manufacturing include two main interrelated blocks (in other words, there are two main components in the context of system engineering): product development and production development, Fig. 3. In the traditional engineering approach of Taylorism, the successor process can start only when its predecessor is completed. In this approach, the production planner receives considerably complete information regarding the product from the product developer and transfers the complete planning information to the next block after completing their own activities—this prolongs the development time and consequently the time-to-market. To keep competitiveness alive, it is vital to reduce the time-to-market. Recently, the approach of simultaneous engineering (SE) or cross enterprise engineering (CEE) has been introduced in the context of NPD [19]. Parallelism, distribution, and connection of product and production starts in the early phase of development. On the one hand, these approaches support the enterprise in reaching the goal of reducing the time-to-market while decreasing the cost of development [20]. On the other hand, they drastically increase the information flow and uncertainty, due to the mutual dependencies between the organizational units that are responsible for the development of products and production, even though the involvement of production development in the NPD project, and accordingly the mutual dependencies, starts in the early phase of NPD.

In the early phase, product engineers design, construct and build the first prototype, at the same time as production engineers plan production facilities. By product release, the production planner releases the planned facility and a supplier constructs and builds the production plant. After the product-release milestone, prototyping and testing of product will occur. From one side, if design engineers found a problem or an opportunity for product optimization at this stage, the product change would take place. As an example: the reinforcement of a car body to optimize crash test behavior can be mentioned. In some cases, this optimization will require adding a new component or new joining elements in the car body. From another side, if the supplier of production planning found a problem regarding manufacturability or optimization possibilities, the request for product change could be issued. For instance, if a supplier discovered a problem with manufacturing tools colliding with the product or having accessibility issues in joining components, the request for product change may be issued.

In the development processes of a car different organizational units are involved in internal interaction while, due to the nature of product, within the organizational units themselves there are several tailored divisions such as press shop, body shop and assembly shop engaged in development processes. This makes NPD and change management processes in the automobile industry much more sophisticated than in other industries.

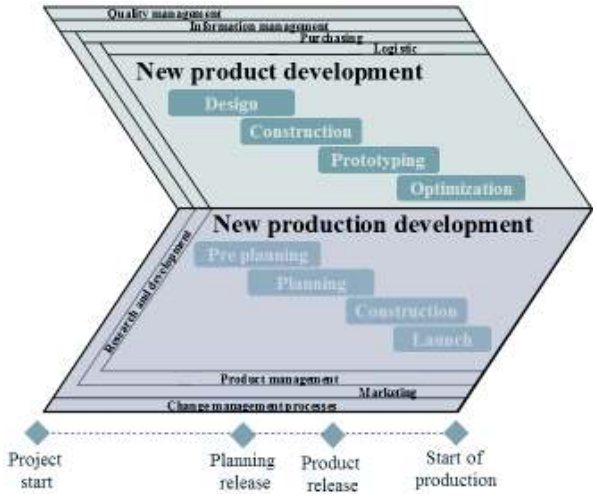

Fig. 4 Product and production processes of a car manufacturing company

III. Complexity in ECM

As mentioned in the previous section, changes are a significant part of the product lifecycle. Thus, coping with changes to product or product-related processes is conditionally essential for the success of the company [23]. Changes in NPD in particular are often illustrated as a sub process, while Fricke et al. [21] describe NPD in its entirety as a continual change management. More specifically, in an industrial context, EC comprises adjustments or modifications of the structure (e.g., shape or pattern), behavior (e.g., stability) or functionality (e.g., performance) [21]. Engineering change process (ECP) represents the procedure and sequence of the change implication. ECM can consolidate the necessary internal company processes and organizational structure as well as external framework conditions (e.g., law, competition, innovation etc.) [5], [22]. In relation to this, Fricke et al. identify five attributes for a successful ECM [21]:

- Less (prevention of EC)
- Earlier (frontloading)
- Effective (effectiveness in the assessment)
- Efficient (efficiency in terms of optimization)
- Better (accepting and understanding changes)

In accordance with these attributes, it is necessary to comprehend the causes and effects of EC. Within the common literature different perspectives of causes of EC are given. Usually, these causes can be classified as:

- Trigger – emergent matters (product or product-oriented e.g., correcting of an error, modifying the functionality or quality and safety issues) or external matters (e.g., customers, market or competition) [23]
- Urgency – running change, emergency change and instant change
- Initiation – early, mid production or late insertion [24]
- Necessity – mandatory changes such as deficient functionality, laws and norms which have to be realized; failing to meet this necessity will affect the successful marketing of the product or go against regulations (e.g., emission regulations); optional changes such as innovation, product or cost optimizations for the purpose of customer acquisition (e.g., optimization of the emission as merchandise).

Otherwise, EC itself can affect different issues like product-process-resources (PPR) and thereby costs, quality or time [25]. However, it is necessary to point out the importance of EMC regarding EC, since aside from potential negative aspects EC can achieve positive effects as part of a continuous improvement concept e.g., optimization, innovation or higher customer satisfaction [21].

Fig. 5 VDA ECM reference process [12]

A successful ECM requires reliable processes and organization. Reference models, e.g., DIN 199 part 4, provide a common foundation of procedures and structure. In the context of this paper and the domain of industrial engineering, in particular the automotive sector, this paper refers to the VDA ECM reference process. This recommendation subdivides the ECM into five sequential phases, see Fig. 5. Usually, ECM activities initiate by identifying ideas for improvements (M1: Change Idea) triggered by the causes listed above. After gathering and assessing potential change concepts (M2: Change Potential Identification) alternate solutions will be defined and estimated on basic input quantity (M3: Potential Solution defined). Following this, the change decision is specified into a change request (M4: ECR decided). The process ends with the phases of engineering (M5: EC released) and manufacturing implementation (M6: Manufacturing change released) [12]. The approach presented in this paper specifies the process phase M3, which will be detailed in the next chapter.

IV. Objectives and Requirements of Complexity Management in EC

As explained in the introduction, NPD is considered to be a complex and dynamic process. Depending on the project phase, technical changes (EC) are happening to develop the new product. In literature and in praxis there are very well-established ECM processes, including the six phases detailed above [12], [21] and [23]. However, the EC process is rigid, inflexible and not suitable for complex NPD. From a holistic point of view under different project circumstances there must be different change management processes to bring flexibility for managing complexity. These form the main objectives of the presented approach. Therefore, the first step is the evaluation of changes with consideration of project complexity, aiming to ensure sufficient transparency; (what should be evaluated).

To evaluate changes in a systematic way the complexity management catalogue is suggested as a building basis for further analysis. As NPD is very dynamic and several changes can happen simultaneously or under time pressure, the evaluation of changes must be accelerated. Considering this, the complexity catalogue must support engineers by evaluating and sorting the changes, preferably in a quick and simple way. For this purpose, a suitable method of evaluation must be contemplated. The result of evaluation is the categorized changes (how, when and by whom changes should happen). The next step is assigning a corresponding ECM process for categorized changes. Here, the current ECM process provided from VDA is selected as the basis. Depending on the category of the changes, adjustment of ECM process is suggested. Adjustment of the ECM process forms a flexible change management process and provides agility (how to proceed with complexity).

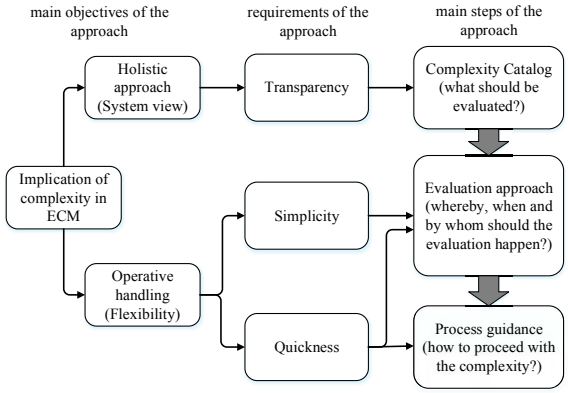

Fig. 6: Proceeding of paper

V. Capturing Complexity of EC

The first step of the approach is to ensure sufficient transparency. In a complex environment it is essential to obtain an overview of the scale and connections through a holistic approach, see Fig. 6. Therefore, ECM and NPD are considered as related systems, since EC might affect not only the ECM but also the next superordinate system NPD. The reason behind using the system point of view is the vast potential of an EC. A simple technical change may trigger non-technical effects on different attributes like process, time or organization. Reflection on the total potential impact of EC allows a rational statement to be made about the existing complexity.

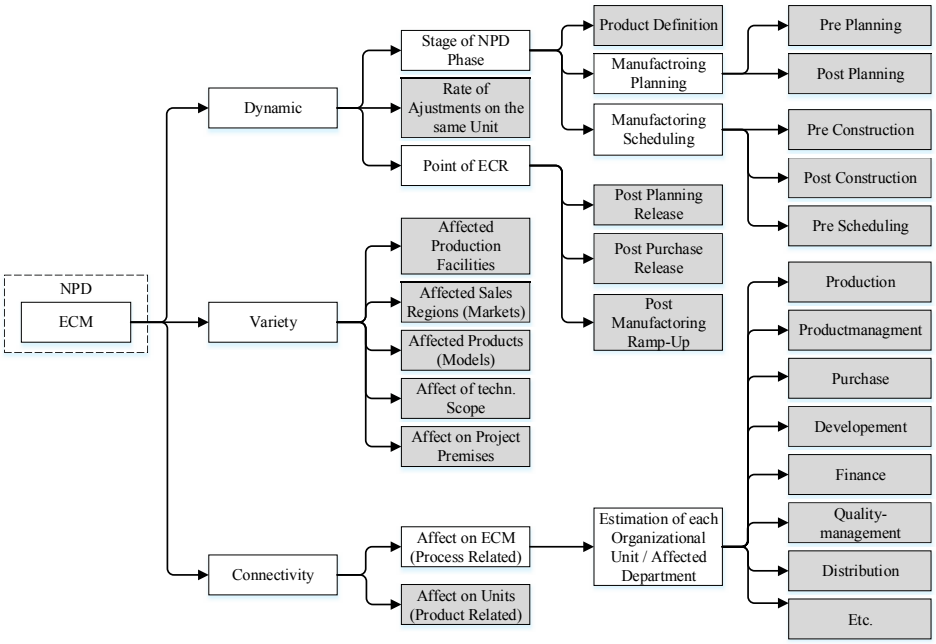

Fig. 7: Complexity catalogue

In order to gather all potential effects, a literature review has been performed. Various information could be deduced from a variety of definitions, illustrations and studies. Additionally, document and process analyses, as well as expert discussions within a major OEM, have been realized. Obtaining a more precise insight into procedures and coherences is important for a better understanding of the system. Furthermore, empirical knowledge could be collected and included. The vast spectrum of gathered information was clustered and successively assigned to the main complexity attributes (variety, connectivity and dynamic) represented in the common literature [1]. Finally, the evaluation and assignment of the cluster results in the complexity catalogue see Fig. 7.

Starting with the ECM and NPD systems, the recorded topics are hierarchically ordered. Assuming EC as the main trigger, each topic represents a cluster of potential qualitative, quantitative or temporal effects on other parts of the system. The final evaluation of the effect happens in the last tier of the path (color-coded).

The dynamic complexity attribute consolidates primary temporal effects relating to the phase of NPD (e.g., project-related changes in the planning, scheduling or construction phase) and/or the point of the Engineering Change Request (ECR), e.g., product related changes such as releases. Likewise, the total amount of changes on the same unit over time is evaluated. The variety attribute focuses on quantitative effects (e.g., affected models, facilities and sales regions) as well as technical consequences (e.g., the scope of the change or alteration of the project premises). Finally, the connectivity attribute considers effects on other units (e.g., intra- or inter-product related unit adjustment) and/or effects on the ECM process itself. Those processual effects are recorded over affected organizational units or departments. All the evaluated potential effects represented in the complexity catalogue have to be considered in the estimation process of each EC. If not, the EC can result in unexpected additional negative cost, time or resource consumptions.

VI. Determination of Systematics for Change Evaluation

Considering the complexity catalogue explained in last section, the aim of this section is to determine an appropriate evaluation method for comprehensive analysis and classifying of changes in NPD. The methods which can classify and set priorities are deliberated.

- FMEA – "Failure mode and effects analysis" is a powerful method that systematically defines and classifies potential risks of failure and accordingly sets priorities for action. This is a bottom-up method, considering all systems from a small component of a process or product up to high levels of a system being impacted from lower hierarchical levels [26]. Although FMEA provides a systematic way to identify the risk priority number (RPN), it does not support identification of the interaction of system components and its possible failure in a systematic way. For the purpose of classification, specifically classification of changes in NPD, the detailed bottom-up analysis provides precise information to categorize changes. However, it also postulates methodical knowledge and is highly time-consuming. Although it supports engineers to have a detailed overview of changes and their impacts, the lack of information in the early stages of ECM means it may not assist engineers expediently.
- ABC method – Based on the Pareto principle (also known as the law of the vital few), a useful method is to divide and categorize items in three classes according to specific criteria; A (very important), B (intermediate) and C (least important). The ABC method provides a simple and swift systematic procedure to identify and classify items with regard to the significance of their impact on the outcome of the system. The results provide a solid structure for further decision making and focusing specially on key aspects. Regarding the evaluation of changes in NPD, this method provides quick results in a simple way by analyzing available information at an early stage of the change request.
- Eisenhower Matrix – The Eisenhower Matrix is a tool for efficient and productive decision making. Based on the criteria 'important/not-important' and 'urgent/not-urgent', tasks or items can be classified into four different ranks of significance. This method has been used widely in the field of management because of its simplicity and efficiency. As with the ABC method, it provides a quick result in respect of EC evaluation in NPD.
- AHP – Analytic Hierarchy Process (also known as the Saaty method) is a quantitative technique from the scientific field of decision making and primarily serves to structure and analyze complex situations. Based on three sequenced phases the user evaluates necessary information, defines hierarchies and establishes priorities [27]. This approach allows a choice between multiple alternatives based on the highest value. Similar to FMEA, it can help engineers involved in ECM more explicitly in later steps when the information is completed. Although it matches the complexity requirement of ECM in NPD, it demands high methodical knowledge and could be a time-consuming approach.
- Delphi – The Delphi method is a qualitative approach to collect and evaluate the opinions of a panel of experts selected for their qualifications, in order to approach a consensus opinion on the selected topic. Delphi is mainly used for problems where quantitative analysis cannot be practiced. Delphi is an interactive process beginning with the collection of the opinions of each expert on the same topic [28]. Afterwards the results (all opinions) are presented to all experts with the opportunity to adjust their own previously submitted argument. In order to densify the results, this process is repeated up to three times. Gaining an appropriate result regarding the evaluation of changes in ECM demands time-consuming and well-organized discussions. Similar to AHP and FMEA, it can provide precise evaluation once sufficient information is available.

In order to identify the optimal method for the presented approach, a systematic comparison is necessary. Cost-Utility-Analysis (CUA) is a simple concept to select between different alternatives. By defining overall criteria and measures the user is able to evaluate the alternatives on the same basis. Each measurement criterion can be weighted by the user's preference, resulting in a highly qualitative approach that is highly practical at the same time. The CUA is performed in sequenced steps:

- Select the relevant alternatives for estimation
- Define and weight the evaluation criteria
- Evaluate and take the alternative with the highest value

To achieve the objectives of the approaches introduced in this paper, simplicity, quickness and precision are defined as the criteria for CUA.

- Simplicity is picked because in the dynamic phase of NPD, saving time through a simple decision-making process is gaining importance. Simplicity is becoming a leading design principle in developing new product [29]. Therefore, this principle must also be transferred to the evaluation approach of CUA used in this paper. Simplicity can be obtained by eliminating the redundant elements of processes or the replacement of interfaces. In other words, removing unnecessary elements of the process can provide ease of use. This follows the suggestion of Cunha and Rego for facilitating complexity though simple rules [30].
- Quickness is a criterion that has a strong relationship with simplicity. In fact, simplicity provides quickness, as expressed by Jack Welch: ''we found in the 1980s that becoming faster is tied to becoming simpler… If we are not simple we cannot be fast ... and if we were not fast we cannot win'' [30]. Quickness in responding to changes in product is one of the most important factors reducing the cost of product development and time-to-market. For instance, if a change happens before product release and the process of change evaluation allows engineers to consider the change quickly and before product release, the change should be cost effective to implement [8]. The longer the evaluation process affecting the implementation of changes, the more expensive the changes could be.

- Precision means that although making a precise decision regarding the type of changes in product is an important factor, in comparison to the other two factors it gains less attended. Indeed, in a dynamic NPD, a rough estimation for change categorization causes a lower risk compared to the factor of quickness. Specifically considering ECM processes, providing precision at the beginning has no relevance because only the change request and possible solution are identified, see Fig. 8.

The five methods introduced above have been analyzed based on these three criteria. According to the requirement of ECM in NPD, quickness and simplicity are high weighting in comparison to precision. Analysis of CUA is completed by gathering information from a group of experts with sufficient experience in the field of change management in praxis. For ranking, the Likert scale has been used, with scaling from one to five; where one is "not matching" and five is "completely matching".

TABLE I
COST-UTILITY-ANALYSIS

	precision	simplicity	Quickness	Quantity
Weighting	0.1	0.4	0.5	1.0
Eisenhower	1	4	4	3.7
ABC Analyses	2	5	5	4.7
FMEA	5	3	1	2.2
AHP	3	1	2	1.7

This analysis shows that ABC is the highest-ranking method. Accordingly, it is selected as the optimal evaluation method for the presented approach. Determination of the ABC method as an optimal evaluation method is therefore the response to the necessity for an appropriate system to provide flexibility to the ECM. When and by whom the evaluation must take place are the next concerns that need to be answered, see Fig. 6.

As depicted in Fig. 8, in the second step of ECM a team including experts from different departments define possible solutions to the change request. This is the earliest step at which relatively sufficient information is available to evaluate the change. Therefore, the recommendation of the presented approach is implementation of ABC-Analysis in the second step of ECM, where the team of experts are gathered together.

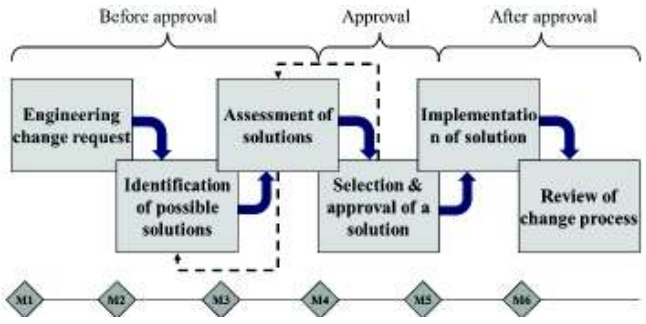

Fig. 8 ECM processes (adopted from [23])

To assign A, B or C for a change in NPD, all 24 items (see Fig. 7) from the complexity catalogue have to be separately evaluated and assigned as A, B or C. Determination of the category of each item is based on experiences of experts with process responsibilities. The items can be sorted in different categories with differing weights depending on the type of company in question. For instance, for automotive companies with diverse manufacturing penetration, the weighting of changes on e.g., production or purchasing can be variable. Even the weighting of items within the same company can vary in different projects based on project premises. Therefore, the weights for items are considered as a variable parameter which has to be defined in the early phase of the project. The weight of items is defined by w_i, and the category of items by x_i where i is the item and x can be "A", "B" or "C". For example, the Likert scale can be used for weighting. A change is assigned with an index calculated by

$$\sum_{i=1}^{24} w_i x_i \quad (1)$$

The index includes all three categories (A, B or C). The calculated result (highest number) defines the category of EC. In the case of an identical number of categories, final determination of A, B or C rating depends on the opinion of the concerned parties.

VII. Defining Case-Related Process Guidance

While the previous subchapter dealt with the issues of complexity content and the evaluation method, the final step of the approach is a response to the question of how to proceed with the results. After evaluating the complexity catalogue via ABC-Analysis, each EC can result in a differing complexity intensity, e.g. A for high complexity intensity, B for medium complexity intensity and C for low complexity intensity. In order to grant maximum flexibility, this approach suggests three different procedures depending on the complexity intensity, see Fig. 9. A quick and adequate response is an important factor when handling complex systems. The sooner the existing complexity and its potential impact are assessed, the better the chance to prevent negative effects.

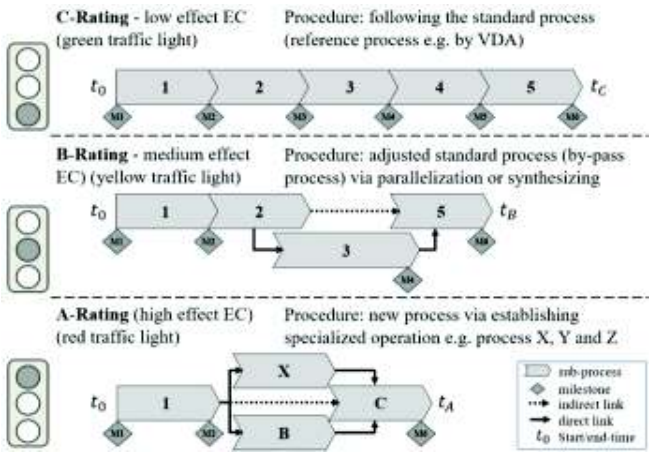

Fig. 9 Process guidance overview for different EC category

ECs with a low complexity intensity are considered as having

a low effect on the viewed system (ECM and NPD). These are rated via ABC-Analysis as C and visualized with the green traffic light, meaning proceeding with the existing standard processes (ECP) without any further changes is adequate, e.g., reference process by VDA. Because of the low intensity no further significant negative impacts are likely to be expected.

B-rated ECs are considered to have a medium complexity intensity (yellow traffic light). It must be assumed that these ECs will have an impact on the viewed system (ECM and NPD) resulting in possible negative cost, quality, technical or temporal effects. In order to respond quickly to the potential extra effort hidden in these ECs, an adjustment of the standard process is necessary. By-pass processes are suitable for such cases because they are based on the principle of shortening or compressing of the existing processes. This can be achieved by reshaping the standard process via elimination of process/ milestones or redefining the process flow/structure [31], as shown in Fig. 9. In daily business, by-pass processes for B-rated ECs have to be prioritized, treated with higher attention or estimated by different premises than C-rated ECs in order to achieve a more time efficient procedure (see Fig. 9, new t_B).

ECs with an A-rating have a high complexity intensity (red traffic light). These are particularly critical changes and anticipated to have highly potential negative impacts on the other parts of the system e.g., unintentional harmful consequences. After identifying change potential via the ABC-Analysis in milestone M2, this approach suggests a radical deviation of the procedure, since the standard process or the by-pass process is no longer considered to be sufficient. ECs with such high effects need to be treated separately, and therefore new specialized ECM processes have to be defined and implemented (see Fig. 9, new specialized operations X, Y and Z). In daily business, for example task forces can be formed by a team of experts. These task forces are responsible solely for A-rated ECs. Other necessary adjustments include defining fitting estimation premises, quick decision making and continuous auditing. Therefore, a minimum in loss of time can be provided.

VIII. Discussion

The literature research exposed that on one hand a comprehensive analysis of EC process in a system of NPD, its causes and impacts are missing. And on the other hand, EC process is formed as a not flexible procedure. The approach presented in this paper responding these two points by the three following steps; complexity capturing, identification of evaluation methodic and defining corresponding process guidance. Introduction of traffic light systematic to the change process enables the organization to improve communication within EC. Once change occurs and the request of change is issued, the team of experts from different organizational units discusses and rates the changes. Rating the changes appends very necessary composed information to the process with two significant functions. The first preliminary function is defining which process should be selected to proceed the change request. Selecting a proper process increases the efficiency of ECM by providing commensurate reaction to the changes. The second function is providing transparency which makes necessary information more evident. Assigning red, yellow or green sign to the change simplifies the transfer of information in very quick way within (procedural view) and as well between (organizational view) department units.

Presented approach contributes to ease knowledge management in ECM. For rating a change parallel to the common change evaluation, required information is collected by team of experts. Gathered information supports to categorize a change request in A,B or C-Rating categories. In fact, a correlation between the collected information and rated changes is formed. Considering this information as experience of experts, building of this correlation is a systemic approach to manage knowledge in ECM. Strictly speaking, collected information from previous EC is transferred to knowledge supporting new EC with appropriate anticipation regarding changes. Eventually, the contributions of introduced approach will provide flexibility in ECM by facilitating communication and stablishing a systematics to knowledge management. This will increase efficiency of ECM by e.g. reduction of change costs, enabling an organization by better resource allocation and appropriate reaction on changes.

IX. Conclusion and Outlook

The initial purpose of the presented approach is to provide transparency and flexibility to manage the complexity of EC in NPD. The first step of most complexity management methods introduced in research papers comprises analysis of the system, the connectivity of its elements and the impact of status changes of elements providing transparency [32], [33] meaning that capturing complexity is an essential factor in the presented concept. The complexity catalogue demonstrated in this research yields a systematic comprehensive evaluation method to provide transparency in ECM. It supports experts in classifying EC in different categories. Clustering, and consequently assigning, the changes is a fundamental step towards providing flexibility in ECM. Indeed, the final result of the approach is to provide several ECM processes matching the features of defined change categories. Based on the category of EC, experts have the option of selecting various procedures. Strictly speaking, according to the law of requisite variety [34] providing variety in ECM processes is the key to managing their complexity. Another aspect considered in this paper is the time intensity of new product development in the automobile industry which is an important complexity driver. Due to time pressure, a quick decision regarding the type of EC is a necessary factor. The quickness of the method used to evaluate EC is ensured by using a proper evaluation tool. In fact, quickness helps to reduce time intensity and increase flexibility again. Generally, a group of experts evaluates and clusters EC based on know-how, which could be considered as a subjective evaluation. To intensify the quickness of evaluation and decrease the subjectivity, the authors recommend the extension of the presented approach with data-mining methods as a suggestion for future work. With proper data mining methods, information gathered from previous projects could be sorted

into different categories. A change request in a project can be immediately matched with a determined category and suitable change process can be assigned. Consequently, a transition from qualitative to quantitative evaluation would be achieved. Furthermore, a completely automated precise evaluation of complexity by means of machine learning could be available.

REFERENCES

[1] Kirchhof R. „Ganzheitliches Komplexitätsmanagement“. Wiesbaden: Springer Fachmedien Wiesbaden GmbH. 2003.

[2] MirRashed S. A., Rostami-Mehr M., Mißler-Behr M. and Lüder A. “Analyzing the causes and effects of complexity on different levels of automobile manufacturing systems”. IEEE 21st International Conference on Emerging Technologies and Factory Automation (ETFA). 2016.

[3] Huang G.Q., Yee W.Y. and Mak K.L. “Current Practices of Engineering Change Management in Hong Kong Manufacturing Industries.” Journal of Modern African Studies 2003, 13.139: 481-487.

[4] Deutsches Institut für Normung 1990. “DIN 6789-3. Teil 3.

[5] Hamraz B., Caldwell N. H. M. and Clarkson P. J. “A Holistic Categorization Framework for Literature on Engineering Change Management”. System Engineering, 2013, Vol. 16 No. 4: 473-505.

[6] Li W. and Moon Y. B. “Modelling and managing engineering changes in a complex product development process”. Proceedings of the 2011 Winter Simulation Conference S. Jain, R.R. Creasey, J. Himmelspach, K.P. White, and M. Fu, eds, 2011.

[7] Ström M. “Redesign of the engineering change process of a supplier in the automotive industry”. Göteborg: 2nd Nordic Conference on Product Lifecycle Management – 2009, NordPLM’09. p. 28-29.

[8] Eger T., Eckert C. M. and Clarkson P. L. “Engineering change analysis during ongoing product development”. Paris: International conference on engineering design, Paris, France, 2007.

[9] Reddi, K. R. and Moon, Y. B. "Modelling Engineering Change Management in a New Product Development Supply Chain". Mechanical and Aerospace Engineering 16, 2013.

[10] S. Leng, L. Wang, G. Chen and D. Tang. 2015. “Engineering Change information propagation in aviation industrial manufacturing execution processes”, Int. J. Adv. Manuf. Technol. p. 1–11.

[11] Subrahmanian; E., Lee, C., Granger, H., “Managing and supporting product life cycle through Engineering Change Management for a complex product”, Res. Eng., 2015. Des. 26. p. 1–29.

[12] VDA Verband der Automobilindustrie. „ECM Recommendation: Part 0 (ECM)”. 2010., Darmstadt: SASIG VDA 4965, Part 3.0

[13] Kocar, V. and Akgunduz, A. “ADVICE: A virtual environment for Engineering Change Management”, 2010, Computers in Industry 61. p. 15–28.

[14] Oyama, K.; Learmonth, G.; Chao, R. “Analyzing complexity science to new product development” Modelling considerations, extensions, Journal of Engineering and Technology Management, 2015, No.35, P.1-24.

[15] Ulrich, K. T. Eppinger, S. D. “Product design and development”, fifth edition, 2008.

[16] Vogel, W. “Complexity management approach for resource planning in variant-rich product development”, Springer Fachmedien Wiesbaden GmbH, 2017.

[17] Grussenmeyer, R; Blecker, T. “Requirement for the design of a complexity management method in new product development of internal and modular products”, international journal of engineering, science and technology, 2013, Vol.5, No. 2, P. 132-149.

[18] Porter, M. E. „Wettbewerbsstrategie: Spitzenleistungen erreichen und behaupten“, Campus Verlag Frankfurt Main, 1986.

[19] Kerga, E.; Taisch, M.; Terzi, S. “Manufacturing process planning in Set-Based concurrent engineering paradigm, International federation for information processing”, 2012, IFIP AICT 388, P. 158- 169.

[20] Wannenwetsch, H. „Integrierte Materialwirtschaft, Logistik und Beschaffung“ (German), fifth edition, Springer Vieweg, Berlin, 2014.

[21] Fricke E., Gebhard B., Negele H. and Igenbergs E. “Coping with Changes: Causes, Findings and Strategies”. System Engineering, 2000. Vol.3 No. 4: 169-179.

[22] Hollauer C., Wickel M. and Lindemann U. “Learning from Past Changes: Towards a Learning-oriented Engineering Change Management”. Proceedings of the 2014 IEEE IEEM: 1081-1085.

[23] Ullah I., Tang D. and Yin L. “Engineering product and process design changes: A literature overview”. Procedia CIRP 56:. 25-33.

[24] Jarratt T. A. W., Eckert C. M. and Caldwell N. H. M. 2011. “Engineering change: an overview and perspective on the literature”. 2016, Res Eng Design 22: 103-124.

[25] Köhler C. „Technische Produktänderungen: Analyse und Beurteilung von Lösungsmöglichkeiten auf Basis einer Erweiterung des CPM/PDD-Ansatzes“. Saarbrücken: Schriftenreihe Produktionstechnik Band 45, 2009.

[26] Peeters, J.F.W., Basten, R.J.I. and Tinga, T. “Improving failure analysis efficiency by combining FTA and FMEA in a recursive manner”, Reliability Engineering and System Safety, 2018.

[27] Brunelli, M. “Introduction to the Analytic Hierarchy Process”. Springer, London, 2014.

[28] Young, S.J. and Jamieson, L.M. “Delivery methodology of the Delphi: A comparison of two approaches”. Journal of Park and Recreation Administration. 2001. 19(1), p. 42-58.

[29] Eytama, E., Tractinsky, N., Lowengart, O. “The paradox of simplicity: Effects of role on the preference and choice of product visual simplicity level”, International Journal of Human – Computer Studies, 2017, 105. p. 43–55

[30] Cunha, M. And Rego, A. “Complexity, simplicity, simplexity”. European Management Journal, 2010, 28. p. 85– 94.

[31] Lindemann U. and Reichwald R. „Integriertes Änderungsmanagement“. Springer, 2013.

[32] Asan S. “A Methodology Based on Theory of Constraints’ Thinking Processes for Managing Complexity in the Supply Chain”. Dissertation, 2009.

[33] Kluth, A., Jäger, J., Schatz, A. and Bauernhansl, T. „Method for a Systematic Evaluation of advanced Complexity Management Maturity”, Robust Manufacturing Conference (RoMaC), 2014.

[34] Ashby W.R. “Requisite variety and its implications for the control of complex systems”, Cybernetica, 1958. 1:2, p. 83-99.

Vietnam's International Trade Is Showing Signs of Recovery after the COVID-19 Pandemic

Nguyen Thi Thu Hoan

***Abstract*—** On a global scale, Vietnam is a low-middle income country with high openness and an effective export-oriented trade model. This article analyses the impacts of the COVID-19 pandemic on Vietnam's trade in 2020. The analysis, which is based on reports and data collected from international organisations and governmental bodies (notably the International Monetary Fund (IMF), Ministry of Industry and Trade, and General Department of Vietnam Customs), highlights how Vietnam's import and export situation has been affected by the Covid-19 pandemic and gives some major recommendations for the post-pandemic period. In specific, the article focuses on analysing changes in the trade balance, import-export turnover, major trade partners of Vietnam, and USD/VND exchange rate. Research results show that, although Vietnam's trade has been affected by the pandemic in some ways, in general, the trade balance is not affected much, and there is a clear sign of recovery in Q3/2020 thanks to the effectiveness of the government's responses to the pandemic. On that basis, this study provides a number of solutions to the increased efficiency of Vietnam's trade in the coming time.

***Keywords*—** Vietnam, international trade, COVID-19 pandemic, recovery.

Nguyen Thi Thu Hoan is with the Diplomatic Academy of Vietnam, Vietnam (e-mail: ngthuhoan@gmail.com).

FEM Investigation of Inhomogeneous Wall Thickness Backward Extrusion for Aerosol can Manufacturing

Jemal Ebrahim, Dessie, Zsolt Lukacs

***Abstract*—** The wall of the aerosol can is extruded from the backward extrusion process. Necking is another forming process stage developed on the can shoulder after the backward extrusion process. Due to the thinner thickness of the wall, buckling is the critical challenge for current pure aluminum aerosol can industries. Design and investigation of extrusion with inhomogeneous wall thickness could be the best solution for reducing and optimization of neck retraction numbers. FEM simulation of inhomogeneous wall thickness has been simulated through this investigation. From axisymmetric Deform-2D backward extrusion, an aerosol can with a thickness of 0.4 mm at the top and 0.33 mm at the bottom of the aerosol can have been developed. As the result, it can optimize the number of retractions of the necking process, and manufacture defect-free aerosol can shoulder due to the necking process.

***Keywords*—** Aerosol can, Backward extrusion, Deform-2D, Necking.

Jemal Ebrahim Dessie is with the University of Miskolc, Hungary (e-mail: metjemal@uni-miskolc.hu).

Strongly Coupled Finite Element Formulation of Electromechanical Systems with Integrated Mesh Morphing using Radial Basis Functions

D. Kriebel, J. E. Mehner

***Abstract*—** The paper introduces a method to efficiently simulate nonlinear changing electrostatic fields occurring in micro-electromechanical systems (MEMS). Large deflections of the capacitor electrodes usually introduce nonlinear electromechanical forces on the mechanical system. Traditional finite element methods require a time-consuming remeshing process to capture exact results for this physical domain interaction.

In order to accelerate the simulation process and eliminate the remeshing process, a new formulation of a strongly coupled electromechanical transducer element will be introduced which uses a combination of finite-element with an advanced mesh morphing technique using radial basis functions (RBF). The RBF allows large geometrical changes of the electric field domain while retain high element quality of the deformed mesh. Coupling effects between mechanical and electrical domains are directly included within the element formulation. Fringing field effects are described accurate by using traditional arbitrary shape functions.

***Keywords*—** Electromechanical, electric field, transducer, simulation, modeling, finite-element, mesh morphing, radial basis function

I. Introduction

The continually improving manufacturing technology of micro-electromechanical systems (MEMS) leads to increasingly smaller and more geometrical complex structures. With the decreasing size of functional elements, the physical behavior can show an increase of nonlinear effects. In electrostatic driven actuators or sensors, the large deflection of the mechanical structures results in nonlinear changing electric fields. In addition, fringing field effects can become more dominant. At this point electromechanical lumped elements are not valid anymore. To efficiently describe the behavior of such complex systems a strongly coupled electromechanical finite element is introduced. This element is combined with an advanced mesh morphing technique to avoid time consuming remeshing of the electric domain. By using traditional shape function in the element formulation, the new element is compatible with the interfacing mechanical structure. The strong coupling between mechanical and electrical domain of the element gives the possibility to apply small signal analysis as modal or harmonic analysis.

In the following first the state of the art of simulating electromechanical coupled domains is investigated. After this the theory behind the new element formulation and the mesh morphing algorithm using radial basis functions is depicted. The resulting transducer element is validated on well-known electrode setups used in MEMS. The advantages of the element using an integrated and automated mesh morphing algorithm is shown on some more complex examples.

II. State of the Art

The investigation of electromechanical coupled field elements has been done with different methods in the literature. There are mainly weakly coupled and strongly coupled approaches. The weakly coupled approaches need sequentially computation of the mechanical and electrical domain [1]. This leads to slower convergence rates and the use of small signal analysis procedures is not possible.

Using boundary element method (BEM), a meshless electromechanical domain can be described [2]. The problem here is the element formulation itself which requires special solvers and the BEM domain must interfacing with FE domain in non-traditional ways.

Strongly coupled electromechanical elements which can convert electrostatic energy into mechanical energy and vice versa were formulated with different approaches. A variational approach was applied to a 2D domain in [3]. Another energy based concept was proven in [4] on a 2D with only triangular shape function which limits the complexity. In all approaches the deformation of the mesh is one of the key problems. The quality of the mesh correlates with the quality of the results.

III. Element Formulation

The coupling between electrical and mechanical domains can be described as an energy transfer between these two domains. The capacitance changes with a mechanical motion of the electrodes. Thereby electrical energy is converted to mechanical and produces a nonlinear mechanical force on the domain interface. For this reason, we are using an energy approach. The electrostatic energy W_e is given in (1) where ε is the electric permittivity, E is the electric field and Ω the domain volume.

$$W_\mathrm{e} = \frac{1}{2}\int_\Omega E^T\,\varepsilon E\;\mathrm{d}\Omega \tag{1}$$

The electric field E is a function of the electric potential ϕ and the shape function $N(P)$ depending on the global node

David Kriebel is with the Chemnitz University of Technology, Germany (e-mail: david.kriebel@etit.tu-chemnitz.de).

coordinates P of the element [1].

$$E = -\nabla N(P)\,\phi = -J^{-1}\nabla N(\xi)\,\phi \tag{2}$$

Applying the virtual work principle, the tangent element stiffness matrix which couples mechanical degree of freedom (DOFs) x and electrical DOFs ϕ can be modeled as following [4]:

$$\begin{bmatrix} K_{xx} & K_{x\phi} \\ K_{\phi x} & K_{\phi\phi} \end{bmatrix} \begin{bmatrix} \Delta x \\ \Delta\phi \end{bmatrix} = \begin{bmatrix} \Delta F_{\mathrm{el}} \\ \Delta Q \end{bmatrix} \tag{3}$$

The components of the right-hand side are the electrostatic forces F_{el} and charges Q. Using the fact that the shape functions is a function of the isoparametric coordinates ξ and the Jacobi matrix J, the electric energy can be differentiated against mechanical and electric DOFs, since the Jacobi matrix can be expressed as a function of mechanical DOFs. The domain volume Ω is also a function of the Jacobi matrix which makes it differentiable.

$$F_{\mathrm{el}} = \frac{\partial W_{\mathrm{e}}}{\partial x} = \int \frac{\partial E^T}{\partial x}\,\varepsilon E\,\mathrm{d}\Omega + \int \frac{1}{2} E^T \varepsilon E \frac{\partial \Omega}{\partial x} \tag{4}$$

$$Q = \frac{\partial W_{\mathrm{e}}}{\partial \phi} = \int \frac{\partial E^T}{\partial \phi}\,\varepsilon E\,\mathrm{d}\Omega \tag{5}$$

The components of the stiffness matrix consist of 3 different terms since the matrix is symmetrical ($K_{\phi x} = K_{x\phi}^T$). All terms are generated in the same way as the right-hand side by using the product rule. We drop high order derivatives, but hold mixed partial derivatives.

$$K_{\phi\phi} = \frac{\partial^2 W_{\mathrm{e}}}{\partial \phi^2} = \int \frac{\partial E^T}{\partial \phi}\,\varepsilon \frac{\partial E}{\partial \phi}\,\mathrm{d}\Omega \tag{7}$$

$$\begin{aligned} K_{xx} &= \frac{\partial^2 W_{\mathrm{e}}}{\partial x^2} \\ &= \int \frac{\partial E^T}{\partial x}\,\varepsilon \frac{\partial E}{\partial x}\,\mathrm{d}\Omega + 2\int \frac{\partial E^T}{\partial x}\,\varepsilon E \frac{\partial \Omega}{\partial x} \end{aligned} \tag{6}$$

$$\begin{aligned} K_{\phi x} &= \frac{\partial^2 W_{\mathrm{e}}}{\partial x \partial \phi} \\ &= \int \frac{\partial^2 E^T}{\partial x \partial \varphi}\,\varepsilon E\,\mathrm{d}\Omega + \int \frac{\partial E^T}{\partial x}\,\varepsilon \frac{\partial E}{\partial \varphi}\,\mathrm{d}\Omega \\ &\quad + \int \frac{\partial E^T}{\partial \varphi}\,\varepsilon E \frac{\partial \Omega}{\partial x} \end{aligned} \tag{8}$$

$K_{\phi\phi}$ describes the electric field, K_{xx} is the electrostatic softening effect on the mechanical structure and $K_{\phi x}$ is the strong coupling between mechanical and electrical domain. These definitions make nonlinear coupled field simulation possible.

It is important to mention that only on the domain interface nodes the mechanical DOFs are considered in the element definition. These mechanical DOFs are coincident with the ones on the mechanical structure and don't create additional DOFs. In the electrical domain every node has an electrical DOF. The coordinates of non-interface nodes of all nodes are updated using an advanced mesh morphing algorithm.

IV. Mesh Morphing

The main problem on quite every electromechanical FE technology are large geometrical changes. This is caused by the missing mechanical force equilibrium. The electrical domain usually consists of air, which has no mechanical properties in a traditional way. This makes it hard to apply force balancing algorithms. Remeshing can be done, but it's the one of the most time-consuming operations.

The preferred way to compute the node displacements of the inner nodes is to use mesh smoothing or mesh morphing algorithms. Mesh smoothing can be done by using a Laplace smoother [5]. This method works quite well as long as the mesh deformation doesn't exceed a critical level. If a critical level is reached, elements could overlap each other or even invert. Both cases cause false results. These critical levels are reached fast especially around singularities, like sharp corners. With application to typical MEMS structures like comb drives, perforated membranes or micro mirrors, large displacements and deformations typically occur. To overcome these problems a mesh morphing algorithm using radial basis functions (RBF) is used [6–8].

The resulting meshes of an example structure with large displacement is compared in the following figure (Figure 1). The mechanical structure (grey filled) is moved and the resulting mesh is shown after applying the Laplace smoother and the RBF mesh morphing algorithm. An element overlapping occur with the Laplace equation because every direction in space is independently solved. A perfect alignment of the deformed mesh is achieved by using RBFs.

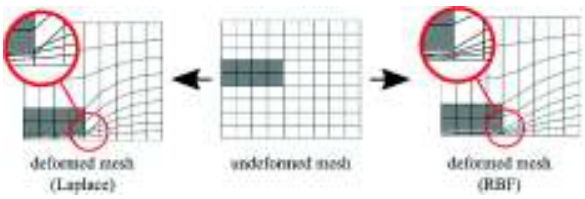

Fig. 1: Mesh deformation on a sample structure. Undeformed mesh (Middle), Laplace smoother result (Left), Mesh morphing with RBF (Right).

The theory behind this mesh morphing technique is presented in the following. The displacements x on the mechanical interface/boundary nodes and n_{m} are known. The remaining node displacements are approximated using a sum of basis functions and a linear polynomial.

$$x(P) = \sum_{j=1}^{n_{\mathrm{b}}} \alpha_j \Phi(\|P - P_{\mathrm{m},j}\|_2) + p(P) \tag{9}$$

There are two different coefficient vectors $\boldsymbol{\alpha}$ and $\boldsymbol{\beta}$ which are determined through the known displacements at the interface and boundary nodes on the mechanical domain. The first coefficient $\boldsymbol{\alpha}$ is related to the distance or Euclidian norm

wrt. the mechanical nodes. The second coefficient $\boldsymbol{\beta}$ is related to a linear polynomial term $p(P)$ which takes the global node coordinates P into account. This term generates an additional dependence between all directions in space (10), where P_m is a $n_\mathrm{m} \times 4$ matrix consists of 3D interface and boundary node coordinates with its components $[1 \quad P_{\mathrm{m},x} \quad P_{\mathrm{m},y} \quad P_{\mathrm{m},z}]$.

$$p(P) = [1 \quad P_x \quad P_y \quad P_z] \cdot \boldsymbol{\beta} \tag{10}$$

TABLE I
COMMON RADIAL BASIS FUNCTIONS

Radial basis function	$\Phi(r)$
Polyharmonic spline	r^k , odd k
Multiquadratic	$\sqrt{1+r^2}$
Inverse multiquadratic	$\frac{1}{\sqrt{1+r^2}}$
Inverse quadratic	$\frac{1}{1+r^2}$
Gaussian	e^{-r^2}

The function Φ represents a meshless interpolation function. It computes the distance from any point to every mechanical interface node and weight them with a radial basis function. There are many different radial symmetric functions available. In the following table the most common and useable RBFs are given [9].

It turns out that polyharmonic splines and normal/inverse multiquadratic basis function are the best choice in terms of mesh morphing. The polyharmonic splines have the advantage of less computation effort.

To compute the coefficient vectors $\boldsymbol{\alpha}$ and $\boldsymbol{\beta}$ the following system of equations in matrix form is solved in (11). The matrix $M_{\mathrm{m,m}}$ is a $n_\mathrm{m} \times n_\mathrm{m}$ contains the evaluated radial basis functions $\Phi_{\mathrm{m}_i,\mathrm{m}_j} = \Phi(\|P_{\mathrm{m}_i} - P_{\mathrm{m},j}\|_2)$. Thereby only nodes with known displacements x are considered. The coefficient vectors are solved for every direction in space and can be done fast since the system matrix is symmetrical.

$$\begin{bmatrix} x_\mathrm{m} \\ 0 \end{bmatrix} = \begin{bmatrix} M_{\mathrm{m,m}} & P_\mathrm{m} \\ P_\mathrm{m}^T & 0 \end{bmatrix} \begin{bmatrix} \boldsymbol{\alpha} \\ \boldsymbol{\beta} \end{bmatrix} \tag{11}$$

The back transformation from computed coefficients to unknown displacements of the mesh can be done using (9). In that way a mesh morphing algorithm can be realized. The computation of the coefficients is either precomputed in respect to the undeformed mesh or iteratively computed with the use of the updated node coordinates. Both ways are acceptable to achieve good results in a large deformed mesh. The electrical properties are nearly independent to the degree of deformation. That means the elements can have large distortion and the resulting effects are still in an acceptable range.

V. VALIDATION

To validate the strongly coupled electromechanical element with integrated mesh morphing we investigate in typical MEMS capacitive actuators. We compare the results with an ANSYS model containing exactly the same mesh. The electrical domain in the ANSYS model is remeshed.

A good validation sample is a comb drive cell. It consists of one moving and one fixed comb drive finger structure. In addition, there a top and bottom electrode modelled which are connected to ground potential. The moving finger can move in every space direction. We cover gap-varying and area-varying capacitances. The capacitance C and electrostatic force F_{el} are compared to the ANSYS results. We can prove that there is a negligible small error between the remeshed ANSYS model and our model using mesh morphing.

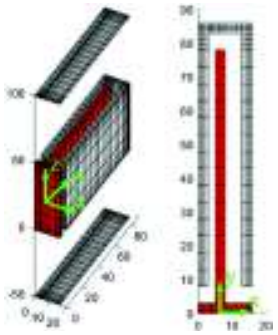

Fig. 2: Comb cell used for validation

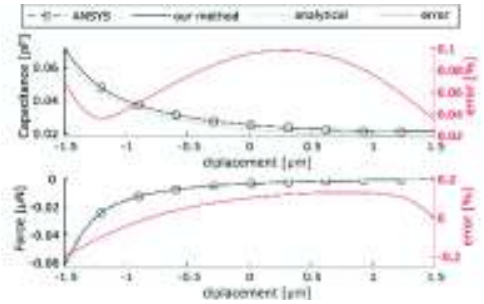

Fig. 3: Capacitance vs. x-displacement (top), electrostatic force vs. x-displacement (bottom)

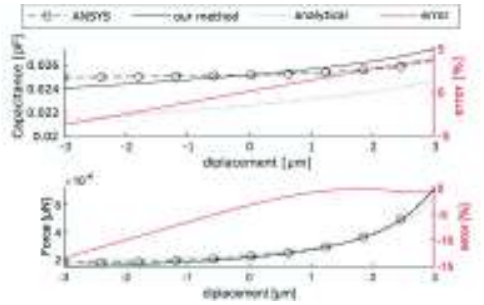

Fig. 4: Capacitance vs. y-displacement (top), electrostatic force vs. y-displacement (bottom)

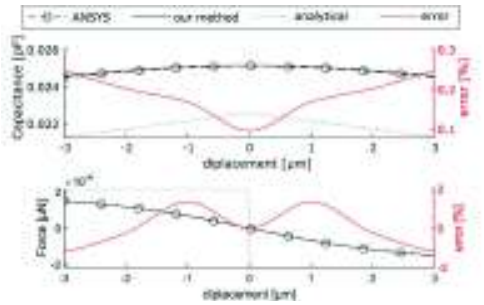

Fig. 5: Capacitance vs. z-displacement (top), electrostatic force vs. z-displacement (bottom)

VI. Further Examples

In order to show the spectrum of possible usages of this FE formulation, more complex models were created. Only a sectional view is shown to make the complex meshes depictable. The mechanical structure (solid gray) is shown undeflected on the top and large deflected on bottom. An electrical field was also computed to demonstrate the independence of element distortion. The deformed meshes containing no invalid/inverted elements.

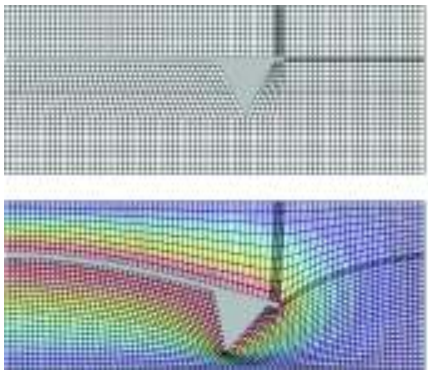

Fig. 6: AFM-tip - undeflected (top), deflected (bottom)

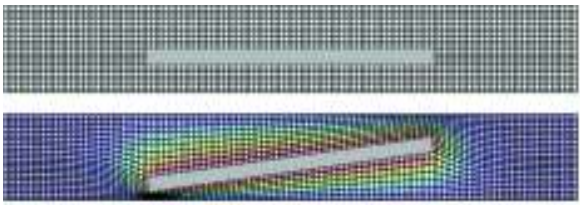

Fig. 7: Micro mirror - undeflected (top), deflected (bottom)

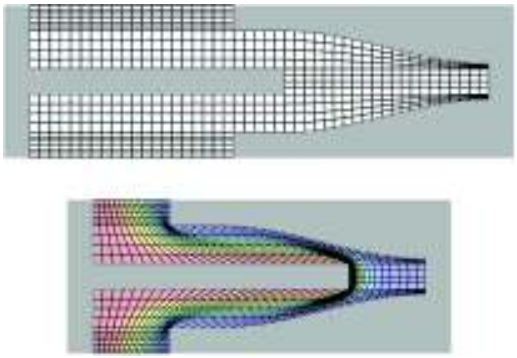

Fig. 8: Complex comb drive - undeflected (top), deflected (bottom)

VII. Conclusion

A new formulation for electromechanical transducer elements was introduced. By differentiating the electrical energy an accurate description of the energy transfer phenomena in electrostatic field problem was found. This formulation uses an integrated mesh morphing algorithm which makes a time consuming remeshing of the model while simulating unnecessary. Moreover, the radial basis function approach in the mesh morphing algorithm allows also highly deformed meshes while overlapping or inverting elements are avoided. Usage of traditional shape functions and solvers makes this method fully integrable into existing FE simulation tools. The spectrum of application is widespread in the field of MEMS. Especially structures with large nonlinear deformable mechanical structures which usually required remeshing are comfortable solvable. Some more complex models which demonstrates that the FE formulation is independent of the complexity. Structures like micro mirrors, AFM tips, micro switches or even more complex is aimed to solved. The effects of nonlinear changing capacitances, electrostatic softening and fringing field effects are included in the method. The strongly coupled matrix formulation opens up the possibility to use any kind of analysis, as modal or harmonic analysis. Furthermore, additional reduced order model techniques can be to create an even more faster simulation model.

References

[1] M. Kaltenbacher, *Numerical Simulation of Mechatronic Sensors and Actuators: Finite Elements for Computational Multiphysics,* 3rd ed. Berlin, Heidelberg: Springer Berlin Heidelberg, 2015. [Online]. Available: http://ebooks.ciando.com/book/index.cfm/bok_id/1868085

[2] S Mukhopadhyay and N. Majumdar, *Use of the neBEM solver to Compute the 3D Electrostatic Properties of Comb Drives*, 2007. [Online]. Available: https://www.researchgate.net/publication/2177896_Use_of_the_neBEM_solver_to_Compute_the_3D_Electrostatic_Properties_of_Comb_Drives

[3] V. Rochus, D. J. Rixen, and J.-C. Golinval, "Monolithic modelling of electro-mechanical coupling in micro-structures," *Int. J. Numer. Meth. Engng.*, vol. 65, no. 4, pp. 461–493, 2006, doi: 10.1002/nme.1450.

[4] M. Gyimesi, I. Avdeev, and D. Ostergaard, "Finite-Element Simulation of Micro-Electromechanical Systems (MEMS) by Strongly Coupled Electromechanical Transducers," *IEEE Trans. Magn.*, vol. 40, no. 2, pp. 557–560, 2004, doi: 10.1109/TMAG.2004.824592.

[5] L. R. Herrmann, "Laplacian-Isoparametric Grid Generation Scheme," *J. Engrg. Mech. Div.*, vol. 102, no. 5, pp. 749–756, 1976, doi: 10.1061/JMCEA3.0002158.

[6] A. de Boer, M. S. van der Schoot, and H. Bijl, "Mesh deformation based on radial basis function interpolation," *Computers & Structures*, vol. 85, 11-14, pp. 784–795, 2007, doi: 10.1016/j.compstruc.2007.01.013.

[7] M. E. Biancolini, "Mesh Morphing and Smoothing by Means of Radial Basis Functions (RBF)," in *Advances in Computer and Electrical Engineering, Handbook of Research on Computational Science and Engineering*, S. Patnaik, J. Leng, and W. Sharrock, Eds.: IGI Global, 2012, pp. 347–380.

[8] A. Beckert and H. Wendland, "Multivariate interpolation for fluid-structure-interaction problems using radial basis functions," *Aerospace Science and Technology*, vol. 5, no. 2, pp. 125–134, 2001, doi: 10.1016/S1270-9638(00)01087-7.

[9] M. E. Biancolini, Ed., *Fast Radial Basis Functions for Engineering Applications*. Cham: Springer, 2018.

Generating links that are both quasi-alternating and almost alternating

Hamid Abchir[1] and Mohammed Sabak[2]

[1]Hassan II University. EST. Route d'El Jadida Km 7. B.P. 8012. 20100 Casablanca. Morocco.
e-mail: hamid.abchir@univh2c.ma
[2]Hassan II University. Ain Chock Faculty of sciences. Route d'El Jadida Km 8. B.P. 5366. Maarif.
20100 Casablanca. Morocco. e-mail: mohammed.sabak-etu@etu.univh2c.ma

1st March 2021

Abstract

We construct an infinite family of links which are both almost alternating and quasi-alternating from a given either almost alternating diagram representing a quasi-alternating link, or connected and reduced alternating tangle diagram. To do that we use what we call a dealternator extension which consists in replacing the dealternator by a rational tangle extending it. We note that all not alternating and quasi-alternating Montesinos links can be obtained in that way. We check that all the obtained quasi-alternating links satisfy Conjecture 3.1 of Qazaqzeh et al. (JKTR 22 (06), 2013), that is the crossing number of a quasi-alternating link is less than or equal to its determinant. We also prove that the converse of Theorem 3.3 of Qazaqzeh et al. (JKTR 24 (01), 2015) is false.

1 Introduction

The set of quasi-alternating links appeared in the context of link homology as a natural generalization of alternating links. They were defined in [19] where the authors showed that they are homologically thin for both Khovanov homology and knot Floer homology as alternating links with which they share many properties. On the other hand, it was shown in [19] that every non split alternating link is quasi-alternating and that the branched double cover of any quasi-alternating link is an L-space.
If D is a link diagram, we denote by $\mathcal{L}(D)$ the link for which D is a projection. Quasi-alternating links are defined recursively as follows:

Definition 1. The set $\mathcal{Q}$ of **quasi-alternating links** is the smallest set of links satisfying the following properties:

1. The unknot belongs to $\mathcal{Q}$,
2. if L is a link with a diagram D containing a crossing c such that
   (a) for both smoothings of the diagram D at the crossing c denoted by D_0^c and D_∞^c as in figure 1), the links $\mathcal{L}(D_0^c)$ and $\mathcal{L}(D_\infty^c)$ are in $\mathcal{Q}$ and,
   (b) $\det(L) = \det(\mathcal{L}(D_0^c)) + \det(\mathcal{L}(D_\infty^c))$.

   Then L is in $\mathcal{Q}$. In this case we will say that c is a *quasi-alternating crossing* of D and that D is quasi-alternating at c.

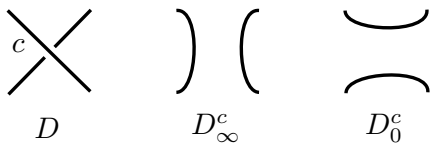

Figure 1: The link diagram D and its smoothings D_0^c and D_∞^c at the crossing c.

Champanerkar and Kofman proved that quasi-alternating property is inheritable via *rational extension* of a quasi-alternating crossing [4], that is the operation which consists in replacing a quasi-alternating crossing of a diagram by a rational tangle extending it as in Fig. 13.
Champanerkar and Kofman proved the following theorem.

Theorem 1.1 (Theorem 2.1, [4])**.** *If D is a quasi-alternating link diagram, let $D^{c\leftarrow T}$ be the link diagram obtained by replacing any quasi-alternating crossing c with an alternating rational tangle T that extends c. Then $D^{c\leftarrow T}$ is quasi-alternating.*

Thus the last theorem provides a way to get new quasi-alternating diagrams from former ones.
Note that when one extends a quasi-alternating crossing, all crossings of the inserted tangle become quasi-alternating also, including the extended crossing itself.
In this paper we will give an other way to build new quasi-alternating diagrams also relying on rational extensions. Nevertheless, unlike what was done in [4], the crossing which will be extended will not be quasi-alternating. To do that, we will start with an almost alternating link diagram D, i.e. a diagram in which one crossing change makes it alternating. We suppose that $\mathcal{L}(D)$ is quasi-alternating. Then we consider a crossing the change of which makes the diagram alternating. Such a crossing is called a *dealternator* of D. Note that an almost alternating diagram can have more than one dealternator. But that cannot occur when that diagram is the projection of a quasi-alternating link (Proposition 2.2, [25]). Our first observation is that a dealternator cannot be a quasi-alternating crossing as mentionned in Corollary2. However, we show that there is a rational extension of D at the dealternator which generates a quasi-alternating diagram. We call such operation a *dealternator extension* of D. We get the following Theorem which is one of our main results.

Theorem 1.2. *Let D be an almost alternating diagram representing a quasi-alternating link. If c is the dealternator of D, then there exists a dealternator extension of D where c becomes a quasi-alternating crossing.*

The proof will be given in section 3 after a more detailed statement (Theorem 3.4).

On the other hand, we show that all non alternating quasi-alternating Montesinos links can be obtained by some dealternator extensions of rational links. In corollary 6, we check that any quasi-alternating link arising as a dealternator extension of an almost alternating diagram which represents a quasi-alternating link satisfies the following conjecture formulated by Khaled Qazaqzeh, Balqees Qublan and Abeer Jaradat in [20] and which compares the crossing number $c(L)$ of a quasi-alternating link L to its determinant $\det(L)$.

Conjecture 1.1. Every quasi-alternating link L satisfies $c(L) \leq \det(L)$.

The paper is organized as follows. In the second section we recall the main tools needed to prove our results, mainly graphs and tangles. We give a brief overview on the link families which we will deal with. We recall some of their properties. In the third section, we show Theorem 1.2 where the technique of dealternator extension is introduced and show some relative results. In the fourth section, we give some applications of Theorem 1.2. We describe a method of generating links which are both almost alternating and quasi-alternating. Then we show how that process allows to construct all non alternating quasi-alternating Montesinos links. The fifth section, is devoted to the consolidation of the conjecture 1.1. In the last section we answer the question asked by K. Qazaqzeh, N. Chbili and B. Qublan at the end of [21].

2 Preliminaries

2.1 Graphs

To prove some of our results, we will need some graph-theoretical machinery which will be found in [23].
For any connected link diagram D, we can associate a connected graph $G(D)$, called the Tait graph of D by checkerboard coloring complementary regions assigning a vertex to every shaded region, an edge to every crossing and a $\pm$ sign to every edge according to the convention in Fig. 2. Note that there are two choices for the checkerboard coloring which give dual graphs.

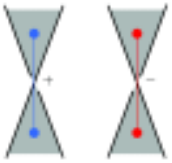

Figure 2: The sign convention for the Tait graph of a link diagram.

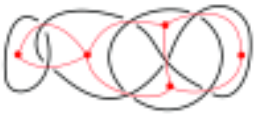

Figure 3: A Tait graph with only negative edges.

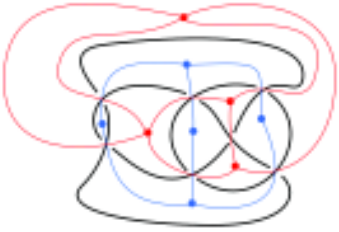

Figure 4: A Tait graph with only positive edges (in blue) and its dual (in red).

Since an edge and its dual have opposite signs, we will always choose the Tait graphs which have more positive edges than negative ones. Note that the edges of a Tait graph of an alternating link diagram are all of the same sign.

Graphs allow to get some link invariants like the determinant. A. Champanerkar and I. Kofman showed the following lemma [4].

Lemma 2.1. *For any spanning tree T of $G(D)$, let $v(T)$ be the number of positive edges in T. Let $s_k(D) = \#\{$ spanning trees T of $G(D) \mid v(T) = k\}$. Then*

$$\det(D) = \left| \sum_k (-1)^k s_k(D) \right|.$$

Remark 1. In particular, the determinant of an alternating link is the number of the spanning trees in a Tait graph of any alternating diagram of that link.

2.2 Tangles

In this paper, we call a *tangle* T any proper embedding of two disjoint arcs and a (possibly empty) set of loops in a 3-ball B^3. Two tangles T and T' are *equivalent* if there is an ambient isotopy of B^3 which is the identity on the boundary and which takes T to T'.
We assume that the four endpoints lie in the great circle of the boundary sphere of B^3 which joins the two poles. That great circle bounds a two disk B^2 in B^3. We consider a regular projection of B^3 on B^2. The image of a tangle T by that projection in which the height information is added at each of the double points is called a *tangle diagram* of T. Two tangle diagrams will be equivalent if they are related by a finite sequence of planar isotopies and Reidemeister moves in the interior of the *projection disk* B^2. Two tangles will be *equivalent* iff they have equivalent diagrams.
Depending on the context we will denote by T the tangle or its projection.

The four endpoints of the arcs in the diagram are usually labeled NW_T,NE_T,SE_T, and SW_T with symbols referring to the compass directions as in the Fig. 5.

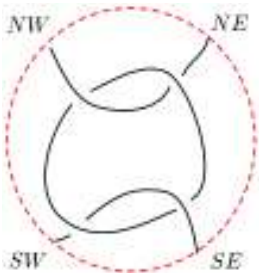

Figure 5: An alternating tangle diagram T.

A tangle diagram T is said to be *disconnected* if either there exists a simple closed curve embedded in the projection disk, called a *splitting loop*, which do not meet T, but encircles a part of it, or there exists a simple arc properly embedded in the projection disk, called a *splitting arc*, which do not meet T and splits the projection disk into two disks each one containing a part of T. A tangle diagram is *connected* if it is not disconnected.

A tangle diagram is *reduced* if its number of crossings can not be reduced by any tangle equivalence.

A tangle diagram T is said to be *locally knotted* if there exists a simple closed curve C embedded in the interior of the disk projection, called a *factorizing circle* of T, which meets T transversally at two points and bounds a disk inside the disk projection which meets T in a knotted spanning arc.

We adopt the notations used for rational tangles by L. J ay R. Goldman and H. Kauffman in [8] and L. H. Kauffman and S. Lambroupoulou in [12]. In the figure 6, we recall some operations defined on tangles.

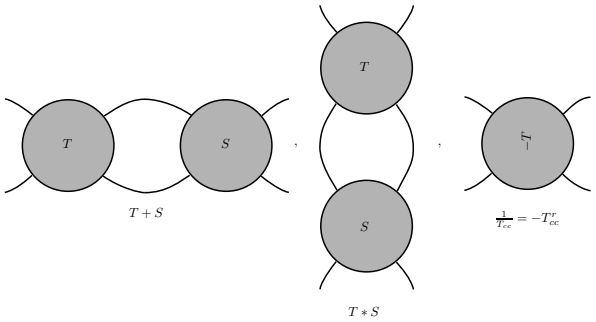

Figure 6: Some operations on tangle diagrams.

A $(-\pi)$ rotation of a tangle diagram T in the horizontal axis is called *horizontal Flip* and will be denoted by T_h. That is the tangle diagram obtained by rotating the ball containing T in space around the horizontal axis as shown in Fig. 7 and then project the new tangle by the same projection function as that used to get T. Note that if T is an alternating tangle diagram, then T_h is also alternating. Note that the Flip operation preseves the isotopy class of a rational tangle (Flip Theorem 1. [8]).

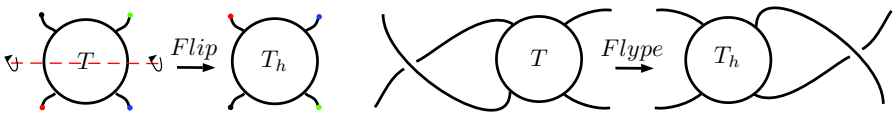

Figure 7:

A *flype* is an isotopy of tangles that is depicted by the Fig. 7.

A tangle diagram T provides two link diagrams: the *Numerator* of T, denoted by $n(T)$, which is obtained by joining with simple arcs the two upper endpoints (NW_T, NE_T) and the two lower endpoints (SW_T, SE_T) of T, and the *Denominator* of T, denoted by $d(T)$, which is obtained by joining with simple arcs each pair of the corresponding top and bottom endpoints (NW_T, SW_T) and (NE_T, SE_T) of T (see Fig. 8). We denote $N(T)$ and $D(T)$ respectively the corresponding links.

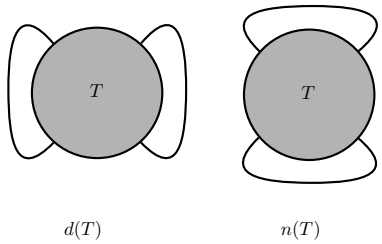

Figure 8: The denominator and the numerator of a tangle diagram T.

As in the case of link diagrams, one can associates to each tangle diagram T a signed planar graph by choosing a checkerboard coloring of T. This graph will also have a dual graph. The signed planar graph of T may be put inside the projection disk such that two of its vertices are evenly spaced on the boundary circle and which we call *boundary vertices*. We denote it by $G_d(T)$ when its boundary vertices happen to be on the lateral sides of the boundary circle. If one boundary is on the upper arc and the other on the lower arc of the boundary circle, we will denote the graph by $G_n(T)$. Note that $G_n(T)$ and $G_d(T)$ are respectively Tait graphs of $n(T)$ and $d(T)$ (see Fig. 9).

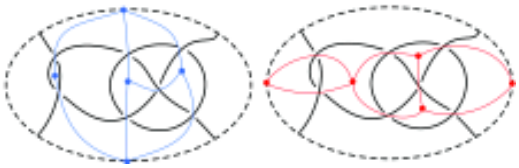

Figure 9: The graph $G_n(T)$ on the left and $G_d(T)$ on the right.

If T is a connected tangle diagram, then $G_n(T)$ and $G_d(T)$ are both connected graphs (see [10]).
Denote by u and v the boundary vertices of $G_d(T)$. We join u to v by a simple arc in the exterior of the disk projection. If we coalesce u and v by contracting that arc, then we get the dual of $G_n(T)$ which is also a Tait graph of $n(T)$ (compare the three graphs in Fig. 3 and Fig. 4).

A tangle diagram T is called *alternating* if the "over" or "under" nature of the crossings alternates as one moves along any arc of T. A tangle is said to be *alternating* if it admits an alternating diagram. A tangle diagram T is alternating iff all the edges of $G_d(T)$ are of the same sign.

We will need the following lemma.

Lemma 2.2. *If T is an alternating connected locally unknotted tangle diagram, then $n(T)$ or $d(T)$ is prime.*

Proof. Let us assume that $d(T)$ is not prime. Then there exists a closed simple curve C in the plane meeting $d(T)$ transversely in two points x and y, and which factorizes $d(T)$. The curve C bounds a disk Δ in the plane. It is easy to see that the only possible case for x and y is that they are both located inside the disk projection B^2.
Consider the connected graph $G_d(T)$ introduced above with its boundary vertices u and v. We can assume that $G_d(T)$ meets C in only one cut vertex a. Furthermore Δ contains a single denominator closure arc, then each connected component of $G_d(T) \setminus a$ contains a boundary vertex. Denote by H_u and H_v the connected components of $G_d(T) \setminus a$ containing respectively u and v. Let o and o' be two vertices of $G_d(T)$ contained respectively in H_u and H_v and distinct from a. By connectedness of $d(T)$ and Theorem 6 in [26], there exists a chain c from u to v, passing through o, a, and o'. When coalescing u and v, the chain c becomes a cycle c' of $G_n(T)$ containing u, v, o, a, and o'. Note that any cycle of $G_d(T)$ is also a cycle of $G_n(T)$ by coalescing u and v. We conclude that, if o and o' are not already contained in some cycle of $G_d(T)$, then they are contained in the cycle c' of $G_n(T)$. The graph $G_n(T)$ is then non-separable by Theorem 7 in [26]. Since, as stated in [23], non-separable graphs correspond to prime link diagrams, hence, $n(T)$ is prime.
Since $n(T) = d(\frac{1}{T}_{cc})$, then the above argument shows that when $n(T)$ is composite, $d(T)$ is prime. □

Let T be an alternating connected tangle diagram. Consider the arc of T which have NW_T as an endpoint. Suppose that when we move along that arc starting at NW_T we pass below at the first encountered crossing.

Then all edges of $G_n(T)$ will be positive, all edges of $G_d(T)$ will be negative, the arc of T which ends at the point SE_T will also pass below at the last encountered crossing before reaching SE_T and the arc of T which starts at NE_T will pass over at the first encountered crossing. It is easy to see that the arcs of T coming from diametrically opposite endpoints both pass over or below at the first encountered crossing. That remark enables us to distinguish two types of alternating connected tangle diagrams which we call *type 1* tangles and *type 2* tangles as shown in the Fig. 10. Throughout the rest of this paper, all the considered alternating tangle diagrams will be assumed to be of type 1 unless otherwise stated.

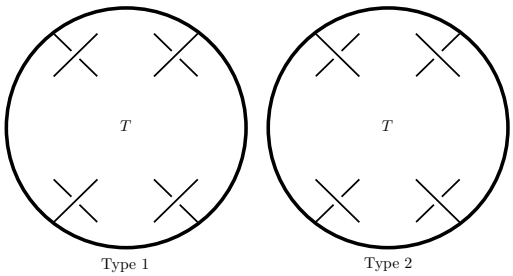

Figure 10: Type 1 and Type 2 alternating tangle diagrams.

Let T be an alternating tangle diagram in B^2. Then $n(T)$ and $d(T)$ are both alternating diagrams. If $n(T)$ and $d(T)$ are also connected and reduced, then T is said to be *strongly alternating*.

2.3 Rational tangles

A *rational tangle* t is a tangle in B^3 such that the pair (B^3, t) is homeomorphic to $(B^2 \times [0,1], \{x, y\} \times [0,1])$, where x and y are points in the interior of B^2. The elementary rational tangle diagrams 0, ± 1, ∞ are shown in Fig. 11.

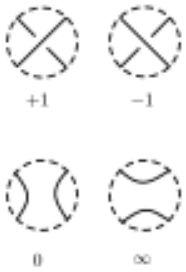

Figure 11: Elementary rational tangles.

The sum of n copies of the tangle diagram 1 or of n copies of the tangle -1 are respectively the *integral tangle diagrams* denoted also by n and $-n$. If t is a rational tangle diagram then $\frac{1}{t_c}$ and $\frac{1}{t_{cc}}$ are equivalent and both represent the *inversion* of t denoted by $\frac{1}{t}$.

Let t be a rational tangle diagram and $p, q \in \mathbb{Z}$, we have the following equivalences:

$$p + t + q = t + p + q \, , \, \frac{1}{p} * t * \frac{1}{q} = t * \frac{1}{p+q}.$$

$$t * \frac{1}{p} = \frac{1}{p + \frac{1}{t}} \, , \, \frac{1}{p} * t = \frac{1}{\frac{1}{t} + p}.$$

Using the above notations and equivalences one can naturally associate to any continued fraction

$$a_1 + \cfrac{1}{a_2 + \cfrac{1}{\ddots + \cfrac{1}{a_{n-1} + \cfrac{1}{a_n}}}}, \;\; a_i \in \mathbb{Z},$$

a tangle diagram as shown in Fig. 12 denoted by $[a_1, ..., a_n]$.

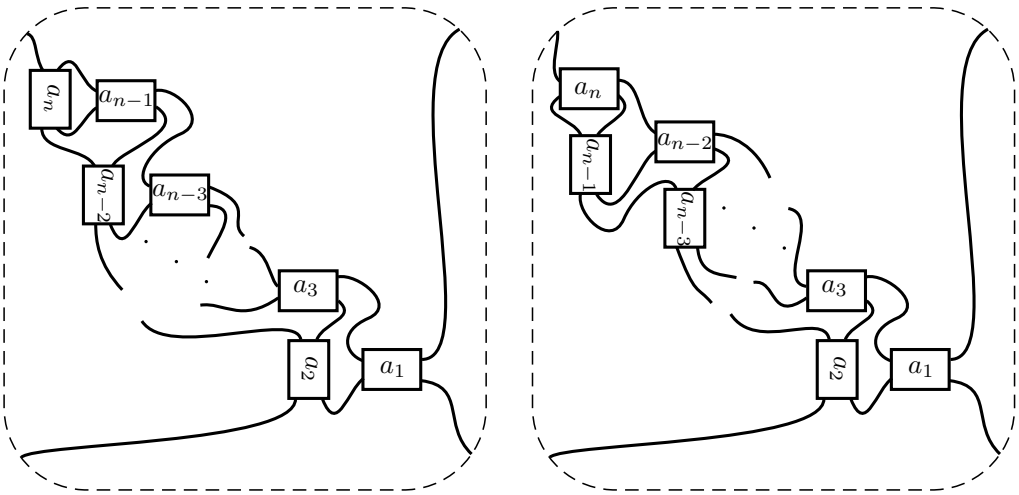

Figure 12: The standard rational tangle diagram $[a_1, ..., a_n]$ according to n is even (left) or odd (right).

Conversely, it is known that for any rational tangle t, there exists an integer $n \geq 1$ and integers $a_1 \in \mathbb{Z}$, $a_2, ..., a_n \in \mathbb{Z} \setminus \{0\}$, all of the same sign, such that $t = [a_1, ..., a_n]$. Then t corresponds to a continued fraction and then to a rational number called the fraction of the tangle.

J. H. Conway showed in [7] that two rational tangles are equivalent if and only if they have the same fraction. Then any rational tangle t can be represented by a continued fraction $[a_1, ..., a_n] = \frac{a}{b}$ where a and b are two coprime integers.

The *standard diagram* of a rational tangle t will be the alternating connected reduced locally unknotted diagram naturally associated to the continued fraction of t described above. In what follows a rational tangle diagram will mean the standard one.

2.4 Rational extensions

Let c be a crossing of some link diagram. It can be considered as a 2-tangle with marked end points. By using Conway's notation for rational tangles, we assign to c the number $\varepsilon(c) \in \{-1, 1\}$ according to whether the overstrand has negative or positive slope as depicted in the figure below.

$\varepsilon(c) = 1$ $\quad$ $\varepsilon(c) = -1$

We recall the technic of rational extension used by A. Champanerkar and I. Kofman in [4]. We say that a rational 2-tangle $t = [a_1, ..., a_n]$ *extends* the crossing c if t contains c and for all i, $a_i.\varepsilon(c) \geq 1$. That means that all crossings of t have the same Conway sign as that of c. One can always replace a crossing c in some link diagram D with a rational 2-tangle t which extends it to get a new link diagram which we will denote by $D^{c \leftarrow t}$. This diagrammatic operation is called a *rational extension* of c with t. We will say that c is *the extended crossing*, and t is an *extension tangle* of c. The link diagram $D^{c \leftarrow t}$ will be called a rational extension of D at c.

A rational extension with fraction $\frac{13}{4} = 3 + \frac{1}{4}$ of the diagram of the Hopf link is depicted in the Fig. 13.

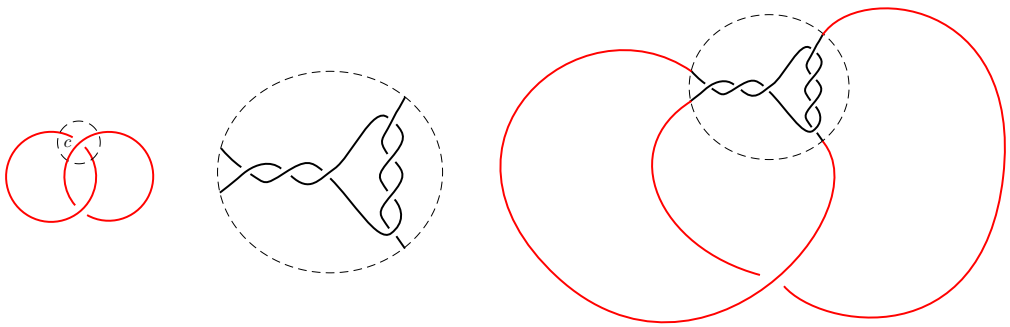

Figure 13: From the left: Hopf link, rational tangle $[3,4] = \frac{13}{4}$ and rational extension $D^{c\leftarrow\frac{13}{4}}$.

2.5 Almost alternating links

A link diagram D is said to be *almost alternating* if one crossing change makes it alternating. A crossing whose change yields an alternating diagram is called a *dealternator*. A link L is said to be almost alternating if it is not alternating and has an almost alternating diagram. Recall that the category of almost alternating links was first introduced by Adams, Brock, Bugbee, Comar, Huston, and Jose in [2].

Note that if a link diagram is an almost alternating diagram with one dealternator then the edges of its Tait graph are all of the same sign except that associated to the dealternator which will be of opposite sign. Throughout the rest of the paper, we will consider only the Tait graphs for which the edge corresponding to the dealternator is negative.

Let D be an almost alternating link diagram with dealternator c. We will consider c as the rational tangle -1 (rotate D if necessary). If both smoothings D_0^c and D_∞^c of D at c are reduced alternating link diagrams, then D is said to be *dealternator reduced*. If those both smoothings are connected alternating link diagrams, then D is said to be *dealternator connected*. A typical example of a dealternator connected reduced link diagram that we will need in the following is the link diagram $n(-1+T)$ where T is a strongly alternating tangle diagram.

Remark 2. Let L be an almost alternating link. Let D be an almost alternating diagram of L which has the smallest crossing number among all almost alternating diagrams of L. Then D has only one dealternator c and it is a dealternator connected reduced diagram as showed in the proof of the Corollary 4.5 in [2]. It is easy to show that the diagram D is equivalent to the numerator $n(-1+T)$ where T is a strongly alternating tangle diagram. Hence L is equivalent to $N(-1+T)$.

On the other hand, in the following, we will need to study if a link $L = N(-1+T)$ is quasi-alternating. Actually it is sufficient to restrict to the cases where T is locally unknotted as explained in the following remark.

Remark 3. Consider a link $L = N(-1+T)$. If T is locally knotted, then L has at least an alternating factor. Let C be a factorizing circle of T. Denote by a and b the intersection points of C and T. Remove the disk bounded by C and containing the alternating factor.Then, replace it with a disk containing one simple arc joining a to b. We can repeat this operation until all alternating factors will be removed. Then we get a link $L^{'} = N(-1+T^{'})$ where $T^{'}$ is a locally unknotted tangle diagram. Those operations preserve the property of being quasi-alternating. Furthermore, the link L is the connected sum of $L^{'}$ with some alternating factors. Since the connected sum of any quasi-alternating links is quasi-alternating [19], then if $L^{'}$ is quasi alternating then so will be L.

3 Dealternator extensions

Let D be an almost alternating diagram with dealternator c. The determinant of D is given in term of the determinants of D_0^c and D_∞^c as stated in the following Proposition.

Proposition 3.1. *Let D be an almost alternating diagram with dealternator c. Then*

$$\det(D) = \left|\det\left(D_0^c\right) - \det\left(D_\infty^c\right)\right|.$$

Proof. Let G_D be the Tait graph of D such that the unique negative edge is that one corresponding to c. Call that edge e_c. The set $\mathcal{T}(G_D)$ of spanning trees of G_D admits a partition $\mathcal{T}_0^c(G_D) \uplus \mathcal{T}_\infty^c(G_D)$ where:

$$\mathcal{T}_\infty^c(G_D) = \{T \in \mathcal{T}(G_D)/e_c \in T\} \text{ , and } \mathcal{T}_0^c(G_D) = \{T \in \mathcal{T}(G_D)/e_c \notin T\}.$$

A tree in $\mathcal{T}_0^c(G_D)$ can be seen as a spanning tree of $G_{D_0^c}$. And if we contract the edge e_c in a tree in $\mathcal{T}_\infty^c(G_D)$ we get a spanning tree of $G_{D_\infty^c}$. Those correspondences are actually one-to-one following [4]. Let $T \in \mathcal{T}(G_D)$, then $e(T) = e_+(T) + e_-(T) = v(G_D) - 1$. If T is in $\mathcal{T}_\infty^c(G_D)$, then $e(T) = e_+(T) + 1 = v(G_D) - 1$, which gives $e_+(T) = v(G_D) - 2$. If T is in $\mathcal{T}_0^c(G_D)$, then $e(T) = e_+(T) = v(G_D) - 1$. This way we have

$$\begin{aligned}\sum_k (-1)^k s_k(D) =& (-1)^{v(G_D)-1} s_{v(G_D)-1}(D) + (-1)^{v(G_D)-2} s_{v(G_D)-2}(D) \\ =& (-1)^{v(G_D)-1} \#\mathcal{T}_0^c(G_D) + (-1)^{v(G_D)-2} \#\mathcal{T}_\infty^c(G_D) \\ =& (-1)^{v(G_D)-1} \#\mathcal{T}(G_{D_0^c}) + (-1)^{v(G_D)-2} \#\mathcal{T}(G_{D_\infty^c}) \\ =& (-1)^{v(G_D)-1} \det(D_0^c) + (-1)^{v(G_D)-2} \det(D_\infty^c) \\ =& (-1)^{v(G_D)-1} \left(\det(D_0^c) - \det(D_\infty^c)\right)\end{aligned}$$

The result then follows using Theorem 2.1. □

Remark 4. Links with vanishing determinants are not quasi-alternating. This implies that if an almost alternating diagram D is representing a quasi-alternating link, then the determinants of D_0^c and D_∞^c must differ if c is the dealternator of D. When $\mathcal{L}(D)$ is also almost alternating, this diffrence has a lower bound (see Corollary 1.2, [16]).

Corollary 1. *Let D be an almost alternating link diagram with dealternator c. Suppose that $L(D)$ is quasi-alternating, then*

$$\det\left(D_0^c\right) \neq \det\left(D_\infty^c\right).$$

If $\mathcal{L}(D)$ is also almost alternating, then $\left|\det\left(D_0^c\right) - \det\left(D_\infty^c\right)\right| \geq 8$.

Corollary 2. *An almost alternating diagram is never quasi-alternating at its dealternator.*

Proposition 3.2. *Let T be an alternating tangle diagram and let $\frac{\alpha}{\beta} > 0$ be a rational number. We have the following*

1. $\det(n(\frac{\alpha}{\beta} + T)) = \beta \det(n(T)) + \alpha \det(d(T))$.
2. $\det(n(-\frac{\alpha}{\beta} + T)) = \left|\beta \det(n(T)) - \alpha \det(d(T))\right|$.

Remark 5. If t and T are respectively a rational and an alternating tangle diagrams, the link diagram $n(t+T)$ is equivalent, up to mirror image, to the link diagram $n(\frac{1}{t} + \frac{1}{T_c})$ as shown in the figure below. Since the tangle diagram $\frac{1}{T_c}$ is also alternating, one can only restrict to the case where $0 < |t| < 1$ when considering the numerator closure of t summed with an alternating tangle diagram.

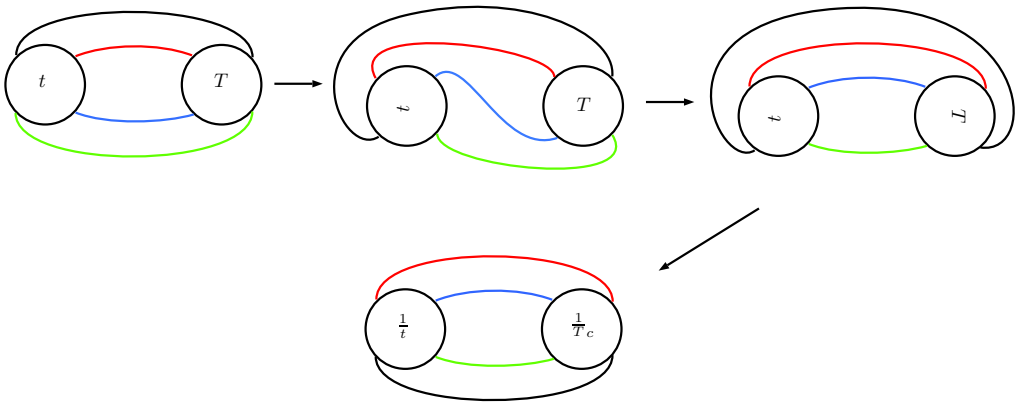

Proof of Proposition 3.2. First part of the proposition: by Remark 5, we can assume that $0 < \frac{\alpha}{\beta} < 1$ and then we write $\frac{\alpha}{\beta} = [0, a_1, ..., a_k]$ where k is a positive integer such that $a_i \geq 1$ for each i. We will use induction on the number k of integer tangles which consist the rational tangle diagram corresponding to the fraction $\frac{\alpha}{\beta} = [0, a_1, ..., a_k]$. For $k = 1$, we have $\frac{\alpha}{\beta} = \frac{1}{p}$ for some integer $p \geq 1$. In this case we have $n(\frac{\alpha}{\beta}+T) = n(\frac{1}{p}+T)$ which is an alternating link diagram which we denote by D_p. Let us label by $c_1, ..., c_p$ the crossings of the vertical tangle $\frac{1}{p}$ respectively from the top. It is clear that $(D_j)_0^{c_s} = D_{j-1}$ and $(D_j)_\infty^{c_s} = n(T)$ for each j, $1 \leq j \leq p$, and for each s, $1 \leq s \leq j$. Since the link diagram D_j is quasi-alternating at the crossing c_j, we have

$$\begin{aligned}\det(n(\frac{1}{p} + T)) &= \det(D_p)\\ &= \det(D_{p-1}) + \det(n(T))\\ &\vdots\\ &= p\det(n(T) + \det(d(T))).\end{aligned}$$

Suppose the result holds until some rank k. Put $\frac{\alpha}{\beta} = [0, a_1, ..., a_k]$ and $\frac{\gamma}{\delta} = [0, q, a_1, ..., a_k]$ for some integer $q \geq 1$. It is clear that $[0, q, a_1, ..., a_k] = [a_1, ..., a_k] * \frac{1}{q}$. Thus, we have $\frac{\gamma}{\delta} = \frac{\beta}{\alpha} * \frac{1}{q} = \frac{1}{q+\frac{\alpha}{\beta}} = \frac{\beta}{q\beta+\alpha}$. Denote by $\mathcal{D}_j$ the link diagram $n(\frac{\beta}{\alpha} * \frac{1}{j} + T)$ for each j, $0 \leq j \leq q$. Also denote by $c_1, ..., c_j$ the crossings of the vertical tangle $\frac{1}{j}$ respectively from the top. It is clear that $(\mathcal{D}_j)_0^{c_j} = \mathcal{D}_{j-1}$, and $(\mathcal{D}_j)_\infty^{c_j} = n(\frac{\beta}{\alpha})\#n(T)$. Now since the link diagram $\mathcal{D}_j$ is quasi-alternating at the crossing c_j for every $1 \leq j \leq q$, we have

$$\begin{aligned}\det(\frac{\gamma}{\delta} + T) &= \det(\mathcal{D}_q)\\ &= \det(\mathcal{D}_{q-1}) + \beta\det(n(T))\\ &\vdots\\ &= \det(n(\frac{\beta}{\alpha} + T)) + q\beta\det(n(T)).\end{aligned}$$

By Remark 5, we have $\det(n(\frac{\beta}{\alpha} + T)) = \det(n(\frac{\alpha}{\beta} + \frac{1}{T_c}))$. Since $\frac{\alpha}{\beta} = [0, a_1, ..., a_k]$ consists of k integer tangles, then by the induction hypothesis we have

$$\begin{aligned}\det(n(\frac{\beta}{\alpha} + T)) &= \det(n(\frac{\alpha}{\beta} + \frac{1}{T_c}))\\ &= \beta\det(n(\frac{1}{T_c})) + \alpha\det(d(\frac{1}{T_c}))\\ &= \beta\det(d(T)) + \alpha\det(n(T)).\end{aligned}$$

This way we have

$$\begin{aligned}\det(\frac{\gamma}{\delta} + T) &= \det(n(\frac{\beta}{\alpha} + T)) + q\beta\det(n(T))\\ &= \beta\det(d(T)) + \alpha\det(n(T)) + q\beta\det(n(T))\\ &= (\alpha + q\beta)\det(n(T)) + \beta\det(d(T))\\ &= \delta\det(n(T)) + \gamma\det(d(T)).\end{aligned}$$

This completes the induction argument.
Second part of the proposition: Let D denote the almost alternating link diagram $n(-1 + \frac{b-a}{b} + T)$ and let c denote its dealternator. The link diagram D is equivalent to $n(\frac{-a}{b} + T)$ by the rational tangle equivalence $-1 + \frac{b-a}{b} = \frac{-a}{b}$. The link diagrams D_0^c and D_∞^c are respectively equivalent to $n(\frac{b-a}{b} + T)$ and $d(\frac{b-a}{b})\#d(T)$. We have $\det(D_0^c) = (b-a)\det(d(T)) + b\det(n(T))$, and $\det(D_\infty^c) = b\det(d(T))$. By Proposition 3.1 we

have

$$\begin{aligned}\det(D) &= \det(n(-\frac{a}{b}+T)\\ &= \left|\det(n(\frac{b-a}{b}+T))-\det(d(\frac{b-a}{b})\#d(T))\right|\\ &= |(b-a)\det(d(T))+b\det(n(T))-b\det(d(T))|\\ &= |b\det(n(T))-a\det(d(T))|\,.\end{aligned}$$

□

Corollary 3. *Let D be an almost alternating link diagram with dealternator c. Then*

$$\det\left(D^{c\leftarrow\frac{1}{-n}}\right)=|n\times\det\left(D_0^c\right)-\det\left(D_\infty^c\right)|\,,\det\left(D^{c\leftarrow -n}\right)=|n\times\det\left(D_\infty^c\right)-\det\left(D_0^c\right)|\,.$$

Proof. D can be represented as $n(-1+T)$ where T is an alternating tangle diagram (not necessarily strongly alternating in this case). The link diagrams D_0^c and D_∞^c would be equivalent to $n(T)$ and $d(T)$ respectively. The result follows using Proposition 3.2. □

Take two strongly alternating tangle diagrams T and S of different types. The link diagram $n(T+S)$ is said to be *semi alternating*. A link is *semi alternating* if it admits a semi alternating diagram. Semi alternating links are non split as shown in Proposition 6 of [15]. Semi-alternating links represent a special case of *adequate links*, which we do not define in this paper. Adequate links are non quasi-alternating links since they have thick Khovanov homology (Proposition 7 in [13]). By using the notion of semi-alternating links, we get the following proposition.

Proposition 3.3. *Let T be a strongly alternating tangle diagram and $0<\frac{a}{b}<1$ be a rational number. If the link $N(-\frac{a}{b}+T)$ is quasi-alternating, then $\frac{\det(n(T))}{\det(d(T))}>\frac{a}{b}$.*

Proof. Since $N(\frac{-a}{b}+T)$ is quasi-alternating, then its determinant is not zero. Hence by Proposition 3.2 we have $\frac{\det(n(T))}{\det(d(T))}\neq\frac{a}{b}$.

Suppose that $\frac{\det(n(T))}{\det(d(T))}<\frac{a}{b}$ and let D' denote the link diagram $n(-1+\frac{-a}{b}+T)$ and let c' denote the leftmost crossing of D'. The link diagram D' is equivalent to $n(-2+\frac{b-a}{a}+T)$ because of the rational tangle equivalence $-2+\frac{b-a}{a}=-1+\frac{-a}{b}$. By Proposition 3.2 we have

$$\begin{aligned}\det(D') &= \det(n(-2+\frac{b-a}{a}+T))\\ &= \left|2\det(d(\frac{b-a}{a}+T))-\det(n(\frac{b-a}{a}+T))\right|\\ &= (b+a)\det(d(T))-b\det(n(T)).\end{aligned}$$

On the other hand, the link diagrams $D_0'^{c'}$ and $D_\infty'^{c'}$ are respectively equivalent to $n(\frac{-a}{b}+T)$ and $d(\frac{-a}{b})\#d(T)$, which implies that $\mathcal{L}(D_0'^{c'})$ and $\mathcal{L}(D_\infty'^{c'})$ are quasi-alternating, the first by assumption and the second being a connected sum of alternating links. We get the following

$$\begin{aligned}\det(D_0'^{c'})+\det(D_\infty'^{c'}) &= a\det(d(T))-b\det(n(T))+b\det(d(T))\\ &= (b+a)\det(d(T))-b\det(n(T))\\ &= \det(D').\end{aligned}$$

This implies that the link diagram D' is quasi-alternating at the crossing c'. Hence, by Theorem 1.1 , the link diagram $D'^{c'\leftarrow\frac{-1}{2}}$, which is equivalent to the semi-alternating diagram $n((\frac{-1}{2}+\frac{-a}{b})+T)$, is quasi-alternating. This is absurd since semi-alternating links are non quasi-alternating. Consequently, the inequality $\frac{\det(n(T))}{\det(d(T))}>\frac{a}{b}$ is true. □

Example 1. Consider the link $L = N(-[0,1,10,1,6] + T)$ depicted in Fig. 14. We show, by the use of Proposition 3.3, that the link L is not quasi-alternating. Indeed, we have $\frac{\det(n(T))}{\det(d(T))} = \frac{65}{71}$ which is a number less than $[0,1,10,1,6] = \frac{76}{83}$.

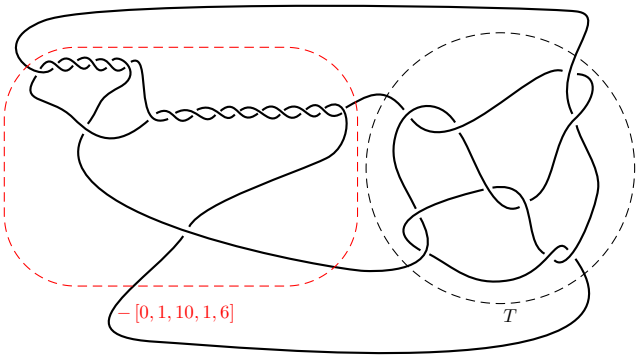

Figure 14:

Remark 6. For a rational tangle diagram $0 < t < 1$ and a strongly alternating tangle diagram T we have an obstruction for the link $L = N(-t+T)$ to be quasi-alternating in Proposition 3.3, namely that $\frac{\det(n(T))}{\det(d(T))} > t$. This is only a necessary condition for L to be quasi-alternating, since if we put $t = \frac{1}{2}$ and take $T = \frac{1}{3} + \frac{1}{3}$ to be the sum of two copies of the rational tangle diagram $\frac{1}{3}$, we observe that the condition holds and yet the link $N(-t+T)$, which is equivalent to the Montesinos link $M(-1;2,3,3)$, is not quasi-alternating by Theorem 4.1.

Corollary 4. *Let T be a strongly-alternating tangle diagram.*

1. *If $N(\frac{-1}{2}+T)$ is quasi-alternating, then the link diagram $n(\frac{-1}{k}+T)$ is quasi-alternating at every crossing of the vertical tangle $\frac{-1}{k}$ for every integer $k \geq 3$.*
2. *If $N(-2+T)$ is quasi-alternating, then the link diagram $n(-k+T)$ is quasi-alternating at every crossing of the integer tangle $-k$ for every integer $k \geq 3$.*

Proof. 1. If $N(\frac{-1}{2}+T)$ is quasi-alternating, then by Proposition 3.3 we have $\frac{\det(n(T)}{\det(d(T))} > \frac{1}{2}$, which is equivalent to $2\det(n(T)) - \det(d(T)) > 0$. This last condition is enough to show that the link diagram $n(\frac{-1}{3}+T)$ is quasi-alternating at each crossing of the vertical tangle $\frac{-1}{3}$. The result then follows by Theaorem 1.1.

2. The result follows by an analogous argument.

□

Now we are ready to prove Theorem 1.2. We will start by giving an expanded version.

Theorem 3.4. *Let D be an almost alternating diagram representing a quasi-alternating link. Denote c its dealternator. We have the following properties*

1. *If $\det(D_0^c) > \det(D_\infty^c)$, then the rational extension with fraction $-\frac{1}{2}$ of D at c yields a quasi-alternating diagram.*
2. *$\det(D_0^c) < \det(D_\infty^c)$, then the rational extension with fraction -2 of D at c yields a quasi-alternating diagram.*

Proof. First, sufficient and necessary conditions will be exhibited for $D^{c\leftarrow -\frac{1}{2}}$ to be quasi-alternating at c. $D^{c\leftarrow -\frac{1}{2}}$ is quasi-alternating at c if and only if

$$\mathcal{L}\left(\left(D^{c\leftarrow -\frac{1}{2}}\right)_0^c\right), \mathcal{L}\left(\left(D^{c\leftarrow -\frac{1}{2}}\right)_\infty^c\right) \in \mathcal{Q}, \text{ and} \tag{1}$$

$$\det\left(D^{c\leftarrow-\frac{1}{2}}\right)=\det\left(\left(D^{c\leftarrow-\frac{1}{2}}\right)_0^c\right)+\det\left(\left(D^{c\leftarrow-\frac{1}{2}}\right)_\infty^c\right) \tag{2}$$

Since $\mathcal{L}\left(\left(D^{c\leftarrow-\frac{1}{2}}\right)_0^c\right)=\mathcal{L}(D_0^c)$ is alternating and $\mathcal{L}\left(\left(D^{c\leftarrow-\frac{1}{2}}\right)_\infty^c\right)=\mathcal{L}(D)$ is quasi-alternating by assumption, then condition (1) is always satisfied. On the other hand, condition (2) is , by Proposition 3.2 and Corollary 1, equivalent to $\det(D_0^c)>\det(D_\infty^c)$. Finally we get that, under the assumptions of the theorem, $D^{c\leftarrow-\frac{1}{2}}$ is quasi-alternating at c if and only if $\det(D_0^c)>\det(D_\infty^c)$. By an analogical reasoning we obtain that $D^{c\leftarrow-2}$ is quasi-alternating at c if and only if $\det(D_0^c)<\det(D_\infty^c)$. Following Corollary1, either $D^{c\leftarrow-\frac{1}{2}}$ or $D^{c\leftarrow-2}$ is quasi-alternating at c. □

Example 2. We consider the link diagram on the left of the Fig. 15. It is an almost alternating diagram which is quasi-alternating at the marked crossing and which represents the tabulated link $L7n2$ in [3]. By applying Theorem 3.4, we get the quasi-alternating diagram on the right of the Fig. 15 which has one additional component and which represents the tabulated link $L9n28$ in [3].

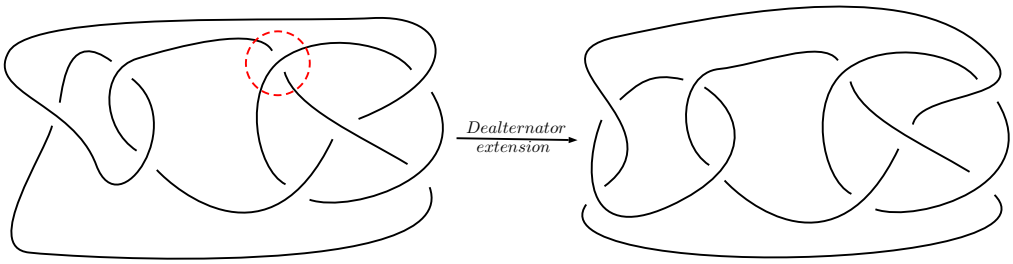

Figure 15: A dealternator extension of a diagram of the link $L7n2$ that yields the quasi-alternating link $L9n28$.

4 Applications

4.1 Generating non alternating and quasi-alternating Montesinos links

Let $t_i\neq 0,\pm1$, for $i\in[\![1,n]\!]$, be rational numbers, and let e be an integer. A *Montesinos link* is defined as $M(e;t_1,...,t_n):=N(e+\frac{1}{t_1}+...+\frac{1}{t_n})$. Those links were introduced by Montesinos in [18].

Let $t=\frac{\alpha}{\beta}$ be a rational number with $\beta>0$. The *floor* of t is $\lfloor t\rfloor=max\{x\in\mathbb{Z}/x\leq t\}$, and the *fractional part* of t is $\{t\}=t-\lfloor t\rfloor<1$. For $t\neq1$, define $\hat{t}=\frac{1}{\{\frac{1}{t}\}}>1$. We also put $\left(\frac{\alpha}{\beta}\right)^f=\begin{cases}\frac{\alpha}{\beta-\alpha} & \text{if } \frac{\alpha}{\beta}>0\\ \frac{\alpha}{\beta+\alpha} & \text{if } \frac{\alpha}{\beta}<0\end{cases}$

Let L be the Montesinos link $M(e;t_1,...,t_n)$. We define $\varepsilon(L)=e+\sum_{i=1}^{n}\lfloor\frac{1}{t_i}\rfloor$. The link L is isotopic to $M(\varepsilon(L);\hat{t_1},...,\hat{t_n})$ (Proposition 3.2 , [5]). The link $M(\varepsilon(L);\hat{t_1},...,\hat{t_n})$ is called the *reduced form* of the Montesinos link $L=M(e;t_1,...,t_n)$.

A complete classification of quasi-alternating Montesinos links is given in [9].

Remark 7. Any Montesinos link is either alternating or almost alternating [1].

Theorem 4.1 (Theorem 1, [9]). *Let $L=M(e;t_1,...,t_n)$ be a Montesinos link and $M(\varepsilon(L);\hat{t_1},...,\hat{t_n})$ its reduced form. Then L is quasi-alternating if and only if*

1. $\varepsilon(L)>-1$, *or*
2. $\varepsilon(L)=-1$ *and* $\left|\hat{t_i}^f\right|>\hat{t_j}$ *for some* $i\neq j$, *or*
3. $\varepsilon(L)<1-n$, *or*
4. $\varepsilon(L)=1-n$ *and* $\left|\hat{t_i}^f\right|<\hat{t_j}$ *for some* $i\neq j$.

By Theorem 10 in [15], the only non alternating and quasi-alternating Montesinos links are those with a reduced form $M(\varepsilon;\hat{t_1},...,\hat{t_n})$ where $\varepsilon=-1$ and $\left|\hat{t_i}^f\right|>\hat{t_j}$ for some $i\neq j$, and their reflections. We will show in the following Theorem that the latter are almost alternating links which can be constructed iteratively by using the technique developed in Theorem 3.4.

Theorem 4.2. *Each non-alternating quasi-alternating Montesinos link can be obtained from some Montesinos link $M(-1,\frac{\lambda}{\gamma},\frac{\eta}{\delta})$ by a finite sequence of dealternator extensions, isotopies, rational extensions and likely flype moves.*

Proof. Let L be a non alternating quasi-alternating Montesions link. Let $M(\varepsilon;\frac{\alpha_1}{\beta_1},...,\frac{\alpha_n}{\beta_n})$ be its reduced form. Since L is non alternating, then $n\geq 3$ as proved in Proposition 3.1 in [5]. Furthermore, as the link L is quasi-alternating, then by Theorem 4.1 $\varepsilon=-1$ and there exist $i\in[\![1,n]\!]$ and $j\in[\![1,n]\!]\setminus\{i\}$ such that $\left|\left(\frac{\alpha_i}{\beta_i}\right)^f\right|>\frac{\alpha_j}{\beta_j}$. Note that we may have $\varepsilon=1-n$. But the latter case corresponds to the mirror image of the former one and then we can restrict ourselves to $\varepsilon=-1$. For convenience, let us denote $\frac{\alpha_i}{\beta_i}=\frac{\lambda}{\gamma}$ and $\frac{\alpha_j}{\beta_j}=\frac{\eta}{\delta}$ and we suppose without loss of generality that $i<j$.
Let D_1 be the almost alternating link diagram $n\left(-1+\frac{\gamma}{\lambda}+\frac{\delta}{\eta}\right)$. Let c_1 be its dealternator. Note that the link $\mathcal{L}(D_1)$ is the alternating Montesinos link $M\left(-1,\frac{\lambda}{\gamma},\frac{\eta}{\delta}\right)$. By Proposition 4.1 in [5], we have

$$\det(D_1)=\left|\lambda\eta\left(-1+\frac{\gamma}{\lambda}+\frac{\delta}{\eta}\right)\right|.$$

Since $\left|\left(\frac{\lambda}{\gamma}\right)^f\right|>\frac{\eta}{\delta}$, which is equivalent to $\frac{\gamma}{\lambda}+\frac{\delta}{\eta}>1$, then $\det(D_1)\neq 0$. This shows that $\mathcal{L}(D_1)$ is non-split, hence it is quasi-alternating.

Now, starting from D_1, we will build the link L by using a finite sequence of operations which preserve the property of being quasi-alternating. Let $k\in[\![1,n]\!]\setminus\{i,j\}$ be a fixed integer.
Step 1: If $i>1$ and $k<i$, this step will be skipped. If not, according to whether $i<k<j$ or $j<k$, we use Flype moves to slide the dealternator c_1 in order to put it between the tangles $\frac{\gamma}{\lambda}$ and $\frac{\delta}{\eta}$ or to the right of the tangle $\frac{\delta}{\eta}$. So we get a new diagram D_2 which is equivalent to D_1 and is almost alternating. Let c_2 denote its dealternator.
Step 2: it is easy to see that $\mathcal{L}\left((D_2)_0^{c_2}\right)=M\left(0;\frac{\lambda}{\gamma},\frac{\eta}{\delta}\right)$ and $\mathcal{L}\left((D_2)_\infty^{c_2}\right)=(\frac{\gamma}{\lambda})\#(\frac{\delta}{\eta})$. On the other hand, we have $\det\left(M\left(0;\frac{\lambda}{\gamma},\frac{\eta}{\delta}\right)\right)=\lambda\eta\left(\frac{\gamma}{\lambda}+\frac{\delta}{\eta}\right)$ and $\det\left(d\left(\frac{\gamma}{\lambda}\right)\#d\left(\frac{\delta}{\eta}\right)\right)=\lambda\eta$. Then $\det\left((D_2)_0^{c_2}\right)>\det\left((D_2)_\infty^{c_2}\right)$. Hence by Theorem 3.4, the diagram $(D_2)^{c_2\leftarrow-\frac{1}{2}}$ is a quasi-alternating link diagram at each crossing of the extension tangle $-\frac{1}{2}$.
Step 3: now since $-\frac{1}{2}=-1+\frac{1}{2}$, then we may replace the tangle $-\frac{1}{2}$ in $(D_2)^{c_2\leftarrow-\frac{1}{2}}$ with the tangle $-1+\frac{1}{2}$ to get an equivalent almost alternating diagram D_3 which is either $n\left(-1+\frac{1}{2}+\frac{\gamma}{\lambda}+\frac{\delta}{\eta}\right)$, or $n\left(\frac{\gamma}{\lambda}+(-1+\frac{1}{2})+\frac{\delta}{\eta}\right)$, or $n\left(\frac{\gamma}{\lambda}+\frac{\delta}{\eta}+(-1+\frac{1}{2})\right)$ depending on the location of k as mentioned in the first step. One can easily check that D_3 is quasi-alternating at each crossing of the tangle $\frac{1}{2}$. Let c_3 be the dealternator of D_3. By using flype moves if needed, we can assume that c_3 is the first rational tangle on the left in the rational parametrization of D_3. Note that it is easy to check that D_3 is quasi-alternating at each of the crossings τ_1 and τ_2 of the tangle $\frac{1}{2}$.
Step 4: now we are ready to insert the rational tangle $t=\frac{\beta_k}{\alpha_k}$. By Theorem 1.1 $(D_3)^{\tau_1\leftarrow\frac{t}{1-t}}$ is quasi-alternating at each crossing of the tangle $\frac{t}{1-t}$ and also at τ_2. Now since $\frac{t}{1-t}*1=t$, then we may consider τ_2 as a crossing of the tangle t. Finally we built one of the following links: $M\left(-1;\frac{\alpha_k}{\beta_k},\frac{\lambda}{\gamma},\frac{\eta}{\delta}\right)$, or $M\left(-1;\frac{\lambda}{\gamma},\frac{\alpha_k}{\beta_k},\frac{\eta}{\delta}\right)$, or $M\left(-1;\frac{\eta}{\delta},\frac{\lambda}{\gamma},\frac{\alpha_k}{\beta_k}\right)$ depending on the initial position of $t=\frac{\alpha_k}{\beta_k}$ in the rational parametrization of L. This ends what we call the first loop of the building process. The next loop will start with the ouput of the last one and will allow the insertion of a new tangle $\frac{\alpha_h}{\beta_h}$. The same arguments used in the four last steps work again. Then after $n-2$ loops we will get the wanted rational parametrisation of L.

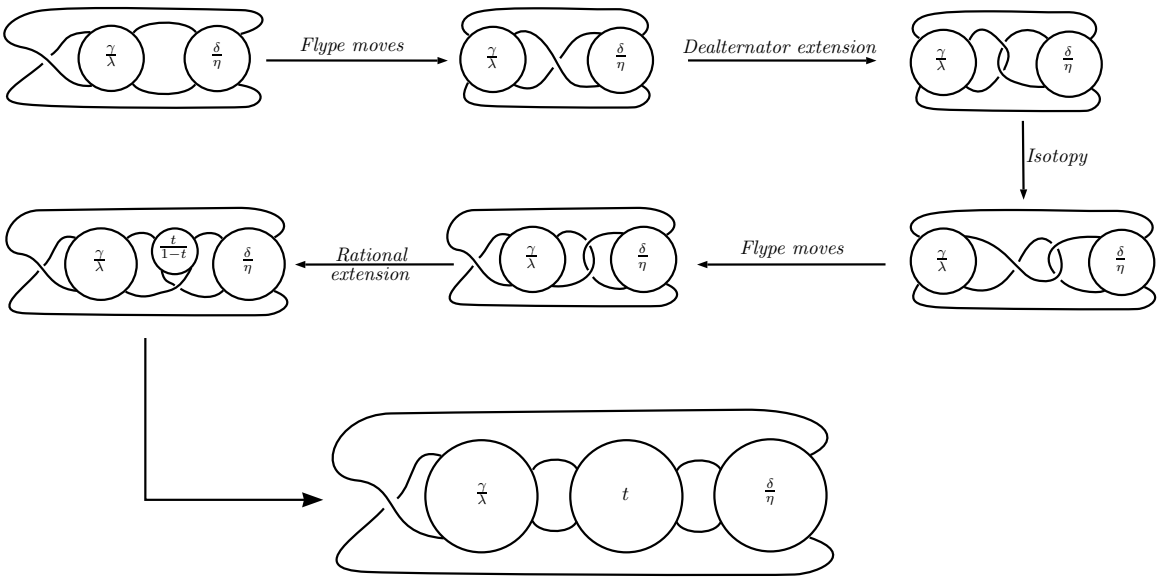

Figure 16: An illustrative diagram of the first iteration where $i < k < j$.

□

4.2 Generating almost alternating and quasi-alternating links

Recall the following definitions. A link $L \subset S^3$, other that the unknot, is *prime* if every 2-sphere in S^3 that intersects L transversely at two points bounds on one side of it, a ball that intersects L in precisely one unknotted arc. A diagram $D \subset S^2$, of a link other that the unknot, is a *prime* diagram if any simple closed curve in S^2 that meets D transversely at two points bounds, on one side of it, a disk that intersects D in a diagram U of the unknotted ball-arc pair.
We will use the Kauffman polynomial $\Lambda_L(a, z) \in \mathbb{Z}[a, a^{-1}, z, z^{-1}]$ which is an invariant of regular isotopy for unoriented link diagrams L. It satisfies the following relations

1. $\Lambda_{\bigcirc} = 1$.
2. $\Lambda_{\times} + \Lambda_{\times} = z(\Lambda_{\times} + \Lambda_{\times})$.
3. $\Lambda_{\times} = a\Lambda_{\smile}$.
4. $\Lambda_{\times} = a^{-1}\Lambda_{\smile}$.

If L is a link or a link diagram, then $c(L)$ is the crossing number of L.

Proposition 4.3. *Let T be a strongly alternating tangle diagram such that $n(T)$ is prime. If t is a rational tangle diagram such that $0 < t < 1$ and $\det(N(-t+T)) \neq 0$, then the link $N(-t+T)$ is almost alternating.*

To prove the proposition we will need the following lemma.

Lemma 4.4. *Let T be a strongly alternating tangle diagram such that $n(T)$ is prime. If t is a rational tangle diagram such that $0 < t < 1$, then*

$$\deg_z \Lambda_{n(-t+T)}(a, z) = c\left(n(-t+T)\right) - 2.$$

Proof. We will prove the lemma by induction on the number k of the integer tangles consisting the diagram t.
First step: If $k = 1$, since $t < 1$ then $t = \frac{1}{p}$ for some integer $p \geq 2$. Then $n(-t+T) = n(-\frac{1}{p}+T)$. To prove

the result, we will do another induction on p: if $p = 2$, we apply the skein relation satisfied by the polynomial L at the top crossing of the tangle $-\frac{1}{2}$, then we get

$$\Lambda_{n(-\frac{1}{2}+T)} = za\Lambda_{n(T)} + z\Lambda_{n(-1+T)} - \Lambda_{d(T)}.$$

By Theorem 4 in [24], we have $\deg_z \Lambda_{n(T)} \leq c(n(T)) - 1$. Since $n(T)$ is prime, according to the discussion which follows from Theorem 5 in [24], we have

$$\deg_z \Lambda_{n(T)} = c(n(T)) - 1.$$

By applying once again Theorem 4 cited above, we have also

$$\deg_z \Lambda_{n(-1+T)} \leq c(n(-1+T)) - 3 = c(n(T)) - 2, \text{ and } \deg_z \Lambda_{d(T)} \leq c(d(T)) - 1.$$

Furthermore we know that $c(n(T)) = c(d(T))$. Finally we get that

$$\begin{aligned}\deg_z \Lambda_{n(-\frac{1}{2}+T)} &= \deg_z \left(za\Lambda_{n(T)}\right) \\ &= 1 + c(n(T)) - 1 = c(n(-\frac{1}{2}+T)) - 2.\end{aligned}$$

Now if the result holds up to an integer p, $p \geq 2$, by applying a new time the skein relation at the top crossing of the integer tangle $-\frac{1}{p+1}$ we obtain that $\deg_z \Lambda_{n(-\frac{1}{p+1}+T)} = c(n(-\frac{1}{p+1}+T)) - 2$.

Second step: let $k \geq 1$ be a fixed integer and suppose that the lemma holds up to k. Let t be a rational tangle diagram consisting of $k+1$ integer tangles. We can write $t = [0, a_1, ..., a_k, p]$. Note that if $p = 1$, by adding p with the integer tangle a_k the tangle t becomes a rational tangle consisting of k integer tangles for which the result holds by the induction hypothesis. So we can suppose that $p \geq 2$. Without loss of generality, we may assume that k is even, in which case the integer tangle p will be vertical. We do an other induction on p. If $p = 2$, then $n(-t+T) = n(-[0, a_1, ..., a_k, 2] + T)$. by applying a new time the skein relation at the top crossing of the integer tangle 2 we get

$$\Lambda_{n(-[0,a_1,...,a_k,2]+T)} = z\Lambda_{n(-[0,a_1,...,a_k+1]+T)} + za\Lambda_{n(-[0,a_1,...,a_k]+T)} - a^{a_k}\Lambda_{n(-[0,a_1,...,a_{k-1}]+T)}.$$

By the induction hypothesis, we get

$$\begin{aligned}\deg_z \Lambda_{n(-[0,a_1,...,a_k,2]+T)} &= \deg_z \left(z\Lambda_{n(-[0,a_1,...,a_k+1]+T)}\right) \\ &= 1 + c(n(-[0, a_1, ..., a_k + 1] + T)) - 2 \\ &= c(n(-[0, a_1, ..., a_k, 2] + T)) - 2.\end{aligned}$$

Now if we assume that the result holds for any integer up to p, $p \geq 2$, it easy to proof the result for $p+1$ by writing the skein formula and by using the induction hypothesis, and the proof is done. □

Proof of Proposition 4.3. We prove that $N(-t+T)$ is not alternating and we provide an almost alternating link diagram of it.
Suppose that the link $N(-t+T)$ is alternating. Since $\det(n(-t+T)) \neq 0$, then $N(-t+T)$ has a connected, reduced and alternating diagram D. By using Theorem 1 in [23], we have $Br\langle D\rangle = 4c(D)$ where $Br\langle D\rangle$ is the breadth of $\langle D\rangle$, i.e. the difference between the maximal degree and the minimal degree of the indeterminate that occur in the Kauffman bracket polynomial $\langle D\rangle$. On the other hand, by using the tangle isotopy $-t = -1 + (\frac{1-t}{t} * 1)$ (see Fig. 17), we get that D is equivalent to the dealternator reduced and dealternator connected diagram $n(-1 + (\frac{1-t}{t} * 1) + T)$ as shown in Fig. 18.

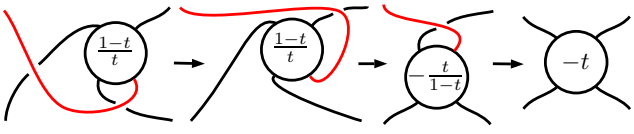

Figure 17: A equivalence of $-1 + (\frac{1-t}{t} * 1)$ and $-t$.

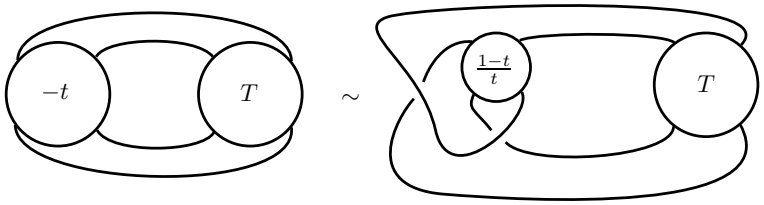

Figure 18: The link diagram $n(-t+T)$ (left) and the equivalent almost-alternating, dealternator reduced, and dealternator connected diagram $n(-1+(\frac{1-t}{t}*1)+T)$.

By Theorem 4.4 in [2], we have

$$Br\langle n(-1+(\frac{1-t}{t}*1)+T)\rangle \leq 4\left(c(n(-1+(\frac{1-t}{t}*1)+T))-3\right).$$

We can easily see from Fig. 17 that $c(n(-1+(\frac{1-t}{t}*1)+T)) = 1+c(n(-t+T))$. Hence, $c(D) \leq c\,(n(-t+T))-2$. By Theorem 4 in [24], we have $\deg_z \Lambda_D \leq c(D)-1$. Hence, by Lemma 4.4 we have $c(n(-t+T))-2 \leq c(D)-1$. This is absurd since $c(D) \leq c(n(-t+T))-2$. □

Theorem 4.5. *Let T be a strongly alternating tangle diagram, let k be an integer, $k \geq 1$, and let $\{t_1,\ldots,t_k\}$ be a family of rational tangle diagrams such that $0 < t_i < 1$, for each i. If the link $N(-1+T)$ is quasi-alternating, $n(T)$ is prime, and $\det(n(T)) > \det(d(T))$, then the link $N(-1+t_1+...+t_k+T)$ is almost alternating and quasi-alternating.*

Denote by $T_k = \frac{1}{2}+...+\frac{1}{2}+T$ the sum of k copies of the rational tangle $\frac{1}{2}$ and the tangle T.

Remark 8. The following results easily follow from the assumptions assumed in the statement of the theorem above. for each $k \geq 1$, the tangle diagram T_k is strongly alternating and locally unknotted. Since $d(T_k)$ is composite then by using Lemma 2.2, the link diagram $n(T_k)$ is prime. Furthermore by simple calculations, one can prove the following relations

$$\det(d(T_k)) = 2^k \det(d(T)) \text{ and } \det(n(T_k))) = 2^k \det(n(T)) + k2^{k-1}\det(d(T)).$$

Hence $\det(n(T_k)) > \det(d(T_k))$.

Lemma 4.6. *Let T be a strongly alternating tangle diagram such that $n(T)$ is prime, the link $N(-1+T)$ is quasi-alternating and $\det(n(T)) > \det(d(T))$. Then for each k, the link $N(-1+T_k)$ is almost alternating and quasi-alternating.*

Proof. We will do an induction on k.
If $k=1$: we must show the result for the link $N(-1+T_1)$. Note that the rational tangles $-\frac{1}{2}$ and $-1+\frac{1}{2}$ are the same then the links $N(-\frac{1}{2}+T)$ and $N(-1+(\frac{1}{2}+T)) = N(-1+T_1)$ are equivalent. The tangle diagram T is strongly alternating and $n(T)$ is prime. Since the rational tangle $\frac{1}{2}$ is less than one, then by Proposition 4.3 the link $N(-\frac{1}{2}+T)$ is almost alternating.
On the other hand, $n(-1+T)$ is an almost alternating diagram of a quasi-alternating link. Remembering that $n(T)$ and $d(T)$ are exactly the smoothings of $n(-1+T)$ at c, since $\det(n(T)) > \det(d(T))$, then by using Theorem 3.4, the dealternator extension of the diagram $n(-1+T)$ by $-\frac{1}{2}$ which is $N(-\frac{1}{2}+T)$ is quasi-alternating.
Now, assume that the result is true for $k-1$. That is $N(-1+T_{k-1})$ is almost alternating and quasi-alternating. By the remark above, the tangle T_{k-1} satisfies the same conditions as T. By applying the same arguments used for the case $k=1$ with T_k instead T, we obtain that the link $N(-\frac{1}{2}+T_{k-1}) = N(-1+\frac{1}{2}+T_{k-1}) = N(-1+T_k)$ is both quasi-alternating and almost alternating. □

Proof of Theorem 4.5. We start by noting that the link diagram $n(-1+T_k)$ is quasi-alternating at each crossing of its rational tangles $\frac{1}{2}$. Indeed, for any integer j, $1 \leq j \leq k$, the two smoothings of $n(-1+T_k)$ at the top

crossing of the j-th tangle $\frac{1}{2}$ are exactly $n(-1+T_{k-1})$ and $n(T_{k-1})$ which are both quasi-alternating. Moreover $\det(n(-1+T_{k-1})) = \det(n(-1+T_k)) + \det(n(T_{k-1}))$. By a similar argument one can show that the bottom crossing of the j-th tangle $\frac{1}{2}$ is also quasi-alternating.
Now, for each i, $1 \leq i \leq k$, we extend the link diagram $n(-1+T_k)$ at the top crossing of the i-th tangle $\frac{1}{2}$ by the rational tangle by $\frac{t_i}{1-t_i}$. By using the rational tangle equivalence $\frac{t_i}{1-t_i} * 1 = t_i$, we see that those extensions provide the link diagram $n(-1+t_1+...+t_k+T)$ which is then quasi-alternating by Theorem 1.1.
To see that $n(-1+t_1+...+t_k+T)$ is almost alternating, one can apply Proposition 4.3 by considering the rational tangle $(1-t_1) < 1$ and the tangle $t_2+...+t_k+T$.

□

Based on a large number of verifications, we formulate the following conjecture.

Conjecture 4.1. If T is a strongly alternating diagram such that $n(T)$ is a prime link diagram, then

$$\det(n(T)) \geq \det(d(T)).$$

Note that if Conjecture 4.1 is true, then the conditions in Theorem 4.5 would be reduced.

Corollary 5. *Let T be a strongly alternating tangle diagram, let k be an integer, $k \geq 1$, and let $\{t_1, \ldots, t_k\}$ be a family of rational tangle diagrams such that $0 < t_i < 1$, for each i. If the link $N(-1+T)$ is quasi-alternating, $d(T)$ is prime, and $\det(d(T)) > \det(n(T))$, then the link $N(-1+t_1+...+t_k+\frac{1}{T}_{cc})$ is almost alternating and quasi-alternating.*

Proof. The main observation is that link diagram $n(-1+\frac{1}{T}_{cc})$ is equivalent to $n(-1+T)$ up to mirror image as one can see in the figure 19. Hence the link $N(-1+\frac{1}{T}_{cc})$ is quasi-alternating.

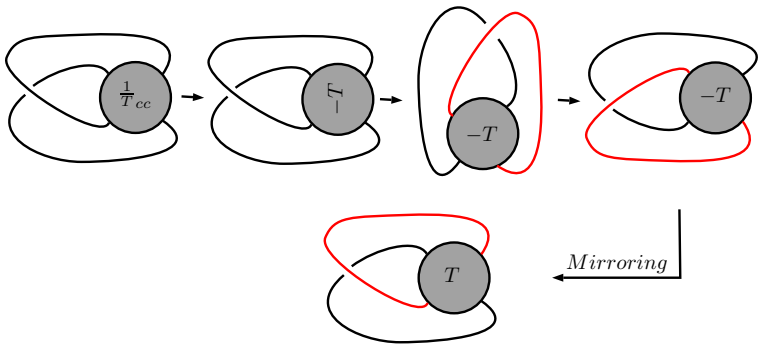

Figure 19: Equivalence between $n(-1+T)$ and $n(-1+\frac{1}{T}_{cc})$.

On the other hand, $\frac{1}{T}_{cc}$ is strongly alternating and $n(\frac{1}{T}_{cc}) = d(-T) = -d(T)$. Then

$$\det(n(\frac{1}{T}_{cc})) = \det(d(T)) > \det(n(T)) = \det(-(-n(T))) = \det(n(-T)) = \det(d(\frac{1}{T}_{cc})).$$

Then we apply Theorem 4.5 to the tangle $\frac{1}{T}_{cc}$ instead T. □

Example 3. We consider the quasi-alternating and almost alternating link diagram on the left in the Fig. 20. By applying Theorem 4.5 we get the quasi-alternating and almost alternating whose diagram is on the right in the same figure.

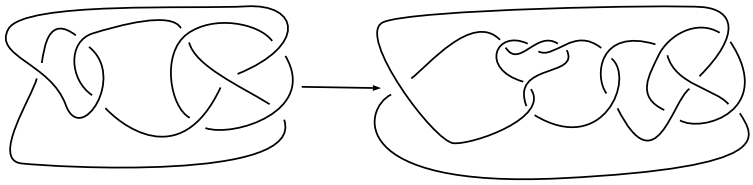

Figure 20:

Theorem 4.7. *Every connected, locally unknotted, reduced alternating tangle diagram generates infinitely many quasi alternating and almost alternating links.*

Proof. Let $t = [0, a_1, ..., a_k]$ be a rational tangle such that $k \geq 2$ is an even integer and T be a connected, locally unknotted, reduced alternating tangle diagram. We denote by $T \star t$ the tangle diagram depicted in the figure below.

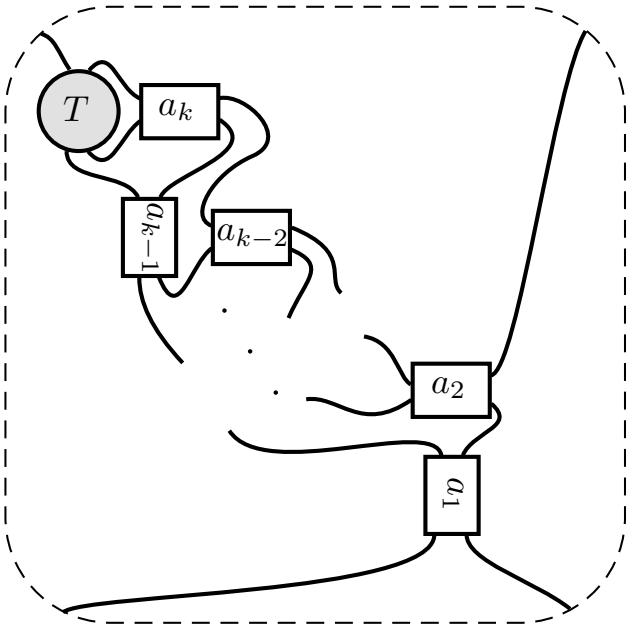

Figure 21: The tangle diagram $T \star t$.

We note that the link diagram $n(-t + T \star t)$ equivalent to $n(T)$ or $n(T_h)$ according to the parity of a_k (the links $N(T)$ and $N(T_h)$ are the same). The Fig. 22 exhibits that equivalence for a particular rational tangle $[0, n, 2m]$. The link $N(-t + T \star t)$ is alternating. It is non split by connectedness of T. By using the rational tangle equivalence $-t = -1 + (\frac{1-t}{t} * 1)$, the link diagram $n(-t + T \star t)$ is equivalent to the almost alternating, dealternator connected, and dealternator reduced link diagram $n\left(-1 + (\frac{1-t}{t} * 1) + (T \star t)\right)$. Denote by S the tangle diagram $(\frac{1-t}{t} * 1) + (T \star t)$. It is clear that S is strongly alternating and Lemma 2.2 provides that $n(S)$ is prime. Furthermore, simple calculations show that $\det(n(S)) > \det(d(S))$. We can then apply Theorem 4.5 to generate infinitely many quasi-alternating and almost alternating links starting with the link diagram $n(-1 + S)$, which represents the non split alternating link $N(T)$. □

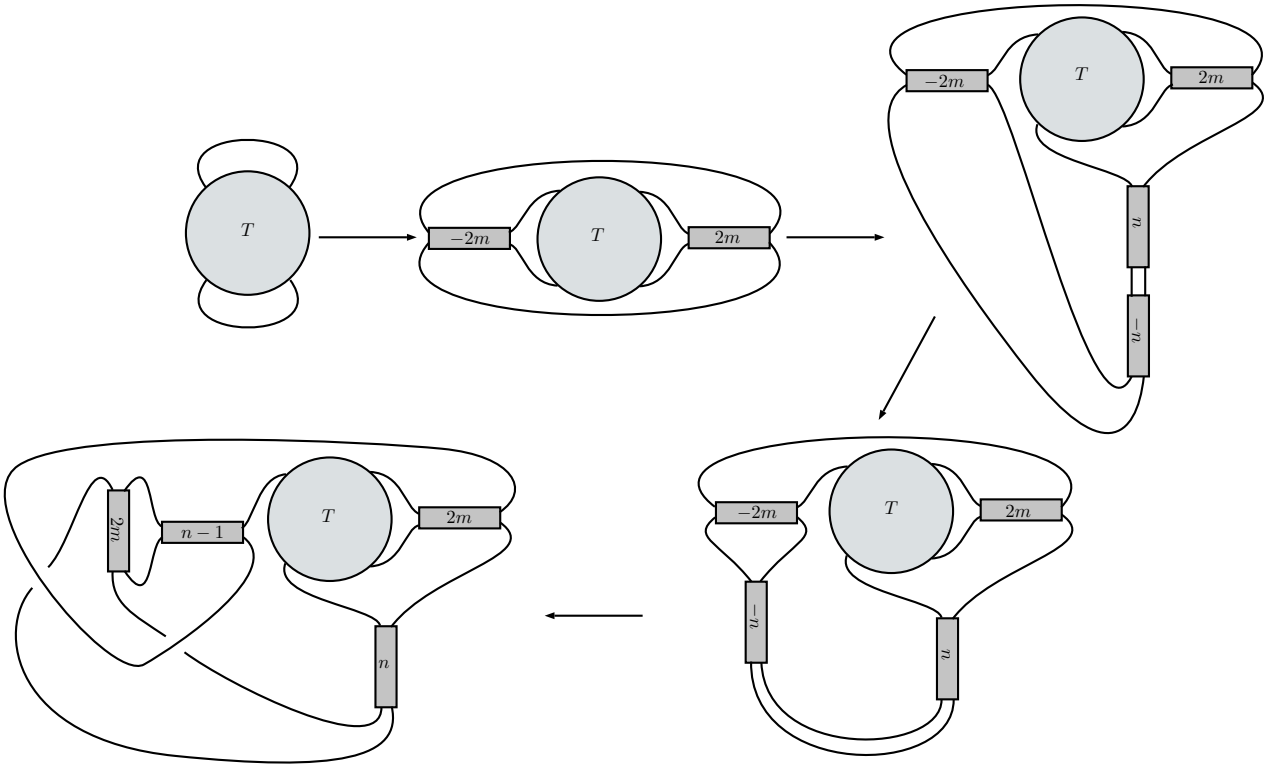

Figure 22: The link diagram $n(T)$ is equivalent to $n(-[0,n,2m]+T)$ which is it self equivalent to the almost alternating link diagram $n(-1+[0,1,n-1,2m]+T\star[n,2m])$.

5 Crossing numbers and determinants of links arising as dealternator extensions

Qazaqzeh et al. showed that the cossing number of any alternating (non-split) link is less than its determinant (see Proposition 2.2 in [20]). Then following many verifications for some known families of quasi-alternating links, they stated the conjecture 1.1. Our aim in this section is to check that the conjecture is satisfied by all links provided by dealternator extensions.

Proposition 5.1. *Let D be an almost alternating link diagram with dealternator c such that $\mathcal{L}(D)$ is quasi-alternating and $c(D) \leq \det(D)$. Let $D^{c\leftarrow\omega}$, where ω is equal either to $-\frac{1}{2}$ or -2, be the quasi-alternating dealternator extension of D obtained by Theorem 3.4. Then every rational extension $\mathcal{D}$ of $D^{c\leftarrow\omega}$ at c satisfies $c(\mathcal{D}) \leq \det(\mathcal{D})$.*

Proof. We first consider the case where the quasi-alternating dealternator extension given by Theorem 3.4 is $D^{c\leftarrow-\frac{1}{2}}$. Note that this occurs if and only if $\det(D_0^c) > \det(D_\infty^c)$. We have $c\left(D^{c\leftarrow-\frac{1}{2}}\right) = c(D)+1 \leq \det(D)+1$. Now since $D^{c\leftarrow-\frac{1}{2}}$ is by assumption quasi-alternating at c, then

$$\det\left(D^{c\leftarrow-\frac{1}{2}}\right) = \det(D_\infty^c) + \det(D_0^c).$$

Since $\det(D_0^c) > \det(D_\infty^c) \geq 0$ and D_∞^c is equivalent to D, then

$$c\left(D^{c\leftarrow-\frac{1}{2}}\right) = c(D)+1 \leq \det(D)+1 \leq \det\left(D^{c\leftarrow-\frac{1}{2}}\right)$$

Now if $\mathcal{D}$ is a rational extension of $D^{c\leftarrow-\frac{1}{2}}$ at c, which is a quasi-alternating crossing in $D^{c\leftarrow-\frac{1}{2}}$, then by Theorem 2.3 in [20] we get that $c(\mathcal{D}) \leq \det(\mathcal{D})$. A similar argument gives the result in the case where the quasi-alternating dealternator extension given by Theorem 3.4 is $D^{c\leftarrow-2}$. □

Proposition 5.2. *Let D be an almost alternating link diagram, dealternator reduced and dealternator connected, with dealternator c and such that $\mathcal{L}(D)$ is quasi-alternating. Let $D^{c\leftarrow\omega}$, where ω is equal either to $-\frac{1}{2}$ or -2, be the quasi-alternating dealternator extension of D obtained by Theorem 3.4. Then every rational extension $\mathcal{D}$ of $D^{c\leftarrow\omega}$ at c satisfies $c(\mathcal{D}) \leq \det(\mathcal{D})$.*

Proof. We first consider the case where the quasi-alternating dealternator extension given by Theorem 3.4 is $D^{c\leftarrow-\frac{1}{2}}$. Note that this case occurs when $\det(D_0^c) > \det(D_\infty^c)$. Suppose that $c\left(D^{c\leftarrow-\frac{1}{2}}\right) > \det\left(D^{c\leftarrow-\frac{1}{2}}\right)$, then

$$c(D) + 1 = c(D_\infty^c) + 2 > 2\det(D_0^c) - \det(D_\infty^c). \tag{3}$$

But since D_∞^c is alternating and reduced, then by Proposition 2.2 in [20] we get that $c(D_\infty^c) \leq \det(D_\infty^c)$. Hence, (3) implies that

$$\det(D_\infty^c) + 2 > 2\det(D_0^c) - \det(D_\infty^c)$$

Which is equivalent to

$$\det(D_\infty^c) \geq \det(D_0^c)$$

Which is absurd. This allows to conclude that $c\left(D^{c\leftarrow-\frac{1}{2}}\right) \leq \det\left(D^{c\leftarrow-\frac{1}{2}}\right)$. Now if $\mathcal{D}$ is a rational extension of $D^{c\leftarrow-\frac{1}{2}}$ at c, which is a quasi-alternating crossing in $D^{c\leftarrow-\frac{1}{2}}$, then by Theorem 2.3 in [20] we get that $c(\mathcal{D}) \leq \det(\mathcal{D})$.
We prove in a similar way the result when the quasi-alternating dealternator extension given by Theorem 3.4 is $D^{c\leftarrow-2}$. □

Corollary 6. *Every quasi-alternating and almost alternating link provided by Theorem 4.5 or Theorem 4.7 satisfies the Conjecture 1.1.*

Proof. The links provided by Theorem 4.5 and Theorem 4.7 are obtained by dealternator extensions of dealternator reduced and dealternator connected diagrams which represent quasi-alternating links. Then, they satisfy Conjecture 1.1 by Proposition 5.2. □

Proposition 5.3. *Let T be a strongly alternating tangle diagram such that $n(T)$ is prime and let $0 < t < 1$ be a rational tangle. If the link $N(-t+T)$ is quasi-alternating, then $c(N(-t+T)) \leq \det(N(-t+T))$.*

Proof. By Lemma 4.4, we have $\deg \Lambda_{n(-t+T)} = c(n(-t+T)) - 2$. By using Theorem 1.2. in [22], we have $\deg \Lambda_{n(-t+T)} = c(n(-t+T)) - 2 \leq \det(N(-t+T)) - 2$. Then the result follows easily. □

Corollary 7. *Every quasi-alternating Montesinos link L satisfies Conjecture 1.1.*

Proof. The result for quasi-alternating Montesinos links which are also alternating is provided by Proposition 2.2 in [20].

Let L be a non alternating, quasi-alternating Montesions link. Then by Theorem 4.1 there exists an integer $n \geq 3$ and an ordered set of rationals $\{\frac{\alpha_k}{\beta_k}\}_{1\leq k\leq n}$ all greater than one where L is isotopic, up to mirror image, to the link $M\left(-1; \frac{\alpha_1}{\beta_1}, ..., \frac{\alpha_n}{\beta_n}\right)$ which is the same as $N\left(-1 + \frac{\beta_1}{\alpha_1}, ..., \frac{\beta_n}{\alpha_n}\right)$. Put $t = \frac{\alpha_1-\beta_1}{\alpha_1}$ and $T = \frac{\beta_2}{\alpha_2} + ... + \frac{\beta_n}{\alpha_n}$. The tangle t is a rational tangle and we have $-t = -1 + \frac{\beta_1}{\alpha_1}$. On the other hand, the tangle diagram T is strongly alternating and $n(T)$ is prime by Lemma 2.2. Now since the link L is equivalent to $N(-t+T)$, the result follows by Proposition 5.3. □

6 The converse of Theorem 1.1 is false

Let D be a link diagram in the plane. Suppose that there exists a disk in the plane meeting D transversely four times and enclosing a tangle diagram T. We say that T is *embedded* in D.

Take an almost alternating diagram D such that $\mathcal{L}(D)$ is quasi-alternating and denote by c the dealternator of D. Without loss of generality, let us assume that $\det(D_0^c) > \det(D_\infty^c)$. Then Theorem 3.4 shows that the

diagram $D^{c\leftarrow\frac{1}{-2}}$ is quasi-alternating at each crossing of the tangle $\frac{1}{-2}$. When replacing this tangle by a single crossing of his, we get D back and Corollary 2 ensures that D is not quasi-alternating at c. This observation motivates the following question asked by the authors in [21]

Question 1 (Question 1, [21])**.** *Let D be a quasi-alternating diagram at a crossing c that is a part of a rational tangle diagram t embedded in D. Let D' be the link diagram obtained by replacing the projection disk of t by the single crossing c. Is the link $\mathcal{L}(D')$ quasi-alternating ?*

Question 1 asks essentially if the converse of Theorem 1.1 is true. In order to answer this question, we exhibit some almost alternating diagrams representing non quasi-alternating links whose dealternator extensions yield quasi-alternating diagrams.

Lemma 6.1. *Let $L = N(T + S)$ be a semi-alternating link. Then L admits a dealternator reduced and dealternator connected almost-alternating diagram D. Furthermore, if we denote by c the dealternator of D, then the link $\mathcal{L}\left(D^{c\leftarrow\frac{1}{-2}}\right)$ is a non-split alternating link.*

Proof. Assume without loss of generality that T is of type 1 and S is of type 2. Let S' denote the type 1 tangle diagram $(-\frac{1}{S}_{cc})_h$ and D denote the link diagram $n(-1 + (S' + 1) * (T + 1))$. We have $\mathcal{L}(D) = N(T + S)$ as shown in Fig. 23. Furthermore, the diagram D is almost-alternating, dealternator reduced, and dealternator connected.

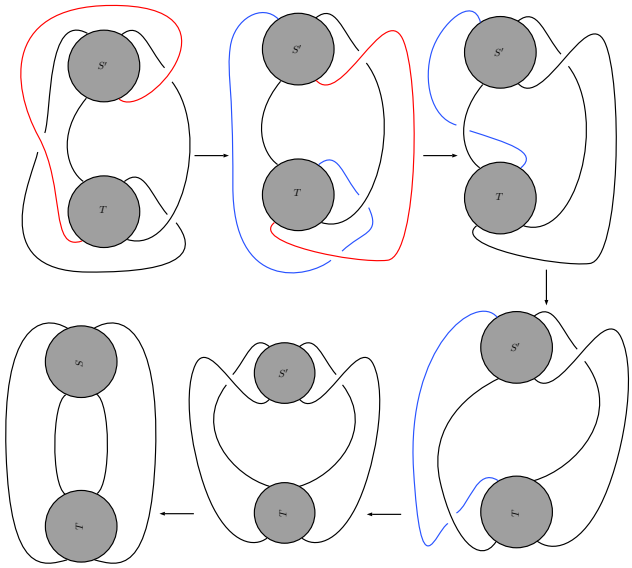

Figure 23: The link diagram $n(-1+(S'+1)*(T+1))$ is equivalent to the semi alternating diagram $n(T+S)$.

Denote by c the dealternator of D. Fig. 24 shows that $D^{c\leftarrow\frac{1}{-2}}$ is equivalent to a connected alternating diagram. Hence $D^{c\leftarrow\frac{1}{-2}}$ is a non-split alternating link.

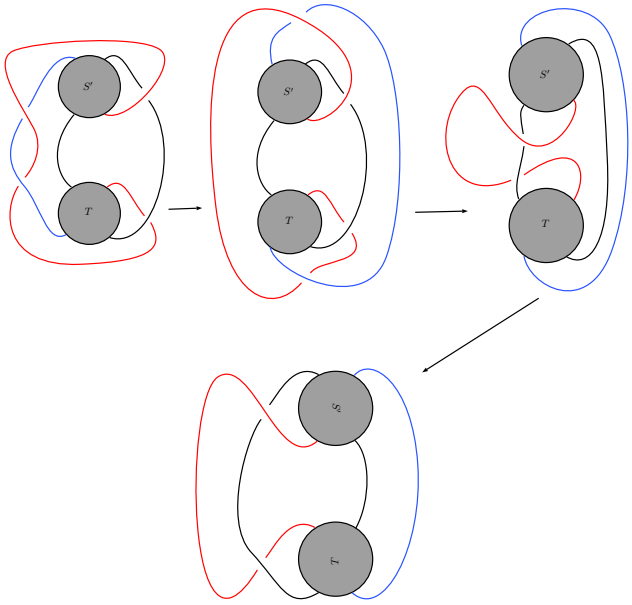

Figure 24: The link diagram $D^{c\leftarrow\frac{1}{-2}}$ is equivalent to an alternating diagram.

□

Proposition 6.2. *There exists a link diagram D which is quasi-alternating at some crossing c that is a part of an embedded rational tangle t such that the replacement of t with the single crossing c yields a non quasi-alternating link.*

Proof. Let T where T and S are strongly alternating tangle diagrams of type 1 and type 2 respectively and put $S' = (-\frac{1}{S})_{cc})_h$. Take D to be the link diagram $n(-\frac{1}{3} + (S'+1) * (T+1))$ and denote by c the top crossing of the vertical tangle diagram $-\frac{1}{3}$. Denote by d the almost alternating diagram $n(-1 + (S'+1) * (T+1))$ and let c' denote its dealternator. Clearly D is exactly the diagram $d^{c'\leftarrow\frac{1}{-3}}$. Lemma 6.1 shows that the link $\mathcal{L}(d^{c'\leftarrow\frac{-1}{2}}) = N(\frac{-1}{2} + (S'+1) * (T+1))$ is alternating none split and then it is quasi-alternating. By Corollary 4 D is quasi-alternating at the crossing c.

If we replace in D the vertical tangle diagram $-\frac{1}{3}$ with the single crossing c we obtain the diagram d. Lemma 6.1 shows that the link $\mathcal{L}(d)$ is semi alternating, hence non quasi-alternating. □

Proposition 6.2 answers negatively Question 1 by exhibiting an infinite family of counterexamples.

Remark 9. Note that Proposition 6.2 shows also that the converse of Theorem 3.3 in [21] is false. To see that let us reconsider the link D in the proof of Proposition 6.2. We can extend the crossing c in D with any sum of rational tangles and the obtained diagram will still be quasi-alternating by Theorem 3.3 in [21]. Replacing this sum of rational tangles with the only crossing c will get us back to a semi-alternating, hence non quasi-alternating link.

Let $0 < t < 1$ be a rational tangle diagram and T a strongly alternating tangle diagram and consider the link $L = N(-t+T)$. In Proposition 3.3, we found a necessary but not sufficient condition for the link L to be quasi-alternating, namely that $\frac{\det(n(T))}{\det(d(T))} > t$. One may rely on this observation and consider that an attempt to characterize the quasi-alternating links of the form $L = N(-t+T)$ through an algebraic formula involving only the two rational numbers $\frac{\det(n(T))}{\det(d(T))}$ and t would be inconvenient. Nevertheless, it is true that in the case of non alternating and quasi-alternating Montesinos links, which all admit the form $N(-t+T)$, it has been found that such a formula is sufficient to provide the characterization (Theorem 4.1).

Question 2. *Are the two rational numbers t and $\frac{\det(n(T))}{\det(d(T))}$ the only data needed to know if the link $N(-t+T)$ is quasi-alternating or not?*

Chbili and Qazaqzeh have recently stated a conjecture about quasi-alternating links in term of the coefficients of their Jones polynomials. Write the Jones polynomial of a link L as $V_L(t) = \sum_{i=0}^{m} a_i t^i$, where $m \geq 0$, $a_0 \neq 0$, and $a_m \neq 0$. The conjecture is formulated as follows.

Conjecture 6.1 (Conjecture 2.3, [6])**.** If L is a prime quasi-alternating link, other than $(2, n)$-torus link, then the coefficients of the Jones polynomial of L satisfy $a_i a_{i+1} < 0$ for all $0 \leq i \leq m-1$.

Question 3. *Do the quasi-alternating links arising as dealternator extensions satisfy Conjecture 6.1?*

References

[1] Tetsuya Abe and Kengo Kishimoto. The dealternating number and the alternation number of a closed 3-braid. Journal of Knot Theory and its Ramifications, 19(09):1157–1181, 2010.

[2] Colin C Adams, Jeffrey F Brock, John Bugbee, Timothy D Comar, Keith A Faigin, Amy M Huston, Anne M Joseph, and David Pesikoff. Almost alternating links. Topology and its Applications, 46(2):151–165, 1992.

[3] J. C. Cha and C. Livingston. Knotinfo: Table of knot invariants, 2016.

[4] Abhijit Champanerkar and Ilya Kofman. Twisting quasi-alternating links. Proceedings of the American Mathematical Society, 137(7):2451–2458, 2009.

[5] Abhijit Champanerkar and Philip Ording. A note on quasi-alternating montesinos links. Journal of Knot Theory and Its Ramifications, 24(09):1550048, 2015.

[6] Nafaa Chbili and Khaled Qazaqzeh. On the jones polynomial of quasi-alternating links. Topology and its Applications, 264:1–11, 2019.

[7] John H Conway. An enumeration of knots and links, and some of their algebraic properties. In Computational Problems in Abstract Algebra (Proc. Conf., Oxford, 1967), pages 329–358, 1970.

[8] Jay R Goldman and Louis H Kauffman. Rational tangles. Advances in Applied Mathematics, 18(3):300–332, 1997.

[9] Ahmad Issa. The classification of quasi-alternating montesinos links. arXiv preprint arXiv:1701.08425, 2017.

[10] Taizo Kanenobu, Hirofusa Saito, and Shin Satoh. Tangles with up to seven crossings. Interdisciplinary information sciences, 9(1):127–140, 2003.

[11] Louis H Kauffman. An invariant of regular isotopy. Transactions of the American Mathematical Society, 318(2):417–471, 1990.

[12] Louis H Kauffman and Sofia Lambropoulou. On the classification of rational tangles. Advances in Applied Mathematics, 33(2):199–237, 2004.

[13] Mikhail Khovanov. Patterns in knot cohomology, i. Experimental mathematics, 12(3):365–374, 2003.

[14] WB Raymond Lickorish. An introduction to knot theory, volume 175. Springer Science & Business Media, 2012.

[15] WB Raymond Lickorish and Morwen B Thistlethwaite. Some links with non-trivial polynomials and their crossing-numbers. Commentarii Mathematici Helvetici, 63(1):527–539, 1988.

[16] Tye Lidman and Steven Sivek. Quasi-alternating links with small determinant. In Mathematical Proceedings of the Cambridge Philosophical Society, volume 162, pages 319–336. Cambridge University Press, 2017.

[17] Ciprian Manolescu and Peter Ozsváth. On the khovanov and knot floer homologies of quasi-alternating links. arXiv preprint arXiv:0708.3249, 2007.

[18] JÜSF M MONTESINOS. Una familia infinita de nudos representados no separables. Revista Math. Hisp. Amer.(IV), 33:32–35, 1973.

[19] Peter Ozsváth and Zoltán Szabó. On the heegaard floer homology of branched double-covers. Advances in Mathematics, 194(1):1–33, 2005.

[20] K Qazaqzeh, B Qublan, and A Jaradat. A remark on the determinant of quasi-alternating links. Journal of Knot Theory and Its Ramifications, 22(06):1350031, 2013.

[21] Khaled Qazaqzeh, Nafaa Chbili, and Balkees Qublan. Characterization of quasi-alternating montesinos links. Journal of Knot Theory and Its Ramifications, 24(01):1550002, 2015.

[22] Masakazu Teragaito. Quasi-alternating links and kauffman polynomials. Journal of Knot Theory and Its Ramifications, 24(07):1550038, 2015.

[23] Morwen B Thistlethwaite. A spanning tree expansion of the jones polynomial. Topology, 26(3):297–309, 1987.

[24] Morwen B Thistlethwaite. Kauffman's polynomial and alternating links. Topology, 27(3):311–318, 1988.

[25] Tatsuya Tsukamoto. A criterion for almost alternating links to be non-splittable. In Mathematical Proceedings of the Cambridge Philosophical Society, volume 137, pages 109–133. Cambridge University Press, 2004.

[26] Hassler Whitney. Non-separable and planar graphs. In Classic Papers in Combinatorics, pages 25–48. Springer, 2009.

Relationship of Fractional Diffusion Equation with SchröDinger Equation and Investigation of Solution with Fractional Mathematics.

Safi Kolkiran

***Abstract*—** Fractional mathematics is a field in mathematical analysis related to the application and identification of ordinary-order derivatives and integrals. Recent studies have shown that fractional mathematics is used to encompass fractals in different areas of physics and engineering. The inadequacy of standard mathematical physics to describe the dynamic of complex physical systems and the importance of fractional mathematics describing the systems stochastically close to reality suggest that some differential equations in mathematical physics have shown that solutions with fractional mathematics can be done. Today, fractal geometry and fractional mathematics are applied to phenomological theories for complex systems. The fractional approach is also a mathematical tool that reveals the relationship between natural systems' force law form and the behavior they deviate from this form. From this point of view, the relation of the fractional diffusion equation, which is one of the fractional differential equations, to the Schrödinger equation will be discussed and the importance of the Mittag-Leffler function.

***Keywords*—** Fractional Calculus, Schrodinger Equation, Mittag Leffler Function, Liouville Equation.

Safi Kolkiran is with the Mugla Sitki Kocman University, Turkey (e-mail: safikolkiran@yahoo.com).

Fast Pattern Mining Inference Applied to Predictive Maintenance of the French High-Speed Train Fleet

Amir Dib, Mathilde Mougeot

***Abstract*—** In the railway industry, maintenance represents a large part of total costs spanning from 20 to 50% of total production cost. Predictive maintenance applied to rolling stock or infrastructure has a very high potential for increased safety, availability and reliability, cost reduction, and process efficiency. Research on model-based failure detection relying on the underlying physical degradation process recently trimmed back in favor of a data-driven approach that aims to apply generic statistical-models from condition monitoring. Most of these researches focus on real-valued multivariate signals (such as vibrations or electrical measurements) even though railway maintainers often need to deal with a large database of sequences from high dimensional unordered sets such as log sequences. Traditional methods ignoring the unordered property of the feature space typically fail to capture important patterns, and deterministic pattern mining methods have exponential complexity with respect to the size of the database. The present study proposes a probabilistic model for the pattern mining problem coupled with a mean-field variational inference with deterministic sampling to infer the set of interesting patterns in the sequences of symbols. The model is applied to pattern extraction for predictive maintenance on the French High-Speed train fleet by searching for the discriminative patterns. The method successfully retrieves the pattern and their frequencies with small relative error with a large computational time gain of one order of magnitude. As this framework provides a fast algorithm for predictive maintenance with easily interpretable output, we hope that it will be applied to different predictive maintenance use cases and other sequential data such as ones encountered in speech analysis, DNA classification, or shopping recommendations system.

***Keywords*—**Bayesian learning, pattern mining, predictive maintenance, variational inference.

A. D. Université Paris-Saclay, CNRS, ENS Paris Saclay, Centre Borelli, SNCF (e-mail: dib.amir@gmail.com).

M. M. Université Paris-Saclay, CNRS, ENS Paris Saclay, Centre Borelli (e-mail: mathilde.mouget@ens-paris-saclay.fr).

Preparation of Papers - Life Cycle Analysis of Railway Infrastructure in the Face of Vulnerabilities Generated by Climate Change

F. B. Ribeiro, A.F. Rosa, L.C.A. Menezes, M.A.V. Silva

***Abstract*—** Considering the effects of climate changes in the railway transport, this study aims to measure the impact of increased rainfall on track performance, since the variations in moisture content is a factor of vulnerability. The mechanical properties of the subgrade, which are affected by its moisture content, are modelled and used to compare different scenarios of a track design, evaluating the use of different materials in the pavement long-term performance. For this, the concepts of railway track mechanics were applied, and internationally known inventories of emissions and impacts. Finally, as a result, it was observed that the subgrade of the railway pavement, subjected during long periods to high moisture contents, tends to undergo higher permanent strains than in its optimum water content. Furthermore, from an environmental point of view, in scenarios with the use of artificial materials as reinforcement solutions, such as cement, emulsion, and HMA, the trade-off between performance gain versus cost and emission was advantageous, but in any case, the best solution was to avoid variations in the subgrade moisture content.

***Keywords*—** railway, life cycle, infrastructure, climate change, pavement

Filipe Ribeiro is with the Federal University of Rio de Janeiro, Brazil (e-mail: filiperibeiro@pet.coppe.ufrj.br).

Architecture and Convalescence - Biophilic and Neuroscience Approach in the Context of Covid-19

Anna Wróblewska

***Abstract*—**In 2020 due to the coronavirus (COVID-19) pandemic, the way how we see the built environment has changed. Buildings become places of forced isolation, treatment, or convalescence, often with tough restrictions to leave. For this reason, there is an urgent need to rethink how architectural spaces are designed. If we take into account that we spend most of our lifetime indoors, we are more likely to make an informed choice. Nowadays, when it comes to the building we have more than ever a variety of options among materials, build technologies, locations, scales, and layouts of spaces. The fact that being within the built environment is a part of our everyday life, should be used as additional subliminal support of human well-being, this dependency is effortlessly recognized in the natural environment. Hence, the biophilic approach in architectural design is the response to the nowadays challenge of confinement. The health of one became in the interest of all. The study show relationship between the built environment and human stress, which is a significant factor contributing to disease occurrence and convalescence. The bridging built environment with a natural environment lowers the stress triggered by demanded confinement. Building consciousness of the role of build environment in human health is crucial for the post-pandemic society convalescence. The study indicates how neuroscience for architecture along with biophilic guidance can help find solutions for supporting the convalescence of people in the context of Covid-19.

***Keywords*—**Biophilia, Biophilic Design, Covid-19 Convalescence, Human Well-Being, Neuroarchitecture, Science-Informed Design.

Anna Wróblewska is a PhD candidate at University of Technology of Gdansk, Poland (email: anna.wroblewska@pg.edu.pl).

Evaluation of Spatial Correlation Length and Karhunen-Loeve Expansion Terms for Predicting Reliability Level of Long-term Settlement in Soft Soils

Mehrnaz Alibeikloo, Hadi Khabbaz, Behzad FatahiFirst A. Author, Second B. Author, Jr., Third C. Author

***Abstract*—**Spectral random filed method is one of the widely used methods to obtain more reliable and accurate results in geotechnical problems involving material variability. Karhunen-Loeve (K-L) expansion method was applied to perform random field discretization of cross correlated creep parameters. Karhunen-Loeve expansion method is based on eigen-functions and eigen-values of covariance function adopting Kernel integral solution. In this paper, the accuracy of Karhunen-Loeve expansion was investigated to predict long-term settlement of soft soils adopting elastic visco-plastic creep model. For this purpose, parametric study was carried to evaluate the effect of K-L expansion terms and spatial correlation length on reliability of results. The results indicate that small values of spatial correlation length require more K-L expansion terms. Moreover, by increasing spatial correlation length, the coefficient of variation (COV) of creep settlement increases confirming more conservative and safer prediction.

***Keywords*—** Karhunen-Loeve expansion, Long-term settlement, Reliability Analysis, Spatial Correlation Length

Mehrnaz Alibeikloo. Author is PhD Candidate, School of Civil and Environmental Engineering, University of Technology Sydney (UTS), Sydney, Australia (phone: +61422838911; e-mail: mehrnaz.alibeikloo@student.uts.edu.au).

Hadi Khabbaz. Author is Associate Professor of Geotechnical Engineering (Ph.D, MEng, BEng), School of Civil and Environmental Engineering, University of Technology Sydney (UTS), Sydney, Australia (e-mail: hadi.khabbaz@uts.edu.au)

Behzad Fatahi. Author is Associate Professor of Geotechnical Engineering (Ph.D, MEng, BEng, CPEng, NPER), School of Civil and Environmental Engineering, University of Technology Sydney (UTS), Sydney, Australia (e-mail: behzad.fatahi@uts.edu.au)

Reliability-Based Design of an Earth Slope Taking into Account Unsaturated Soil Properties

Siacara A.T. , Beck A.T, Futai A.A.

***Abstract*—** This paper shows how accurately and efficiently reliability analyses of geotechnical installations can be performed by directly coupling geotechnical software with a reliability solver. An earth slope is used as the study object. The limit equilibrium method of Morgenstern-Price is used to calculate factors of safety and find the critical slip surface. The deterministic software package Seep/W and Slope/W is coupled with the StRAnD reliability software. Reliability indexes of critical probabilistic surfaces are evaluated by the first-order reliability methods (FORM). By means of sensitivity analysis, the effective cohesion (c´) is found to be the most relevant uncertain geotechnical parameter for slope equilibrium. The slope was tested using different geometries taking into account unsaturated soil properties. Finally, a critical slip surface, identified in terms of minimum factor of safety, is shown here not to be the critical surface in terms of reliability index.

***Keywords*—**Slope, unsaturated, reliability, safety, seepage.

Adrian Torrico Siacara is with the University of São Paulo, Brazil (e-mail: adriantorricosiacara@gmail.com).

Finite Difference Based Probabilistic Analysis to Evaluate the Impact of Correlation Length on Long-Term Settlement of Soft Soils

Mehrnaz Alibeikloo, Hadi Khabbaz, Behzad Fatahi

***Abstract*—**Probabilistic analysis has become one of the most popular methods to quantify and mange geotechnical risks due to the spatial variability of soil input parameters. Correlation length is one of the key factors of quantifying spatial variability of soil parameters which is defined as a distance within which the random variables are correlated strongly. This paper aims to assess the impact of correlation length on long-term settlement of soft soils improved with preloading. The concept of "worst case" spatial correlation length was evaluated by determining probability of failure of a real case study of Vasby test fill. For this purpose, a finite difference code was developed based on axisymmetric consolidation equations incorporating the non-linear elastic visco-plastic model and Karhunen-Loeve expansion method. The results show that correlation length has a significant impact on post-construction settlement of soft soils in a way that by increasing correlation length, probability of failure increases and the approach to asymptote.

***Keywords*—** Karhunen-Loeve Expansion, Probability of Failure, Soft Soil Settlement, "Worst Case" Spatial Correlation Length

Mehrnaz Alibeikloo. Author is PhD Candidate, School of Civil and Environmental Engineering, University of Technology Sydney (UTS), Sydney, Australia (phone: +61422838911; e-mail: mehrnaz.alibeikloo@student.uts.edu.au).

Hadi Khabbaz. Author is Associate Professor of Geotechnical Engineering (Ph.D, MEng, BEng), School of Civil and Environmental Engineering, University of Technology Sydney (UTS), Sydney, Australia (e-mail: hadi.khabbaz@uts.edu.au)

Behzad Fatahi. Author is Associate Professor of Geotechnical Engineering (Ph.D, MEng, BEng, CPEng, NPER), School of Civil and Environmental Engineering, University of Technology Sydney (UTS), Sydney, Australia (e-mail: behzad.fatahi@uts.edu.au)

The Role of Virtual Reality in Mediating the Vulnerability of Distant Suffering: Distance, Agency, and the Hierarchies of Human Life

Z. Xu

***Abstract*—**Immersive virtual reality (VR) has gained momentum in humanitarian communication due to its utopian promises of co-presence, immediacy, and transcendence. These potential benefits have led the United Nations (UN) to tirelessly produce and distribute VR series to evoke global empathy and encourage policymakers, philanthropic business tycoons and citizens around the world to actually do something (i.e. give a donation). However, it is unclear whether or not VR can cultivate cosmopolitans with a sense of social responsibility towards the geographically, socially/culturally and morally mediated misfortune of faraway others. Drawing upon existing works on the mediation of distant suffering, this article constructs an analytical framework to articulate the issue. Applying this framework on a case study of five of the UN's VR pieces, the article identities three paradoxes that exist between cyber-utopian and cyber-dystopian narratives. In the "paradox of distance", VR relies on the notions of "presence" and "storyliving" to implicitly link audiences spatially and temporally to distant suffering, creating global connectivity and reducing perceived distances between audiences and others; yet it also enables audiences to fully occupy the point of view of distant sufferers (creating too close/absolute proximity), which may cause them to feel naïve self-righteousness or narcissism with their pleasures and desire, thereby destroying the "proper distance". In the "paradox of agency", VR simulates a superficially "real" encounter for visual intimacy, thereby establishing an "audiences–beneficiary" relationship in humanitarian communication; yet in this case the mediated hyperreality is not an authentic reality, and its simulation does not fill the gap between reality and the virtual world. In the "paradox of the hierarchies of human life", VR enables an audience to experience virtually fundamental "freedom", epitomizing an attitude of cultural relativism that informs a great deal of contemporary multiculturalism, providing vast possibilities for a more egalitarian representation of distant sufferers; yet it also takes the spectator's personally empathic feelings as the focus of intervention, rather than structural inequality and political exclusion (an economic and political power relations of viewing). Thus, the audience can potentially remain trapped within the minefield of hegemonic humanitarianism. This study is significant in two respects. First, it advances the turn of digitalization in studies of media and morality in the polymedia milieu; it is motivated by the necessary call for a move beyond traditional technological environments to arrive at a more novel understanding of the asymmetry of power between the safety of spectators and the vulnerability of mediated sufferers. Second, it not only reminds humanitarian journalists and NGOs that they should not rely entirely on the richer news experience or powerful response-ability enabled by VR to gain a "moral bond" with distant sufferers, but also argues that when fully-fledged VR technology is developed, it can serve as a kind of alchemy and should not be underestimated merely as a "bugaboo" of an alarmist philosophical and fictional dystopia.

Z. Xu is a PhD candidate with the University of Cologne, Cologne, Köln 51063 Germany (e-mail: xuzhe.edu.ac@hotmail.com).

***Keywords*—**Audience, cosmopolitan, distance, distant suffering, humanitarian communication, mediation, presence, virtual reality.

The Vulnerability of Climate Change to Farmers, Fishermen and Herdsmen in Nigeria

Idris N. Medugu

***Abstract*—** This research is aimed at assessing the vulnerability of climate change to rural communities (farmers, herdsmen and fishermen) in Nigeria with the view to study the underlying causes and degree of vulnerability to climate change and examine the conflict between farmers and herdsmen as a result of climate change. This research employed the use of quantitative and qualitative means of data gathering techniques as well as physical observations. Six states (Kebbi, Adamawa, Nasarawa, Osun, Ebonyi, and Akwa Ibom) have been selected on the ground that they are key food production areas in the country and are therefore essential to continual food security in the country. So also, they also double as fishing communities in order to aid the comprehensive study of all the effects on climate on farmers and fishermen alike. Community focus group discussions were carried out in the various states for interactive session and also to have firsthand information on their level of awareness on climate change. Climate data from the Nigerian Meteorological Agency over the past decade were collected for the purpose of analyzing trends in climate. The study observed that the level of vulnerability of rural dwellers most especially farmers, herdsmen and fishermen to climate change is very high due to their socioeconomic, ethnic and historical perspective of their trend. The study therefore recommends that urgent step needs to be put in place to help control natural hazards and manmade disasters and serious measures is also need in order to minimize severe societal, economic and political crises; some of which may either escalate to violent conflicts or could be avoided by efforts of conflict resolution and prevention by the initiation of a process of de-escalation. So this study has recommended the best-fit adaptive and mitigation measures to climate change vulnerability in rural communities of Nigeria.

***Keywords*—**adaptation, farmers, fishermen, herdsmen.

I. N. Medugu is with Nasarawa State University, Keffi, Nigeria. PMB 1022 Keffi. (phone: 08042157979; e-mail: nasiru@nsuk.edu.ng

An Artificial Potential Field Based Swarm Algorithm for Fixed Wing Unmanned Aerial Vehicles

Kemal Güven, Andaç T. Şamiloğlu

***Abstract*—** In this study, an artificial potential field based swarm algorithm has been developed to establish line formation with fixed wing unmanned aerial vehicles. Total potential field for each agent was calculated according to the determined target location and the position of each agent. For each agent, heading angle and speed values were determined using potential field vector. Performance verifications of the swarm controller methods and algorithms have been studied primarily for situations where dynamics are not in the calculation. First of all, UAVs are modeled as simple massless points. Line formation algorithms were verified with limited maneuver models (simplified dynamic behavior). For this purpose, Matlab program was used. The algorithms determined as a result of these studies were used in the Gazebo environment, where the dynamics of UAVs, such as mass, thrust forces, and weather conditions, are calculated and thus have more realistic models. Delta wing model was chosen as the aircraft model. The heading and speed values obtained with the output of the swarm algorithm are used as reference in flight controls of the UAVs. Thrust control was done by using PID controller in order to reach the desired flight speed values in aircraft in the Gazebo environment. Heading was controlled by using roll angle of UAVs. Flight with line formation was carried out with a swarm of 5 UAVs in Gazebo platform.

***Keywords*—**Artificial Potential Field, Swarm Algorithm, Unmanned Aerial Vehicles, Multi Agent Systems

K. Güven is with Baskent University, Ankara, Turkey (corresponding author, phone: +90-536-867-1001; e-mail: kemalguven@baskent.edu.tr).

A. T. Şamiloğlu is with Baskent University, Ankara, Turkey (e-mail: andacsam@baskent.edu.tr).

Experimental and Numerical Determination of the Freeze Point Depression of a Multi-Phase Flow in a Scraped Surface Heat Exchanger

Carlos A. Acosta, Amar Bhalla, Ruyan Guo

***Abstract*—** Scraped surface heat exchangers (SSHE) use a rotor shaft assembly with scraping blades to homogenize viscous fluids during the heat transfer process. Obtaining in-situ measurements is difficult because the rotor and scraping blades spin continuously inside the mixing chamber obstructing the instrumentation pathway. Computational fluid dynamics simulations provide useful insight about the flow behavior around the scraper blades for a variety of fluids and blade geometries. However, numerical solutions often focus on the fluid dynamics and heat transfer phenomena of rotating flow ignoring the glass-transition temperature and freezing point depression. This research studies the multi-phase fluid dynamics and freezing point depression inside the SSHE with non-isothermal conditions in a time dependent process using an aqueous solution that contains 13.5 wt. % high fructose corn syrup and CO_2. The computational results were validated with in-situ pressure, temperature, and optical spectroscopy measurements. Results from the numerical model show good quantitatively agreement with experimental values.

***Keywords*—** Computational fluid dynamics, freezing point depression, phase-transition temperature, multi-phase flow.

I. Introduction

The prediction of microscopic fluid flow using computational techniques is done by solving the nonlinear partial differential equations that govern fluid dynamics. For multi-phase flows, the accurate definition of boundary conditions and physical properties is an essential step to fully characterize the system of equations [1]. However, is not always possible to obtain in-situ physical and chemical properties in engineering applications due to irregular or unsteady flow conditions that lead to erroneous measurements. On the other hand, scraped surface heat exchangers (SSHE) use a rotor shaft and scraping blades to mix viscous fluids inside a rigid sealed cylinder while heat is transferred through the cylinder walls. The heat transfer process typically takes place by installing a copper tube around the cylinder longitudinal wall where a working fluid (refrigerant) boils to remove heat from the mixing chamber (see Fig. 1).

Due to the continuous mixing inside the chamber, fluid and thermal boundary layers develop between the scraping blades and the rigid wall [2] enhancing the heat transfer throughout the flow. Typically, the system operates at elevated pressures and phase-transition temperatures to produce chemical reactions [3]. Therefore, monitor points to retrieve data in-situ are difficult to install and expensive to maintain.

Governing equations that describe the microscopic heat and mass transfer of the system are difficult to derive [4] due to the complex dynamics of multi-phase rotational Taylor-Couette flows [5] in the SSHE. Unfortunately, Particle image velocimetry (PIV), electro-magnetic tomography (EMT), and other optical field experimental techniques are virtually impossible to implement [6] due to the copper tube and the rigid stainless-steel wall that separates the refrigerant from the mixing fluid in the chamber.

Predicting the fluid dynamics in the mixing chamber is not trivial because the scraping blades create local vortices within the rotating flow [7] while the fluid temperature decreases reaching the phase-transition point. Past studies found in literature model the flow behavior in the SSHE using single phase flows [8] or tow-dimensional domains [9] to predict the temperature and velocity fields.

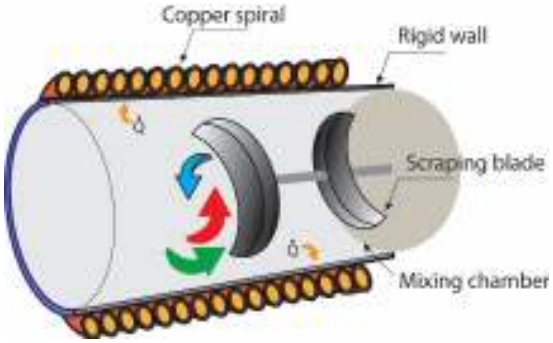

Fig. 1 Schematic of the mixing principle in a scraped surface heat exchanger (SSHE).

Experimental studies reported flow patterns using PIV in a SSHE for steady and isothermal conditions [10] demonstrating the complicated dynamics developing around the scraping blades. An innovative method to measure in-situ wall temperature for a SSHE determined the macroscopic characterization of the heat transfer coefficient during the

C. A. Acosta is with the Computer and Electrical Engineering department at the University of Texas at San Antonio, San Antonio, TX 78249 USA (corresponding author, e-mail: carlos.acosta2@utsa.edu).

A. Bhalla is a distinguished researcher in the college of engineering at the University of Texas at San Antonio, San Antonio, TX 78249 USA (e-mail: amar.bhalla@utsa.edu).

R. Guo is the program director of the advanced materials engineering program with the Electrical Engineering Department, University of Texas at San Antonio, San Antonio, Tx 87249 USA (e-mail: ruyan.guo@utsa.edu).

cooling process using a custom evaporator design [11].

The goal of this research is to study the freezing point depression and phase-transition temperature of a viscous solution in a SSHE. A time dependent non-isothermal CFD simulation was developed in order to study the fluid and heat transfer mechanisms of the multi-phase flow. An experimental workbench was constructed to measure the thermal and optical properties of the flow in-situ. The results from the simulation show good agreement with the experimental temperature values obtained experimentally.

II. Materials and Methods

Chlorinated water with an electrical conductivity of $211\left(\frac{\mu S}{cm}\right)$ has been used as the solvent. High fructose corn (HFCS) syrup $(4.6pH)$ containing 56% sucrose was dissolved at a 13.5% concentration by weight. Since HFCS dissolves in the solution, the freezing point depression of the mixture decreases, and the dynamic viscosity increases [12].

Initially, the mixing chamber is filled with HFCS and H_2O at $20(℃)$ until the in-situ pressure sensor installed on the back wall of the chamber reached $20\ (kPa)$. Then, CO_2 gas (g) was injected in the mixing chamber until the pressure sensor measured $200\ (kPa)$. At this instant the refrigeration system and electric motor were activated to remove heat from the fluid while it mixes continuously and an optical probe measured optical absorption inside the chamber. The nominal angular velocity of the electric motor was $175(RPM)$. A gas flow meter captured $17.5(L)$ of CO_2 (g) injected in the chamber (total amount for the process). A temperature probe and a pressure transducer were installed on the front and back wall of the chamber respectively to capture the fluid temperature and pressure in-situ and in real time as shown in Fig 2.

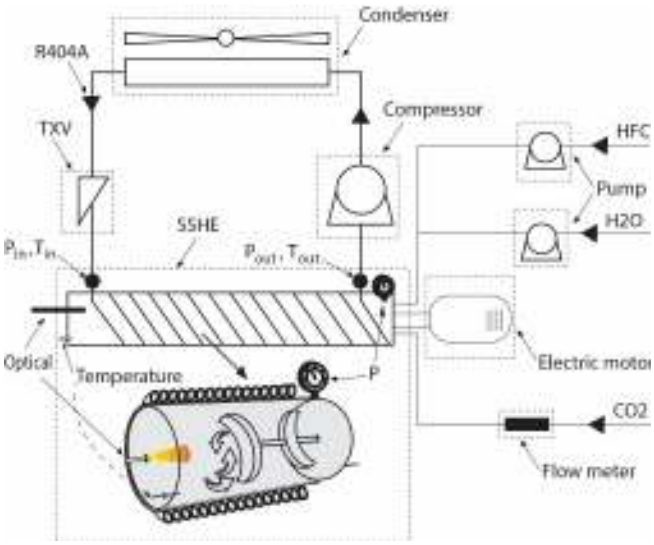

Fig 2. Experimental setup.

The optical probe and temperature sensor installed on the front wall of the chamber captured the optical absorbance of the solution during the freezing and mixing process while capturing the corresponding phase transition temperature and freezing point depression. The pressure transducer installed on the rear wall captured the variations in static pressure during the process. The temperature and pressure values gathered in-situ were used to determine the CO_2 solubility. Table I shows the accuracy in the instrumentation used for the experimental setup.

TABLE I
INSTRUMENTATION USED IN THE EXPERIMENTAL SETUP

Sensor	Manufacturer	Accuracy (%)
Pressure	Omega (PX-309)	0.2
Temperature	Omega (RTD PR-20)	0.1
Flow	Omega (FMA 400)	0.1
Spectrometer	Ocean Optics (HR 4000)	0.02

Pressure gauges and thermocouples were installed at the inlet and outlet of the copper tube spiral to capture the thermodynamic states of the refrigerant (R404A) in the evaporator. The enthalpy at the inlet and outlet were computed using the thermodynamic properties of the refrigerant [13] in order to estimate the effective evaporative power applied to the longitudinal wall of the mixing chamber.

The mean evaporative power and in-situ (averaged) pressure measurements (shown in Fig 3.) were used as time dependent boundary conditions for the CFD simulation. The cooling rate provided by the evaporator is $0.071\left(\frac{℃}{s}\right)$.

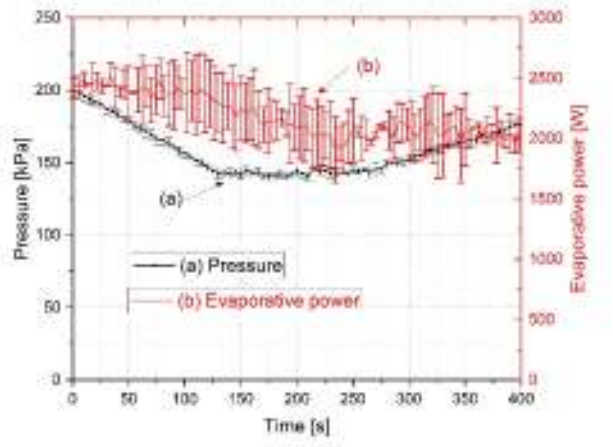

Fig. 2 Pressure measurements in-situ and computed evaporative power from refrigerant properties.

During the cooling process the temperature in the chamber decreases and the CO_2 (g) dissolves in the liquid. Since the concentration of dissolved gas increases the pressure in the chamber decreases reaching a minimum at the phase-transition point. Then, the static pressure in the chamber increases due to the ice formation and CO_2 (g) precipitation out of the solution.

III. Governing Equations

The Navier-Stokes equations are set of non-linear partial differential equations that mathematically characterize fluid flow [14]. Due to the rotating periods of the shaft and scraping blades in the mixing chamber, a convenient mathematical formulation used to solve CFD flows in SSHE applications is

the rotating frame of reference approach [15]. For a multi-phase flow containing two phases (liquid and gas) the volume fractions are expressed as follows [16]:

$$\alpha_l + \alpha_g = 1 \tag{1}$$

Where α_l and α_g are the volume fractions of liquid and gas respectively. The multi-phase density is:

$$\rho = \alpha_l \rho_l + \alpha_g \rho_g \tag{2}$$

where ρ_l and ρ_g are the densities of the liquid and gas. The multi-phase mass fraction is:

$$\varphi_l + \varphi_g = 1 \tag{3}$$

for which $\varphi_l = \frac{\rho_l \alpha_l}{\rho}$ and $\varphi_g = \frac{\rho_g \alpha_g}{\rho}$.
Similarly, the heat capacity is:

$$c_p = \varphi_l c_{p_l} + \varphi_g c_{p_g} \tag{4}$$

and the thermal conductivity is:

$$k = \alpha_l k_l + \alpha_g k_g. \tag{5}$$

The velocity vector is:

$$\vec{u} = \varphi_l \vec{u}_l + \varphi_g \vec{u}_g. \tag{6}$$

The continuity equation for the liquid phase is expressed as:

$$\frac{\partial \alpha_l \rho}{\partial t} + \nabla \cdot \left(\rho \alpha_l \vec{u_l}\right) = \Gamma \tag{7}$$

And for the gas phase is:

$$\frac{\partial \alpha_g \rho}{\partial t} + \nabla \cdot \left(\rho \alpha_g \vec{u}_g\right) = S - \Gamma \tag{8}$$

where Γ is the mass transfer rate and S is a source term associated with the CO_2 (g) precipitating out of the solution due to the dynamics from the continuous mixing. Consequently, the momentum equation in the x-direction from a rotational frame of reference approach is:

$$\frac{\partial \rho u_x}{\partial t} + \nabla \cdot (\rho \vec{u} u_x) = -\frac{\partial p}{\partial x} + \nabla \cdot (\mu_l \nabla u_x) - \nabla \cdot \left(\mu_l \alpha_g \nabla u_{x_g}\right) + \left(\mu \alpha_g \nabla u_{x_g}\right) - \nabla \cdot \left\{\frac{\rho \alpha_g}{\alpha_l}\left(u_x - u_{x_g}\right)\left(\vec{u} - \vec{u}_g\right)\right\} + F + \rho \vec{g} + \vec{\omega}^2 r - 2\vec{\omega} \times \vec{u} \tag{9}$$

where μ is the multi-phase viscosity, $\vec{g}$ is gravity, p is the dynamic pressure, and r is the direction vector. Furthermore, the momentum equations in the y-direction is:

$$\frac{\partial \rho u_y}{\partial t} + \nabla \cdot \left(\rho \vec{u} u_y\right) = -\frac{\partial p}{\partial y} + \nabla \cdot \left(\mu_l \nabla u_y\right) - \nabla \cdot \left(\mu_l \alpha_g \nabla u_{y_g}\right) + \left(\mu \alpha_g \nabla u_{y_g}\right) - \nabla \cdot \left\{\frac{\rho \alpha_g}{\alpha_l}\left(u_y - u_{y_g}\right)\left(\vec{u} - \vec{u}_g\right)\right\} + F + \rho \vec{g} + \vec{\omega}^2 r - 2\vec{\omega} \times \vec{u} \tag{10}$$

and the momentum equations in the z-direction is:

$$\frac{\partial \rho u_z}{\partial t} + \nabla \cdot (\rho \vec{u} u_z) = -\frac{\partial p}{\partial z} + \nabla \cdot (\mu_l \nabla u_z) - \nabla \cdot \left(\mu_l \alpha_g \nabla u_{z_g}\right) + \left(\mu \alpha_g \nabla u_{z_g}\right) - \nabla \cdot \left\{\frac{\rho \alpha_g}{\alpha_l}\left(u_z - u_{z_g}\right)\left(\vec{u} - \vec{u}_g\right)\right\} + F + \rho \vec{g} + \vec{\omega}^2 r - 2\vec{\omega} \times \vec{u}. \tag{11}$$

where F contains the lift and drag forces. The temperature field is computed using the energy equation such that:

$$\frac{\partial \left(\rho c_p T\right)}{\partial t} + \nabla \cdot \left(\rho c_p \vec{u} T\right) = \nabla \cdot (k \nabla \mathrm{T}) + \frac{\partial (\rho \delta_g L)}{\partial t} + \nabla \cdot \left(\rho \delta_g \vec{u}_g L\right) \tag{12}$$

where T is the temperature scalar field and L is the latent heat.

IV. Numerical Solution

The non-isothermal and time-dependent numerical solution for the CFD simulation was obtained in ANSYS CFX 17.2, finite volume commercially available software. The three-dimensional computational geometry was generated based on the exact dimensions from the test bed. The mesh (generated in ICEM-CFD) and geometry details are shown in fig. 3.

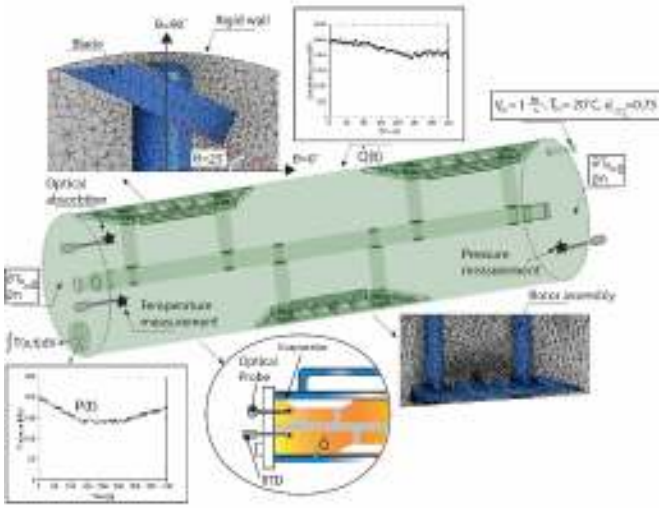

Fig. 3 Mathematical domain and boundary conditions

The computational solution was obtained ignoring the heat by radiation and assuming the heat loss between the SSHE and ambient are negligible. Also, it was assumed that the CO_2 (g) dissolves in the water before and after ice forms.

The CO_2 concentration is computed using Henry's law of solubility such that:

$$c^{CO_2} = \mathrm{H} \cdot e^{\left[A\left(\frac{1}{T}-\frac{1}{T_{in}}\right)\right]} \cdot P^{CO_2} \quad (13)$$

where c^{CO_2} is the computed volumetric concentration of CO_2 (g) in the solution, H is Henry's solubility constant, A is the *activity* coefficient in the liquid phase, P^{CO_2} is the gas partial pressure, and $\bar{T} = \int T(t,\tilde{x})dV$ is the average temperature field for the 3D fluid domain $\tilde{x}$ in the chamber. The total simulation time was 400 seconds with a time step of 0.1 (s). The inlet boundary condition was specified as a Dirichlet type with a multiphase velocity of $1\frac{m}{s}$ and a CO_2 (g) volume fraction of 75%. The outlet pressure and the heat flux across the longitudinal chamber wall were specified as a periodic boundary conditions from the average values obtained experimentally (shown in Fig. 2). The CO_2 (g) concentration at the outlet was computed using Eq. (12). The front and back surfaces of the chamber were insulated $\left(\frac{\partial T}{\partial n}\right)$ and assigned a no-slip condition.

The mesh metrics and element specifications are shown in Table II.

TABLE II
MESH PARAMETERS

Parameter	Specification
Mesh type	Unstructured
Element type	Tetrahedral
Interface	Conformal
# elements	4253537
# nodes	830944
Max. element size	2.6E-002(m)
Min. element size	5.3E-002(m)
Max. Skewness	0.82

The single and multi-phase viscosity as well as the density were measured as a function of temperature (see Table III) with viscometer (SV-100) and a high precision scale (Uline H1654). The temperature dependent specific heat, enthalpy and thermal conductivity we obtained from [17], [18], and [19] respectively.

TABLE II
FLUID PROPERTIES

Temperature (℃)	Viscosity (cP)	Density $\left(\frac{kg}{m^3}\right)$
20	1.7 ± 0.01	1099 ± 0.5
15	4.1 ± 0.01	1161 ± 0.5
10	8.3 ± 0.01	1189 ± 0.5
5	12.4 ± 0.02	1210 ± 0.5
0	16.2 ± 0.05	1202 ± 0.9
-2	36.7 ± 0.1	1080 ± 1.5
-3	735 ± 11	951 ± 1.9
-4	936 ± 16	907 ± 3.2
-5	1315 ± 25	875 ± 4.5

The viscous, thermal, and mass properties of the fluid were programmed into ANSYS-CFX to capture the phase-transition point in the computational solution though the temperature dependent material properties.

V. RESULTS AND CONCLUSIONS

The time dependent CFD simulation as well as in-situ temperature, pressure, and optical absorbance measurements were captured for the first 400 seconds of the process. The temperature solution (see Fig. 4) corresponds to the local solution obtained at the exact coordinates where the experimental temperature measurements were collected.

The temperature results from the simulation display a larger temperature compared to the experimental results due to the uniform heat flux boundary condition applied to the longitudinal chamber wall. In practicality, the refrigerant evaporates at specific locations throughout the evaporator generating colder regions not captured in the simulation.

The experimental measurements exhibit larger deviations after the phase-transition point due to the intrinsic variations from the multi-phase flow dynamics [20] and the growth or nucleation of ice crystals.

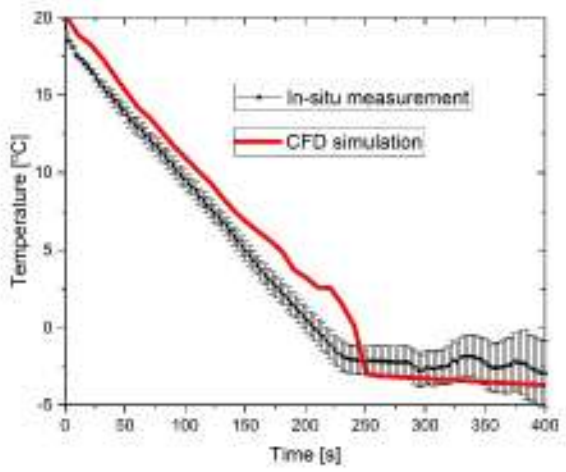

Fig. 4 Comparison between CFD results and experimental measurements in-situ

The carbonic acid forming in solution from CO_2 dissolved in water was not considered in the numerical simulation. Nonetheless, good agreement can be observed between the predicted temperature values and the values measured experimentally. In-situ optical absorbance measurements shown in Fig. 5 were obtained during the freezing process in order to capture the phase-transition temperature.

There are several distinguishing features shown. First, the characteristic signatures of sucrose in the ultra-violet (UV) spectrum $(230 - 450\,nm)$ are captured confirming values found in literature for similar aqueous solutions [21], [22]. Second, the optical absorbance of the liquid mixture at 20℃ shows characteristic sucrose signatures around 300 nm at maximal light absorbance spanning for almost 100 nm. Third, since water in a static state does not absorb light from any wavelength in the visible (VIS) spectrum [23], it is inferred that the optical absorbance detected from $\lambda = 400(nm)$ to $\lambda = 1000(nm)$ corresponds to the energy induced by the flow dynamics while mixing. Fourth, at $T = -2.55$℃ the signatures

of sucrose and water molecules are not perceptible due to the change in symmetry in the fluid molecules suggesting a phase-transition from the liquid state to an ice slurry.

For lower temperatures ($T = -3.5℃$), the absorbance measurements obtained are uniform through the UV, VIS, and near-infra-red spectrum implying the presence of ice crystals in the fluid.

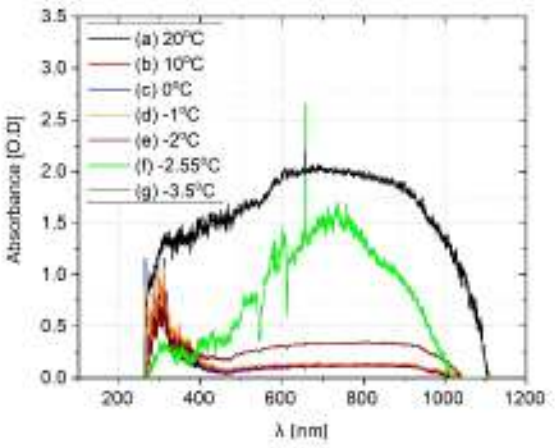

Fig. 5 Optical absorbance measurements in-situ

The velocity field of the liquid phase at $t = 250$ seconds is shown in Fig. 6. The velocity was rendered in the gap between the scraper blade and the rigid wall.

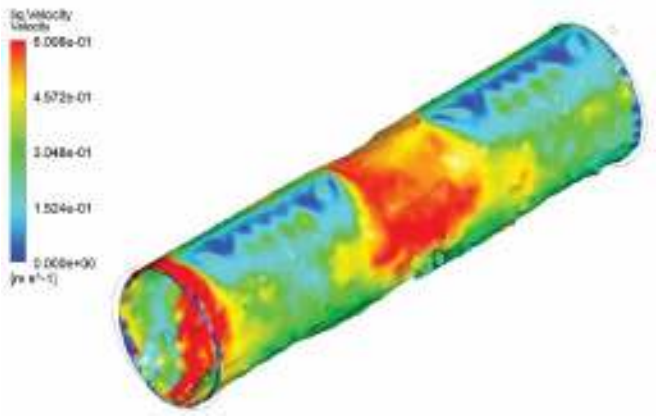

Fig. 6 Velocity field for the liquid phase at $t = 250$ seconds.

According to the numerical results the largest velocity region developed in the center of the chamber, especially in the core domain. The flow dynamics behind the blade display low velocities compared to the rest of the system. Clearly, the velocities are virtually identical for the rest of the flow.

Fig. 7 depicts the CO_2 volume fraction at $t = 250$ seconds. Interestingly, there were localized areas with CO_2 volume fraction around 80% at the front and back of the domain. Also, results show that the CO_2 volume fraction was close to 40% in the center of the chamber corresponding to the flow region displaying the largest velocity. The CO_2 volume fraction was controlled using Eq. (13) by computing the volumetric gas concentration in the solution. This approach assumes that the *activity* coefficient and solubility constant remain invariant through the latent heat offset associated with the phase change.

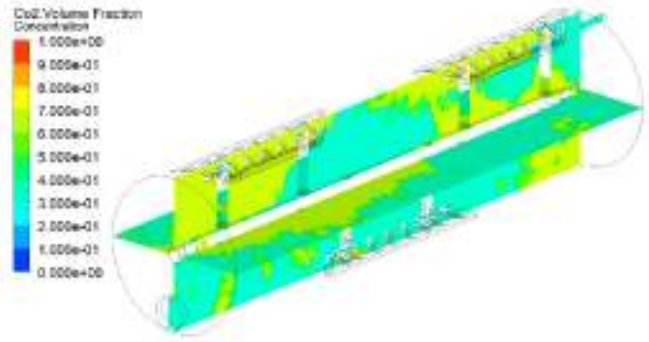

Fig. 7 Concentration of CO_2 at t=250 seconds.

VI. Conclusions

Experimental values of temperature, pressure, and optical absorbance were obtained in-situ in a SSHE to determine the phase-transition temperature and freezing point depression of an aqueous solution containing CO_2 and sucrose in a SSHE. A time dependent CFD simulation was developed and validated against temperature data found experimentally to study the microscopic fluid flow and heat transfer behavior during the freezing process.

From the experimental and numerical results, the following observations are made:

1) Optical absorbance captures the phase transition details of turbulent flows in the UV and VIS spectrum rendering the microscopic symmetry changes during the phase-transition process.
2) The computed freezing point depression using the cryoscopic constant of water was $-1.65℃$. However, the phase-change temperature measured experimentally was $-2.55℃$ evidencing the effect of fluid forces in the decrease of the freezing point. Therefore, Determining the freezing point depression mathematically is not trivial because the rotor velocity and blade geometry directly affect the fluid dynamics inside the SSHE.
3) The CFD simulation shows CO_2 segregation in the multi-phase Taylor-Coutte multi-phase flow, especially in regions with flow stagnation or low velocity.

Acknowledgment

This research work has been partially supported by industrial sponsorship under grant UTSA #1000002380.

References

[1] M. Wang, Y. Feng, Y. Wang and T. Zhao, "Periodic boundary conditions of discrete element method-lattice Boltzmann method for fluid-particle coupling," *Granular Matter,* vol. 19, no. 3, pp. 1-100, 2017.

[2] H. Abichandani and S. A. H. Sarma, "Heat transfer and power requirements in horizontal thin film scraped surface heat exchangers.," *Chemical Engineering Science,* vol. 43, no. 4, pp. 871-881, 1988.

[3] L. Erlbeck, D. Wössner, K. Schlachter, T. Kunz, F.-J. Methner and M. Rädle, "Investigation of a novel scraped surface crystallizer with included ice-pressing section as new purification technology," *Separation and Purification Technology,* vol. 228, no. 1, p. 15748, 2019.

[4] J. Solano, A. García, P. Vicente and A. Viedma, "Flow pattern assessment in tubes of reciprocating scraped surface heat exchangers," *International Journal of Thermal Sciences,* vol. 50, no. 5, pp. 803-815, 2011.

[5] D. Crespí-Llorens, P. Vicente and A. Viedma, "Flow pattern of non-Newtonian fluids in reciprocating scraped surface heat exchangers," *Experimental Thermal and Fluid Science,* vol. 76, no. 1, pp. 306-323, 2016.

[6] P. Błasiak and S. Pietrowicz, "An experimental study on the heat transfer performance in a batch scraped surface heat exchanger under a turbulent flow regime," *International Journal of Heat and Mass Transfe,* vol. 107, no. 1, pp. 379-390, 2017.

[7] R. De Goede and E. De Jong, "Heat transfer properties of a scraped-surface heat exchanger in the turbulent flow regime," *Chemical Engineering Science,* vol. 48, no. 8, pp. 1393-1404, 1993.

[8] K. Nilpueng and S. Wongwises, "Experimental study of single-phase heat transfer and pressure drop inside a plate heat exchanger with a rough surface," *Experimental Thermal and Fluid Science,* vol. 68, no. 1, pp. 268-275, 2015.

[9] P. Błasiak and S. Pietrowicz, "Towards a better understanding of 2D thermal-flow processes in a scraped surface heat exchanger," *International Journal of Heat and Mass Transfer,,* vol. 98, no. 1, pp. 240-256, 2016.

[10] M. Yataghene, F. Francine and L. Jack, "Flow patterns analysis using experimental PIV technique inside scraped surface heat exchanger in continuous flow condition," *Applied Thermal Engineering,* vol. 31, no. 14, pp. 2855-2868, 2011.

[11] D. Martínez, F. Illán, J. Solano and A. Viedma, "Embedded thermocouple wall temperature measurement technique for scraped surface heat exchangers," *Applied Thermal Engineering,* vol. 114, no. 1, pp. 793-801, 2017.

[12] P. W. Wilson and A. D. J. Haymet, "Effect of solutes on the heterogeneous nucleation temperature of supercooled water: an experimental determination," *Physical Chemistry Chemical Physics,* vol. 11, no. 15, pp. 2679-2682, 2009.

[13] I. H. Bell, J. Wronski, S. Quoilin and V. Lemort, "Pure and Pseudo-pure fluid thermophysical property evaluation and the open-source thermophysical property library CoolProp," *Industrial Engineering Chemistry Research,* vol. 53, no. 6, pp. {2498-2508, 2014.

[14] W. Sheng, "A revisit of Navier–Stokes equation," *European Journal of Mechanics,* vol. 80, no. 1, pp. 60-71, 2020.

[15] M. Yataghene and J. Legrand, "A 3D-CFD model thermal analysis within a scraped surface heat exchanger," *Computers and Fluids,* vol. 71, no. 1, pp. 380-399, 2013.

[16] B. Liu, X. Liu, C. Lu, A. Godbole, G. Michal and A. K. Tieu, "Multi□ phase decompression modeling of CO2 pipelines," *Greenhouse Gases: Science and Technology,* vol. 7, no. 4, pp. 665-679, 2017.

[17] A. Magoń, A. Wurm, C. Schick, P. Pangloli, S. Zivanovic, M. Skotnicki and M. Pyda, "Heat capacity and transition behavior of sucrose by standard, fast scanning and temperature-modulated calorimetry," *Thermochimica Acta,* vol. 589, no. 1, pp. 183-196, 2014.

[18] E. Tombari, G. Salvetti, C. Ferrari and G. P. T. E. Johari, "Kinetics and thermodynamics of sucrose hydrolysis from real-time enthalpy and heat capacity measurements.," *The journal of physical chemistry,* vol. 111, no. 3, pp. 496-501, 2007.

[19] D. A. Maccarthy and N. Fabre, "Thermal Conductivity of Sucrose," in *Food Properties and Computer-Aided Engineering of Food Processing Systems*, Cork, Springer, 1989, pp. 105-111.

[20] Y. Liu, W. Sun and S. Wang, "Experimental investigation of two-phase slug flow distribution in horizontal multi-parallel micro-channels," *Chemical Engineering Science,* vol. 158, no. 1, pp. 267-276, 2017.

[21] M. Hennemeyer, S. Burghardt and R. W. H. M. Stark, "Cantilever Micro-rheometer for the Characterization of Sugar Solutions.," *Sensors,* vol. 8, no. 1, pp. 10-22, 2008.

[22] W. C. Stagner, S. Gaddam, R. Parmar and A. K. Ghanta, "Sucrose octaacetate," in *Profiles of drug substances, excipients, and related methodology*, Cambridge, Academic Press , 2019, pp. 267-291.

[23] K. Molt and Y. Cho, "Analysis of aqueous solutions by near-infrared spectrometry (NIRS). I. Titrations of strong acids with strong bases," *Journal of Molecular Structure,* vol. 349, no. 1, pp. 345-348, 1995.

Air Impingement Drying of the Macroalgae *Sargassum muticum*: Effects of the Temperature on the Drying Kinetics

Jeanne Le Loeuff, Virginie Boy, Pascal Morançais, Nathalie Bourgougnon, Jean-Louis Lanoisellé

***Abstract*—**The brown alga *Sargassum*, which is an invasive species, causes public health troubles because of their massive groundings on beaches. For example, in 2014, 58.5 ktons of dried biomass grounded in Martinique (French West Indies). One of the main issues to cross for the recovery of this raw material is the seasonal nature of groundings. In this context, the goal of this work is to add value to this biomass through the development of a biorefinery in order to use the deposit for longer periods. Owing to their high moisture content, this raw material should be first stabilized to be used for biorefineries input. The drying aims to obtain a stabilized product available the entire year. The thermal drying is a complex process, which is energy intensive. Therefore, modern drying technology focuses on energy saving, as well as on the quality of the product. Air impingement technology aims to enhance the hot air drying process. Thanks to this technology, the air impingement dryer permits to decrease the drying time and the temperature levels.

A prototype of air impingement dryer designed by the company CIMS (Sablé-sur-Sarthe, France) was used. The alga *Sargassum muticum* was dried in different conditions. The experiments were carried out at four different temperatures (40, 50, 60 and 70 °C) at 40 m s^{-1}. The biomass used was both fresh algae stored in fridge (+4 °C) in salt water and frozen algae stored in freezer (–18 °C).

To reach a moisture content of 10 % (wet basis), the drying time varied between 21 and 81 min for the fresh product and between less than 11 min and 31 min for frozen algae. For each temperature, it took much time to achieve this moisture content for fresh algae than for the frozen product. Fick's diffusional model was fitted to the drying kinetics and the model was applied to determine the effective moisture diffusivity, D_{eff}. For all the conditions, D_{eff} varies between 1.85 10^{-9} and 3.60 10^{-9} m s^{-1} and the value is higher for the fresh algae as for the frozen ones regardless of temperature. Eleven curve fitting equations were applied on the experimental data. To determine the model which best fits the experimental data, the quality of the models was evaluated by four statistical parameters: the adjusted coefficient of determination (R^2), the residual sum of squares (RSS), the chi-square (χ^2) and the root-mean-square-error (RMSE). Low values of RSE, χ^2, RMSE and high adjusted R^2 are expected. At 60 °C for fresh algae, the Logarithmic and Midilli-Kucuk models best fit the experimental data ($R^2 > 0.9999$; $\chi^2 < 6\ 10^{-6}$; $RSS < 9\ 10^{-5}$; $RMSE < 3\ 10^{-3}$). This study shows that the effective moisture diffusivity depends on drying temperature and storage conditions of the biomass before the drying.

J. L.L. Author is with the Univ. Bretagne Sud, UMR CNRS 6027, IRDL, F-56300 Pontivy (e-mail: jeanne.le-loeuff@univ-ubs.fr).

V. B. Author is with the Univ. Bretagne Sud, UMR CNRS 6027, IRDL, F-56300 Pontivy (e-mail: virginie.boy@univ-ubs.fr).

P. M. Author is with the Univ. Bretagne Sud, UMR CNRS 6027, LBCM, F-56017 Vannes (e-mail: pascal.morancais@univ-ubs.fr).

N. B. Author is with the Univ. Bretagne Sud, UMR CNRS 6027, LBCM, F-56017 Vannes (e-mail: nathalie.bourgougnon@univ-ubs.fr).

J. L.L. Author is with the Univ. Bretagne Sud, UMR CNRS 6027, IRDL, F-56300 Pontivy (e-mail: jean-louis.lanoiselle@univ-ubs.fr).

***Keywords*—**Air impingement drying, effective moisture diffusivity, macroalgae, modelling.

On Chip Magnetic Microparticles Migration for Layer-by-Layer Deposition

Amaury de Hemptinne, Iwona Ziemecka, Wim De Malsche

***Abstract*—** Microfluidics is a powerful tool to produce microparticles with a high level of mono-dispersity. In addition, Layer-by-Layer (LbL) deposition is a fast and easy technique to structure a material in consecutive layers. In this work the advantages of microfluidics and LbL deposition are combined to produce structured microparticles.

The structured microparticle is made of a core particle on which we deposit different layers. A laminar flow transports the core particles along the microfluidic chip. Layers can be added by displacing the core into various solutions, each flowing in different interconnected microfluidic channels. The core particles are made of superparamagnetic nanoparticles fixed in a matrix of polystyrene. Handling of the superparamagnetic core particles is done by external magnets.

Two externals channels contain solutions of polyelectrolytes (P1 and P2) and a central channel contains a washing solution (WS). Particles are injected in the chip with the WS. By changing the positions of the magnets, trajectory of the core microspheres can be manipulated, forming a zigzag pattern. We aim to produce particles with three layers, two with P1 and one with P2.

With the use of walls and the limited number of fluidic links between the channels, the mixing of solutions between channels is kept to a minimum, which gives good prospect to increase the channel length and cycle number without experiencing excessive dilution.

A theoretical study of the trajectory and forces acting on particles was also performed. To this end, the resulting forces on the particles were calculated and the magnetic particle susceptibility was measured.

To design this experiment, we considered the different forces in the direction of the magnet. Using Newton's seconds law, we can sum the magnetic and Stokes drag force driving the particles and find an equation for the magnetic susceptibility of the particle.

The magnetic susceptibility of the core particles is determined by measuring the particles trajectory and velocity in a known magnetic field. In our study, we used polystyrene superparamagnetic particles with a diameter of 89µm and a magnetic susceptibility of 0.045.

With knowledge of the magnetic susceptibility, the required magnetic field as well as the particle–magnet distance in the microfluidic channel can now be determined. After optimization of the chip we can run particles in the respective channels. The liquid flow controls the residence time in each solution.

We are currently producing and characterizing particles with this developed methodology.

In conclusion, we developed a device enabling the continuous production of nanostructured microparticles. We have a full control of the movement of the particles thanks to the measure of the magnetic susceptibility, the calculation of the forces and the optimized chip design. The first step was done with three layers. We aim to create an extended tool to increase the number of layers and increase the potential of the concept.

Keywords **—** Layer-by-Layer deposition, magnetic susceptibility, particles migration, superparamagnetic particles

Amaury de Hemptinne is with Vrije Universiteit Brussels, 1050 Brussels, Belgium (phone: 0032 629 1084, e-mail: amaury.de.hemptinne@vub.be).

Iwona Ziemecka is with Vrije Universiteit Brussels, 1050 Brussels, Belgium (Iwona.ziemecka@vub.be

Wim De Malsche is with Vrije Universiteit Brussels, 1050 Brussels, Belgium (phone: 0032 2 629 3781, e-mail: wim.de.malsche@vub.be).

Numerical Method for Productivity Prediction of Water-producing Gas Well with Complex 3D Fractures - Case study of Xujiahe Gas Well in Sichuan Basin

Hong Li, Haiyang Yu, Shiqing Cheng, Nai Cao, Zhiliang Shi

***Abstract*—**Unconventional resources have gradually become the main direction for oil and gas exploration and development. However, the productivity of gas wells, the level of water production, and the seepage law in tight fractured gas reservoirs are very different. These are the reasons why production prediction is so difficult. Firstly, a three-dimensional multi-scale fracture and multiphase mathematical model based on Embedded Discrete Fracture Model (EDFM) is established. And using the material balance method to calculate the water body multiple according to the production performance characteristics of water-producing gas well. This will help construct a "virtual water body". Based on these, this paper presents a new numerical simulation process that can adapt to different production modes of gas wells.

The research results show that fractures have a double-sided effect. The positive side is that it can increase the initial production capacity, but the negative side is that it can connect to water body which will lead the gas production drop and the water production rise both rapidly, showing a "scissor-like" characteristic. It is worth noting that fractures with different angle have different ability to connect with the water body. The higher the angle of gas well development, the earlier the water maybe breakthrough. When the reservoir is a single layer, there may be a stable production period without water before the fractures connect with the water body. Once connected, a “scissors shape” will appear. If the reservoir has multiple layers, the gas and water will produce at the same time. The above gas-water relationship can be matched with the gas well production date of Xujiahe gas reservoir in Sichuan Basin. This method is used to predict the productivity of a new well with hydraulic fractures in this gas reservoir, and the prediction results are in agreement with on-site production data by more than 90%. It shows that this research idea has great potential in productivity prediction of water-producing gas well. Early prediction results are of great significance to guide the design of development plans.

***Keywords*—**EDFM, Multiphase, Multilayer, Water body.

H. Li. Author is with China university of petroleum Beijing, CO 102249 China (phone: +86-184-28386011; e-mail: lihong660@163.com).

H.Y. Yu. Author is with China university of petroleum Beijing, CO 102249 China (e-mail: haiyangyu.cup@139.com).

S.Q. Cheng. Author is with China university of petroleum Beijing, CO 102249 China (e-mail: chengsq973@163.com).

N. Cao. Author is with China university of petroleum Beijing, CO 102249 China (e-mail: caonai99@163.com).

Z.L. Shi. Author is with SINOPEC Petroleum Exploration & Production Research Institute, Beijing, CO 100083, China (e-mail: 569809365@qq.com).

High Pressure Multiphase Flow Experiments: the Impact of Pressure on Flow Patterns Using an X-Ray Tomography Visualisation System

S. Black, C. McLaughlin, A. Pranzitelli, M. Laing

***Abstract*—** Multiphase flow structures of two-phase multicomponent fluids were experimentally investigated in large diameter high pressure pipeline up to 130 bar at TÜV SÜD's National Engineering Laboratory Advanced Multiphase Facility. One of the main objectives of the experimental test campaign was to evaluate the impact of pressure on multiphase flow pattern as much of the existing information is based on low pressure measurements. The experiments were performed in a horizontal and vertical orientation in both 4-inch and 6-inch pipework using nitrogen, Exxsol^{TM} D140 oil and a 6% aqueous solution of NaCl at incremental pressures from 10 bar to 130 bar. To visualise the detailed structure of the flow of the entire cross-section of the pipe, a fast response X-ray tomography system was used. A wide range of superficial velocities from 0.6 m/s to 24.0 m/s for gas and 0.04 m/s and 6.48 m/s for liquid were examined to evaluate different flow regimes. The results illustrated the suppression of instabilities between the gas and the liquid at the measurement location and that intermittent or slug flow was observed less frequently as the pressure was increased. CFD modelling of low and high pressure simulations were able to successfully predict the likelihood of intermittent flow; however further tuning is necessary to predict the slugging frequency. The dataset generated is unique as limited datasets exist above 100 bar and is of considerable value to multiphase flow specialists and numerical modellers.

***Keywords*—** High pressure**,** Multiphase, X-ray tomography.

S. Black C. McLaughlin, A. Pranzitelli, M. Laing are with TÜV SÜD National Engineering Laboratory, East Kilbride, Glasgow, G75 0QF, United Kingdom (phone: +44(0)1355 593700; e-mail: sandy.black@tuvsud.com).

Mycoflora Associated with Maize Grains Sampled from All over Egypt

Yasser M. Shabana, Khaled M. Ghoneem, Nehal S. Arafat, Younes M. Rashad, Dalia G. Aseel, Bruce D. L. Fitt, Aiming Qi, Benjamin Richard, Haitham Sayed

***Abstract*—** Maize is one of the main staple food crops in Egypt. Pests and diseases are estimated to cause yield losses of c. 20% for this crop. Climate change will directly influence crop diseases, and their hosts, decreasing crop yields and increasing numbers of people at risk of hunger. In order to better protect the maize crop and secure food supply in Egypt, investigations on the occurrence and diversity of the seed-borne mycoflora in maize were conducted at 200 local sites from all 25 maize-cultivating governorates in Egypt. Maize grain samples were collected from four districts/counties in each governorate. In each county, two villages and one maize field from each village was selected for sampling. Each grain sample weighed 1 kg. At each sampling site, the crop information was recorded and the location was georeferenced using the global positioning system (GPS). In total, two hundred samples of maize grains from 200 villages (i.e. 25x4x2) were collected in 2020 and stored at 4oC. They were subsequently screened for their seed-borne mycoflora. A total of 23 genera and 40 species of fungi were recovered from the seed samples using a deep-freezing blotter method. The genera identified were: Absidia, Alternaria, Arthrobotrys, Aspergillus, Bipolaris, Cephalosporium, Cladosporium, Curvularia, Epicoccum, Fusarium, Geotrichum, Melanospora, Mucor, Nigrospora, Penicillium, Phomopsis, Rhizoctonia, Rhizopus, Stemphylium, Trichoderma, Trichothecium, Ulocladium, and Ustilago. Among the 23 genera, 4 genera of seed-borne fungi consisting of 9 species and 23 strains that are known to be plant pathogens were tested for their pathogenicity and transmission on maize seedlings. Fusarium verticillioides was the most frequent and was recovered from almost all samples. A washing test was done for all maize grain samples to detect the common smut fungus Ustilago maydis. Pathogenicity tests showed that Bipolaris maydis, F. verticillioides, F. incarnatum, F. proliferatum, followed by Acremonium strictum, caused high percentages of rotted seeds and seedling mortality. Transmission studies showed that F. verticillioides, B. maydis, A. flavus and A. niger were transmitted to the germinating maize seeds. These results are vital for guiding research priorities for developing future strategies for managing these diseases.

***Keywords*—** Egypt, maize, mycoflora, seed-borne fungi.

Shabana Y.M., Arafat N.S. are with the Plant Pathology Dept., Faculty of Agric., Mansoura University, Mansoura, Egypt (e-mail: Yassershabana2@yahoo.com).

Ghoneem K.M. is with the Seed Pathology Research Department, Plant Pathology Research Institute, Agricultural Research Center, Giza, Egypt.

Rashad Y.M., Aseel D.G. are with the Plant Protection and Biomolecular Diagnosis Department, Arid Lands Cultivation Research Institute, City of Scientific Research and Technological Applications, Alexandria, Egypt.

Fitt B.D.L., Qi A., Richard B., Sayed H. are with the School of Life and Medical Sciences, University of Hertfordshire, Hatfield, Hertfordshire, AL10 9AB, UK.

Study of Effects of Hydraulic Retention Time and Organic Loading Rate on the Performance of Two-Stage Semi-Continuous Mesophilic Anaerobic Digestion of Food Waste during System Startup

A. Khadka, A. Parajuli, B. Thapa, S. Dangol, L. Sapkota, A. Ghimire

***Abstract*—** The starting-up of two-stage anaerobic digestion (AD) processes is challenging due to the dynamics of the different microbial communities that are dependent upon the operational conditions. The major operational parameters such as hydraulic retention time (HRT) and organic loading rate (OLR) in two-stage AD needs to be controlled to ensure steady-state operation and prevent any inhibition or reactor failure. Therefore, this study aims to investigate the effect of HRT and OLR in the semi-continuous two-stage AD during the start-up phase. The study reports the performance of the two-stage AD digestion of food waste using anaerobic digestate as start-up inoculum at the mesophilic condition (35℃). The working volumes of the first and second stage reactors were 0.4 L and 0.8 L, respectively. The performance of the two-stage systems in terms of volumetric biogas production and gas composition was studied under different OLR (0.25 – 0.5 gVS/L/d) and HRT (10, 20, 40 days). The start-up OLR and HRT in the reactors were 0.25 g VS/L/d and 20 days and 40 days for the first and second stage, respectively. It was observed that the methane (CH4) composition decreased from 18.20% to 0.06% in 44 days when HRT in the first stage was reduced to 10 days from 20 days and OLR was increased from 0.25 gVS/L/d to 0.5 gVS/L/d. When the volatile fatty acids (VFA)/alkalinity ratio in the second stage was 0.76, which indicated an alarm for the souring of the reactor, the feeding was stopped for a week until the pH was restored to 7.0. The restoration of healthy methanogens in the second stage was also indicated by an increase in methane (CH4) content in biogas, 39.15% to 67.48%. Lowering the HRT in the first stage reactor to 10 days will wash out the methanogens from the first reactor and could aid in the production of biohydrogen (H2). Thus, a two-stage AD could pave a way for the production of multiple biofuels, i.e. H2 and CH4.

***Keywords*—** biogas, anaerobic digestion, food waste, hydraulic retention time, organic loading rate.

A.Khadka is with the Soil Water and Air Testing Laboratories Pvt. Ltd., GPO 25752, Babarmahal, Kathmandu, 44600, Nepal (email:aakash.swat@gmail.com)

A. Parajuli is with Creasion (Centre for Research and Sustainable Development), Lamingtan, Sheetal Marg, Baluwatar, Nepal (email: anmolparajuli7@gmail.com)

B.Thapa is with the Nawa Paila, Sisir-Marg-11, Babarmahal, Kathmandu Nepal (email:thapabijay88@gmail.com)

S.Dangol is with the Nawa Paila, Sisir-Marg-11, Babarmahal, Kathmandu Nepal (email:sheila.dangol@gmail.com)

L.Sapkota is with the Department of Environmental Science and Engineering, Kathmandu University, Dhulikhel, 45200, Nepal and Soil Water and Air Testing Laboratories Pvt. Ltd., GPO 25752, Babarmahal, Kathmandu, 44600, Nepal (email:lokesh.sapkota.27@gmail.com)

A. Ghimire is with the Department of Environmental Science and Engineering, Kathmandu University, Dhulikhel, 45200, Nepal (email:anishghimire@ku.edu.np; anishghimire@gmail.com)

Access to Reproductive Health Care for Internally Displaced Women in Northern Nigeria: A Critical Ethnography Study

Oluwakemi C. Amodu, Bukola O. Salami, Solina Richter, Philomina Okeke-Ihejirika.

Abstract— Boko Haram terrorists and Herdsmen in Northern Nigeria have forcibly displaced over one million women from their homes into relief camps. Exposure to sexual activities, both consensual and forced, without the use of contraceptives, predisposes women to unique reproductive health challenges. According to the author's knowledge, little research is published about the reproductive health care experiences of women displaced by Boko Haram terrorists in Nigeria. Based on the intersectionality framework of analysis as proposed by Kimberlé Crenshaw, the ethnographic investigation was conducted to explore the socio-structural factors influencing reproductive health access for internally displaced women living in a relief settlement in Nigeria. My project keys into the Nigerian humanitarian response plan (January, 2019 – December, 2021) supported by the Ministry of Budget and National Planning, which is a bold initiative aimed at transitioning all program interventions from a humanitarian perspective to a recovery and development perspective. Thirty-nine participants, including internally displaced women, health service providers and policymakers were recruited for the study in Nigeria. Women narrated traumatic stories of abuse, loss of loved ones and livelihoods to Boko Haram attacks. Imperative reproductive health concerns identified among women include widespread urogenital infection symptoms and noticeable high rate of childbearing associated with a need to replace children lost to terrorist attacks. Cultural practices of women's ancestral villages, including home birthing practices and seeking spousal consent before obtaining care continued to influence health-seeking decisions of affected women. There was staff shortage and limited medical supplies in primary health facilities serving affected women. Further, it was found that many women relied heavily on a patent medicine vendor who provided care to them on credit. Cultural connectedness with the health provider influenced the decision to seek care. Moreover, analysis of the Nigerian social policy context identified contradictions in the subnational provision for reproductive rights and healthcare for displaced women. In 2016, the Nigerian Senate voted against the gender and equal opportunities bill 2016 (GEO bill SB 301 C 1955) — a provision of the United Nations convention on the elimination of all forms of discrimination against women (CEDAW), aiming to accord women rights equal to those of men in various spheres of life. Overall, the Nigerian government is overly reliant on aid agencies to support displaced women's health needs. As funding to humanitarian agencies is scaled back, displaced women are left to depend on grossly inefficient primary health care facilities. Conclusively, this study highlights important structural factors that undermine reproductive health access for affected women: poor governance of the primary health care sector in Nigeria and insufficient co-ordination between the federal government and implementing agencies. Results have implications for policy and administrative restructuring in the primary health sector, as well as for improved funding allocation for the provision of reproductive health services, including voluntary family planning, urogenital infections treatment and maternal healthcare. The Federal Government and all institutions managing healthcare funds should implement strategies to ensure strong leadership and accountability in health development assistance and practices for internally displaced persons.

Keywords—Critical ethnography, internally displaced women, intersectionality, reproductive health.

O. C. Amodu, Faculty of Nursing, University of Alberta, Level 3—Edmonton Clinic Health Academy, Edmonton, AB, T6G 1C9, Canada. amodu@ualberta.ca

B. O. Salami, Faculty of Nursing, University of Alberta, Level 3—Edmonton Clinic Health Academy, Edmonton, AB, T6G 1C9, Canada. bukola.salami@ualberta.ca

S. R. Richter, Faculty of Nursing and Global Nursing Office, University of Alberta, Level 5—Edmonton Clinic Health Academy, Edmonton, AB, T6G 1C9, Canada. solina.richter@ualberta.ca

P. Okeke-Ihejirika, Department of Women and Gender Studies, University of Alberta, 6-5 Humanities Center, Edmonton, AB, T6G 1C9, Canada. pokeke@ualberta.ca

Disparities and Prevailing Situation of Afghan Refugee in Pakistan: A Research Assessment Study with Focus On Baluchistan Province

Bashir Ahmed

***Abstract*—** For the last 35 years, Afghan refugees are coming to Pakistan. Due to war and local conflicts in Afghanistan. These refugees are facing several issues of basic rights and going through the stress that is affecting their health and psychological well-being. The aim of this research is to highlight the issues and problems Afghan refugees that they are facing in Pakistan with refugee status. For the comprehensive coverage of the problem Mixed method research approach was adopted for the study. The quantitative method was used for conducting a perception survey for gathering quantifiable information from the primary target group (Afghan Refugees in Balochistan). From the qualitative methods perspective Key Informant Interviews (KIIs) and Focus Group Discussions were conducted by selecting respondents from the secondary groups of population (Refugee's Intellectuals/elders, government officials and personnel from UNHCR and UNHCR Partners from the Province). District Quetta and Pishin were the universe of the study. The study revealed that Afghan refugees are more vulnerable compared to the local population of the area as refugees have very limited access to basic rights and needs. One of the most major issues highlighted by the research that refugees facing very sever level of protection issues due to the behavior of local law enforcement agencies.

***Keywords*—** migration, refugees, Afghan refugee, protection issues

Bashir Ahmed is with the Balochistan University of Information Technology, Engineering and Management Sciences, Pakistan (e-mail: bashirchurmai@yahoo.com).

Skills Mismatch of Displaced Professionals in Canada

Camelia Tigau

***Abstract*—** This paper explores the disconnect between the humanitarian discourse surrounding refugees, on the one hand, and the fact that many refugees in Canada are highly-skilled. Their experience is different from the overall cohort of unskilled or medium skilled refugees, an issue that has been many times left behind from the humanitarian discourse of Canadian diplomats and politicians. Skilled mobility has been pictured as a best scenario of emigration, in which individuals actually get to choose the place where they want to live, and they even prepare their leave through education in foreign languages. However, there are cases when skilled migrants are forced to migrate in the same way as the unskilled ones; wars, poverty and violence may cause sudden or half planned decisions to migrate. Canada has been described as a model host society, protected by its multiculturalism against populist and anti-migrant discourses that other main countries of destination of skilled migration, such as the US, the UK and Australia, are experiencing at present. Canada is even shown to benefit from a possible spillover effect, that causes certain foreign workers from the US to move to cosmopolitan technological hubs such as Toronto, ¨the world in a city¨ (Anisef and Laphnier, 2003, Wadhwa et al., 2007). Canada was also leading the refugee submissions by destination as of January 2020. (UNHCR, 2020)

In spite of its excellent migration diplomacy practice, many refugees were shown to have difficulties in their integration to the job market (Enns, 2017; Nichles and Nyce, 2018). Many displaced professionals do not carry their diplomas and even when they do, they lack Canadian experience; furthermore, the definition for certain skills in their country of origin is not the same as in their country of destination. As a matter of fact, these differences in skills definition are quite common among various knowledge economies (Lo, Li and Yo, 2019)

Several theoretical approaches may serve as a background for this study. For instance, Boswell (2009) and Banulescu-Bogdan (2018) have both outlined knowledge utilization in the politics of migration, meaning that migration issues have frequently been characterized as a typical subject for risk construction for many countries of destination. Canada may be a different case, due to the relevance of migrants to its economy and national identity. Previous work by Roberts (2015) has deconstructed the role of hospitality in the Canadian identity, including its outcome on the integration of new migrants. Other studies are dedicated to the privatization of refugee costs in Canada (Hyndman, Payne and Jiménez, 2017) and to mental health problems that may hinder the labour integration of skilled immigrants in Canada (Kaushik and Drolet, 2018). My research will also consider the intervention of private actors such as World Education Services and Talent Beyond Boundaries in the certification of foreign professionals. This study will be conducted in two levels of analysis: a) pragmatic discourse analysis of diplomatic messages on refugees and displaced migrants in Canada; b) biographical research based on in-depth interviews with skilled refugees.

***Keywords*—** skilled refugees, skills mismatch, deskilling, Canada.

Camelia Tigau is with the National Autonomous University of Mexico, Mexico (e-mail: ctigau@unam.mx).

Economic Implications of the Arrival of Syrian Refugees in Jordan

Ammar Z. Alwrekiat, Sara Ojeda González, María José Miranda Martel, Antonio Mihi-Ramírez

***Abstract*—** This paper analyses the economic situation in Jordan, which has been the political asylum destination for Syrians since 2011. We analyze the effects of Jordanian situation through following indicators: international aid, gross domestic product, remittances and unemployment. A correlation analysis has been used to identify the main connections of these parameters with the reception of refugees. Although the economic effects of Syrian refugees in Jordan are uncertain, it involves an important challenge in the development of migration policies. Jordan has a special economic situation and limited capacities, but the country has provided humanitarian assistance to Syrian refugees. In this case, the support of the international community is of particular importance, taking an important role in the negotiation of international agreements on refugees.

***Keywords*—** correlation analysis, economic implications, migration, refugees.

Ammar Z. Alwrekiat is PhD candidate, University of Granada, Spain (e-mail: ammarziad@correo.ugr.es).

Sara Ojeda González., is PhD, University of Las Palmas de Gran Canaria (e-mail: sara.ojeda@ulpgc.es).

María José Miranda Martel is Professor in Department of Ecnomomy and Business, University of Las Palmas de Gran Canaria (e-mail: mariajose.miranda@ulpgc.es)

Antonio Mihi Ramírez is Professor in Department of International and Spain' Economics, University of Granada (amihi@ugr.es)

How Afghan Female Refugees in Germany Navigate Reproductive Health: A Photovoice Project through Coronavirus Pandemic

Naseem S. Tayebi

***Abstract*—** Afghan nationals rank third in number applying for asylum in Europe, following Syrian and Iranian refugees (UNHCR, 2018). The number of Afghan refugees in Germany has doubled since 2015. Research suggests that Afghan refugees and asylum seekers often have mental health problems resulting from prolonged exposure to war and the insecurity of seeking international protection, as well as the challenges they face while seeking asylum, often beginning in childhood, and in multiple countries. The current qualitative study includes data from 18 in-depth interviews (13 Afghan refugee women and 5 German volunteers from Helferkreis) in a suburb of Munich /Germany, as well as field notes and observations collected while accompanying refugee families as a translator as they interfaced with health care providers and government authorities in 2019-2020. Participants have mentioned their experiences with the German health system and the difficulties they had to overcome, especially related to language barriers and medical/comorbidity issues (e.g., missing vaccinations, tuberculosis). The crucial role of volunteers is another theme which was emphasised by the participants that allows women refugees to overcome the barriers they face in accessing health care and maternity care. Eight out of thirteen of these Afghan refugee women cooperated in photovoice and 4 participatory meetings, where they could share their experiences and challenges during the pandemic and lockdown (March 2020 until October 2020). This sharing of experiences via participatory meetings was especially uplifting and could promote the women's self-confidence and empower others in their community.

***Keywords*—** Afghan women refugees, coronavirus pandemic, participatory research, reproductive health.

Naseem Sadat Tayebi is with the Ludwig Maximilian University, Germany (e-mail: nasim_st@yahoo.com).

How Schools can support a Sense of Belonging in Female Students from Refugee Backgrounds

Van der Putten, Sonja A.

***Abstract*—** There are over 50 million children from refugee backgrounds under the age of 18 years old worldwide today. Due to the unique cognitive, social, and emotional needs of developing children, the United Nations Convention on the Rights of the Child recommends that countries make special provisions for refugee student populations. Education plays an essential role in creating a sense of belonging and preserving hope amongst adolescents from refugee backgrounds. To better understand the significance of sense of belonging on students from refugee backgrounds, this study used narrative inquiry to collect data from seven-female adolescent students from refugee backgrounds in one Canadian secondary school. The study triangulated data from interviews, observations, field note journals, and artwork to better understand students' experiences. A strength-based lens framed students as being resilient, resourceful, and optimistic of their futures, despite the on-going challenges that they continued to experience upon resettlement. Findings indicated that a sense of belonging was influenced positively and negatively by feelings of inclusion/exclusion both in the community and amongst peer groups, teacher-student relationships, and the availability of support services. The female experience was also uniquely influenced by additional familial obligations and responsibilities. The study concluded that schools that are able to foster a positive sense of belonging amongst students from refugee backgrounds, increase their pro-social outcomes and decrease their negative well-being outcomes. The positive academic, behavioural, and psychological outcomes of students who feel a strong sense of belonging in school results in improved self-efficacy, motivation and reduced social-emotional distress.

***Keywords*—** belonging, education, female, refugees.

Van der Putten, S. is a Doctoral Candidate in the Faculty of Education at Simon Fraser University, in British Columbia (e-mail: svanderp@sfu.ca).

Identifying the Effects of the COVID-19 Pandemic on Syrian and Congolese Refugees' Health and Economic Access in Central Pennsylvania

Mariam Shalaby, B.Phil., B.S., Kayla Krause, B.S., Raisha Ismail, B.S., and Daniel George, Ph.D.

***Abstract*— Introduction**: The Pennsylvania State College of Medicine Refugee Initiative is a student-run organization that works with eleven Syrian and Congolese refugee families. Since 2016, it has used grant funding to make weekly produce purchases at a local market, provide tutoring services, and develop trusting relationships. This case study explains how the Refugee Initiative shifted focus to face new challenges due to the COVID-19 pandemic in 2020. **Methodology**: When refugees who had previously attained stability found themselves unable to pay the bills, the organization shifted focus from food security to direct assistance such as applying for unemployment compensation since many had recently lost jobs. When refugee families additionally struggled to access hygiene supplies, funding was redirected to purchase them. Funds were also raised from the community to provide financial relief from unpaid rent and bills. **Findings**: Systemic challenges were encountered in navigating federal/state unemployment and social welfare systems, and there was a conspicuous absence of affordable, language-accessible assistance that could help refugees. Finally, as struggling public schools failed to maintain adequate English as a Second Language (ESL) education, the group's tutoring services were hindered by social distancing and inconsistent access to distance-learning platforms. **Conclusion**: Ultimately, the pandemic highlighted that a charity-based arrangement is helpful but not sustainable, and challenges persist for refugee families. Based on the Refugee Initiative's experiences over the past year of the COVID-19 pandemic, several needs must be addressed to aid refugee families at this time, including: increased access to affordable and language-accessible social services, educational resources, and simpler options for grant-based financial assistance. Interventions to increase these resources will aid refugee families in need in Central Pennsylvania and internationally.

***Keywords*—** COVID-19, health, pandemic, refugees, access

All authors are affiliated with the Pennsylvania State University College of Medicine in Hershey, Pennsylvania, USA.

Predictive Behavioral Modeling of Global Asylum Adjudications-United States versus European Union

Hari Krishnamurthy

***Abstract*—** The 1948 Universal Declaration of Human Rights (UDHR) guarantees the right to seek asylum, as does the 1980 U.S Refugee Act. In reality, around 60 % of asylum applications are denied in the US and the EU. The goal of this novel study was to compare the predictive analytics of asylum adjudication in the U.S to that in the European Union. An individualized data set containing several 100K each of US and EU case records was developed and machine learning models (Bagged Tree algorithm-based) created using the datasets. The vetted Bagged Tree classifier model was used on more than 400,000 US asylum case records obtained using the Freedom of Information Act through the TRAC software provided by Syracuse University. The US model predicted, with 91% accuracy, asylum decisions using few predictors like jurisdictional region, representation, nationality, detention, and application type. Jurisdictional Region was as important a predictor as being detained in the home country, suggesting regional judicial behavioral bias. The model was tested on around 900,000 asylum cases in the EU obtained through Eurostat and the predictability was found to be lower at 81.8%. Asylee sex had a great impact in the EU, with a significantly higher positive grant rate for female asylees. EU female asylum seekers were 20 % more likely to be granted asylum even though there was a higher number of male applicants. EU Jurisdictional country and number of attempts were not significant areas of bias in the EU. For the first time, the effect of US asylum judge gender was analyzed. Overall, in the US, Female U. S asylum judge's grant rate was significantly higher (51%to 35%, $p < 0.001$). In areas with low overall grant rates like Texas, female judges had a lower grant rate than male judges, but in areas like California with overall high grant rates, female judges were granted at significantly higher rates than male judges. In conclusion, there is higher behavioral bias in the US asylum adjudication process shown by the greater than 90% predictability compared to lower predictability in the EU. In the EU, asylee sex is the main factor, while regional bias is the key factor in the US. Overall, female US asylum judges grant asylum at higher rates compared to males, but regional variations impact this also. Future applications include the creation of a user-friendly app to assist global refugees and refugee aid agencies assess refugee's chances and to use these findings to advance legislative policy to eliminate regional biases in the U.S. Creation of a federal panel, an appeals process, and audits could be considered by the US congress to tackle the regional bias.

***Keywords*—** behavioral bias, machine learning model, judge gender, jurisdictional bias.

Hari Krishnamurthy is with the Canyon Crest Academy, United States (e-mail: rupaca@yahoo.com).

Access to Livelihoods for Urban Refugees in Kenya: The Case Study of Somalis Living in Eastleigh

Nancy Njoka. Author, Manuela Ramos. Author,

***Abstract*—**In Kenya, refugee situations are becoming increasingly protracted, stretching over the years or even decades. As urbanization rates increase, so do the numbers of urban refugees in the country. Refugees living in urban areas face a range of challenges. In their efforts to pursue livelihoods, refugees have identified strategies to confront these challenges. In the same manner, humanitarian actors have come up with different interventions to promote access to livelihoods working through obstacles and barriers created by host governments. This paper seeks to understand the experience of Somali urban refugees living in the urban area of Eastleigh, Nairobi, both by investigating their own actions towards creating avenues to access livelihoods and by understanding their social, economic and policy context in which they forge livelihoods. The empirical data collected through fieldwork in Nairobi in 2020 serves as the basis of this qualitative case study. Drawing upon the themes of urban refugee movement, Somali ethnicity, citizenship discrimination and the livelihoods of refugees, the paper highlights how the actions of the Kenyan government and international non-governmental organization (INGO)s affect access to livelihoods and the consequences of these actions for Somali urban refugees. The results of the paper found that Somali urban refugees are taking active steps to create livelihoods for themselves. This is seen in the growth of Eastleigh as an economic hub in Kenya which is owned and run mostly by Somalis. Indeed, the Somali community is central to the establishment of networks in the neighborhood. Somali urban refugees are marginalized by the Kenyan government, reducing their opportunity to create dignified lives in Eastleigh. Findings also point out the community-based approaches used by INGOs in livelihood interventions. The relevance of this research lies in the interconnection of humanitarian development interventions for protracted refugees and the promotion of livelihoods in an urban and global context.

***Keywords*—**Livelihoods, Kenya, Somali, Urban Refugees.

Nancy Njoka is, Roskilde University; Denmark e-mail: nknjoka@ruc.dk
Manuela Ramos, Roskilde University, Denmark e-mail: Mramosc@ruc.dk

The Role of Social Media in Changing the Attitudes of Upper Egyptian Females towards Early Marriage

Amany Bassyouny

***Abstract*—** The increasing dependence on social media and its increasing effects on all societies worldwide has been evident in the past few years. According to 2020 statistics, there are over 42 million social media users in Egypt . This indicates that social media is becoming a very influential factor in shaping Egyptian people's attitudes towards many social issues and it also reflects the increasing power of Egyptian citizens to tell their stories and share their views regarding societal problems. The early (child) marriage phenomenon is one of the persistent problems in Upper Egypt that hinder all the developmental efforts in Upper Egypt and negatively affects the women status and development in Egypt. This research aims at describing the phenomenon of increasing use of social media by the Upper Egyptian women and its effect on their attitudes towards early marriage problem. This study intends to shed light on the least- studied upper Egyptian female community as many sources confirm the scarcity of field studies on Upper Egyptian women. The descriptive study will use the qualitative research method of focus groups with representatives of the Upper Egyptian female community to explore their social media habits and to assess their attitudes towards early marriage phenomenon.

***Keywords*—** social media, Upper Egypt, females, early marriage.

Amany Bassyouny is with the The British University in Egypt, Egypt (e-mail: Amany.bassyouny@bue.edu.eg).

Transferring Stress Patterns

Kathrin Feindt

***Abstract*—** Emphasis in the form of relative prominence in comparison to other syllables within a word is produced by modification of the acoustic parameters duration, intensity, and fundamental frequency (F0). A stressed syllable then is marked by stronger pitch movements and lengthening of the nucleus and is also louder than surrounding syllables. Through interlinguistic difference in deploying these parameters stress assignment is a specific issue in L3 acquisition. Thus, duration is the most important cue in German and English, while changes in pitch are crucial in Turkish. To investigate which linguistic system leaves traces in bilinguals' foreign language English, the oral performance of 29 bilingual Turkish-German students in school year 7 and 9 was examined for word stress, with 37 monolingual German participants in the same age to act as control group. The data examined here are recordings of spoken language that was gathered for the quasi-longitudinal research project Mehrsprachigkeitsentwicklung im Zeitverlauf (MEZ). The recordings are analysed to filter out which of the acoustic correlates is most dominantly used, whereby examination is restricted to bisyllabic words that meet certain requirements. The total amount of stressed syllables in the corpus is condensed into a sub-corpus containing bisyllabic words that occur in any other position than utterance-final and are not associated with semantic or pragmatic novelty or paradigmatic/syntagmatic contrasts. While the word <breakfast> is always stressed on the first syllable, stress falls on the second syllable in roughly 40% of the cases in the word <coffee> and with that the difference is even highly statically significant (p-value = 0,000; X^2 =3,73; df = 1). The observation that learners deviate from the English stress pattern in pronouncing the word <coffee> can be explained by considering the cognates in German and Turkish. In German, there is (regional) variation. Although stressed first syllable prevails the Northern German dialect, diachronic analysis showed a tendency towards stressing the second syllable in modern German. For the Turkish /kʌh've/, stress always falls on the last syllable. Thus, whereas the acoustic parameters unveiled positive transfer, the influence of the background languages is negative in this case**.**

***Keywords*—**Phonological development, word stress, L3-acquisition, linguistic transfer

Kathrin Feindt is with the University of Hamburg, Hamburg, Germany. (phone: +49 (040) 42838-4854; e-mail: kathrin.feindt@uni-hamburg.de).

Paying Less and Getting More: Evidence on the Effect of Corporate Purpose from Two Natural Field Experiments

Nikolai Brosch, Alwine Mohnen

***Abstract*—** Academics and business leaders increasingly call for a (re)definition of a corporate purpose beyond profit-maximization to contribute to the welfare of society. This study investigates the effect of communicating such a pro-social corporate purpose on three employee-level outcomes that constitute major cost components for most organizations: workers reservation wage, work quality and work misbehavior. To provide causal evidence, two natural field experiments were conducted with almost 2,000 workers recruited from different online labor marketplaces. Workers were randomly assigned to treatments manipulating weather or not they received information about the employer's corporate purpose and subsequently performed a short, real-effort task for payment. The main findings in both experiments show that receiving information about an employer's pro-social corporate purpose causes workers to accept lower wages (9% lower in first experiment and 28% lower in the second experiment) for the same job. Workers that personally assess a high importance to organizations having a pro-social purpose are most responsive. At the same time, sacrificing wage for a corporate purpose comes at no cost of quality and even decreases the likelihood of engaging in work misbehavior. In a broader context, the results provide some evidence that the (re)definition of corporate purpose in commercial organizations is not ultimately at odds with creating profits.

***Keywords*—** Corporate purpose, natural field experiment, reservation wage, work misbehavior, work quality.

N. Brosch is with the TUM School of Management of Technical University of Munich, Munich, 80333 Germany (phone: +49-151-67520302; e-mail: n.brosch@tum.de).

A. Mohnen is with the TUM School of Management of Technical University of Munich, Munich, 80333 Germany (e-mail: a.mohnen@tum.de).

The Use of Ward Linkage in Cluster Integration with a Path Analysis Approach

Adji Achmad Rinaldo Fernandes

***Abstract*—** Path analysis is an analytical technique to study the causal relationship between independent and dependent variables. In this study, the integration of Clusters in the Ward Linkage method was used in a variety of clusters with path analysis. The variables used are character (x_1), capacity (x_2), capital (x_3), collateral (x_4), and condition of economy (x_5) to on time pay (y_2) through the variable willingness to pay (y_1). The purpose of this study was to compare the Ward Linkage method cluster integration in various clusters with path analysis to classify willingness to pay (y_1). The data used are primary data from questionnaires filled out by customers of Bank X, using purposive sampling. The measurement method used is the average score method. The results showed that the Ward linkage method cluster integration with path analysis on 2 clusters is the best method, by comparing the coefficient of determination. Variable character (x_1), capacity (x_2), capital (x_3), collateral (x_4), and condition of economy (x_5) to on time pay (y_2) through willingness to pay (y_1) can be explained by 58.3%, while the remaining 41.7% is explained by variables outside the model.

***Keywords*—**Cluster Integration, Linkage, Path Analysis, Compliant Paying Behavior

I. INTRODUCTION

According to [1], KPR is one of the credit services provided by banks to customers who apply for special loans to meet the needs of a residence.

According to [1], KPR is one of the credit services provided by banks to customers who apply for special loans to meet the needs of a residence.

One of the problems in KPR is the existence of debtors who are not smooth in paying their obligations. This causes losses to the bank. Therefore, it is necessary to have supervision in customer credit services, namely the classification used to determine the characteristics of debtors who are able to meet credit obligations or not. Statistical methods that can be used to deal with these problems are using cluster integration and path analysis.

There are several studies regarding research related to cluster integration with path analysis, namely those investigated by [2] with the title "An improved path-based Clustering algorithm" shows that path analysis with Cluster integration provides results that outperform other Cluster algorithms.

This study aims to classify the willingness to pay for credit types of KPR purchases at Bank X by integrating cluster analysis with path analysis. Furthermore, comparing 2, 3, and 4 clusters to find out the best integration of Clusters with the Ward Linkage method. The data used in this study are primary data from variable character / character (x_1), customer capacity (x_2), capital (x_3), collateral (x_4), and conditions of economy (x_5). on time to pay (y_2) through the variable willingness to pay / willingness to pay (y_1).

Adji Achmad Rinaldo Fernandes is with the University of Brawijaya, Indonesia (e-mail: fernandes@staff.ub.ac.id).

II. LITERATURE REVIEW

Cluster analysis (group analysis) is an analysis method that aims to group objects into several groups, the objects in the group are homogeneous (the same) while other group members are heterogeneous (different) [3]. According to [4] in the method of forming groups in the hierarchical method, there are two approaches, namely the agglomerative hierarchical method and devisive hierarchical methods. The method that is often used is the agglomerative hierarchy method. The agglomerative hierarchy method algorithms used in group formation include:

a. Ward Linkage Method

$$SSE = \sum_{j=1}^{p}\left(\sum_{i=1}^{n}\varepsilon_{ij}^2 - \frac{1}{n}\left(\sum_{i=1}^{n}\varepsilon_{ij}^2\right)^2\right)$$

where:

X_{ij}: the value for to-i object of the to-j Cluster

p : the number of variables

n : the number of respondents in the formed cluster

b. Complete Linkage Method

$$d_{(ij)k} = max\left(d_{ik}, d_{jk}\right)$$

where:

$d_{(ij)k}$: the distances between the subsample (ij) and the Cluster k

d_{ik}: distance of subsample i and Cluster k

d_{jk}: distance of sub sample j and Cluster k

c. Metode *Average linkage*

$$d_{(IJ)k} = \frac{\sum_I \sum_J d_{(IJ)}}{N_{IJ} N_K}$$

$d_{(ij)k}$: the distances between the subsample (ij) and the Cluster k

d_{ik}: distance of subsample i and Cluster k

d_{jk}: distance of sub sample j and Cluster k

d. Cluster Analysis Distance

$$d\left(x_i, x_j\right) = \sqrt{\sum_{z=1}^{p}\left(x_{ki} - x_{kj}\right)^2}$$

where:

$d\left(x_i, x_j\right)$: the Euclidean distance between the to-i object and the-j object

x_{ki} : the value of to-i object in the variable k

x_{kj} : the value of to-j object in the variable k

z : variabel ke z, $z=1,2,3,\ldots, p$

Path Analysis

The model in path analysis is as follows: $Y_1 = \beta_{10} + \beta_{11}X_1 + \beta_{12}X_2 + \beta_{13}X_3 + \varepsilon_1$

$$Y_2 = \beta_{20} + \beta_{21}X_1 + \beta_{22}X_2 + \beta_{23}X_3 + \beta_{24}Y_1 + \varepsilon_2$$

Then do the standardization so that the units of each variable are the same. The equation obtained is:

$$Z_{Y_1} = \beta_{10} + \beta_{11}Z_{X_1} + \beta_{12}Z_{X_2} + \beta_{13}Z_{X_3} + \varepsilon_1$$

$$Z_{Y_2} = \beta_{20} + \beta_{21}Z_{X_1} + \beta_{22}Z_{X_2} + \beta_{23}Z_{X_3} + \beta_{24}Z_{Y_1} + \varepsilon_2$$

Perform Cluster integration with path analysis. The cluster integration model in path analysis is written in the following equation.

$$Z_{Y_1} = \beta_{11}Z_{X_{1i}} + \beta_{12}Z_{X_{2i}} + \beta_{13}Z_{X_{3i}} + \beta_{14}D_{1i}Z_{X_{1i}} + \beta_{15}D_{2i}Z_{X_{1i}} + \beta_{16}D_{1i}Z_{X_{2i}} + \beta_{17}D_{2i}Z_{X_{2i}} + \beta_{18}D_{1i}Z_{X_{3i}} + \beta_{19}D_{2i}Z_{X_{3i}} + \varepsilon_{1i}$$

$$Z_{Y_2} = \beta_{21}Z_{Y_{1i}} + \beta_{22}Z_{X_{1i}} + \beta_{23}Z_{X_{2i}} + \beta_{24}Z_{X_{3i}} + \beta_{25}D_{1i}Z_{Y_{1i}} + \beta_{26}D_{2i}Z_{Y_{1i}} + \beta_{27}D_{1i}Z_{X_{1i}} + \beta_{28}D_{2i}Z_{X_{1i}} + \beta_{29}D_{1i}Z_{X_{2i}} + \beta_{210}D_{2i}Z_{X_{2i}} + \beta_{211}D_{1i}Z_{X_{3i}} + \beta_{212}D_{2i}Z_{X_{3i}} + \varepsilon_{2i}$$

Selection of the best linkage using model validity. Choose the best linkage from the 3 linkages used, namely Ward, Complete, and Average linkage by using the total determination coefficient.

$$R_m^2 = 1 - P_{e1}^2 P_{e2}^2 \ldots P_{ep}^2$$

where:

$$P_{ei} = \sqrt{1 - R_i^2}$$

information:

P_{ei} : residual effect on each equation (i=1,2,…,p)

R_i^2 : the coefficient of determination in each equation

R_m^2: total determination coefficient

The greater the total determination coefficient value approaching 100%, then the model is said to be good.

Hypothesis of Linear Parameter Function (HLPF)

a) Formulating a Linear Parameter Function Hypothesis.

[5]explains that there are procedures that can be used to write general and specific hypotheses. Hypothesis testing of linear parameter functions is used to simultaneously test the equations formed in the study. This hypothesis can be written in the form of a matrix as follows:

$$H : \mathbf{K'\beta = m}$$

b) Hypothesis Testing for Linear Function Parameters

$$\frac{Q}{s\sigma^2} = \frac{\left(\mathbf{K'\hat{\beta} - m}\right)' \left[\mathbf{K'(X'X)^{-1}K}\right]^{-1} \left(\mathbf{K'\hat{\beta} - m}\right)}{s\sigma^2} \sim F_{db_1, db_2}$$

III. RESEARCH METHODS

Data Source

The data used in the study are primary data on attitude variables, subjective norms, behavior control, intention to comply with paying, and obedient paying behavior at Bank X. The number of respondents in this study were 100 respondents who visited Mount Bromo. The sampling technique used purposive sampling.

Steps

The steps of this research are as follows:

1. Scaling the data using the method of measuring the average score of the indicators. According to [3], the scale average method is carried out by using the average scale of all indicators for each variable so that the scale average data is obtained which is the data of the latent variable in question.
2. Perform Cluster analysis with Ward, Average, and Complete linkage methods using the Euclidean distance.
3. Establishing a dummy variable matrix.
4. The path diagram used in this study is as shown in Figure 1.

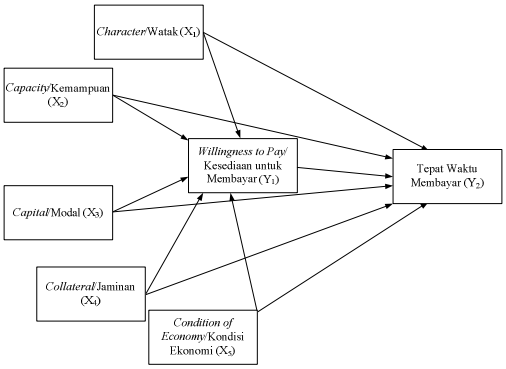

Figure 1. Research Diagram

5. Creating a path analysis model.
6. Perform cluster integration with path analysis.
7. Estimate the path coefficient using OLS

$$\hat{\beta} = (\mathbf{X'X})^{-1}\mathbf{X'}y$$

8. Check path analysis assumptions.
9. Dealing with the breached path analysis assumptions.
10. Selection of the best linkage using model validity.
11. Formulate Hypothesis of Linear Parameter Function.
12. Hypothesis Testing for Linear Function Parameters
13. Model interpretation.

IV. RESULTS AND DISCUSSION

Latent Variable Measurement Method

The results of the method of measuring demographic variables use an average score for each variable. The results of the average score can be seen in Table 4.1

TABLE 4.1
QUANTIFICATION RESULTS

No	X1	X2	X3	X4	X5	Y1	Y2
1	2,7	3,3	3,8	3,0	2,8	2,8	2,8
2	2,8	2,8	3,0	3,3	3,2	3,2	3,8
3	3,5	3,5	2,5	1,5	1,7	2,6	2,5
⋮	⋮	⋮	⋮	⋮	⋮	⋮	⋮
98	3,7	2,2	3,3	3,3	2,8	2,2	2,5
99	2,7	3,0	4,2	2,5	2,8	3,3	3,8
100	1,5	3,8	4,0	4,0	2,2	3,2	3,5

Cluster Analysis

Determination of Multiple Clusters

Determination of the best number of clusters using a dendogram. The following are the cluster results for each linkage method.

a. Ward Linkage Method

TABLE 4.2
NUMBER OF MEMBERS OF EACH CLUSTER WARD LINKAGE METHOD 2 CLUSTERS

Cluster	Number of Cluster Members

1	57
2	43

b. Complete linkage method

TABLE 4.3
THE NUMBER OF MEMBERS OF EACH CLUSTER WARD LINKAGE METHOD 3 CLUSTERS

Cluster	Number of Cluster Members
1	19
2	38
3	43

c. Average linkage method

TABLE 4.4
NUMBER OF MEMBERS OF EACH CLUSTER WARD LINKAGE METHOD 4 CLUSTERS

Cluster	Number of Cluster Members
1	19
2	38
3	26
4	17

Linearity Assumption Test

The linearity assumption test performed using Software R is presented in Table 4.5.

TABLE 4.5
LINEARITY TEST RESULTS

Variable	P-value	Relation
X_1 to Y_1	0,79	Linear
X_2 to Y_1	0,29	Linear
X_3 to Y_1	0,99	Linear
X_4 to Y_1	0,89	Linear
X_5 to Y_1	0,79	Linear
X_1 to Y_2	0,79	Linear
X_2 to Y_2	0,29	Linear
X_3 to Y_2	0,89	Linear
X_4 to Y_2	0,99	Linear
X_5 to Y_2	0,59	Linear
Y_1 to Y_2	0,99	Linear

With a confidence level of 5%, it can be seen that the relationship between variables meets linear assumptions.

4.3.2. Remaining Normality Assumption Test

The test of the remaining normality assumptions performed using Software R is presented in Table 4.6.

TABLE 4.6
REMAINING NORMALITY ASSUMPTION TEST RESULTS

2 Cluster		
Endogenous Variables	P-value	Conclusion
Intentions to Pay (Y_1)	0,45	Normal
Compliant Paying Conduct (Y_2)	0,81	Normal
3 Cluster		
Endogenous Variables	P-value	Conclusion
Intentions to Pay (Y_1)	0,30	Normal
Compliant Paying Conduct (Y_2)	0,50	Normal
4 Cluster		
Endogenous Variables	P-value	Conclusion
Intentions to Pay (Y_1)	0,28	Normal
Compliant Paying Conduct (Y_2)	0,45	Normal

It can be seen from Table 3.6. It can be concluded that with a confidence level of 5% the p-value is more than α. So it can be said that the remainder is normally distributed.

The remaining homogeneity assumption test

The remainder of an equation must be constant or homogeneous. Brief test results can be seen in Table 4.7.

TABLE 4.7.
THE RESULT OF HOMOGENEITY TEST OF THE REMAINING VARIETY

2 Cluster		
Endogenous Variables	P-value	Conclusion
Intentions to Pay (Y_1)	0,06	Variety of remainder is Constant
Compliant Paying Conduct (Y_2)	0,39	Variety of remainder is Constant
3 Cluster		
Endogenous Variables	P-value	Conclusion
Intentions to Pay (Y_1)	0,33	Variety of remainder is Constant
Compliant Paying Conduct (Y_2)	0,36	Variety of remainder is Constant
4 Cluster		
Endogenous Variables	P-value	Conclusion
Intentions to Pay (Y_1)	0,62	Variety of remainder is Constant
Compliant Paying Conduct (Y_2)	0,69	Variety of remainder is Constant

Integrated Cluster Model in the Ward Linkage 2 Cluster Method Path Analysis

Ward linkage 2 Cluster method, then the model formed is like the following equation.

$$Z_{y_{1i}} = 0,2784Z_{x_{1i}} + 0,1887Z_{x_{2i}} + 0,2379Z_{x_{3i}} + 0,1235Z_{x_{4i}} + 0,3277Z_{x_{5i}} - 0,0845D_iZ_{x_{1i}} - 0,0235D_iZ_{x_{2i}} - 0,1469D_iZ_{x_{3i}} + 0,3714D_iZ_{x_{4i}} + 0,1853D_iZ_{x_{5i}}$$

$$Z_{y_{2i}} = 0,8544Z_{y_{1i}} + 0,0311Z_{x_{1i}} - 0,0068Z_{x_{2i}} + 0,0578Z_{x_{3i}} + 0,0164Z_{x_{4i}} - 0,1603Z_{x_{5i}} - 0,3428D_iZ_{y_{1i}} - 0,0511D_iZ_{x_{1i}} + 0,1607D_iZ_{x_{2i}} - 0,0910D_iZ_{x_{3i}} + 0,0764D_iZ_{x_{4i}} + 0,3616D_iZ_{x_{5i}}$$

The low cluster (D = 0) can be seen in the following equation.

$$Z_{y_{1i}} = 0,2784Z_{x_{1i}} + 0,1887Z_{x_{2i}} + 0,2379Z_{x_{3i}} + 0,1235Z_{x_{4i}} + 0,3277Z_{x_{5i}}$$

$$Z_{y_{2i}} = 0,8544Z_{y_{1i}} + 0,0311Z_{x_{1i}} - 0,0068Z_{x_{2i}} + 0,0578Z_{x_{3i}} + 0,0164Z_{x_{4i}} - 0,1603Z_{x_{5i}}$$

Medium cluster (D = 1) can be seen in the following equation.

$$Z_{y_{1i}} = 0,1939Z_{x_{1i}} + 0,1652Z_{x_{2i}} + 0,0910Z_{x_{3i}} + 0,4949Z_{x_{4i}} + 0,5130Z_{x_{5i}}$$

$$Z_{y_{2i}} = 0,5116D_iZ_{y_{1i}} + 0,8033Z_{x_{1i}} + 0,1918Z_{x_{2i}} - 0,0978Z_{x_{3i}} + 0,0928Z_{x_{4i}} - 0,2013Z_{x_{5i}}$$

Integrated Cluster Model in the Ward Linkage 3 Cluster Method Path Analysis

Ward linkage 3 Cluster method, then the model formed is like the following equation.

$$Z_{y_{1i}} = 0,2024Z_{x_{1i}} + 0,1776Z_{x_{2i}} + 0,0661Z_{x_{3i}} + 0,0393Z_{x_{4i}} + 0,4824Z_{x_{5i}} - 0,1263D_{1i}Z_{x_{1i}} - 0,0086D_{2i}Z_{x_{1i}} - 0,0546D_{1i}Z_{x_{2i}} - 0,0213D_{2i}Z_{x_{2i}} + 0,2911D_{1i}Z_{x_{3i}} + 0,0248D_{2i}Z_{x_{3i}} + 0,0458D_{1i}Z_{x_{4i}} + 0,4556D_{2i}Z_{x_{4i}} - 0,3109D_{1i}Z_{x_{5i}} + 0,0305D_{2i}Z_{x_{5i}}$$

$$Z_{y_{2i}} = 1,1055Z_{y_{1i}} + 0,0390Z_{x_{1i}} - 0,0192Z_{x_{2i}} + 0,0905Z_{x_{3i}} - 0,0265Z_{x_{4i}} - 0,2344Z_{x_{5i}} - 0,3836D_{1i}Z_{y_{1i}} - 0,5939D_{2i}Z_{y_{1i}} - 0,1546D_{1i}Z_{x_{1i}} - 0,0591D_{2i}Z_{x_{1i}} - 0,0327D_{1i}Z_{x_{2i}} + 0,1730D_{2i}Z_{x_{2i}} + 0,0754D_{1i}Z_{x_{3i}} - 0,1237D_{2i}Z_{x_{3i}} + 0,0471D_{1i}Z_{x_{4i}} + 0,1193D_{2i}Z_{x_{4i}} - 0,0014D_{1i}Z_{x_{5i}} + 0,4357D_{2i}Z_{x_{5i}}$$

Low clusters ($D_1 = 0$ and $D_2 = 0$) can be seen in the following equation.

$$Z_{y_{1i}} = 0,2024Z_{x_{1i}} + 0,1776Z_{x_{2i}} + 0,0661Z_{x_{3i}} + 0,0393Z_{x_{4i}} + 0,4824Z_{x_{5i}}$$

$$Z_{y_{2i}} = 1,1055Z_{y_{1i}} + 0,0390Z_{x_{1i}} - 0,0192Z_{x_{2i}} + 0,0905Z_{x_{3i}} - 0,0265Z_{x_{4i}} - 0,2344Z_{x_{5i}}$$

Medium clusters ($D_1 = 1$ dan $D_2 = 0$) can be seen in the following equation.

$$Z_{y_{1i}} = 0,0761Z_{x_{1i}} + 0,1230Z_{x_{2i}} + 0,3572Z_{x_{3i}} + 0,0851Z_{x_{4i}} - 0,2626Z_{x_{5i}}$$

$$Z_{y_{2i}} = 0,7219Z_{y_{1i}} - 0,1156Z_{x_{1i}} - 0,0519Z_{x_{2i}} + 0,1659Z_{x_{3i}} - 0,0206Z_{x_{4i}} - 0,2358Z_{x_{5i}}$$

Height clusters ($D_1 = 0$ dan $D_2 = 1$) can be seen in the following equation.

$$Z_{y_{1i}} = 0,1938Z_{x_{1i}} + 0,1563Z_{x_{2i}} + 0,0909Z_{x_{3i}} + 0,4949Z_{x_{4i}} + 0,5129Z_{x_{5i}}$$

$$Z_{y_{2i}} = 0,5116Z_{y_{1i}} - 0,0201Z_{x_{1i}} + 0,1538Z_{x_{2i}} - 0,0332Z_{x_{3i}} + 0,0928Z_{x_{4i}} + 0,2013Z_{x_{5i}}$$

Integrated Cluster Model in the Ward Linkage 4 Cluster Method Path Analysis

Ward linkage 4 Cluster method, then the model formed is like the following equation.

$$Z_{y_{1i}} = 0,2024Z_{x_{1i}} + 0,1776Z_{x_{2i}} + 0,0661Z_{x_{3i}} + 0,0393Z_{x_{4i}} + 0,4824Z_{x_{5i}} - 0,1263D_{1i}Z_{x_{1i}} - 0,0905D_{2i}Z_{x_{1i}} + 0,0856D_{3i}Z_{x_{1i}} - 0,0546D_{1i}Z_{x_{2i}} - 0,0676D_{2i}Z_{x_{2i}} - 0,1687D_{3i}Z_{x_{2i}} + 0,2911D_{1i}Z_{x_{3i}} + 0,1678D_{2i}Z_{x_{3i}} + 0,0379D_{3i}Z_{x_{3i}} + 0,0458D_{1i}Z_{x_{4i}} + 0,4362D_{2i}Z_{x_{4i}} + 0,5445D_{3i}Z_{x_{4i}} + 0,3109D_{1i}Z_{x_{5i}} + 0,0424D_{2i}Z_{x_{5i}} + 0,3014D_{3i}Z_{x_{5i}}$$

$$Z_{y_{2i}} = 1,1055Z_{y_{1i}} + 0,0390Z_{x_{1i}} - 0,0192Z_{x_{2i}} + 0,0905Z_{x_{3i}} - 0,0265Z_{x_{4i}} - 0,2344Z_{x_{5i}} - 0,3836D_{1i}Z_{y_{1i}} - 0,5284D_{2i}Z_{y_{1i}} + 0,1372D_{3i}Z_{y_{1i}} - 0,1546D_{1i}Z_{x_{1i}} - 0,1502D_{2i}Z_{x_{1i}} + 0,0525D_{3i}Z_{x_{1i}} - 0,0327D_{1i}Z_{x_{2i}} + 0,0100D_{2i}Z_{x_{2i}} + 0,4840D_{3i}Z_{x_{2i}} + 0,0754D_{1i}Z_{x_{3i}} + 0,0016D_{2i}Z_{x_{3i}} - 0,1900D_{3i}Z_{x_{3i}} + 0,0471D_{1i}Z_{x_{4i}} + 0,2889D_{2i}Z_{x_{4i}} + 0,1241D_{3i}Z_{x_{4i}} - 0,0014D_{1i}Z_{x_{5i}} + 0,2815D_{2i}Z_{x_{5i}} + 0,6916D_{3i}Z_{x_{5i}}$$

Low clusters ($D_1 = 0$, $D_2 = 0$, $D_3 = 0$) can be seen in the following equation.

$$Z_{y_{1i}} = 0,2024Z_{x_{1i}} + 0,1776Z_{x_{2i}} + 0,0661Z_{x_{3i}} + 0,0393Z_{x_{4i}} + 0,4824Z_{x_{5i}}$$

$$Z_{y_{2i}} = 1,1055Z_{y_{1i}} + 0,0390Z_{x_{1i}} - 0,0192Z_{x_{2i}} + 0,0905Z_{x_{3i}} - 0,0265Z_{x_{4i}} - 0,2344Z_{x_{5i}}$$

Medium clusters ($D_1 = 1$, $D_2 = 1$, $D_3 = 0$) can be seen in the following equation.

$$Z_{y_{1i}} = -0,0144Z_{x_{1i}} + 0,0554Z_{x_{2i}} + 0,5250Z_{x_{3i}} + 0,5213Z_{x_{4i}} + 0,8357Z_{x_{5i}}$$

$$Z_{y_{2i}} = 0,1935Z_{y_{1i}} + 0,2658Z_{x_{1i}} - 0,0419Z_{x_{2i}} + 0,1675Z_{x_{3i}} + 0,3095Z_{x_{4i}} + 0,0457Z_{x_{5i}}$$

Height clusters ($D_1 = 0$, $D_2 = 1$, $D_3 = 1$) can be seen in the following equation.

$$Z_{y_{1i}} = 0,1975Z_{x_{1i}} - 0,0587Z_{x_{2i}} + 0,2718Z_{x_{3i}} + 1,0200Z_{x_{4i}} + 0,8262Z_{x_{5i}}$$

$$Z_{y_{2i}} = 1,1055Z_{y_{1i}} + 0,7143Z_{x_{1i}} - 0,4748Z_{x_{2i}} - 0,0979Z_{x_{3i}} - 0,3865Z_{x_{4i}} - 0,7387Z_{x_{5i}}$$

Selection of the Best Linkage from Model Validity

Selection of the best linkage and model validity is to choose the model that has the largest total R^2, as in the equation, it can be seen in summary in table 4.8.

TABLE 4.8
VALUE IN EACH MODEL

	R^2 Y_1	R^2 Y_2	R^2 total
2 Cluster	0,61	0,56	0,583
3 Cluster	0,61	0,55	0,580
4 Cluster	0,59	0,55	0,572

The path analysis model with the Ward linkage 2 Cluster method cluster integration has the greatest total determination value, so path analysis with the Cluster integration with the Ward linkage 2 Cluster method is the best model. The total determination value of 58.3% is considered good enough to describe the model.

Best Model

TABLE 4.9
AVERAGE VALUE AND EACH CLUSTER

Variable	Average	
	Cluster 1: Low Cluster	Cluster 2: Height Cluster
Character (X_1)	3,289	3,66
Capacity (X_2)	3,202	3,94
Capital (X_3)	3,287	3,60
Collateral (X_4)	3,254	3,84
Condition of economy (X_5)	3,053	3,81
Willingness to pay (Y_1)	3,102	4,03
On time to pay (Y_2)	3,009	4,01

Hypothesis of Linear Parameter Function (HLPF)

Simultaneous testing of path coefficients through testing the Linear Function Hypothesis (HLPF) with the following hypotheses:

Direct influence

1) $H_0 : \beta_{11} = 0$ vs $H_1 : \beta_{11} \neq 0$
2) $H_0 : \beta_{11} + \beta_{14} = 0$ vs $H_1 : \beta_{11} + \beta_{14} \neq 0$
3) $H_0 : \beta_{11} + \beta_{15} = 0$ vs $H_1 : \beta_{11} + \beta_{15} \neq 0$
4) $H_0 : \beta_{12} = 0$ vs $H_1 : \beta_{12} \neq 0$
5) $H_0 : \beta_{12} + \beta_{16} = 0$ vs $H_1 : \beta_{12} + \beta_{16} \neq 0$

6) $H_0 : \beta_{12} + \beta_{17} = 0$ vs $H_1 : \beta_{12} + \beta_{17} \neq 0$
7) $H_0 : \beta_{13} = 0$ vs $H_1 : \beta_{13} \neq 0$
8) $H_0 : \beta_{13} + \beta_{18} = 0$ vs $H_1 : \beta_{13} + \beta_{18} \neq 0$
9) $H_0 : \beta_{13} + \beta_{19} = 0$ vs $H_1 : \beta_{13} + \beta_{19} \neq 0$

Then the results of hypothesis testing are obtained as follows.

TABLE 4.10
HLPF DIRECT EFFECT

No.	Coefficient	*F* count	*F* table	Decision
1	β_{11}	0,032	3,937	Accept H_0
2	$\beta_{11} + \beta_{14}$	0,181	3,937	Accept H_0
3	$\beta_{11} + \beta_{15}$	1,729	3,937	Accept H_0
4	β_{12}	0,306	3,937	Accept H_0
5	$\beta_{12} + \beta_{16}$	0,662	3,937	Accept H_0
6	$\beta_{12} + \beta_{17}$	2,424	3,937	Accept H_0
7	β_{13}	0,148	3,937	Accept H_0
8	$\beta_{13} + \beta_{18}$	5,498	3,937	Reject H_0
9	$\beta_{13} + \beta_{19}$	0,128	3,937	Accept H_0

Indirect influence

1) $H_0 : \beta_{21} = 0$ vs $H_1 : \beta_{21} \neq 0$
2) $H_0 : \beta_{21} + \beta_{25} = 0$ vs $H_1 : \beta_{21} + \beta_{25} \neq 0$
3) $H_0 : \beta_{21} + \beta_{26} = 0$ vs $H_1 : \beta_{21} + \beta_{26} \neq 0$
4) $H_0 : \beta_{22} = 0$ vs $H_1 : \beta_{22} \neq 0$
5) $H_0 : \beta_{22} + \beta_{27} = 0$ vs $H_1 : \beta_{22} + \beta_{27} \neq 0$
6) $H_0 : \beta_{22} + \beta_{28} = 0$ vs $H_1 : \beta_{22} + \beta_{28} \neq 0$
7) $H_0 : \beta_{23} = 0$ vs $H_1 : \beta_{23} \neq 0$
8) $H_0 : \beta_{23} + \beta_{29} = 0$ vs $H_1 : \beta_{23} + \beta_{29} \neq 0$
9) $H_0 : \beta_{23} + \beta_{210} = 0$ vs $H_1 : \beta_{23} + \beta_{210} \neq 0$
10) $H_0 : \beta_{24} = 0$ vs $H_1 : \beta_{24} \neq 0$
11) $H_0 : \beta_{24} + \beta_{211} = 0$ vs $H_1 : \beta_{24} + \beta_{211} \neq 0$
12) $H_0 : \beta_{24} + \beta_{212} = 0$ vs $H_1 : \beta_{24} + \beta_{212} \neq 0$

Then the results of hypothesis testing are obtained as follows.

TABLE 4.11
HLPF INDIRECT EFFECT

No.	Coefficient	*F* count	*F* table	Decision
1	β_{21}	13,676	3,94	Reject H_0
2	$\beta_{21} + \beta_{25}$	0,035	3,94	Reject H_0
3	$\beta_{21} + \beta_{26}$	0,931	3,94	Reject H_0
4	β_{22}	1,243	3,94	Accept H_0
5	$\beta_{22} + \beta_{27}$	1,370	3,94	Accept H_0
6	$\beta_{22} + \beta_{28}$	6,912	3,94	Accept H_0
7	β_{23}	1,029	3,937	Reject H_0
8	$\beta_{23} + \beta_{29}$	0,660	3,94	Accept H_0
9	$\beta_{23} + \beta_{210}$	3,553	3,94	Reject H_0
10	β_{24}	12,586	3,94	Reject H_0
11	$\beta_{24} + \beta_{211}$	7,279	3,94	Accept H_0
12	$\beta_{24} + \beta_{212}$	0,171	3,94	Accept H_0

Based on Tables 4.9 and 4.10, it can be seen that the value of F count> F table which results in the rejection of H0 so that it can be concluded that there is an influence on this path. There is an insignificant path to the intention to comply with paying and the behavior to comply with paying with a dummy or not with a dummy.

Model Interpretation

From the results of the Integrated Cluster R^2 on the path analysis with the Ward method has the highest R^2 value, where the Ward method consists of 2 clusters. For the Ward linkage method with Cluster 1 as many as 57 and Cluster 2 as many as 43. If the average variables for each cluster are compared, it is found that most of the Cluster 2 has the highest average value compared to other Clusters, so Cluster 2 is a high cluster. While Cluster 1 has the lowest average value compared to other clusters, so Cluster 1 is a low cluster.

V. CLOSING

Conclusion

1. The application of the integrated cluster in the path analysis using the ward method results in many different clusters and members of the cluster, causing different dummy variables to form, thus affecting the value of R^2.
2. The best result of R^2 value is the integrated Cluster 2 model with the Ward linkage method.

Recommendation

1. For further research, it is expected to use an integrated cluster with simulation, in order to obtain a maximum R^2 result and produce a significant different R^2 value.
2. The results of this study can be used by Bank 'X' in determining customer credit categories by grouping customers into clusters that have been obtained and then conducting path analysis.

REFERENCE

[1] Kuswati, S.M. *Cara Gampang Membeli Rumah tanpa Modal. Publishing Langit.* 2015.

[2] Liu, G., & Wei, C, "A new multi-path routing protocol based on *Cluster* for underwater acoustic sensor networks", In 2011 International Conference on Multimedia Technology (pp. 91-94). IEEE.

[3] Solimun, Fernandes, A. A. R., dan Nurjannah. *Metode Statistika Multivariat Pemodelan PErsamaan Struktural (SEM) Pendekatan WarPLS. Malang. UB Press*, 2017.

[4] Johnson, R. A. dan Wichern, D. W. *Applied Multivariate. Analysis. Upper Saddle River*, NJ: Prentice Hall, 1992.

[5] Searle, S. R. 1971. *Linear Models*. New York : John Wiley & Sons, Inc.

Closing the Assessment Loop: Case Study in Improving Outcomes for Online College Students during Pandemic

Arlene Caney, Linda Fellag

***Abstract*—** To counter the adverse effect of Covid-19 on college student success, two faculty members at a US community college have used web-based assessment data to improve curricula and, thus, student outcomes. This case study exemplifies how "closing the loop" by analyzing outcome assessments in real time can improve student learning for academically underprepared students struggling during the pandemic. The purpose of the study was to develop ways to mitigate the negative impact of Covid-19 on student success of underprepared college students. Using the Assessment, Evaluation, Feedback and Intervention System (AEFIS) and other assessment tools provided by the college's Office of Institutional Research, an English professor and a Music professor collected data in skill areas related to their curricula over four semesters, gaining insight into specific course sections and learners' performance across different Covid-driven course formats—face-to-face, hybrid, synchronous, and asynchronous. Real-time data collection allowed faculty to shorten and close the assessment loop, and prompted faculty to enhance their curricula with engaging material, student-centered activities, and a variety of tech tools. Frequent communication, individualized study, constructive criticism, and encouragement were among other measures taken to enhance teaching and learning. As a result, even while student success rates were declining college-wide, student outcomes in these faculty members' asynchronous and synchronous online classes improved or remained comparable to student outcomes in hybrid and face-to-face sections. These practices have demonstrated that even high-risk students who enter college with remedial level language and mathematics skills, interrupted education, work and family responsibilities, and language and cultural diversity can maintain positive outcomes in college across semesters, even during the pandemic.

***Keywords*—** AEFIS, assessment, distance education, institutional research center.

Arlene Caney is with the Community College of Philadelphia, United States (e-mail: acaney@ccp.edu).

A Comparative Study on How Social Robots Support Learners' Motivation and Learning

Hae Seon Yun, Maximilian Karl, Johann Chevalere, Niels Pinkwart

***Abstract*—** This paper aims to answer two questions 1) do social robots support motivation and learning and 2) how do social robots support motivation and learning. To answer these questions, this paper compares recent studies that focus on social aspect of robot in a learning context. The paper has compared and derived features of social robots that influence motivation and learning. The findings of this research show that social robot does affect motivation and learning and several studies present common features unanimously which are physical contact, posture, gesture, gaze including eye contact, speech including intonation and pitch and motivating dialog with peer like attitude.

***Keywords*—** social robot, learning companion, motivation, human robotic interaction, human-robot interaction.

Hae Seon Yun is with the Humboldt University, Germany (e-mail: yunhaese@informatik.hu-berlin.de).

The Role of Instruction in Knowledge Construction in Online Learning

Soo Hyung Kim

***Abstract*—**Which of the following is better for learning? Focusing on factual knowledge or focusing on the embedded meaning in the statements? The belief is that each way of learning has positive effects on different question categories, where factual knowledge helps more with simple fact questions and searching for meaning in given information helps learn causal relation and the embedded meaning. To test this belief, two groups of learners (12 male and 39 female adults aged 18-37) watched a ten-minute long Youtube video about various factual events of American history, their meaning, and the causal relations of the events. The fact group was asked to focus on factual knowledge in the video and the meaning group was asked to focus on the embedded meaning in the video. After watching the video, both groups took multiple choice questions which consisted of 10 questions asking the factual knowledge addressed in the video and 10 questions asking embedded meaning in the video such as causal relation between historical events and significance of the event. From ANCOVA analysis, it was found that the factual knowledge showed higher performance on the factual questions than the meaning group, although there was no group difference on the questions about meaning between the two groups. The finding suggests that a teacher instruction plays an important role in learners constructing a different type of knowledge in online learning.

***Keywords*—**Factual knowledge, Instruction, Meaning-based Knowledge, Online learning.

Soo Hyung Kim is with the Stevenson School, Pebble Beach, CA 93953 USA (e-mail: skim22@stevensonschool.org).

Changing Dimensions of Peace and Security in International Relations: Implication on Middle East

Priya Ranjan Kumar

***Abstract*—** Evidently, the conceptual understanding of peace and security has been the core matter of debate and discourse from the very beginning of Westphalian modern nation-state system. Significantly, the approaches to establish peace and security were primarily state centric, where non-state actors were neither considered nor taken both as the sources to enhance international peace or threat to international peace and security. The concepts have become the critical concepts to be analysed both horizontally and vertically by many scholars. Significantly, traditional meaning and scope of peace and security remain crucial point of reference, while new dimensions of the same have been debated and explored many ways in this interconnected, interdependent globalised world. In fact, critical studies have provided multiple meanings and multi-focused interpretations of peace and security where peace became human and environmental centric and idea of security explained to emancipate human from various aspects of threats in the present context. Obtaining life enhancing peace beyond negative and positive peace occupied the centre point of reference in peace studies. At the same time, establishing all-encompassing comprehensive security beyond the collective, cooperative, and common security to build security community or regime became matter of discourse in the security discourse. The environmental security has, in fact, brought the issue around security without enemies. Consequently, no region of this glob is exception to the challenges posed by new dimensions of peace and security in today's world. Historically, Middle East region has been the area where most of theoretical discourses around peace and security have been built and failed to explain the causes of long and enduring nature of peace and security issues. In fact, Middle East has experienced combined interactions of both state and non-state actors in constructing as well as deconstructing peace and security in multidimensional aspects. The perennial nature of existing conflicts, artificial creation of nation-state's boundaries by victorious powers of World War I and II, and continuous external involvements have been reasons for the causes of threat to many aspects of security. Ironically, no theory of international relations has till now provided insightful explanations to the ongoing security scenario along with framework to establish regional peace and security in Middle East. This paper attempts to analyse changing dimensions of peace and security in international relations while keeping referent point as Middle East and try to explore the feasible frameworks for establishing peace and security in the region.

***Keywords*—** peace and security, Westphalia, Middle East, conflict.

Priya Ranjan Kumar is with the Central University of Gujarat, India (e-mail: priya.k.ranjan@gmail.com).

Economic Empowerment before Political Participation: Peacebuilding from the Perspective of Women Activists in the Post-Yugoslav Area

Emilie Fort

***Abstract*—** Two major pitfalls emerge at the intersection of gender and peacebuilding literature: the comprehension of women as a homogeneous category and a focus on women's participation in formal peace processes and state structures. However, women belong (and identify) to distinct ethnic, religious, or social groups, and the variety of their social location impacts their ability to mobilize, to participate in peace processes as well as the way they envision peace. This study is based on interviews conducted (remotely) with women activists from the post-Yugoslav area. It shows that women's economic empowerment and education are central issues that must be addressed for women political participation being effective. This has implications for peace projects –their priorities, scales of implementation, etc.– and the allocation of civil society's funds.

***Keywords*—**ex-Yugoslavia, gender-based issues, peacebuilding, women activism.

Emilie Fort is with the Durham University, Japan (e-mail: emilie.fort@durham.ac.uk).

Theorizing Women's Informal Peacebuilding and Their Strategies

Nandini Gupta

***Abstract*—** The international agendas like 1325 have generated awareness regarding women's participation in peace-making and has also raised the question of 'why women matter in peace?'. But by neglecting marginalized women and overlooking their indigenous ways of peacebuilding it has maintained its hegemonic grip on an elusive question of 'which women matter in peacebuilding?' and neglected the particular ways in which women at the grassroots approach peacebuilding. The question 'which' foregrounds some important deliberations on the aspect of power relations regarding representational discourse in the domain of peacemaking, peacebuilding and peacekeeping . This paper will aim to investigate these embedded power relationships by situating the struggle of these women in the larger framework of feminist peacebuilding and will traverse through their distinctive manoeuvrings of making peace at the grassroots level through sticks and stones. It will also establish the importance for studying and understanding women's informal peacebuilding by discussing the two important theoretical frameworks which are 'Politics of Emotions' and 'Transversal Politics' . I will highlight how both of these frameworks will help in developing a novel understanding of women's informal peacebuilding approach, exploring how the politics of emotion, enable women to build cross-sectarian alliances in pursuing their goal of equality and inclusiveness in conflict-ridden societies.

***Keywords*—** feminist peacebuilding, down-up approach, transversal politics, politics of emotion.

Nandini Gupta is with the Trinity College Dublin, Ireland (e-mail: ngupta@tcd.ie).

English Test Success among Syrian Refugee Girls Attending Language Courses in Lebanon

Nina Leila Mussa

***Abstract*—** Background: The devastating effects of the war on Syria's educational infrastructure has been widely reported, with millions of children denied access. However, among those who resettled in Lebanon, the impact of receiving educational assistance on their abilities to pass the English entrance exam is not well described. The aim of this study was to identify predictors of success among Syrian refugees receiving English language courses in a Lebanese university. Methods: The database of Syrian refugee girls matriculated in English courses at the American University of Beirut (AUB) was reviewed. The study period was 7/2018-09/2020. Variables compared included: family size and income, welfare status, parents' education, English proficiency, access to the internet, and need for external help with homework. Results: For the study period, there were 28 girls enrolled. The average family size was 6 (range 4-9), with eight having completed primary, 14 secondary education, and 6 graduated high school. Eighteen were single-income families. After 12 weeks of English courses, 16 passed the Test of English as Foreign Language (TOEFL) from the first attempt, and 12 failed. Out of the 12, 8 received external help, and 6 passed on the second attempt, which brings the total number of successful passing to 22. Conclusion: Despite the tragedy of war, girls receiving assistance in learning English in Lebanon are able to pass the basic language test. Investment in enhancing those educational experiences will be determinantal in achieving widespread progress among those at-risk children.

***Keywords*—** refugee girls,TOEFL, education, success.

Nina-Leila Mussa is with the Horace Mann School, United States (e-mail: Ninaleila03@gmail.com)

Manifestations of Moral Imagination During the COVID-19 Pandemic in the Debates of Lithuanian Parliament

Laima Zakaraitė, Vaidas Morkevičius

***Abstract*—**The COVID-19 pandemic brought important and pressing challenges for politicians around the world. Governments, parliaments and political leaders had to make quick decisions about containment of the pandemic, usually without clear knowledge about the factual spread of the virus, the possible expected speed of spread and levels of mortality. Opinions of experts were also divided, as some advocated for "herd immunity" without closing down of economy and public life and others supported the idea of strict lockdown. The debates about measures of pandemic containment were heated and involved strong moral tensions with regard to the possible outcomes.

This paper proposes to study the manifestations of moral imagination in the political debates regarding the COVID-19 pandemic. Importantly, moral imagination is associated with twofold abilities of a decision-making actor: ability to discern the moral aspects embedded within a situation and ability to envision a range of possibilities alternative solutions to the situation from a moral perspective. The concept was most thoroughly investigated in the business management studies. However, its relevance for the study of political decision making is also rather clear. The results of the study show to what extent politicians are able to discern the wide range of moral issues related to a situation (in this case, consequences of COVID-19 pandemic in a country) and how broad (especially, from a moral perspective) are discussions of the possible solutions proposed for solving the problem (situation). Arguably, political discussions and considerations are broader and affected by wider and more varied range of actors and ideas compared to decision making in the business management sector. However, the debates and ensuing solutions may also be restricted by ideological maxims and advocacy of special interests. Therefore, empirical study of policy proposals and their debates might reveal the actual breadth of moral imagination in political discussions. For this purpose, we carried out the qualitative study of the parliamentary debates related to the COVID-19 pandemic in Lithuania during the first wave (containment of which was considered very successful) and in the beginning and consequent acceleration of the second wave (when the spread of the virus became uncontrollable)

***Keywords*—**Decision making, moral imagination, political debates, political decision.

L. Zakaraitė is with Institute of Social Sciences, Arts and Humanities, Kaunas University of Technology, Kaunas 44249 Lithuania (phone: 0037067826248; e-mail: laima.zakaraite@ktu.lt).

V. Morkevičius is with Kaunas University of Technology, Kaunas 44249 Lithuania (phone: 0037065541041; e-mail: vaidas.morkevicius@ktu.lt).

Understanding Embryology in Promoting Peace Leadership: A Document Review

Vasudev Das

***Abstract*—** The specific problem is that many leaders of the 21st century do not understand that the extermination of embryos wreaks havoc on peace leadership. The purpose of the document review is to understand embryology in facilitating peace leadership. Extermination of human embryos generates a requital wave of violence which later falls on human society in the form of disturbances, considering that violence breeds further violence as a consequentiality. The study results reveal that a deep understanding of embryology facilitates peace leadership, given that minimizing embryo extermination enhances non-violence in the global village. Neo-Newtonians subscribe to the idea that every action has an equal and opposite reaction. The US Federal Government recognizes the embryo or fetus as a member of Homo sapiens. The social change implications of this study are that understanding human embryology promotes peace leadership, considering that the consequentiality of embryo extermination can serve as a deterrent for violence on embryos.

***Keywords*—** consequentiality, Homo sapiens, neo-Newtonians, violence.

Vasudev Das is with the Walden University, United States (e-mail: glykeria108@gmail.com).

The Role of Businesses in Peacebuilding in Nigeria: A Stakeholder Approach

Jamila M. Makarfi, Yontem Sonmez

***Abstract*—** Developing countries like Nigeria, have recently been affected by conflicts characterized by violence, high levels of risk and insecurity, resulting in loss of lives, livelihoods, displacement of communities, degradation of health, educational and social infrastructure as well as economic underdevelopment. The Nigerian government's response to most of these conflicts have mainly been reactionary in the form of military deployments, as against precautionary to prevent or address the root causes of the conflicts. Several studies have shown that at various points of a conflict, conflict regions can benefit from the resources and expertise available outside the government, mainly from the private sector through mechanisms such as corporate social responsibility (CSR) by businesses. The main aim of this study is to examine the role of businesses in peacebuilding in Northern Nigeria through CSR in the last decade. The expected contributions from this will answer research questions, such as, the key business motivations to engage in peacebuilding, as well as the degree of influence exerted from various stakeholder groups on the business decision to engage. The methodology of the study adopts a multiple case study of over 120 businesses of various sizes, ranging from small, medium and large-scale. A mixed method enabled the collection of quantitative and qualitative primary data, to augment the secondary data. The results indicated that the most important business motivations to engage in peacebuilding were the negative effects of the conflict to economic stability, as well as stakeholder driven motives. On the other hand, out of the 12 identified stakeholders, micro-, small- and medium-scaled enterprises (MSMEs) considered the chief executive officer's interest to be the most important factor, while large companies rated the government and community pressure as the highest. Overall, the foreign stakeholders scored low on the influence chart for all business types.

***Keywords*—** Conflict, Corporate Social Responsibility, Peacebuilding, Stakeholders.

J. M. Makarfi is with the Department of Economics, Policy and International Business, Manchester Metropolitan University, UK (e-mail: J.M.Makarfi@stu.mmu.ac.uk).

Y. Sonmez is a senior lecturer with the Department of Economics, Policy and International Business, Manchester Metropolitan University, UK (e-mail: Y.Sonmez@mmu.ac.uk).

Mnemotopic Perspectives: Communication Design as Stabilizer for the Memory of Places

C. Galasso

***Abstract*—**The ancestral relationship between humans and geographical environment has long been at the center of an interdisciplinary dialogue, which sees one of its main research nodes in the relationship between memory and places. Given its deep complexity, this symbiotic connection continues to look for a proper definition that appears increasingly negotiated by different disciplines. Numerous fields of knowledge are involved, from anthropology to semiotics of space, from photography to architecture, up to subjects traditionally far from these reasonings. This is the case of Design of Communication, a young discipline, now confident in itself and its objectives, aimed at finding and investigating original forms of visualization and representation, between sedimented knowledge and new technologies. In particular, Design of Communication for the Territory offers an alternative perspective to the debate, encouraging the reactivation and reconstruction of the memory of places. Recognizing *mnemotopes* as a cultural object of vertical interpretation of the memory-place relationship, design can become a real mediator of the territorial fixation of memories, making them increasingly accessible and perceptible, contributing to build a topography of memory. According to a mnemotopic vision, Communication Design can support the passage from a memory in which the observer participates only as an individual to a collective form of memory. A mnemotopic form of Communication Design can, through geolocation and content map-based systems, make chronology a topography rooted in the territory and practicable; it can be useful to understand how the perception of the memory of places changes over time, considering how to insert them in the contemporary world. *Mnemotopes* can be materialized in different format of translation, editing and narration and then involved in complex systems of communication. The memory of places, therefore, if stabilized by the tools offered by Communication Design, can make visible ruins and territorial stratifications, illuminating them with new communicative interests that can be shared and participated.

***Keywords*—**Memory of places, design of communication, territory, mnemotope, topography of memory.

I. Historical Background

THE relationship between place and memory is part of deep cultural history. Since ancient Greece poets, oratories, and politicians have relied on *mnemotechnics*, principles used to organize memory, funded on places recollection, which made it possible to keep in mind vast stores of knowledge.

It is not surprising that the importance of places for a virtuous memory has a founding myth. Simonides of Ceos, a famous poet, was hired to give a panegyric during a banquet organized by an influential man, Scopas, in Thessaly. While Simonides had left the hall for a moment, a terrible accident occurred, the entire roof of the house collapsed, and the poet was the only survivor. Thanks to his mnestic abilities, he could identify the position of every person who had been seated at the table just before the tragic event. His great memory was not only a genius expression: precise mnemonic patterns enhanced it. This legend, even if it may appear fable-like, introduces three interconnecting concepts that will define some of the most important issues of the topography of memory. First of all, the hegemony of the sight. Training visual and the imaginative faculty is essential to represent objects, places, and events in mind. The second aspect is the presence of a building, real or fictitious, in which to insert the newly created images in exact order. Finally, the importance of suggestion and engagement: the mental environments have to involve the creator to facilitate their memorization.

The story had a huge success, crossed national borders, was translated in Latin, and quoted in many rhetoric treatises over the following centuries, becoming the milestone for the culture of eloquence, for the long-standing tradition that raised memorization to the level of an *ars memoriae* [29].

In the *Rhetorica ad Herennium*, a work long attributed to Cicero, the anonymous author gave a more detailed description of ancient mnemotechnics, stating that there are two different types of memory coexisting in the human mind: the natural memory, embedded in our minds, born simultaneously with thought, and the artificial memory (*artificiosa*), the one that can be learned and improved by training. The artificial memory includes backgrounds (*loci*), scenes naturally or artificially set off on a small scale, for example, palaces, gardens, vestibules, useful for precisely organizing memories, and images (*imagines*), figures, marks, or symbols of the object to remember [11]. Images and backgrounds interact creating *imagines agentes*, mnestic devices which, due to their great emotional and suggestive impact, can recall large amounts of data.

In 1966 Frances Yates, published *The Art of Memory* [34] and was one of the first scholars to highlight the importance of the mnemonics tradition by reviving its decisive role, from Classicism to the Renaissance. Through her pioneering work, she disclosed the topic as a historical foundation of the connection between place and memory. After her studies, the art of memory was no longer just a way to fix and organize memories in mind but became a source of identity and culture [19].

C. Galasso is with Politecnico di Milano - Design Department (e-mail: clorindasissi.galasso@polimi.it).

II. Places of Memory

Until the eighteenth century, the link between places and memory has been recognized in classical *loci memoriae*. However, starting from Romanticism, it has acquired a deeper philosophical and conceptual articulation, which has freed it from being just a technical ability [18]. The place was moving away from being the setting only of our present, an artificial context for memories, the place was becoming the protagonist of studies that would help the *loci* evolve into actual *places of memory*. In this interdisciplinary discussion, the innovative works by the French sociologist Maurice Halbawchs were particularly significant. In *Les Cadres sociaux de la mémoire* [20] he refused the Freudian thesis that memories are preserved only in the unconscious, affirming that they can last only if "contextualized by the social group to which the individual belongs, be it a family, a social class, or a religious community" [10]. He was already introducing the idea that memory is never truly private, not a purely individual affair, but exists as collective memory, a topic that gives the name to his most famous book, *La mémoire collective* (1950). "Every collective memory unfolds within a spatial framework. [...] It is to space - the space we occupy, traverse, have continual access to, or can at any time reconstruct in thought and imagination - that we must turn our attention" [21]. For Halbawchs the place became one of the foundations of intersubjectivity, vital in creating connections between individuals and social groups [16].

Another author who contributed significantly to what can be defined as the hermeneutics of the places of memory is certainly Pierre Nora. Influenced by Halbwachs, he wrote a monumental work in seven volumes, *Les Lieux de mémoire* (1984-1992), a comprehensive scholarly study about the places of memory. Places where memory crystallizes and secretes [24], mental and physical spaces where a group, a community, or an entire society can recognize itself through a connection with the collective memory [6]. Places of memory are significant units, of material or ideal order, which the will of men or the passage of time have made a symbolic element for communities and societies [24]. Nora distinguishes *lieux de mémoire* from *milieux de mémoire*, tradition-grounded memory, the way the past is "naturally" in the present [15]: "There are *lieux de memoire*, sites of memory, because there are no longer *milieux de memoire*, real environments of memory" [25]. The focus is that the spontaneous and traditional forms of memory, which are irremediably destined to be lost and disappear, have been substituted by the places of memory, artificial and reconstituted objects, moved by commemorative intentions.

Pierre Nora divides *Lieux de mémoire* into three categories: material, symbolical and functional. The first are monuments, museums, archives, memorials, places where the relationship with history prevails; the second ones, like anniversaries or pilgrimages, are related to the mental geography of remembrance and are intended to evoke episodes that are fundamental to the identity of a country [18]. The third typology combines the collective diaries and autobiographies with movies and exhibitions to keep the memory alive. Proceeding his reflections, Nora introduces a significant peculiarity of places of memory, their relation with the symbol. He affirms that even a place that appears merely material, such as an archive depository, is not a place of memory if the imagination does not invest it with a *symbolic aura* [24]. In this statement, we can glimpse the seed of the storytelling of places of memory, that idea of mnestic interpretation and translation that will become a fundamental part of their communication.

Nora's work was fundamental, and starting from his theories, the idea of a place of memory has begun to be understood as a specific place, where the commemorative side prevails and allows us to better understand past events and transmit them to future generations. However, Nora's works also presented a sort of translation issue. *Lieux de mémoire* have been variously transformed into realms of memory, places of memory, or even backgrounds of memory, connecting them with the original idea of *loci*. In Germany the term *erinnerungsorte* is the most used, where the word *erinneren*, to internalize, has passed to mean memory, and also has a didactical connotation, stating for to learn, to teach [1]. What is clear is that *lieux de mémoire* is not a transnational word, not only terminologically but also conceptually. No wonder that after Nora's publications, many countries have worked to seek their own idea of places of memory. Particularly relevant are Mario Isnenghi [23] reflections in Italy and the studies of the American historian Jay Winter, who in the essay *Sites of memory* [35] define the term more narrowly to mean physical sites where commemorative acts occur, real *topoi* with a life history.

Despite the attempt to move away from Nora, these reflections continue to manifest one of his most compelling methodologies, the investigation of memory sites as "plural texts" in the Barthesian sense of the term [18]: "The text is plural. This does not mean only that it has several meanings, but that it fulfills the very plurality of meaning: an irreducible (and not just acceptable) plurality. The text is coexistence of meaning, but passage, traversal" [5]. An intrinsic plurality that undoubtedly defines places of memory complexity.

III. The Mnemotopes

In the literature, to indicate the interaction between places and memory, we can also use another particular term: *mnemotope*, or in a more classical way, *mnemotopos*. This conceptual *portmanteau* is more than a practical synonym of place of memory, used for stylistic reasons when you want to avoid repetition, more than the combination of the ideas of memory and place. The term effectively renders the concepts of place and remembrance as interdependent, entangling their manifestations and significations in one epistemological whole [13]. Mnemotope is a cultural object of territorial interpretation, a plural text, on the border between individual and collective, between private and institutionalized [7]. Inside this term, we can also find the liminal value, highlighted by Nora, between material and symbol, that characterizes the topography of memory.

Mnemotope is not an entirely new word. It has been sporadically used in various fields of knowledge. One of the first authors who mentioned it not as a synonym was Jan Assmann's in his most famous work, *Cultural Memory and Early Civilization* (1992). Referring to Maurice Halbwachs' *La*

topographie legendaire des evangiles en Terre Sainte [22], he affirms that: "The art of memory works with imaginary settings, and memory culture with signs based on Nature. Even, or indeed especially, entire landscapes may serve as a medium for cultural memory. [...] Rome created a sacred landscape during Antiquity, consisting of topographical texts of cultural memory, that is, 'mnemotopes'" [2]. In Assmann's vision, mnemotopes start to be physical and memorable places of a certain amplitude, privileged mediums of cultural memory.

If memory is inevitably concerned with time, we can also discuss whether mnemotope can have a connection with a more successful concept, the *chronotope* theorized by Bakhtin as the "intrinsic connectedness of temporal and spatial relationships that are artistically expressed in literature" [4]. The fusion of temporal and spatial dimensions is an essential part of the literary chronotope, which certainly tends to distance it from the mnemotope, where time plays a constitutive, but not determining role. Moreover, the chronotope remains in the literary territory, and there are many doubts about the possibility of its insertion in other cultural texts. A mnemotope is instead a place of multiple interacting cultural products to produce mnestic knowledge and awareness. Therefore, the issue is still very open: today is missing an unambiguous definition of the term that disconnects it entirely from being a terminological alternative for places of memory. We can find an attempt in *Gedächtnis und Erinnerung. Ein interdisziplinäres Lexicon*, the "Dictionary of Memory and Remembrance" [26], which gathers most of the terms that make up the macrocosm of memory. While echoing Assmann's reflection, the authors emphasize even more that mnemotopes can mark very complex formations of sense, useful to the collective remembrance if identified on the territory and culturally recognized. They can last a long time, and their permanence can strengthen community identity.

Jan Van Rookhuijzen, one of the few scholars to have declared and motivated his mnemotopic choice, claims that mnemotopes are different from objects, monuments, or landscapes, although these categories are closely associated with them [32]. Objects are transportable, not embedded in a surrounding landscape, and less permanent than a mnemotope. Monuments are planned, they are apparatuses that never pretend to be unintentional, while mnemotopes can be the result of a totally spontaneous stratification.

Stefan Bednarek [9] adds that perhaps, in an attempt of definition, it would be useful to distinguish mnemotopes as much as possible from their historical referents *lieux de mémoire*, to give them terminological independence and to remove them from the context of *commemorative bulimia*, to which Nora somberly referred [6]. Definitions by negation certainly help to narrow the mnemotopic multifaceted field but do not entirely solve the puzzle.

Mnemotopes may take any form, they can be man-made structures and natural landmarks, and even empty spaces [32]. We can also identify some specific mnemotopic categories. We can talk about mnemotopes "with trauma", more related to the traditional idea of places of memory, where commemoration and the *memento* play a fundamental role, and mnemotopes "without trauma", linked to positive aspects of reality, with strong creative energy [7], for example literary mnemotopes, birthplaces of famous people, cinematographic locations. Going more into detail, we can also indicate some features common to the entire mnemotopic sphere.

We can start from the word itself mnemotope, focusing on the second segment, *-topoi*. The term *topos* came from Greek τόπος, place, but over time its lexical vocation has evolved to mean a common or recurring topic, something that is repeated and whose connotation is recognized and shared, until it becomes a content itself. Expanding this idea, we can look for specific mnemo-*topoi*, recurring patterns, motifs, building blocks of collective memory, potentially defining a mnemotopic rhetoric, not absolute but constantly updatable and integrable. Basic unifying criteria that can make mnemotopes more intelligible and decipherable.

First, in dealing with mnemotopes, the place, the physical place, is essential. Mnemotopes are not transportable markers of collective identity [14], they have precise location and roots. In this context, we cannot fail to mention the sense of authenticity. When we approach a mnemotope we often expect to have unique access to the past, building a relationship of trust. Feeling the mnemotope as real, as genuine memory bearer, is one of the access keys to its true identity.

Mnemotopes are located. They have topographies (hills, trees, rivers), geographies (cities, towns, capitals), and different scales (region, zone, areas, districts) [14]. Mnemotopes contain narratives. Whether visible or latent, the layers of stories are a fundamental part of the mnemotope and its subsequent dissemination. Mnemotopes have their own communicative value that may be hidden but remains intrinsic as they go from individual to collective horizons.

Mnemotopes are places where vital complexity emerges from a layered stratification. The physical presence of the place fixes memory, situates mnemotopes in a perspective of permanence, able to alleviate disorientation and separation caused by the passage of time [12]. Permanence is not affected by the elimination of monuments or memorials that come up on mnemotopes, and the stability of places finds its faithful ally in representation. The resilience of mnemotopes also depends on their ability to create relationships. These kinds of places can connect territory and people because they can be lived and felt.

The place is one of the main experiences that one can make of memory, and sensoriality is a foundational part of mnemotopic involvement. There is a kind of embodied memory in coming into contact with a mnemotope. Casey [12] suggests that we can talk about an *aura*, an embracing atmosphere, that exists in the place and can surround us. Paradoxically, we can perceive the atmosphere even of inaccessible mnemotopes. This happens not directly but through various translation processes that can increase the already mentioned trust in the mnemotope. Not to be underestimated is the suggestion that a mnemotope can generate up to natural enchantment.

Mnemotopes can also be activators of territorial movements and traveling activities. A visitor that recognizes a place as a mnemotope can experience the curiosity to go in that place, to see, and perceive its memory. Finally, the mnemotopic

identification can stabilize a place without institutionalization, making it emerge on the territory, ready to communicate.

IV. Communication Design as Mnemotopic Stabilizer

The mnemotopic recognition, especially for those non-institutionalized places that have a strong communicative urgency, is not a direct and straightforward operation. We need specific methods and tools to make a place emerge on the territory as the bearer of significant memories.

Today Communication Design, and more specifically, Communication Design for the Territory, can stabilize mnemotopic realities, making them more evident and understandable. This discipline merges traditional know-how with technological innovation [8]; it masters different instruments to translate and represent the place-memory axis, and is able to look to other fields of knowledge, successfully interfacing with them. This happens precisely in the case of mnemotopes, whose study belongs mainly to fields of knowledge that are very distant from design, such as anthropology, sociology, and memory studies. Nevertheless, Communication Design can deal with the description and visualization of mnemotopes, and their translation, transforming them into articulated communicative systems that introduce individual memories into a wider and collective narrative.

The privileged tool of this discipline is cartography, essential when discussing mnestic-spatial representation. For centuries maps, interfaces to describe and act upon the complexity of the territory [27], have helped to reconstruct the past and geolocate historical events. As an interpretation of reality, they are not only conventional visualizations of a geographical area, but they are able to convey the complexity of the elements that compose them. They are the final communicative artifact of a translation process in which different actors are involved: data, information, images, and texts are anchored to the territory revealing their communicative nature. Maps become visual mediums of remembrance, which cannot be thought of as "the passive reproduction of reality but a production of meaning and spaces" [28].

For the design of mnemotopic communication, maps are fundamental. They help geolocalize the memory of places and identify new connections up to the creation of real mnemotopic itineraries. However, maps are not only static devices to identify points and to guide territorial exploration. They can also be useful to reconstruct and visualize narratives, encouraging knowledge and imagination. In this context, one of the most important solutions of topographic mnestic storytelling [30] is the *story maps*, and even more the *digital story maps*. They are spatial structures of stories in relationship with places that can add to the bi-dimensional structure of maps the temporal side and the dynamism; story maps are not created to "define exact locations, determine coordinates or measure distances, but seek to tell and stimulate stories from different places and times" [30]. They can expose the stratified mnemotopes, making contents of different nature interact on a cartographic structure. To clarify the importance of the story maps, we can introduce here a project called *Distretto Testori*, "Testori District", designed for Milano City of Literature UNESCO. It has been realized by DCxT, the research group of Communication Design for the Territory from the Design Department of Politecnico di Milano. It is a map-based web portal, focused on the places quoted by Giovanni Testori [31], a famous Italian writer of the post-war period, specifically choose because he describes Milan as a city that constantly needs localization in order to be able to stand up to the greatness of the events it collects. His works are full of places depicted in detail, up to the specific addresses and districts.

The website is divided into three main sections. The first one, the most important, is a complex story map, based on the quotes from the novel together with pre-selected archival photos describing the precisely geolocalized places. This content is divided into six chapters that remind those of a book. The user can move within the narrative, following the suggested itinerary, or can decide to freely explore the sections and the suggested places.

Fig. 1 *Distretto Testori*. Inside the chapter "I Casermoni". The historical images are geolocalized on the map and combined with Testori's quotes

The second part is related to the principal places of Testori's life, fixed on the map, enriched with historical pictures, and reference dates.

The third section is called "Mnenotopes" and is a map of Testori's places, divided into four different sub-categories: literary mnemotopes, cinematographic mnemotopes, biographical mnemotopes, contemporary mnemotopes (places where Testori's memory is nowadays preserved, like Testori's Archive). In this way, the user can have a general view of the district related to the author and the places that characterize it. At first glance, it seems clear that most of them are not official places, but common places linked to everyday life, which would risk being forgotten if not stabilized by the communicative translation operated by design.

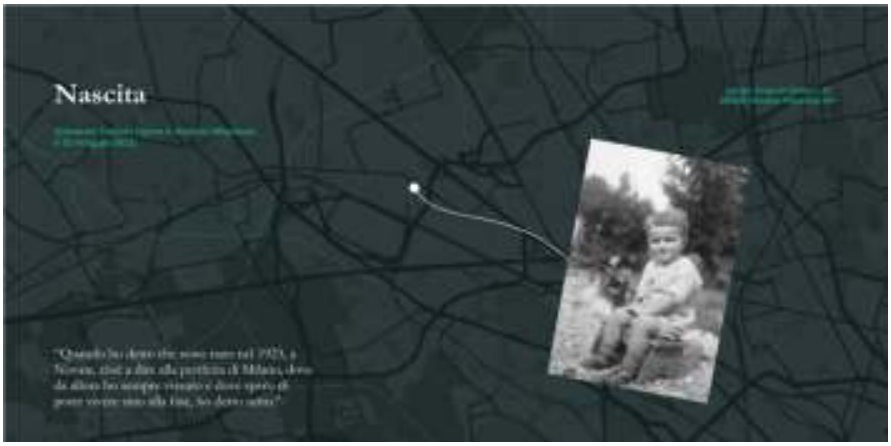

Fig. 2 *Distretto Testori*. Inside the section dedicated to the places of Testori's life

Fig. 3 *Distretto Testori*. Inside the section "Mnemotopes", mapping all the places related to Testori's memory

In this experimental project, Communication Design recognized the places narrated by the author as mnemotopes, highlighting not only points on a map but a dense Testori district in Milan. Literary mnemotopes have been translated and represented through a hybrid system in which coexist maps, archival photos, quotes creating together a new narration. In fact, the website does not report the stories and the characters of Testori on a cartographic medium, but the places narrated by the author, in a specific virtual environment, generate a new geolocalized original story.

Considering mnemotopic communication, what appears to be more important is not the level of individual artifacts, which should also be carefully evaluated and selected, but how they work together within a complex communication system and what apparatuses can generate. It is right through the hybridization of languages, in fact, that the intrinsic complexity of mnemotopes is able to emerge.

The role of Communication Design as a stabilizer of the memory of places can also be experimented within the educational field, especially through teaching activities. This aspect can be demonstrated by analyzing the project "Educazione e Memoria. Un racconto di periferia" [37], with the over-mentioned DCxT group as scientific coordinator. The project intended to involve high school students from the Rosa Luxemburg Technical Institute in Milan, to realize a movie documentary about the Marchiondi Spagliardi Institute. Built between 1954-1958 in a peripheral area of the city by the architect Vittoriano Viganò, the institute was intended to host children in difficulty. The huge complex of buildings was a clear example of the Brutalist current, but today is miserably

abandoned and inaccessible. For this reason, the core of the work was the rediscovery of a past unknown but under everyone's eyes, to understand, validate, and communicate it.

Fig. 4 Marchiondi Spagliardi Institute by Vittoriano Viganò, abandoned and hidden by thick vegetation. Milan, 2021

We proposed a narrative methodology, starting from Communication Design to investigate abandoned architectures that are silent and disregarded. Four seminars have been organized for the students, by setting up a path of recognition of the building as a mnemotope, focused on the pedagogical vocation of the ruins [3]. Fundamental was exploring the original functions of the remaining structures at the historical, mnestic, and architectural level, promoting territorial awareness; atmospheres of memory and places have been another critical theme through which to explore Marchiondi Institute. The didactic translation of the mnemotope has also passed through participatory activities: realization of word-cloud posters and original postcards to put at the center of the reflection on the future of the suburbs, an element of primary importance, memory of place.

Fig. 5 A postcard realized by the students of the project "Educazione e Memoria. Un racconto di periferia", 2021

For the final meeting, we also organized a walking tour around the perimeter of Marchiondi, to test if an abandoned mnemotope can still stimulate curiosity and touristic involvement. Students were given a map to orient themselves around the buildings and recognize their function despite the dense vegetation.

Fig. 6 Students walking around the perimeter of Marchiondi Institute, Milan, 2021

The mnemotopic recognition achieved with the communication design tools made the experience much more engaging. It allowed the students to perceive the building no longer as a ruin to be demolished but as a cultural resource of the neighborhood. These experimentations and the related prototypes feed the idea that the mnemotopes needing most to be inserted in complex communicative systems, are the ones that have not experienced processes of *museification* or institutionalization, whether they are punctual places (Marchiondi) or memory-scapes (Testori District). Communication design can offer them external communication devices, which must necessarily be elaborated, that act as re-activators of dormant memories.

V. Mnemotopes as Activators of Interdisciplinary Discourses

The German art historian Aby Warburg was an energetic ambassador of the interdisciplinary study of culture, pointing out, since the beginning of the 20th century, that researchers should stop policing disciplinary boundaries to gain insight into processes of cultural memory [17].

Mnemotopic communication design is not only limited to referring to other fields of knowledge, but it also manages to generate new interdisciplinary discourses. This is the case of *Mnemosphere project* [36], promoted by the Design Department of Politecnico di Milano, involving PhD students and research fellows. Mnemosphere aims to investigate the different ways in which the memory of places can be designed and communicated through atmospheric spaces capable of stimulating emotions.

The project bases its approach on a synergistic collaboration between different disciplinary fields. The driving force of the research is the dialogue between the design of communication for the territory and the design of installations in the atmospheric dimension; the interdisciplinary nature of the research is enriched with the study of emotions, color perception, and the design of temporary spaces and services.

The project does not aim to give a single definition to the

concept of “mnemosphere”, but intends to investigate its plural substance to communicate its intangibility. We started the investigation from the construction of a shared vocabulary regarding the concepts of “mnemotopes", “atmospheres of spaces” and “atlas of emotions”. Then, we visually expanded the shared lexicon through an Open Call for images that invited artists, designers, photographers, and creative professionals to share their own visual interpretations of the theme. The main idea was to use a tool, the open call, typically addressed to the art world, in a specific design context, to see and evaluate its effects. The Call was articulated through the filling of a form with images and text, that stimulated the participants to reflect on the relationship between the memories, places, atmospheres, and colors. Surprisingly, more than 400 images were received among photographs, illustrations, artworks, and videos.

Fig. 7 Mnemosphere Project. Open call results, 2021

Fig. 8 Mnemosphere Project. Board on collective memory, 2021

The project is still ongoing, and we are now organizing a series of workshops to analyze the collected materials. One of them has been specifically dedicated to mnemotopes; we divided the images from the open call into different categories

related to the mnemotopic sphere: individual memory, collective memory, physical environment, and abstract dimensions. We elaborated four boards from this preliminary distinction, inspired by Warburg *Bilderatlas Mnemosyne* [33], making mnemotopes activators of interdisciplinary discourses.

Once all images are analyzed and integrated into the lexicon, the final goal will be to set up a collective and participated visual archive, a *Mnemosphere Atlas*, where the power of the relationship between images and words will emerge, contributing to narrate the atmospheres of memory in the present time.

VI. Conclusions

From a *mnemotopic perspective*, Communication Design for the Territory can be a valuable resource. It can interact with the other disciplines involved in study of mnemotopes in a supportive way. It is not only a process of enhancement and communicative translation; Communication Design is involved in the very recognition of these complex mnestic realities. It can stabilize the memory of places and make it accessible through mnemotopes representation; it acts in particular on those lesser-known places that time has made almost invisible and manages to make them much more perceptible. Moreover, this field of knowledge, through the use of maps, can create mnemotopic paths and fill them with stories and visual narratives that can be experienced by users even online.

One of the theoretical challenges will be to understand the cultural specificity of mnemotopic research and design, increasingly distinguishing it from other academic discourses, while keeping the concept flourishing in an interdisciplinary environment.

References

[1] J. Agnew, G. Toal, K. Mitchell, *A companion to political geography*. Malden, MA: Blackwell, 2008.

[2] J. Assmann, *Cultural memory and early civilization. Writing, remembrance and political imagination*. Cambridge: Cambridge University Press, 1992.

[3] M. Augé, *Rovine e macerie: il senso del tempo*. Torino: Bollati Boringhieri, 2004.

[4] M. Bakhtin, *The dialogic imagination: four essays*. Austin: University of Texas Press, 1981, p. 84-86.

[5] R. Barthes, *The Rustle of Language*. Berkley, Los Angeles, University of California Press, 1989, pp. 58-59.

[6] M. Bassanelli, *Oltre il memoriale: le tracce, lo spazio, il ricordo*. Milano: Mimesis, 2015.

[7] G. Baule, C. Galasso, "An answer to the complex representation of territory. The fertile ground of mnemotopes and design of communication". In Cumulus Conference*, Design Culture*s, Roma, June 8-11, 2021.

[8] G. Baule, M. Quaggiotto, "Communication of the territory and cartographic interfaces. The spatial turn in communication design". Cumulus Conference, *The Virtuous Circle Design Culture and Experimentation*, Milano, June 3-7, 2015.

[9] S. Bednarek, "Mnemotopika polska". *Przegląd Kulturoznawczy*, Number 1 (11), 2012, pp. 94-111.

[10] C. Bilsel, "Architecture and the Social Frameworks of Memory: A Postscript to Maurice Halbwachs' Collective Memory" *International Journal of Architecture & Planning*, Volume 5, Issue 1, pp. 01-09.

[11] H. Caplan, *Rhetorica ad Herennium*. Cambridge: Harvard University Press, 1954.

[12] E. Casey, *Remembering: A Phenomenological Study*. Bloomington, IN: Indiana University Press, 1987.

[13] S. De Nardi, *The Routledge handbook of memory and place*. Abingdon, New York: Routledge, 2020, pp. 117-119.

[14] G. Dickinson, C. Blair, B. L. Ott, *Places of Public Memory: The Rhetoric of Museums and Memorials*. Tuscaloosa: The University of Alabama Press, 2010, pp. 26-57.

[15] C. Di Pasquale, *Antropologia della memoria: il ricordo come fatto culturale*. Bologna: Il Mulino, 2018, pp- 132-137.

[16] J. Donohoe, *The Betweenness of Monuments. In Interpreting Nature: The Emerging Field of Environmental Hermeneutics*. New York: Fordham University Press, 2013.

[17] A. Erll, A. Nünning, *Cultural Memory Studies*. Berlin, New York: De Gruyter, 2008.

[18] V. Fortunati, E. Agazzi, *Memoria e saperi: percorsi transdisciplinari*. Roma: Meltemi, 2007, pp. 531-546.

[19] C. Galasso, *Zone di memoria. Il design per gli archivi del territorio*. Milano: FreancoAngeli, 2018.

[20] M. Halbwachs*, Les cadres sociaux de la mémoire*. Paris: F. Alcan, 1925.

[21] M. Halbwachs, *The collective memory*, New York: Harper & Row, 1980, pp. 139-140.

[22] M. Halbwachs, *La topographie légendaire des Evangiles en Terre Sainte: Etude de mémoire collective*. Paris: Presses Universitaires de France, 1941.

[23] M. Isnenghi, *I luoghi della memoria: simboli e miti dell'Italia unita*. Roma: Editori Laterza, 1998.

[24] P. Nora, *Le lieux de la mémoire*. Paris: Gallimard, (1984-92).

[25] P. Nora, "Between memory and history: Les lieux de mémoire". *Representations*, 26: 7–25.

[26] N. Pethes, J. Ruchatz, *Dizionario della memoria e del ricordo*, Milano: Mondadori, 2002.

[27] M. Quaggiotto, "A New Atlas for Abstract Spaces. Visual Tools for the Exploration of Complex Contexts". D. Durling, R. Bousbaci, L. Chen, P. Gauthier, T. Poldma, S. Roworth-Stokes, E. Stolterman, *Design and Complexity* - DRS International Conference 2010, 7-9 July, Montreal, Canada.

[28] M. Quaggiotto, *Cartografie del sapere: interfacce per l'accesso agli spazi della conoscenza*. Milano FrancoAngeli, 2012.

[29] P. Ricoeur, *Memory, history, forgetting*. Chicago: University of Chicago Press, 2004, pp. 58–68.

[30] Z. Segal, B. Vannieuwenhuyze, *Motion in Maps, Maps in Motion*, Amsterdam: Amsterdam University Press, 2020

[31] G. Testori, *I segreti di Milano*. Milano: Feltrinelli, 1958.

[32] J. Van Rookhuijzen, *Herodotus and the topography of Xerxes' invasion*. Berlin, Boston: De Gruyter, 2020, pp. 5-19.

[33] A. Warburg, R. Ohrt, A. Heil, *Bilderatlas Mnemosyne: the original*. Berlin Hatje Cantz, 2020.

[34] F. Yates, *The art of memory*. Chicago: The university of Chicago press, 1966.

[35] J. Young, *The texture of memory: Holocaust memorials and meaning*. New Haven: Yale university press, 1993.

[36] Mnmemosphere project website: https://www.mnemosphere.polimi.it/

[37] A. Caccia et al., *Educazione e memoria. Un racconto di periferia*. 2021. Project funded by MIUR (Italian Ministry of Education, University and Research).

Holocaust Fairy Tale

Kinga Anna Gajda

***Abstract*—** In his book, 'Modernity and Holocaust', Zygmunt Bauman proposes to treat the Holocaust as a test of the hidden possibilities of modern society, and Peter Novick lists what lessons can be learned from the Holocaust today. He claims that the events of the Second World War warn against totalitarianism, prove what the decline of humanistic values is leading to, and reveal the good and bad nature of man. By citing the example of the Holocaust, one can not only teach respect for diversity, explain what tolerance is, respect for human rights, counteracting discrimination and exclusion, but also show how important heritage and memory are, also about trauma. The memory of the Holocaust is used primarily to obey and prevent similar genocides, it is treated as a difficult legacy. As Gregory J. Ashworth writes, 'there are few historical events whose memory (and the manner in which that memory is honored) may be more controversial.'

These controversies concern not only the content itself, but also the ways of its transmission, as well as the age from when it begins to be told to children. Some believe that it is not appropriate to familiarize students with the traumatic experience of the youngest graders, others, primarily the survivors, believe that the pedagogue and child therapist Haim Ginott, in his appeal addressed to teachers, called for warning children against hatred from an early age and showing what to do. she drives. He said, 'Help your children to become human.' He also assigned the same responsibility to parents, emphasizing that the language of communication is very important in passing on the heritage.

The survivors, as he writes, Batshewa Dagan (actually Izabella Rubinstein) felt the need to write down their experiences, tell about their experiences and give testimony not only to adults, but also to children. That's why they wrote fairy tales. The goal of these fairy tales, like all other stories addressed to the youngest, was to develop such models of behavior that would give 'value to human life' (Bruno Bettelheim). Moreover, these fairy tales become the basis of knowledge. As an Austrian psychologist and educator writes, 'knowledge of facts benefits the whole of the personality (...) when it transforms into 'subjective knowledge'.

The aim of the presentation / article is a literary and cultural analysis of Holocaust fairy tales.

***Keywords*—** faity tale, heritage, Holocaust, memory, post-memory generation.

Kinga Gajda is with the Institute of European Studies, Poland (e-mail: kinga.gajda@uj.edu.pl).

Effectiveness of Habit Reversal Treatment(Hrt) on Craving,Assertiveness and Emotion Regulation of Addicts Treated with Methadone

Samin Khorrami

***Abstract*—** Objectives: The purpose of this study was to investigate the effectiveness of habit reversal treatment on craving, Assertiveness and Emotion regulation of addicts treated with methadone. Method: The research design was a semi-pilot pre-test،post-test, Together with the control and experimental group. The statistical population was formed of all addicts referred to addiction treatment centers in district 7 of Tehran in the second half of 1396 and the first half of 1397. In a available sampling method, 20 drug addicts treated with methadone with a history of at least 6 months of treatment as a sample of the experimental group as well as 20 addicts with a history of at least 6 months of non-use as a control group were selected. Craving questionnaires, Assertiveness and emotional regulation strategies were used to evaluate variables and multivariate analysis of covariance analysis in order to analyze the data.

Results: The results of this study showed that the use of methadone therapy with by Habit Reversal Treatment in comparison with methadone therapy alone has a significant effect on craving, Assertiveness and Emotion regulation of addicts.

Conclusion: According to the results, it seems that accompanied by methadone therapy, the use of systematic reversal training increases the possibility of success in treatment and decreases the possibility of slipping and returning to re-use of drug.

***Keywords*—** Habit Reversal Treatment, cravin, Effectivenes, Emotion regulation, methadone, treated addicts

Samin Khorrami is with the Islamic Azad University, Chalous Branch, Iran (e-mail: khorrami25@yahoo.com).

Deciphering Electrochemical and Optical Properties of Folic Acid for the Applications of Tissue Engineering and Biofuel Cell

Sharda Nara, Bansi Dhar Malhotra

***Abstract*—** Investigation of the vitamins as an electron transfer mediator could significantly assist in merging the area of tissue engineering and electronics required for the implantable therapeutic devices. The present study report that the molecules of folic acid released by Providencia rettgeri via fermentation route under the anoxic condition of the microbial fuel cell (MFC) exhibit characteristic electrochemical and optical properties, as indicated by absorption spectroscopy, photoluminescence (PL), and cyclic voltammetry studies. The absorption spectroscopy has depicted an absorption peak at 263 nm with a small bulge around 293 nm on day two of bacterial culture, whereas an additional peak was observed at 365 nm on the twentieth day. Furthermore, the PL spectra has indicated that the maximum emission occurred at various wavelengths 420, 425, 440, and 445 nm when excited by 310, 325, 350, and 365 nm. The change of emission spectra with varying excitation wavelength might be indicating the presence of tunable optical bands in the folic acid molecules co-related with the redox activity of the molecules. The results of cyclic voltammetry studies revealed that the oxidation and reduction occurred at 0.25V and 0.12V, respectively, indicating the electrochemical behavior of the folic acid. This could be inferred that the released folic acid molecules in a MFC might undergo inter as well as intra molecular electron transfer forming different intermediate states while transferring electrons to the electrode surface. Synchronization of electrochemical and optical properties of folic acid molecules could be potentially promising for the designing of electroactive scaffold and biocompatible conductive surface for the applications of tissue engineering and biofuel cells, respectively.

***Keywords*—** biofuel cell, electroactivity, folic acid, tissue engineering.

Sharda Nara is with the Delhi Technological University, India (e-mail: sharda23sept@gmail.com).

Identification of Candidate Congenital Heart Defects Biomarkers by Applying a Random Forest Approach on DNA Methylation Data

Kan. Yu, Khui Hung. Lee, Eben. Afrifa-Yamoah, Jing. Guo, Katrina. Harrison, Jack. Goldblatt, Nicholas. Pachter, Jitian. Xiao, Guicheng (Brad). Zhang

Abstract

Background and significance of the study—Congenital Heart Defects (CHDs) are the most common type of birth defects, representing 0.8% of infants at birth and one of the leading causes of infant death. Although the exact etiology remains a significant challenge, epigenetic modifications, such as DNA methylation, are thought to contribute to the pathogenesis of congenital heart defects. At present, no existing DNA methylation biomarkers are used for early detecting CHDs. The existing CHD diagnostic techniques are time-consuming and costly and can only be used to diagnose CHDs after an infant was born. The present study employed a machine learning technique to analyse genome-wide methylation data in children with and without CHDs with the aim to find methylation biomarkers for CHDs.

Methods—The Illumina Human Methylation EPIC BeadChip was used to screen the genome-wide DNA methylation profiles of 24 infants diagnosed with congenital heart defects and 24 healthy infants without congenital heart defects. Primary pre-processing was conducted by using RnBeads and limma packages. The methylation levels of top 600 genes with the lowest p-value were selected and further investigated by using a random forest approach. ROC curves were used to analyse the sensitivity and specificity of each biomarker in both training and test sample sets. The functionalities of selected genes with high sensitivity and specificity were then assessed in molecular processes.

Major findings of the study—Three genes (*MIR663*, *FGF3* and *FAM64A*) were identified from both training and validating data by random forests with an average sensitivity and specificity of 85% and 95%. GO analyses for the top 600 genes showed that these putative differentially methylated genes were primarily associated with regulation of lipid metabolic process, protein-containing complex localization and Notch signalling pathway. The present findings highlight that aberrant DNA methylation may play a significant role in the pathogenesis of congenital heart defects.

Keywords—biomarker, congenital heart defects, DNA methylation, random forest

K. Yu is with the School of Science, Edith Cowan University, Joondalup, Western Australia, Australia (phone: +61 8 6304 2835; e-mail: k.yu@ecu.edu.au)

KH. Lee is with the School of Public Health, Curtin University of Technology, Bentley, Western Australia, Australia (e-mail: khuihung.lee@postgrad.curtin.edu.au)

E. Afrifa-Yamoah is with the School of Science, Edith Cowan University, Joondalup, Western Australia, Australia (e-mail: e.afrifayamoah@ecu.edu.au)

J. Guo is with the School of Public Health, Curtin University of Technology, Bentley, Western Australia, Australia (e-mail: jing.guo@postgrad.curtin.edu.au)

K. Harrison is with the Genetic Services & Familial Cancer Program of WA, King Edward Memorial Hospital for Women, Subiaco, Western Australia, Australia

J. Goldblatt is with the Genetic Services & Familial Cancer Program of WA, King Edward Memorial Hospital for Women, Subiaco, Western Australia, Australia

N. Pachter is with the Genetic Services & Familial Cancer Program of WA, King Edward Memorial Hospital for Women, Subiaco, Western Australia, Australia

J. Xiao is with the School of Science, Edith Cowan University, Joondalup, Western Australia, Australia (phone: +61 8 6304 6056; e-mail: j.xiao@ecu.edu.au)

B. Zhang is with the School of Public Health, Curtin Health Innovation Research Institute, Curtin University, Kent St, Bentley, Western Australia, Australia, is adjunct Associate Professor with Infection and Immunity, School of Biomedical Sciences, University of Western Australia, Crawley, Western Australia, Australia (phone: +61 8 9266 3226 e-mail: brad.zhang@curtin.edu.au)

Systematic Review of Stricturoplasty for Ileal Strictures in Crohn's Disease in the Biologics Times

Mohammed Qayum, Lava Krishna Kannappa, Shahin Hajibandeh, Arun Chockalingam

***Abstract*—** Background: Since the 1980s, stricturoplasty has been one of the options for the surgical management of obstructing small bowel Crohn's disease (CD). Since the advent of biologics, stricturoplasty has gone out of fashion but has been shown to be an increasing trend of fistulating disease behaviour as a risk that increases over time in patients with CD. The long-term, large studies outcome results of the Stricturoplasty have reinforces the resurgence of bowel sparing surgery. Methods: Medline database via PUBMED with terms was (Crohn's), (Surgery), (stricture), and (management) without any restriction to year of Publication. Four hundred and ninety articles were shortlisted. After inclusion and Exclusion criteria following PRISMA guidelines, five articles were included in the study. Systematic review was done with stricturoplasty outcomes in the last 20 years. Results: Recent large studies have estimated the risk of surgical recurrence over a period of 7-8 years post stricturoplasty at 30-34%. The number of patients included were about 1525. Studies of ileocolic resection long-term follow up over 25 years showed a tendency towards an increase in ileal disease from 38% to 67%. The most popular strictureplasty techniques were the Heineke-Mikulicz technique -strictures up to 7 cm, Finney for strictures (7–15 cm), isoperistaltic side-to-side Michelassis for strictures more than 15 cm. Conclusion: The likelihood of multiple bowel resections during the patient's lifetime in Crohn's disease being high, placing patients at a definite risk of developing the short gut syndrome. Strictureplasty remains indicated as part of an overall strategy to conserve intestinal length. Contraindications to strictureplasty include penetrating disease, perforation of the bowel, malnutrition, suspicion of cancer. The effectiveness of biologics should not result in a neglected approach with the risk of intestinal failure among CD patients, and this event must be avoided by means of the application of bowel-sparing surgery in all suitable patients. Recent large studies have estimated the risk of surgical recurrence over a period of 7-8 years post stricturoplasty at 30-34%. Studies of ileocolic resection long-term follow-up over 25 years showed a tendency towards an increase in ileal disease from 38% to 67%.

***Keywords*—** Crohn's, stricture, surgery, management.

Lava Kannappa is with the NHS, United Kingdom (e-mail: lavakrishna@yahoo.com).

How Artificial Intelligence is Changing Healthcare: A Digital Marketing Revolution

Samuel Peek

***Abstract*—** This presentation will discuss what is on the horizon for Artificial Intelligence (AI) technology, and how AI can be used on a small scale to give practice a competitive edge. Artificial intelligence is a topic that sparks much debate, but it is a conversation that one cannot afford to avoid, as it is no longer just a dream. Science fiction often portrays AI as an omniscient force capable of world-changing effects, both good and evil. Although the current capabilities of AI do not include being able to predict a person's life-long partner or initiate a nuclear war against mankind, the changes and possibilities that AI is already bringing to the tech world are, in fact, altering the world as we know it. AI can be used to improve almost everything, from our sleep cycle to creating your perfect social media experience. This is because its learning algorithms mimic cognitive functions—such as learning, problem-solving, and pattern recognition—at efficiency levels unparalleled by humans. Current AI can curate new content, help decrease the cost of acquiring new patients, lower the cost per conversion, and determine how to wisely allocate your budget among marketing tactics. Utilizing the tools at the disposal will help get ahead now, leaving others to face insurmountable barriers later. As AI is changing healthcare, a digital marketing revolution, this study will discuss instances of AI technology being used effectively in the industry. From there, this study will discuss the magnitude of AI technology, and what it means for our industry. Then, taking a look into the future, it will discuss what is on the horizon for AI technology, and how it can be used on a small scale to give human practice a competitive edge. AI algorithms are self-contained systems that bring in new leads, nourish them, and learn from failures to create individually custom and curated experiences as humans advance. These systems can more accurately predict human interactions than humans can. This, therefore, allows it to create unique, personally-tailored experiences on the fly, conduct predictive analysis, and generate sales. Although relinquishing control to an automated AI system sounds risky, the reality is that AI can become a perfect practice manager, best social media expert, and the most knowledgeable ad specialist, without ever tiring. AI technology is the future and will become more widely adopted as the algorithms continue to get more advanced. Time is money, and world has already reached the point where AI can outperform humans in various tasks. AI is the new face of productivity; when data needs to be analyzed and trends to be spotted on immense scales, there is no substitute for what AI offers (Higher Efficiency = Better ROI). AI technology is still in infancy, and the possibilities of what can be accomplished with machine learning may be even more exciting than the current capabilities. Therefore, it is important to begin integrating AI into marketing practices now.

***Keywords*—** artificial intelligence, digital marketing, practice management, ROI.

Sam Peek is with the Incredible Marketing, United States (e-mail: sam@incrediblemarketing.com).

The Day After Tomorrow: How to Market Your Practice Post Pandemic

Samuel Peek

***Abstract*—** Aim: This presentation will illustrate how to optimize plastic surgery services and digital footprint to create meaningful ROI for your business in a post-COVID world. INTRO: In just 12 months, COVID-19 has altered every facet of our lives; from communication, to travel, to making purchases, nothing has been left untouched. Even once a level of widespread vaccinations is reached, the virtual adaptations made to meet the needs of a pandemic world will not be so easily reverted. The pandemic has shown that distance is subjective, and that humans have the resources available to facilitate most business from the comfort of homes. Therefore, if you believe that people will choose the more difficult option of waiting in line to drive to consultations again, then 2021 is going to be rough. These digital adaptations present a new and unique challenge to modern companies to either evolve to fit the patient's needs or fall behind and hope to catch up later. Marketing and advertising has to happen, and the businesses that make the necessary adjustments will be the ones that come out on the other side confident, their message is going to be seen. METHOD: In this presentation, The Day After Tomorrow: How to Market Your Practice Post Pandemic, we will illustrate how to optimize your plastic surgery services and digital footprint to create meaningful ROI for the business in a post-COVID world. This presentation will explain how to leverage the following four tools: 1) Telehealth- Telemedicine is here to stay. 2) Google New Initiatives- Are you a trusted source of information to Google? 3) Websites- Your most important marketing tool. 4) Social Media- Leverage the power of information. RESULTS: By leveraging these four resources to their full potential, you can create an ecosystem that nourishes and educates existing patients, while portraying a welcoming environment for new patients too. COVID has forced us to reevaluate how we conduct business, and although not every change benefits humans, they cannot escape or ignore them. CONCLUSION: With maskless grocery trips and large-scale gatherings still on the horizon, adapting business to cater to the needs of a distanced society will set the business up for success—both in the office and behind a screen. Not only will be the new patients attracted, but the loyal clients will appreciate the efforts in being a practical and visible resource.

***Keywords*—** marketing, practice management, SEO, website development.

Sam Peek is with the Incredible Marketing, United States (e-mail: sam@incrediblemarketing.com).

Exploring Potential for Community Pharmacists to Support Improved Help-Seeking for Dementia among Black, Asian and Minority Ethnic Population

Omaedo Iyoko

***Abstract*—** Background: The Black, Asian and Minority Ethnic (BAME) people are known to be at a higher risk of developing vascular dementia, due to higher exposure to the risk factors such as cardiovascular diseases and being of lower social economic status (Weuve et al., 2018; Moriaty et al. 2014; Bhattacharyya, 2012; Adelman et al., 2011). Thus, by 2051, while a two-fold increase of dementia prevalence is projected among the whole UK population, a seven-fold increase is projected for the BAME population (Nielsen et al. 2018; Mukadam, 2017; Alzheimer's Society, UK, 2015, APPGD, 2013). The BAME people however, remain late help-seekers as they continue to present later to specialist care centres and services for memory problems. This review seeks to explore the interventions that have been developed to support improved help seeking for dementia in this population and what further interventions may be needed. Methods: Adopting the scoping review framework by Arksey and O'Malley (2005) buttressed by the Peters et al., (2015) outline, the identified papers were analysed and themes identified. Results: Intervention themes identified are: awareness targeted, culture targeted and healthcare targeted interventions. Conclusions: This review reveals the lack of research exploring the role of the wider healthcare community in supporting BAME people to seek help for dementia related issues as well as a lack of research involving other community health care settings such as the community pharmacies, a place frequently visited by target populations.

***Keywords*—** BAME people, community pharmacists, dementia, help-seeking.

Omaedo Iyoko is with the Leeds Beckett University, United Kingdom (e-mail: O.Iyoko3395@student.leedsbeckett).

Non-Conveyance Statuses Resulting from Patients-Initiated Refusal for Emergency Medical Services in Riyadh Province, Saudi Arabia.

H. N. Moafa

***Abstract*—** Objectives: We aimed to investigate the association between demographic and operational factors and emergency medical services (EMS) missions ending in non-conveyance (NC) status due to patient-initiated Refusal (PIR). Methods: This was a retrospective population-based registry analysis for the conveyance status resulting from a decision made by patients after the arrival of ambulance crews at the scene between January 1, 2018, and December 31, 2018 Riyadh Province of Saudi Arabia. Conveyance status was categorized as conveyed to the hospital, not conveyed due to patient-initiated Refusal (PIR), and not conveyed due to EMS-initiated Refusal (EIR). Differences in characteristics of the mission were tested using Pearson's chi-squared test. The Mann- Whitney U test was used to compare response time and on-scene time, and total mission time for outcome missions. Unadjusted odds ratios (ORs) and adjusted ORs (AORs) with 95% confidence interval (CI) were calculated. Result: In the total of 67,620, we found 23,991 missions (34.4%) ended in NC due to PIR, and 5,969 missions ended in EIR status (8.6%) while the rest were transported to hospitals' emergency departments. Furthermore, we found that NC rates due to PIR were higher for women, adults, for missions in Riyadh city, during nighttime, for medical emergencies, and for Advance Life Support (ALS) crews. In addition, we found the following additional predictors significantly associated with the odds of NC due to PIR in the adjusted regression analyses: Factors of age category, geographical locations, EMS-shift, time of call, emergency type, and response time. Conclusion: The NC rate represents half of all missions for patients requesting EMS. Further interventions policymakers are required to obscure the progressive increase in NC rate due to PIR, where the rate in Riyadh city has increased compared to previous studies. Most NC cases occur for the highest urgency level of medical emergency type in Riyadh city during the nighttime with ALS crews. NC due to PIR involves younger patients more than the elderly and females more than males. High-quality research involving patients and the public are needed.

***Keywords*—** emergency medical services, ambulance, non-conveyance, conveyannce

Hassan Moafa is with the Maastricht University, Netherlands (e-mail: h.moafa@maastrichtuniversity.nl).

Health Hazards of Performance Enhancing Drugs

Austin Oduor Otieno

***Abstract*—** There is an ingrained belief that the use of performance-enhancing drugs by athletes enable them to perform better. While this has been found to be truth, it also raises ethical and health issues. This paper analyzes the health hazards associated with performance enhancing drugs. It seeks to achieve this through the analysis of different academic journals as well as publications on the relationship between doping in sports and health. It concludes that there are inherent health hazards associated with the use of performance-enhancing drugs as they affect the physical and psychological health and wellbeing of a user (athlete).

***Keywords*—** doping, health hazards, athletes, drugs.

Austin Otieno is with the Masinde Muliro University of Science and Technology, Kenya (e-mail: aoduor24@gmail.com).